Experimental and Theoretical Investigations of the Dielectric and Electro-Optical Properties of Polycarbazoles and Polysiloxanes

Stephen John Mumby, BSc

A thesis presented for the degree of

Doctor of Philosophy

to

The University of Aston in Birmingham

December 1983

Experimental and Theoretical Investigations of the Dielectric and Electro-Optical Properties of Polycarbazoles and Polysiloxanes

A thesis presented for the degree of
Doctor of Philosophy
to
The University of Aston in Birmingham
by
Stephen John Mumby, BSc
1983

Following the availability of sharp fractions of cyclic and linear poly(dimethyl siloxanes), a comparative dielectric study has been undertaken of these materials. The electronic, atomic and orientational polarizations have been determined in the undiluted state for number-average molar masses in the range 160-7700 and dipole moments calculated. For cyclic dimethyl siloxanes containing more than 20 skeletal bonds the dipole moments were found to be the same, within experimental error, as those found for the nearest equivalent linear molecules. However, the dipole moments of smaller cyclic molecules were observed to be substantially less than the dipole moments of the equivalent open chain molecules. Measurements of the static dielectric permittivity of solutions of cyclic and linear poly(dimethyl siloxanes) in cyclohexane indicated a significant specific solvent effect.

Theoretical investigations of the conformational statistics of cyclic and linear dimethyl siloxane oligomers and polymers have been undertaken. Rotational isomeric three-state models were used to calculate electric dipole moments, optical anisotropies and molar Kerr constants. Theoretical dipole moments agreed well with the experimentally determined values.

Samples of poly(N-vinyl carbazole) possessing different tacticities were prepared and carefully characterised. Measurements of their static dielectric and electro-optical properties in solution in 1,4-dioxan have been made. The results of these measurements support the view that the stereostructure of poly(N-vinly carbazole) is sensitive to the mechanism of polymerization. These results, together with carbon-13 N.M.R. data, are discussed in terms of the possible conformations of the polymer chains and the relative orientations of the bulky carbazole side groups.

Polysiloxanes
Polycarbazoles
Static dielectric permittivities
Electric dipole moments
Electro-optical Kerr effect

ACKNOWLEDGEMENTS

I am grateful to the Department of Chemistry for provision of facilities and to the Science and Engineering Research Council for their financial support during the period 1980-1983.

I would like to thank the staff of the Chemistry workshop for the construction of a variety of pieces of apparatus particularly during the first year of this work.

Much of the theoretical work presented in this thesis would not have been possible without the generous facilities offered by the Departement of Computer Science at Aston and help and advice given by the staff of this department.

I am indebted to Dr. S. Whitburn who gave a good deal of her time to obtain the high quality carbon-13 NMR spectra of poly(N-vinyl carbazole) presented in Chapter 3.

My sincere thanks are also extended to Christina Cade for her unswerving moral support and her careful and tireless preparation of figures which help to make this thesis more complete.

Further thanks are extended to Mrs S. Puar for her patient typing of this manuscript and to all friends and colleagues for their encouragement and comments during the course of this work.

Finally, it is simply not appropriate to thank 'my supervisor, Dr M.S. Beevers, for his helpful advice .. etc.' English understatement inhibits a reasonable declaration of the debt which I owe Dr Beevers for his faith, support, intellect and involvement.

CONTENTS

TABLES

ILLUSTRATIONS

CHAPTER 1

INTRODUCTION

Polymers, and in general most organic compounds in the pure state, are known principally for their insulating properties sooner than their ability to conduct an electric current. It was the former attribute, inherent in most polymers, which was first exploited commercially. An early example was the use of the naturally occurring polymer gutta-percha for the insulation of the first trans-Atlantic telephone cables laid in the 1860's. The major advantages of the new synthetic materials, such as polyethylene and polystyrene, are mainly due to the combination of high quality electrical insulation coupled with ease of fabrication by moulding. Synthetic polymers also tend to be less prone to water absorption than their naturally occuring counterparts. Polytetrafluoroethylene,PTFE, is particularly useful as a high voltage insulator because it is not susceptable to tracking.[1] If the insulating ability of polymers, containing aromatic or weakly bonded groups is exceeded an electric current may pass over the surface of the polymer, via a corona discharge, producing narrow tracks of carbon due to charing. These carbonised tracks have a lower resistance than the bulk polymer and will conduct electricity to give local ohmic heating and futher degradation. In the case of PTFE, however, the breakdown products are volatile and no carbon tracks are formed.

Polar, non-conducting, synthetic polymers are also used as

dielectric materials[2-9]. Poly(N - vinyl carbazole) was used as a replacement for mica in capacitors during the second world war[10]. Modern capacitors usually contain polystyrene or polypropylene as the dielectric material, although polycarbonate is also used in 'self-repairing' capacitors. The formation of electrets using polar polymers is also becoming more common[11]. Electrets may be formed by either heating a polar polymer above its glass transition temperature, applying a high voltage electric field across the sample and allowing it to cool, or by charge implantation[1]. The latter method is usually used commerically as it has been shown to produce electrets of long-term stability[12]. Any mechanical movement in an electret will produce a charge displacement, resulting in a potential difference between its surfaces, which may then be amplified. Polymers which are commonly used include poly(ethylene terephthalate) and fluorinated ethylene-propylene copolymer, which are both employed in the construction of electret microphones.

Many specialist applications of insulating polymers rely upon the frequency independence of the dielectric permittivity and dielectric strength. In the area concerned with high frequency, high voltage insulation, if the frequencies employed correspond to the natural orientational frequency of the dipolar units of the polymer, then there will be absorption of energy, which may lead to heating and subsequent breakdown of the material. For this reason it is important that the temperature of application does not exceed, or approach, the glass transition temperature of the polymer. However, the phenomenon of dielectric heating has found widespread use. An important application concerns the pre-heating of plastic preforms immediately prior to moulding. The heating of food in a microwave oven, by causing the water molecules to rotate under the influence of an intense

electric field, oscillating at approximately 22GHz, is another well known example of dielectric heating.

During the 1970's a considerable acceleration of effort occured in the study of polymers for possible use as electronic or electro-active materials[13-16]. The aims of this research to date have been primarily concerned with the development of a processable (mouldable) semiconducting or metallic polymer of demonstrated technological value. Many polymer based systems, often containing high proportions of dopant molecules, have now been prepared which possess varying degrees of electrical conductivity. Indeed, the electrical conductivity of some of these materials is not far removed from that of metals[17-20]. However, many of the polymers used in these systems, such as poly(acetylene), poly(diacetylene), poly(pyrrole), poly(p-phenylene) and poly(suphur nitride) rely on conjugation and a long-range repeating stereostructure for their electron transport mechanisms and tend, therefore, to be very brittle and infusible. However, some of these materials have been employed commercially in applications where they may be cast as films, for instance, in solar cells and in batteries[18]. Although a truly processable electrically conducting polymer has not yet been obtained, many specialist, electro-active polymers have been successfully developed[15]. To date, by far the most economically valuable of these applications is that employing the photoconductive polymer poly(N-vinyl carbazole)[21,22], PVK, which is used in the electrophotographic industry as a replacement for the photoconductor As_2Se_3. The latter is difficult to fabricate since it is brittle and has to be handled by vacuum sublimation techniques. The photoconductive properties of PVK were discovered in 1957 by Hoegl[23]; it is a good insulator in the dark. PVK is an efficient

absorber of ultra violet light (λ_{max} = 360nm), and fluorescesses in the green part of the visible spectrum. However, λ_{max} (absorption) for PVK may be conveniently moved into the visible region of the spectrum by the addition of an electron acceptor such as 2, 4, 7 - trinitrofluorenone[24]. The latter molecule is planar and is believed to form a 'sandwich' type repeating structure by interleaving with the planar carbazole side groups[25].

In the development of polymers as electro-active materials it is important to understand the relationships between molecular structure (e.g. primary sequence, tacticity, morphology) and the resulting macroscopic properties. Maxwell-Wagner effects[26-29], for instance, in which ions collect at the interfaces of domains possessing different dielectric permittivities, may produce totally misleading electrical conductivity or dielectric results for solid polymers, unless the existence of such effects is recognised or avoided. In order to gain maximum insight into the dependence of macroscopic parameters on molecular structure, it is anticipated that a variety of physical methods will be required to probe the molecular conformations and stereostructures of the polymer molecules[30-33]. The measurement of dielectric permittivity[34,35], electrically - induced optical birefringence (Kerr effect)[36-40] and optical anisotropy[41], may be used to provide valuable information about chain conformations and molecular interactions, which may then be correlated with macroscopic quantities, such as charge-carrier mobility, specific electrical conductivity[14,15], etc.

The various physical methods of structure determination referred to above, may also be used, in a more academic sphere, to test molecular models[30-33]. The general approach employed normally involves the

calculation of some physical property of interest which is then compared with an experimentally determined value. Volkenstein[32] demonstrated that rotational isomeric state models could be very successfully used in the analysis of conformational-dependent properties of any type of polymer chain. Such models are now well established and are conspicuously successful when compared with the more simple freely-rotating or freely-jointed models[31]. Rotational isomeric state models are employed extensively in a variety of calculations presented in this thesis. By using models, based on the rotational isomeric state approximation, to calculate the root-mean-square dipole moments[31], for comparison with experimentally determined values[42], the validity of group dipole vector additivity may be tested. The suggestion that group optical polarizations are additive and invariant with conformation is still attracting a great deal of interest[43]. The valence optical scheme may be regarded as a tensor analogue of the vectorial addition method, used in the calculation of molecular dipole moments, and is employed in the calculation of the mean-square optical anisotropy, $\langle\gamma^2\rangle$, and the molar Kerr constant, ${}_mK$[31]. Much of the controversy regarding the valence optical scheme has resulted from the use of a multitude of bond polarizabilities for common types of bonds. However, Patterson and Flory[44] have shown that if experimental measurements of $\langle\gamma^2\rangle$ are carried out on dilute solutions of solutes dissolved in optically isotropic and geometrically symmetric solvents, the results obtained agree well with those predicted by the valence optical scheme.

Since 1977, when the first synthetic cyclic polymers were prepared and characterised by Semlyen and coworkers[45], these materials have received considerable attention[46-56]. They are of interest because

they belong to a class of polymer that is topologically different from the linear, branched and network polymers that have received such close attention during the last five decades. In fact, a detailed knowledge of the properties and molecular conformations of cyclic polymers could lead to a better understanding of the behaviour of linear polymers, as well as to new insights into the properties of rubbers, gels and other systems where closed loops are known to be present. Rotational isomeric state models may also be used to predict the conformational properties of cyclic polymer molecules. This approach represents an extreme test of any given model, since only those conformations of chain molecules which are restricted to a cyclic structure are required, and this situation corresponds to a much reduced conformational population. Semlyen and coworkers[45-56] have demonstrated that valuable information can be obtained by comparing the calculated properties and experimental data of cyclic and linear polymer molecules. This approach provides not only information about the conformational properties of the cyclic molecules, but also gives a novel and useful insight into the conformational statistics of the equivalent linear chains.

The measurement of dipole moments[42,57] has been used for many years as a means of investigating the conformational characteristics of polymeric materials. This has proved to be a convenient and valuable technique since the dipole moment of molecules in solution may be readily determined over the entire range of chain length from monomer through to high molecular weight polymer. In addition there is both theoretical[58-62] and experimental[63] evidence that dipole moments of many chain molecules are unaffected by excluded volume

interactions[30,31]. The chain molecules most extensively studied with regard to the dependence of the dipole moment on chain length, temperature, and the nature of the solvent medium are the dimethyl siloxanes[64-69], and a vast amount of information about the conformations of these interesting materials has been deduced as a consequence of these studies. Polymers with oxygen atoms present in their backbone structure are especially amenable to dielectric studies since they do not rely solely upon side groups for their polarity. Partly for this reason the conformational characteristics of polyoxyalkyls[31,58,59,70-83] have been studied extensively, both in solution and the pure state. Although the polymethylene chain possesses negligible polarity, information on its conformational characteristics has been obtained from the analysis of the dipole moments of α, ω-dibromoalkanes[84-87].

The Kerr effect of synthetic polymers in solution has received considerable attention in a systematic set of studies by Le Fèvre and coworkers[80,88-97]. Recently, there has been a great deal of interest in studying the tacticities of vinyl polymers through measurements[98,99,101] and theoretical calculations[98-101] of the Kerr effect and optical anisotropy. The two vinyl polymers which appear to have received most interest are poly(vinyl chloride)[99-101] and poly (p -chlorostyrene)[99,100]. Extensive calculations of dipole moments of these polymers and their dependence on composition and stereoregularity have been presented by Mark[57]. Unfortunately, it transpires that the dipole moments are often nearly constant over a substantial range of tacticity. Tonelli[100] has calculated Kerr constants for a wide variety of vinyl copolymers and considered variations of both stereoregularity and composition. In general the Kerr constants appear to show greater sensitivity to both sequence and stereostructure.

Saiz et al[99] have obtained good agreement between experimental and theoretical Kerr constants for samples of vinyl polymers, the tacticities of which had been estimated by depolarized light scattering in conjunction with other methods. In recent years there has been considerable interest in re-investigating the effect of excluded volume on dipole moments and Kerr constants of polymers (principally vinyl polymers) determined under non-theta point conditions, and a number of theoretical[102-105] and experimental studies[63,105] have been published.

Dielectric and electro-optical techniques may also be used to study a variety of other molecular systems[38-40,106]. Generally, the measurements are made on dilute solutions and the results extrapolated to infinite dilution. Thus, the solute molecules are assumed to be unperturbed by intermolecular interactions from other solute molecules[107]. This affords considerable simplification when considering the conformations adopted by the solute molecules. However, in certain circumstances, electro-optical and dielectric techniques may in fact be employed in the study of molecular interactions and many studies of this kind have been reported[38-40,106]. The measurement of dielectric permittivity and the Kerr effect have also been used to study the effect of pH and ionic strength on the overall shape and related properties of a variety of macromolecules and suspended particles (protein molecules, viruses, bacteriophages and clays) in aqueous media[108-113].

The rate of orientation of macromolecules in solution may be studied by the dynamic electro-optical Kerr effect and by dielectric relaxation techniques. This has become an important method of studying the sizes and shapes of rigid or semi-rigid macromolecules.

Since rigid molecules often have well defined geometries, and rotate relatively slowly in solution, their rates of rotational diffusion can be accurately measured, thus permitting useful analyses to be performed concerning the dependence of hydrodynamic behaviour on this molecular structure. A number of closely related relaxation techniques have been extensively applied to determine molecular mobility and long-range order in liquid crystals[114-118]. These rod-like molecules often have large molecular dipole moments and are usually highly optically anisotropic, due to the extensive geometrical correlations between the molecules in the liquid-crystalline phase. These systems are very amenable to study by static dielectric and electro-optic techniques. However, due to the rigid molecular structure of these materials (e.g. poly(γ-benzl-L-glutamate) and poly(n-alkyl isocyanates))[117] their rotational relaxation times are often of the order of several milliseconds compared to the much faster relaxation times of 10^{-11} to 10^{-9} seconds exhibited by small molecules in solution. Relaxation times of ca. 10^{-7} seconds or greater can be easily measured by electro-optical methods and useful information thereby obtained[119]. (The range of relaxation times which may be studied by dielectric methods is much greater).

A detailed knowledge of molecular structure is an important prerequisite for a fuller understanding of the macroscopic properties of any material. In addition the ability to correlate desirable physical properties with molecular structure provides a powerful method of testing molecular models. In this thesis the principal experimental techniques used to study the conformationally dependent properties of cyclic and linear polymer molecules, in the pure state (bulk) and in solution, are based on the measurement of dielectric permittivity

and electrically-induced optical birefringence. It is generally accepted that it is valuable to employ techniques which rely upon different aspects of the conformational structure and behaviour of molecules. The parameters so obtained may then be interpreted in parallel, to see if, when considered together, they support, or refute, the conformational possibilities. This use of complementary methods helps to eliminate ambiguities which may arise if reliance is placed upon a single experimental technique. Thus, wherever possible, dielectric and electro-optic data were obtained for the same molecular system. The following chapters describe in detail the methods and results derived using this approach. Two major areas of investigation have been undertaken. The first is concerned with a comparative study of the experimental and theoretical conformational behaviour of cyclic and linear poly(dimethyl siloxanes). The second area is a study of the effect of synthetic route upon the stereostructure of poly(N-vinyl carbozole).

CHAPTER 2

EXPERIMENTAL METHODS

2.01 Introduction

The principal experimental techniques used throughout this thesis are concerned with the measurement of the static dielectric permittivity and the electro-optical Kerr effect. The apparatus and techniques employed to facilitate these measurements are described in this chapter.

The discovery of the first electro-optic effect was reported in 1875 by John Kerr[120,121] who made his initial observations on glasses. However, the techniques have advanced considerably since these pioneering measurements. Kerr's optical detector was his eye and his light source a flickering paraffin candle. (Edison developed the first practical electric lamp in 1880).

The opportunity for the Kerr effect to be used as an investigative technique, rather than merely a scientific curiosity, came with the realization by Gans[122] of the relationship between the Kerr constant and the magnitude of the optical anisotropy of a molecule. After further development of the theoretical relationships between molecular optical properties and light scattering by Debye[2,3,123] and by Debye and Sack[124] during the 1930's, Stuart[125,126] was able to considerably extend the work on optical anisotropy and its dependence on molecular structure.

One of the first groups of workers to apply the Kerr effect to

macromolecules was that of Zimm and O'Konski, who worked at Berkeley California from 1948. The macromolecules studied were biopolymers such as D.N.A. However, since that time a large number of polymers both synthetic and biological have been investigated by means of the Kerr effect and their structures elucidated.

The measurement of the static dielectric permittivity, as a means of determining the dipole moments of molecules, is also a well established technique for investigating molecular structure. It is by far the most popular method, since the experimentation is not too demanding (cf microwaves) and the interpretation of the results is relatively straight-forward.

Debye and Bueche[127] have shown that a comparison of the dipole moment of a polymeric molecule with that of one of its structural units can yield information concerning the average chain configuration. This method has since been employed by many other workers for a variety of polymer types. Thus, it makes an ideal complementary tool, along with the Kerr effect, for the study of the average configurational structures of the polymers in this investigation.

2.02 Dielectric Apparatus

Two sets of dielectric apparatus were used. The first was designed and built to measure the static dielectric permittivity of small sample volumes (cacm^3) of non-volatile liquids. This apparatus was used for the measurements on the cyclic and linear oligomers of dimethyl siloxane and the poly(dimethyl siloxanes). The second type of apparatus was designed to make measurements on larger sample volumes (ca. 20cm^3) of pure liquids and on dilute solutions, and was used principally for measuring the permittivity of solutions of poly(N-vinyl carbazoles).

The methods employed to determine the dielectric permittivity using the two sets of apparatus were somewhat different. For the small sample volume apparatus this was done by measuring the capacitance of the empty cell, using a capacitance bridge, and remeasuring the capacitance when filled with the liquid under investigation. For the equipment employing larger sample volumes a resonance method was used and the capacitances were determined indirectly by the measurement of frequencies.

2.03 Small Sample Volume Dielectric Cell (Dielectric Cell A)

This was a three-terminal cell constructed principally for the measurement of the static dielectric permittivity of fractions of cyclic and linear poly(dimethyl siloxanes) possessing narrow distributions of molecular weight. The cell had a sample volume of ca. 1 cm^3 and this could be adjusted over the range 0.5-1.5cm^3. A cross-sectional diagram of the cell is shown in Fig. 2.01. The high voltage electrode (A), low-voltage electrode (B), inner guard ring (C) and the outer guard ring (D) were turned from solid cylinders of stainless steel. The high-voltage electode forms the base of the cell and the outer guard ring constitutes the wall of the cell. The inner guard ring was fixed by three nylon screws (E) to the low-voltage electrode and secured in position by filling the small intervening gap with an epoxy based resin. The inner and outer guard rings were connected electrically by a short length of P.T.F.E. - coated wire. The outer guard was securely fixed to the high-voltage electrode by six 6mm diameter Allen bolts (F). Each bolt was fitted with a sleve of P.T.F.E. (G) and a disc of Tufnol[a] (H) to ensure electrical isolation between bolts and the high-voltage electrode. The outer guard and high-voltage electrode were electrically insulated from each other by a thin sheet of epoxy-impregnated paper (I) which was cured in situ

[a] Tufnol - phenol resin impregnated cloth

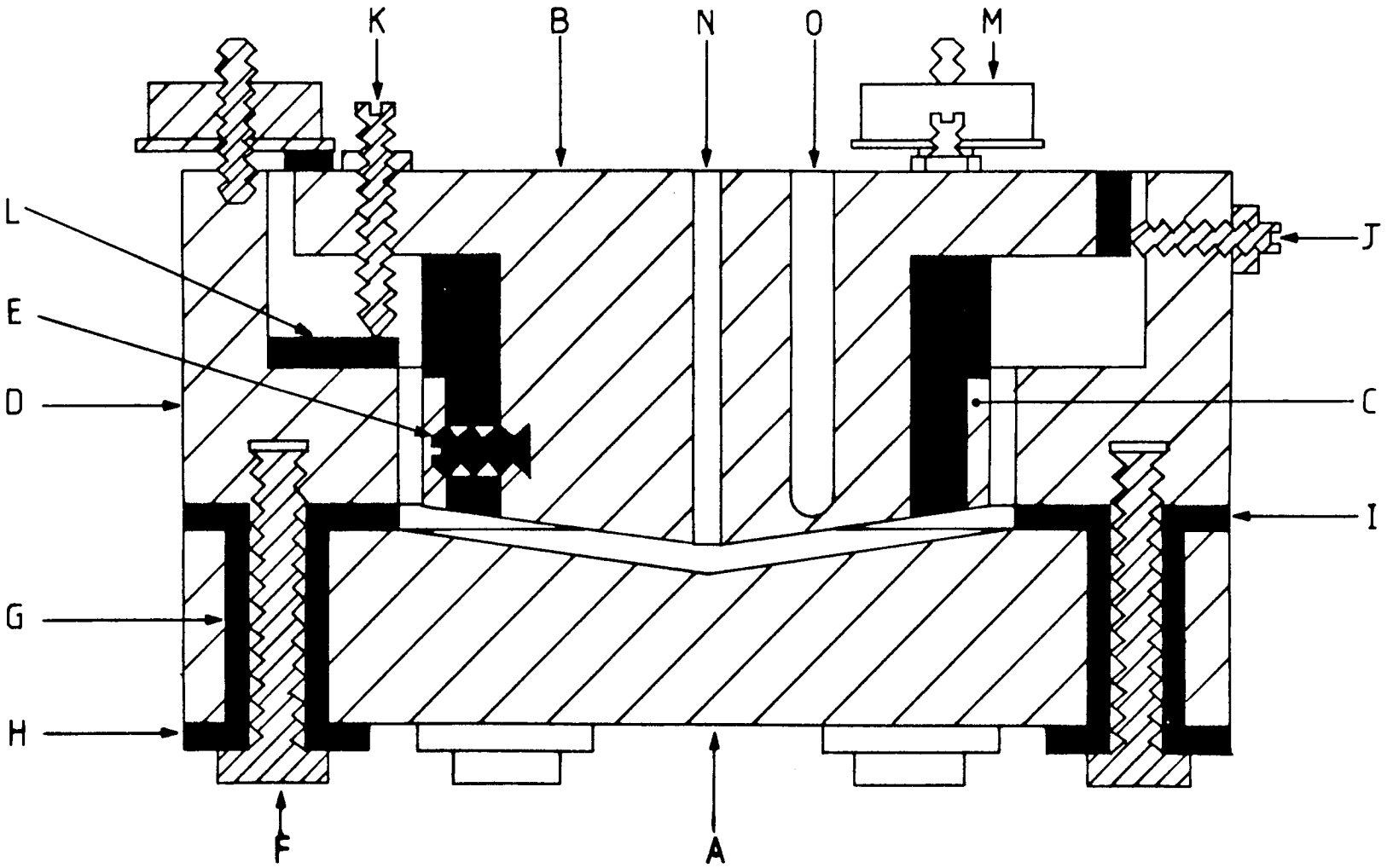

Figure 2.01 Cross-sectional diagram of the small sample volume dielectric cell (dielectric cell A).

at 353K for 24 hours. The paper was dried for several hours at 393K prior to immediate use. The horizontal position of the low-voltage electrode/inner guard ring assembly, relative to the outer guard ring, could be adjusted by three screws (J) set in the wall of the cell. The size of the gap between the high-voltage electrode and the low-voltage electrode was set by three screws (K) located in the rim of the low-voltage electrode. In order to maintain electrical isolation between the electrodes each adjustment screw impinged on a glass insulator (L). All the adjustment screws were fitted with lock-nuts. The low-voltage electrode/inner guard ring assembly could be locked in position by three knurled discs of brass (M), mounted on threaded studs set in the outer guard ring, which engaged with the upper surface of the low-voltage electrode via glass insulators. The facing surfaces of the low-voltage and high-voltage electrodes were conical in profile to facilitate filling and emptying the cell. A hyperdermic syringe was used to fill and empty the cell via a small hole (N) located at the centre of the low-voltage electrode. A larger hole (O) in the low-voltage electrode accommodated either a thermometer or a thermocouple junction. The electrical capacitance of the empty cell, when adjusted for a sample volume of about $1cm^3$, was approximately 70pF.

2.04 Temperature Control of Dielectric Cell A

The cell was enclosed in a perspex box (~20cm square). The latter was fitted with a removable lid, and insulated thermally by thin sheets of expanded polystyrene wrapped in aluminium foil. The air in the box was circulated using a fan and heated by means of a 7 Watt heater. For convenience and to maintain maximum thermal insulation the perspex box was mounted on top of the aluminium control unit by means of four

lengths (~5cm) of platic tube (~2.5cm diameter).

The control unit was housed in an aluminium box (approx 25 x 18 x 10cm) and had numerous holes (~13mm) punched in the sides and bottom to help dissipate heat generated by the transformers and power transistors. The majority of the components of the control circuit, shown in Figures 2.02 and 2.03, were mounted on printed circuit boards designed and built by the author. The pair of 2N3055 power transistors were mounted on a heat sink at the rear of the box, and the temperature sensor (LM3911) was encapsulated in an epoxy resin within a short length of aluminium tube and located in the perspex box. The heating rate and final temperature could be readily adjusted using the potentiometer controls on the front panel of the control unit.

The temperature of the cell could be controlled to within ±0.1K over the range 283-333K.

2.05 Measurement of Static Dielectric Permittivities using Dielectric Cell A

The electrical capacitance of the dielectric cell was measured using a Marconi Universal Bridge (Type T1313A) at a frequency of 10kHz. A substitution method described in reference 37 was used to calculate the static dielectric permittivities of liquids assuming a value[37] of 2.0199 for the static dielectric permittivity of cyclohexane at 298K. This entails making the reasonable assumption that the 'stray capacitance', ΔC, involved with the leads and edge effects does not change upon introducing a liquid into a dry cell. The 'stray capacitance' may then be calculated from the measured capacitances of the empty dry cell, C_{AIR}, and the capacitance, C_{SOLV}, of the cell when filled with freshly distilled solvent, since

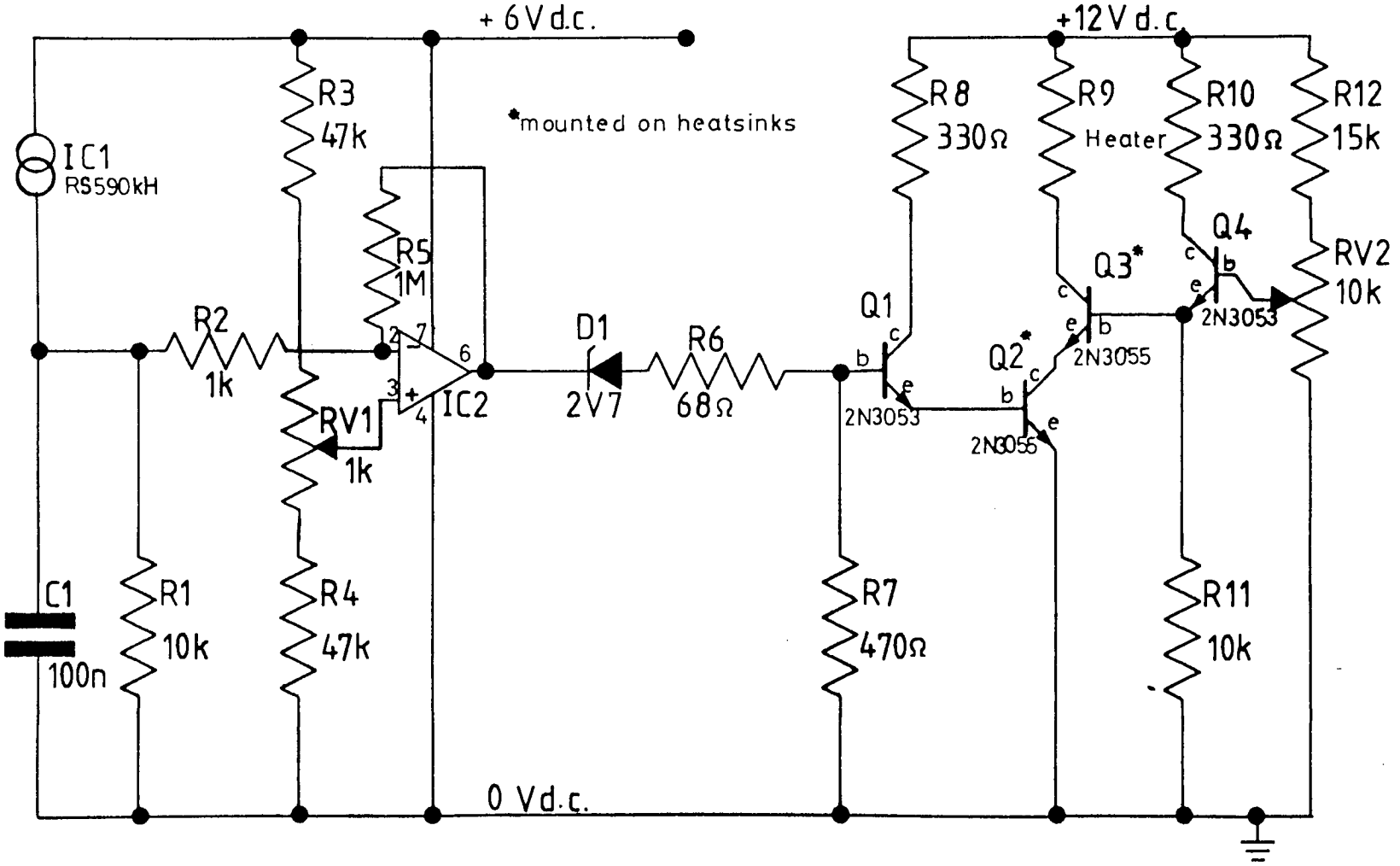

Figure 2.02 Circuitary for temperature control of dielectric cell A.

Parts List for Circuit Shown in Figure 2.02

Resistors

R1 10kΩ

R2 1kΩ

R3 47kΩ

R4 47kΩ

R5 1MΩ

R6 68Ω

R7 470Ω

R8 330Ω

R9 Heater (see Text)

R10 330Ω

R11 10kΩ

R12 15kΩ

RV1 1kΩ potentiometer

RV2 10kΩ potentiometer

Capacitors

C1 0.1 μF disc ceramic

Semiconductors

Q1, Q4 2N3053

Q2, Q3 2N3055 (mounted on heatsinks)

D1 400mW 2.7V zener diode

IC1 Temperature sensor
RS590 kH
(current source $1\mu AK^{-1}$)

IC2 μA741CP

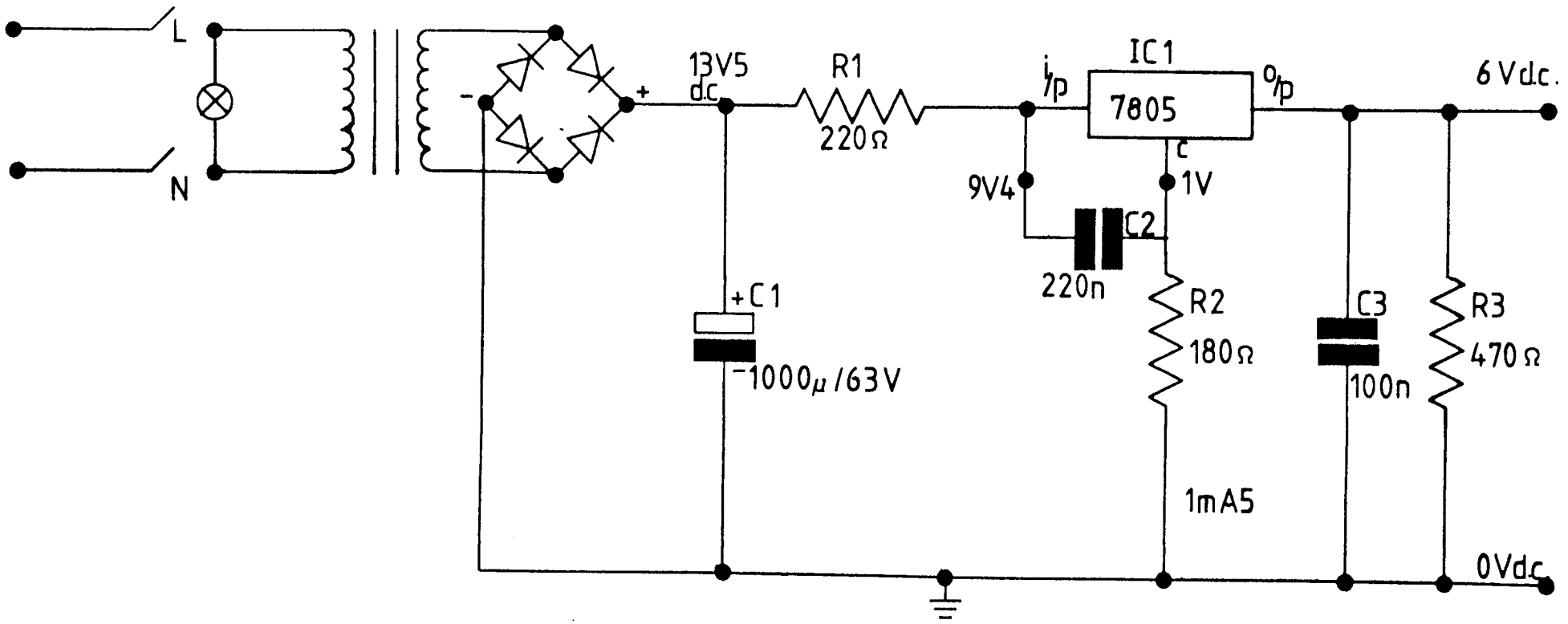

Figure 2.03 6V regulated supply for temperature controller

Parts List for Circuit shown in Figure 2.03

Resistors

R1 220 Ω

R2 180 Ω

R3 470 Ω

Capacitors

C1 1000μF/63V electrolytic

C2 220nF

C3 100nF

Semiconductors

IC1 7805

$$\varepsilon_{SOLV} = \frac{C_{SOLV} - \Delta C}{C_{AIR} - \Delta C} \qquad (2.1)$$

Solving for ΔC gives

$$\Delta C = \frac{C_{SOLV} - \varepsilon_{SOLV} C_{AIR}}{1 - \varepsilon_{SOLV}} \qquad (2.2)$$

From the measurement of the capacitance, C_{AIR}, of the empty cell and the capacitance, C_X, of the cell containing the sample, the static dielectric permittivity of the sample may be calculated using the relationship

$$\varepsilon_X = \frac{C_X - \Delta C}{C_{AIR} - \Delta C} \qquad (2.3)$$

Where ΔC is defined by equation (2.2). The static dielectric permittivity of cyclohexane (2.0199)[37] at 298K, together with the value $(-1.60 \times 10^{-3} K^{-1})$[128] of the temperature coefficient $(d\varepsilon/dT)$ of cyclohexane were used to calculate the static permittivities of liquids between 288K and 313K.

The static dielectric permittivities of the fractions of the cyclic and linear poly(dimethylsiloxanes) at 298K and 313K were obtained using the above procedure. The dielectric permittivities of the cyclic and chain fractions of the poly(dimethylsiloxanes) were estimated to have experimental errors of 0.05% and 0.1%, respectively.

2.06 Large Sample Volume Dielectric Apparatus (Dielectric Cell B)

The configuration of the dielectric apparatus is shown in Figure 2.04. The layout of components on the printed circuit board of the associated variable frequency oscillator (V.F.O.) is reproduced in Figure 2.05.

The dielectric cell (C_{CELL}) was of a German commercial origin. It was constructed of two gold-plated concentric cylinders, the outer cylinder being hollow for passage of coolant liquid, and was electrically guarded. The approximate sample volume of the cell was $20cm^3$.

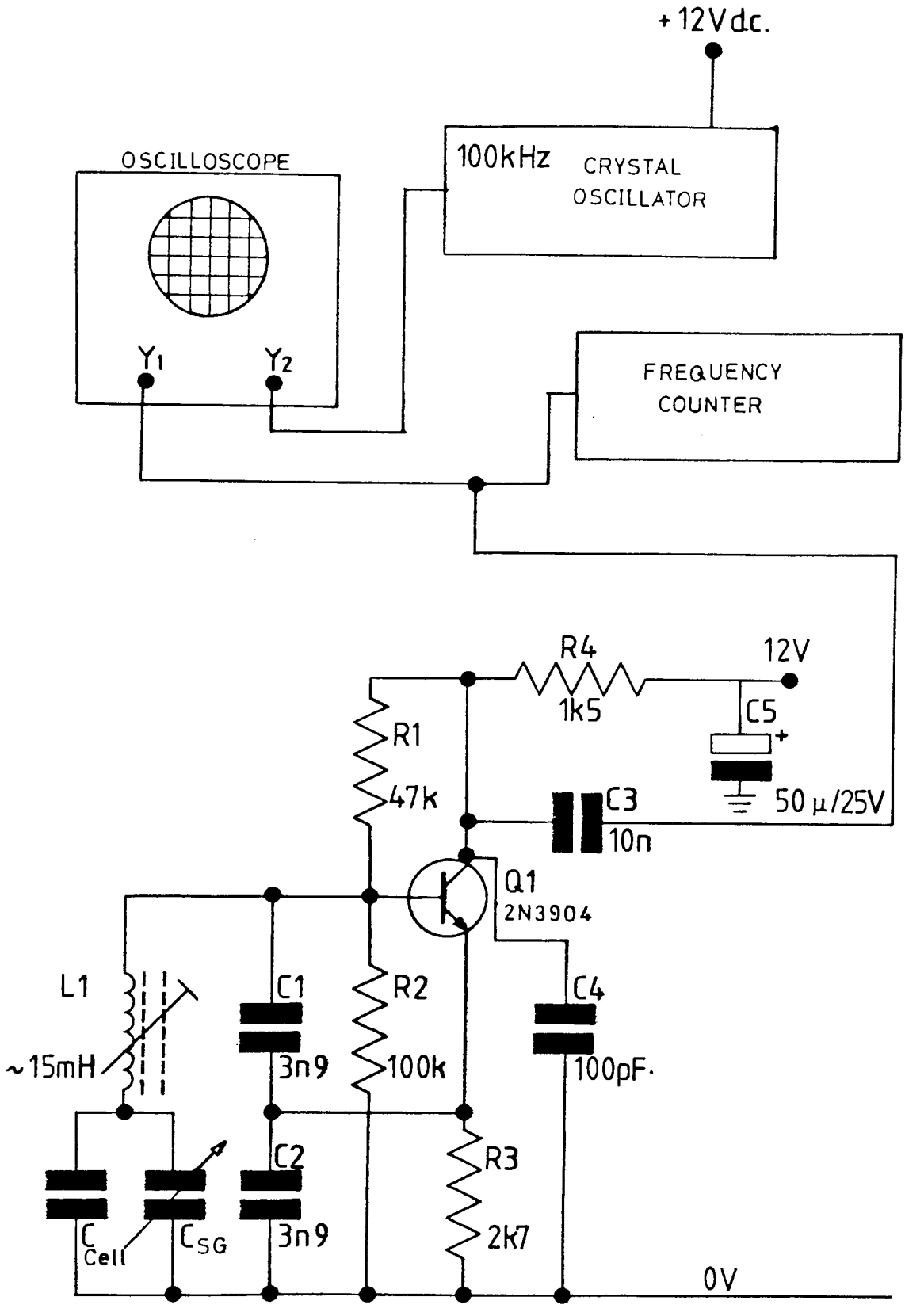

Figure 2.04 Configuration of large sample volume dielectric apparatus.

Parts List for Circuit Shown in Figure 2.04

Resistors

R1 47kΩ

R2 100kΩ

R3 2.7kΩ

R4 1.5kΩ

Capacitors

C1 3.9nF

C2 3.9nF

C3 10nF

C4 100pF

C5 50μF/25V electrolytic

Semiconductors

Q1 2N3904

Inductance

L1 ~ 15mH

Made by pile winding approximately 194 turns of enamelled copper wire (s.w.g. 30) upon a ferrite core (R.S. code 228-258).

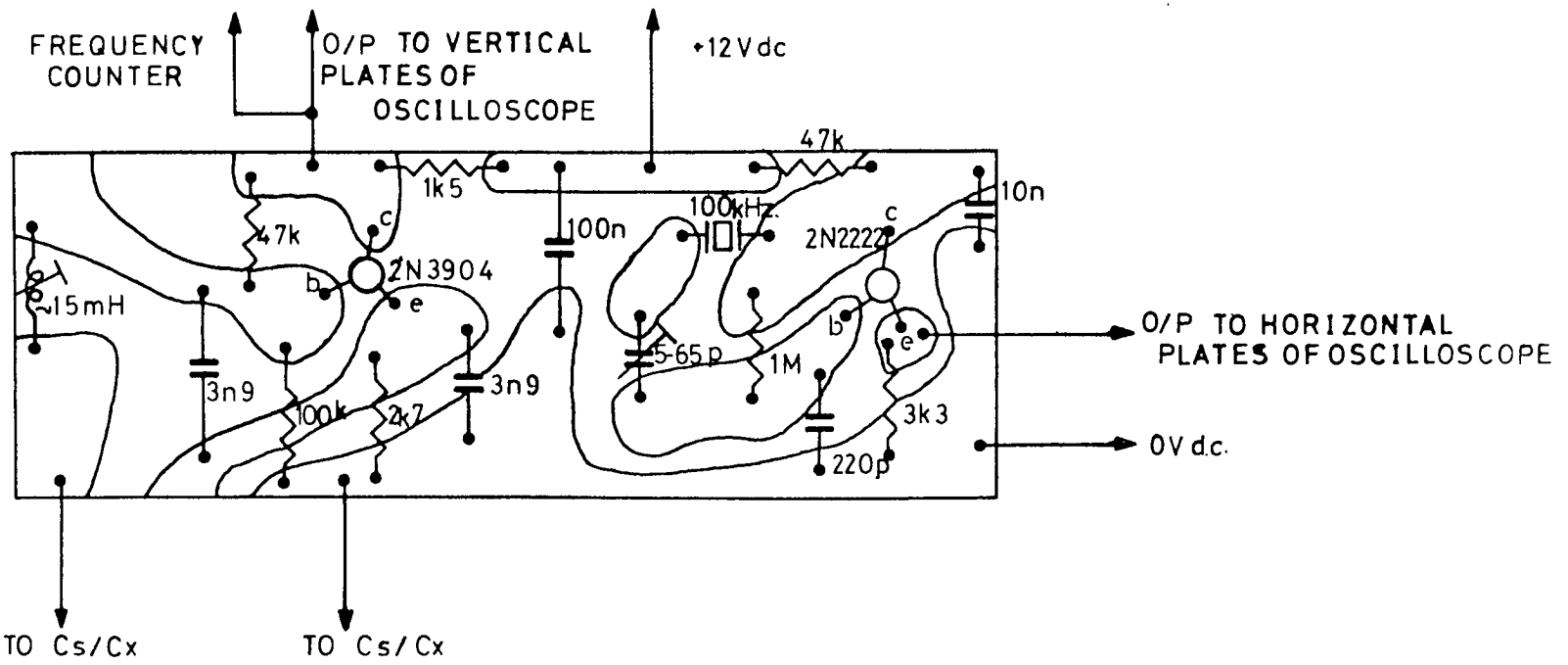

Figure 2.05 Printed circuit board layout for variable frequency and 100kHz oscillators.

Measurements of the dielectric increment could be made by matching the oscillator frequency of the V.F.O. with that of a fixed 100kHz crystal oscillator. This could be done by connecting the V.F.O. to the vertical plates of an oscilloscope (Telequipment, Type D43R), whilst the 100kHz oscillator was connected to the horizontal plates of the oscilloscope. The resulting Lissajous's figures could then be viewed and formed into a perfect circle by adjusting the value of the Sullivan and Griffiths precision variable air capacitor (C_{SG}). It was found that the accuracy of measurement could be significantly improved if the capacitor (C_{SG}) was fixed and any frequency differences were measured by a frequency counter (Venner Electronics Limited, type T5A 6636/2M). The frequency counter method was generally used in this work.

The precaution was taken of housing the 12V d.c. power supply for the V.F.O. and 100kHz oscillator in a separate container, to eliminate any heating effects that the power transformer may have upon the frequency of operation of the two oscillators.

2.07 Measurement of Static Dielectric Permittivities using Dielectric Cell B

It is convenient to denote the measured capacitances of the dielectric cell when filled with air, a standard dielectric and the material under test by C_{AIR}, C_S and C_X, respectively. The static permittivities of the standard and material under test may be represented by ε_S and ε_X respectively. If the capacitor used had no stray capacitance, C_{AIR}, C_S and C_X would be in the ratio $1:\varepsilon_S:\varepsilon_X$. However, for a real capacitor, which is associated with various stray capacitances, this will not be the case. But, since these stray capacitances, ΔC, can usually be assumed to be constant, it follows that

$$\frac{(C_S - \Delta C) - (C_{AIR} - \Delta C)}{(C_X - \Delta C) - (C_{AIR} - \Delta C)} = \frac{C_S - C_{AIR}}{C_X - C_{AIR}} = \frac{\varepsilon_S - 1}{\varepsilon_X - 1} \qquad (2.4)$$

and hence

$$\varepsilon_X = 1 + \left[\frac{C_X - C_{AIR}}{C_S - C_{AIR}}\right] (\varepsilon_S - 1) \qquad (2.5)$$

If the frequency of operation of the V.F.O. is matched to that of the reference (100kHz) crystal oscillator by adjusting the precision variable air capacitor, the readings (C_{AIR}, C_S and C_X) taken from this capacitor may be substituted into equation(2.5) to give the static dielectric permittivity, ε_X, of the unknown. However, since the square of the reciprocal frequency of the V.F.O. is proportional to the values of capacitance, the respective frequency terms may be substituted into equation (2.5) to give

$$\varepsilon_X = 1 + \left[\frac{1/f_X^2 - 1/f_{AIR}^2}{1/f_S^2 - 1/f_{AIR}^2}\right] (\varepsilon_S - 1) \qquad (2.6)$$

This method was generally employed for the measurement of dielectric permittivity since frequency differences could be measured more accurately than could differences in the electrical capacitance of the sample cell.

2.08 Kerr Effect Apparatus

A diagram of the apparatus used to measure the electrically induced phase difference, δ, is shown in Figure 2.06. A parallel plane-polarized beam of monochromatic light is passed through the Kerr cell such that the plane of polarization of the light is at an angle of 45^o relative to the direction of the applied pulsed electric field, E. In the presence of this electric field the light leaving the cell is generally elliptically polarized. After passing through a quarter-wave retarder (de Senarmont compensator) orientated with its principal optical axis at 45^o to the direction of the applied electric field, the light can be nulled by rotating the analyser. The angular

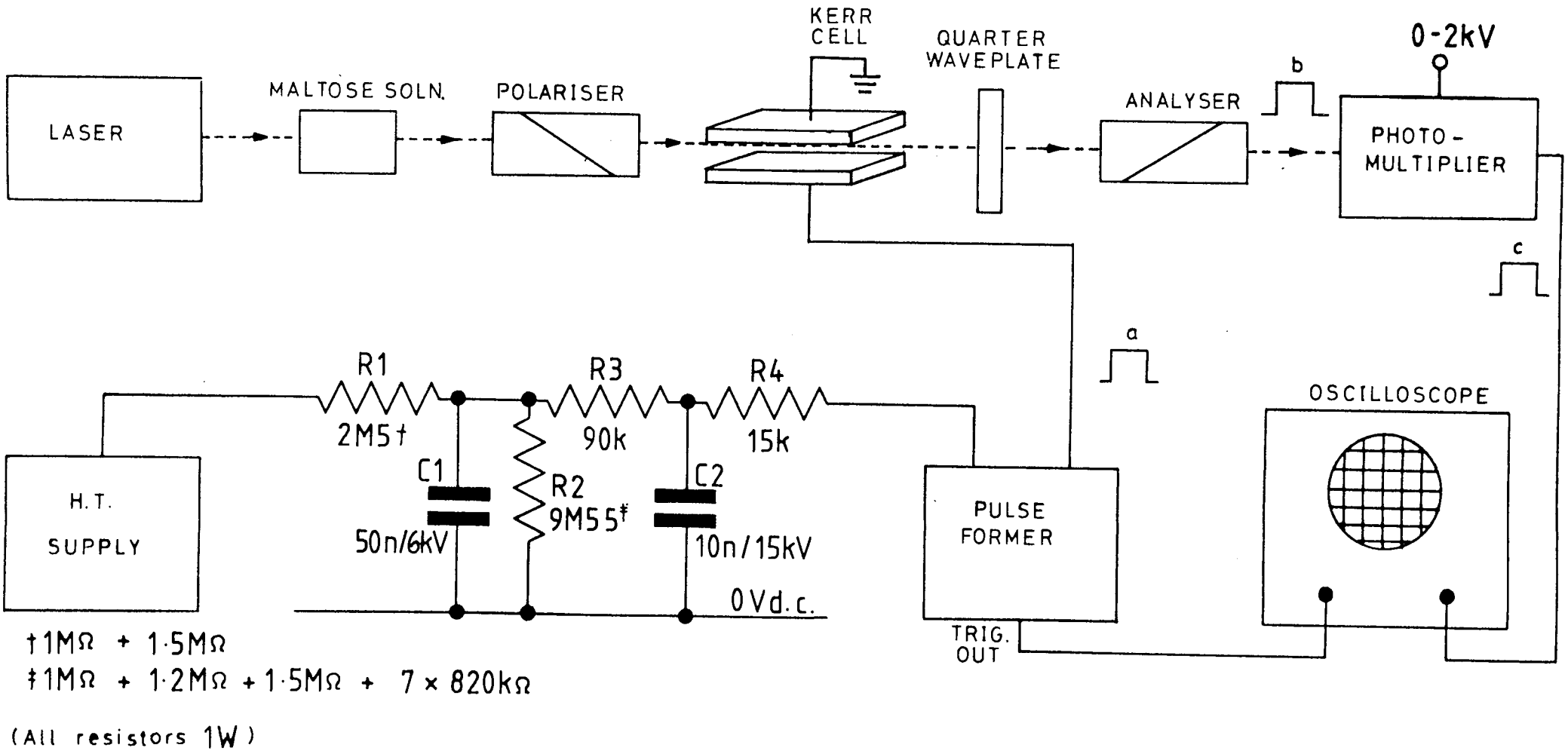

Figure 2.06 Apparatus used to measure the electrically induced phase difference, δ.

difference, α, between the principal planes of the polarizer and the analyser is equal to $\delta/4$ provided that the electric field is applied as a rectangular pulse (Cf $\delta/2$ if a d.c. electric field is used). Further details of the optical theory of the Kerr effect are given in Appendix 1.

The light source was a 2.6m W helium-neon laser (Scientifica and Cook, model SLH/2) emitting at a wavelength of 632.8nm. The plane of polarization of the light emitted from the laser was horizontal. To obtain maximum sensitivity the plane of polarization was rotated to an angle of 45^{o} relative to the applied electric field by passing the light through an optically active sugar solution. The sugar chosen was maltose, which has a large specific rotation $(122.9^{o})^{128}$ at 632.8nm. Specific rotation, $[\alpha]^{293K}_{632.8}$, at 293K and 632.8nm is given by[129]

$$[\alpha]^{293}_{632.8} = \frac{\text{observed rotation (degrees)}}{\text{path length(dm) x concentration(gcm}^{-3})} \qquad (2.7)$$

Thus, the concentration required in a 10cm quartz cell to produce the rotation of 45^{o} was found to be $0.3662 gcm^{-3}$. A few drops of formaldehyde solution were also added to deter bacterial growth.

The degree of polarization of the light entering the Kerr cell was improved by passing the beam through a high quality polarizer. Both the polarizer and analyser were Glan-type prisms (Ealing Beck Ltd) mounted in brass tubes. The analyser could be rotated by means of a series of gears connected to a graduated disc which allowed rotations as small as 0.005 degrees to be read with an accuracy of 0.002 degrees. The quarter wave retarder was of mica (F. Wiggins and Sons Ltd) mounted between glass discs and cleaved for use at 632.8nm.

Changes in levels of light were detected by a photomultiplier. The output of the photomultiplier was connected to an oscilloscope (Tektronix Inc, type 465B) thus enabling the electrically-induced optical pulse to be effectively displayed. The electrical configuration

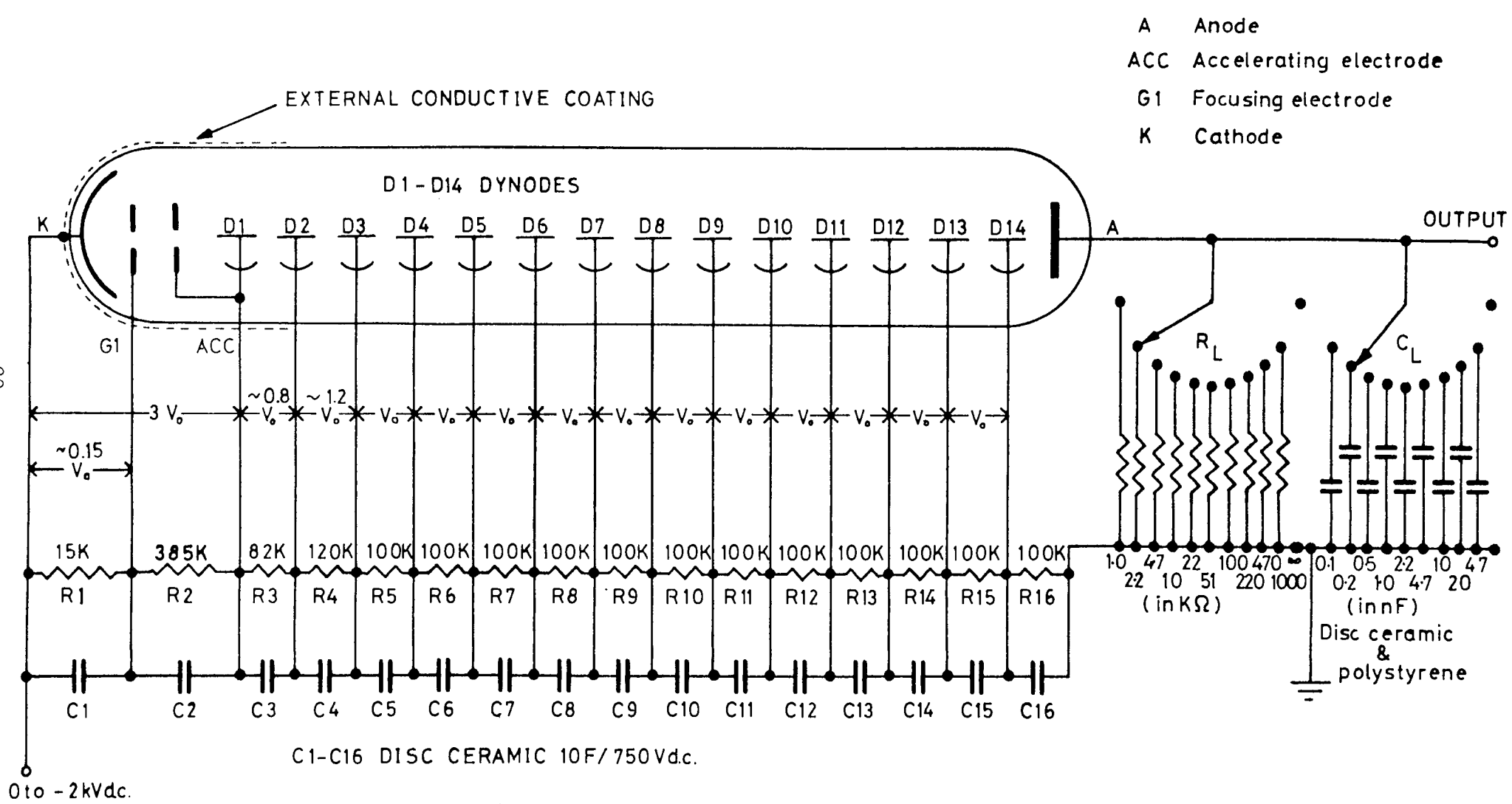

Figure 2.07 Electrical configuration of the electrodes of the photomultiplier tube.

of the electrodes of the photomultiplier tube (E.M.I. 9816B) is shown in Figure 2.07 and is recommended by the manufacturer for high gain usage. A quanta of light impinging upon the semi-transparent caesium-antimony photocathode, k, causes the emission of an electron. After being focused and accelerated this electron gives rise to an avalanche of electrons along the dynode chain, d1 - d14. The resulting electrical photo-induced current is collected at the anode, a. The extent of the gain and/or smoothing of the output from the photomultiplier tube may be adjusted by changing the values of R_L and/or C_L, respectively. A Brandenberg model 472R power pack was used to supply the high tension voltage which was continuously variable in the range 0-2kV.

2.09 High Voltage Pulse Former

The circuit diagram of the high voltage pulse former is shown in Figure 2.08. A relaxation oscillator based on a unijunction transistor (2N2646) and timing components R1, RV1 and C1 provides a narrow negative going exponential pulse at the trigger input pin (2) of IC1, a monostable (7555). The duration of the rectangular pulse output from IC1 is determined by the product of R_A and C2. The leading edge of this pulse triggers IC2, the first time-delay monostable, whilst the trailing edge of the same pulse triggers the second time-delay formed by monostable IC3. Upon triggering IC2 the output pin (3) goes high, switching on transistor Q3 and allowing current to flow through coil L1. The induced magnetic field closes the read switch (RS1) thereby applying a high voltage across the Kerr cell. When the monostable IC3 is triggered its output pin (3) goes high, switching on transistor Q4, allowing current to pass through coil L2, which in turn closes read switch RS2. The high-voltage electrode of the Kerr cell is then crowbarred to ground. The timing diagram of the clock and three monostables is shown in Figure 2.09.

Figure 2.08 Circuit diagram of the high voltage pulse former.

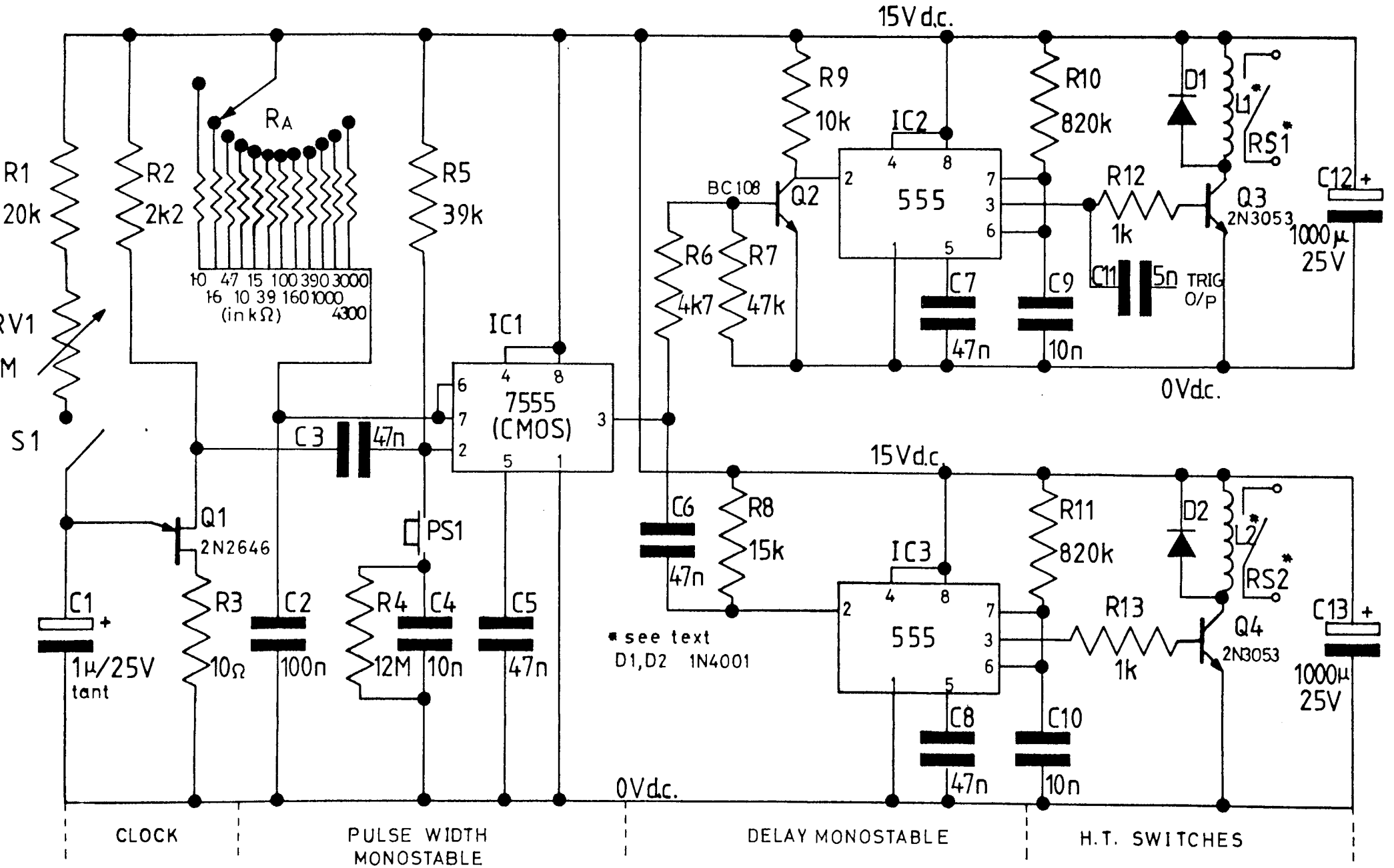

Parts List for Circuit Shown in Figure 2.08

Resistors

R1 220kΩ

R2 2.2kΩ

R3 10Ω

R4 12MΩ

R5 39kΩ

R6 4.7kΩ

R7 47kΩ

R8 15kΩ

R9 10kΩ

R10 820kΩ

R11 820kΩ

R12 1.0kΩ

R13 1.0kΩ

RV1 1MΩ potentiometer

R_A Twelve switched values:-

1.0kΩ

1.6kΩ

4.7kΩ

10kΩ

15kΩ

39kΩ

100kΩ

160kΩ

390kΩ

1.0MΩ

3.0MΩ

4.3MΩ

Capacitors

C1 1μF/25V tantalum

C2 0.1μF disc ceramic

C3 0.047μF disc ceramic

C4 0.01μF disc ceramic

C5 0.047μF disc ceramic

C6 0.047μF disc ceramic

C7 0.047μF disc ceramic

C8 0.047μF disc ceramic

C9 0.01μF disc ceramic

C10 0.01μF disc ceramic

C11 0.005μF disc ceramic

C12 1000μF/25V electrolytic

C13 1000μF/25V electrolytic

Semiconductors

Q1 2N2646

Q2 BC108

Q3, Q4 2N3053

D1, D2 1N4001

IC1 7555CMOS

IC2, IC3 555

Switches

PS1 Press switch

RS1, RS2, DTA 812 (FR Electronics)

10kV read switches, normally open, tungsten contacts

Inductances

L1, L2 90-130 ampere turns wound on P.T.F.E. former.

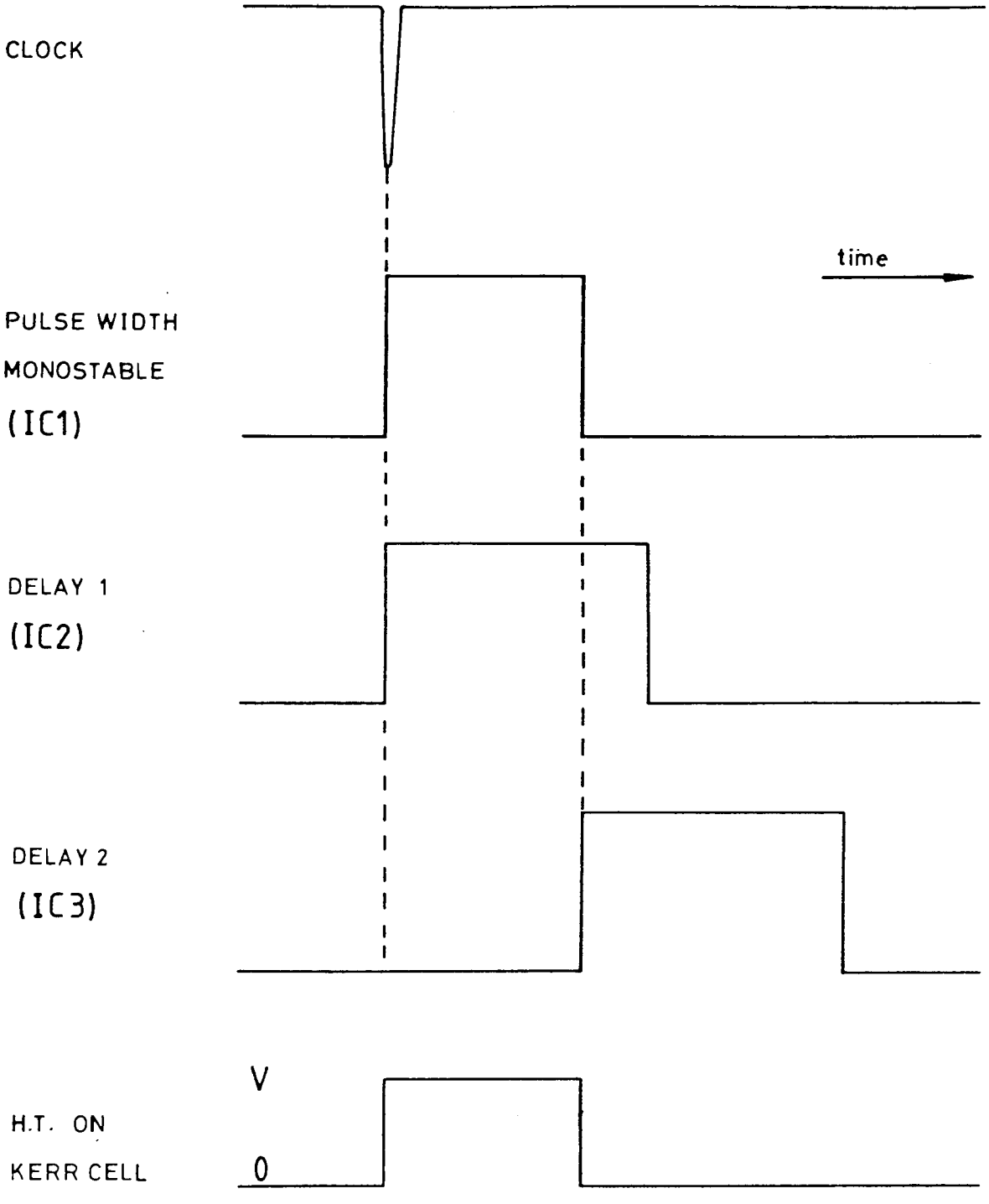

Figure 2.09 Timing diagram of the clock and three monostables in the high voltage pulse former.

The high voltage pulse former may also be used in a 'one-shot' mode by opening switch S1 and thus disconnecting the clock. The pulse width monostable IC1 is then triggered manually by means of press switch PS1 which triggers IC1 by grounding its input pin (2).

2.10 Small Sample Volume Kerr Cell (Kerr Cell A)

A diagram of the small sample volume Kerr cell is shown in Figure 2.10. The body of the cell was fabricated by milling a rectangular channel through one face of a solid stainless steel cuboid. The two electrodes, also of stainless steel, are positioned in this channel. The high-voltage electrode is isolated from the body of the cell by two pieces of glass covering the bottom and one side wall of the channel. The earthed electrode makes electrical contact with the cell body by means of two stainless steel ball bearings housed in the electrodes which may be pressed firmly into contact with the inner wall of the cell by screwing down two Allen-key grub screws. This locking mechanism also serves to keep the electrode assembly rigid. The electrode gap is set by four glass spacers, which fit into opposite holes drilled in the two electrodes. The depth of the holes in the high-voltage electrode may be varied by adjusting four Allen-key grub screws and in this way the electrode gap may be varied. However, for much of the work the electrode gap was set at 1.35mm. The earthed electrode was dressed back 2mm along its upper edge to prevent arcing between the electrode gap above the liquid level. The high-voltage electrode was somewhat shorter than the earthed one to prevent arcing between the ends of the high-voltage electrode and the window assembly. The length of the high-voltage electrode (42mm) was taken as the effective optical path length between the electrodes. The stainless steel window seating rings were fastened to the cell body using three screws and sealed with epoxy resin. The windows of the cell consisted of two optical quality quartz discs which were carefully selected for

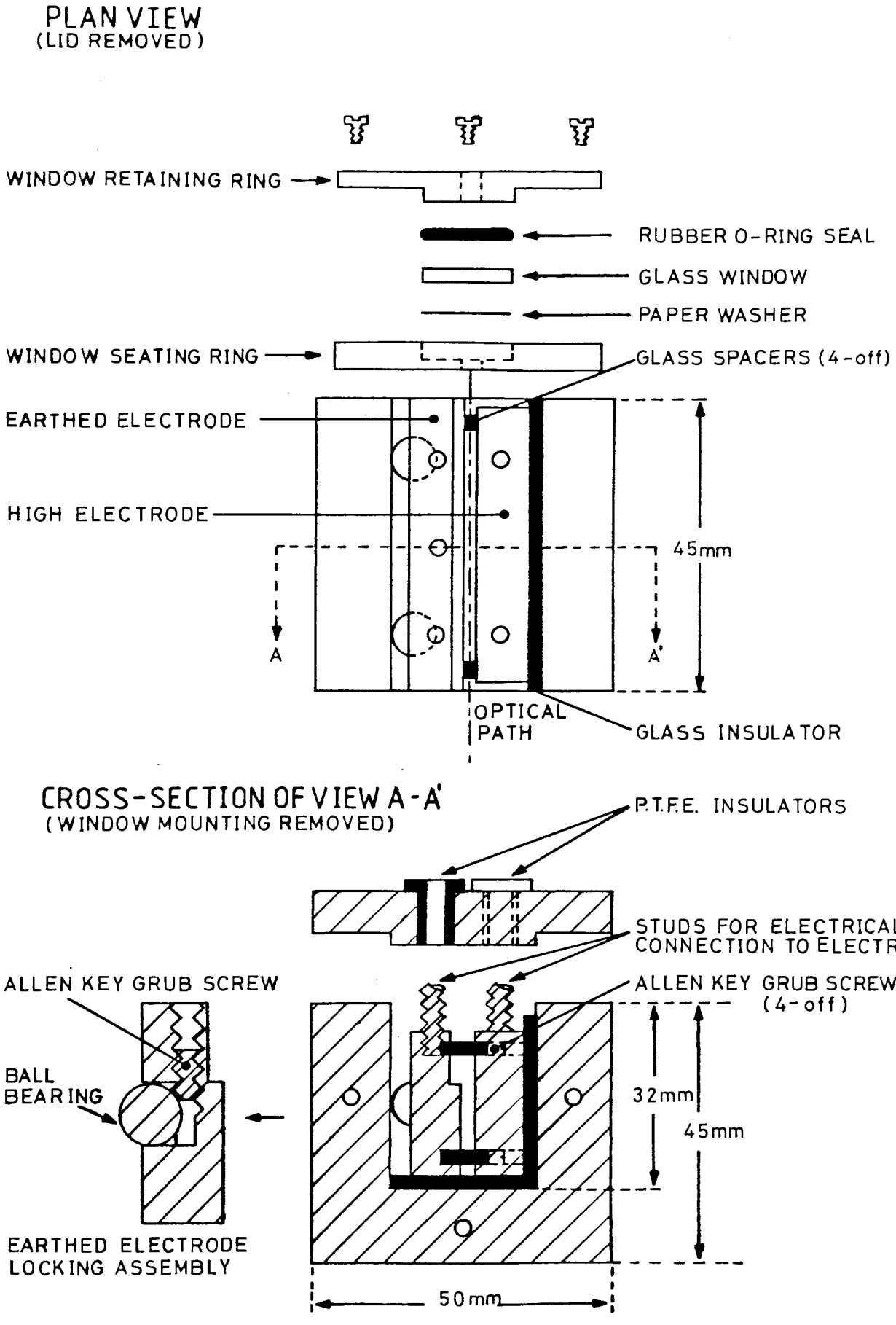

Figure 2.10 Diagram of the small sample volume Kerr cell.

their freedom from strain birefringence. Each window was secured to the cell by a stainless steel retaining ring and three screws. A leak-proof seal was achieved between each window and its mounting using paper washers. A rubber O-ring cushioned the seal of the retaining ring upon the window. The electrical connections to the electrodes passed through holes in the stainless steel lid of the cell and each hole was fitted with an electrically insulating P.T.F.E. sleeve. The temperature of the cell could be controlled to better than ±0.05K by means of a close fitting water-jacket (not shown in Figure 2.10) connected to a Churchill water pump-thermostat.

2.11 Large Sample Volume Kerr Cell (Kerr Cell B)

A cross-sectional diagram of the large sample volume (ca $25cm^3$) Kerr cell is shown in Figure 2.11. The design used in the construction of the Kerr cell resembles that used by other workers[130]. The cylindrical body of the cell and window mountings were made from brass, whilst the two electrodes were made from stainless steel. The cylindrical brass body was electro-plated with nickel (see next section). The lower electrode was semi-circular in cross-section and made electrical contact with the cell wall, which was earthed. The upper electrode, also semi-circular in cross-section, had a smaller radius than the lower electrode and was electrically insulated from the cell by means of a P.T.F.E. sleeve through which passed the high-voltage electrical connection. The central stainless steel screw also served to keep the electrode assembly rigid. The inter-electrode separation was 1.08mm and was set by means of two uniformly ground glass spacers. The length of the electrodes was 99mm and this was taken to be the effective optical path length between the electrodes. The windows of the cell consisted of two optical quality quartz discs

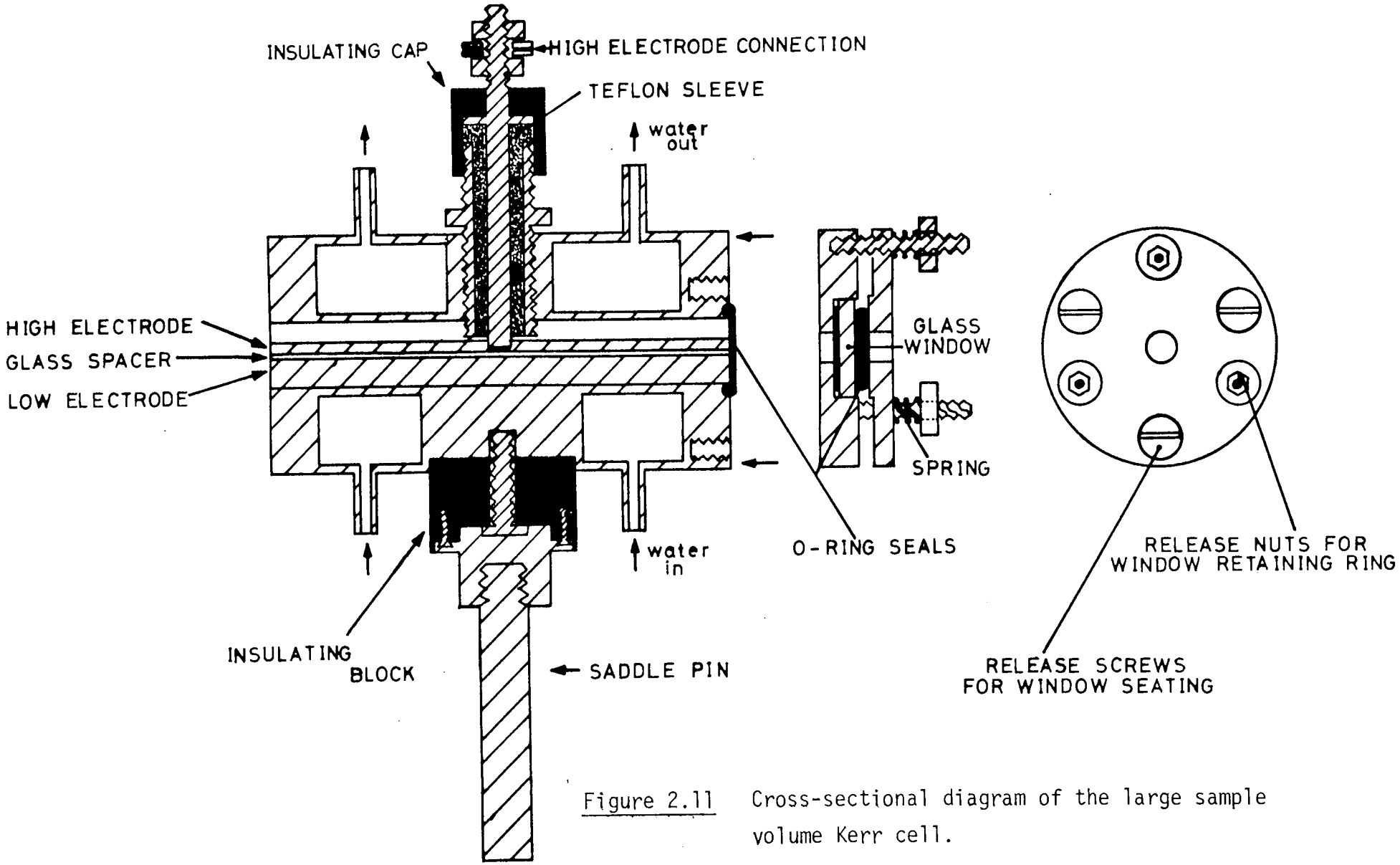

Figure 2.11 Cross-sectional diagram of the large sample volume Kerr cell.

which were carefully selected for their freedom from strain birefringence. Each window was secured between a window seating and a window retaining ring by three spring-loaded nuts. A leak-proof seal was achieved using washers cut from good quality paper. A rubber O-ring separated the window retaining ring from the glass window to minimize optical strain induced by the window mounting assembly. The complete window assembly was fastened to the body of the cell by three screws. A rubber O-ring was used to effect a liquid-tight seal between the window mounting assembly and the end faces of the Kerr cell. A Wallis (Worthing)model S103/3 power pack was used to supply the high tension voltage, which was continuously variable in the range 0-10kV. The voltage applied to the Kerr cell was measured on a $3\frac{1}{2}$ digit Keithley model 616 electrometer. The temperature of the cell could be controlled to better than ± 0.05K by means of the close fitting water-jacket and a Churchill water pump-thermostat.

2.12 Electro-Plating of Kerr Cell B

In order to minimise any possible chemical reactions between samples and the walls of the cell it was decided to coat the wall with nickel. The cylindrical brass body of the large sample volume Kerr cell was plated with nickel using an 'electroless' (chemical reduction) method. The cell was first cleaned by dipping in:-

a) Caustic bath (pH ~ 10) for 10 minutes and passing a current of 2.5A.

b) Washed with water followed by dilute sulphuric acid.

c) Concentrated sulphuric acid.

d) Washed with dilute sulphuric acid followed by water.

e) Cyanide bath (pH ~ 10) for 10 minutes passing a current of 2.5A.

f) Washed with water followed by dilute sulphuric acid.

g) Concentrated sulphuric acid.

h) Washed with dilute sulphuric acid followed by water.

It was then plated for 5 minutes with Watt's nickel passing a current of 2.5mA, and kept in hot water until entering the plating solution which was at 363K.

The plating solution was made up from concentrates obtained from Canning Ltd, Birmingham. Nifoss 80 solution (41) was made up by mixing the 'base' solution N21311 ($100cm^3l^{-1}$) with the 'initial' solution N21312 ($250cm^3l^{-1}$) and making up with distilled water.

2.13 Measurement of Absolute Kerr Constants

The equation which defines the experimentally determined Kerr constant, B, is[36]:-

$$B = \frac{\delta}{2\pi l(V/d)^2} \qquad (2.8)$$

where:-

δ = Electrically induced phase difference between the components of light parallel and perpendicular to the applied electric field, E,

L = Optical path length between the electrodes,

V = Applied voltage

and d = Electrode separation.

For the pulsed electric field method of measuring the Kerr effect the rotation of the plane of polarization, α, is related to the phase difference by

$$\alpha = \frac{\delta}{4} \qquad (2.9)$$

This may be substituted into equation (2.8) and rearranged to give

$$\alpha = \frac{\pi l (V/d)^2 B}{2} \qquad (2.10)$$

Thus, a plot of α against V^2 should give a straight line passing through the origin with a gradient of $(\pi l B)/2d^2$, thereby permitting the experimental value of B to be determined. If straight line plots are obtained using equation (2.10), then the Kerr law is obeyed (i.e. $\alpha : E^2$).

In practice the absolute rotation, α, was not normally measured or plotted. Instead a directly proportional quantity, α^1, was obtained from an arbitrarely calibrated dial. The rotation α is related to α^1 by a constant factor governed by the ratios of the gears used to rotate the analyser and by an additional conversion factor required to change from degrees to radians. Thus, the true angular rotation, α, of the plane of polarization of the light is given by

$$\alpha = 0.9 \times 0.0174532 \times \alpha^1 \qquad (2.11)$$

2.14 Measurement of Relative Kerr Constants

The vast majority of the Kerr effect measurements were not conducted by the absolute method described previously. Instead, the graph of α^1 against V^2 was plotted for the unknown and the gradient, m_X, found. The cell was then calibrated with a liquid of known Kerr constant, B_S. The graph of α^1 against V^2 for the standard liquid gave a gradient, m_S. The Kerr constant, B_X, of the unknown liquid could then be simply found using equation (2.12).

$$B_X = \frac{m_X}{m_S} \times B_S \qquad (2.12)$$

The standard liquid used was normally toluene ($B = 0.81 \times 10^{-14} mV^{-2}$)[131].

CHAPTER 3

SYNTHESIS AND CHARACTERISATION OF MATERIALS

3.01 Introduction

Two of the earliest workers to prepare cyclic siloxane oligomers were Kipping and Robinson[132]. Their original intention was to obtain $R_2Si = O$ groups analogous to $R_2C = O$ structures in organic chemistry. These $R_2Si = O$ compounds were to be called silicones corresponding to conventional ketones. However, instead of obtaining $(C_6H_5)_2 Si = O$ from hydrolysis of dichlorodiphenylsilane, Kipping and Robinson found mainly cyclic and linear low molecular weight polymer products. A cyclic trimer, hexaphenylcyclotrisiloxane, and a cyclic tetramer, octaphenylcyclotetrasiloxane, were isolated and their melting points recorded.

Similar cyclic structures resulting from the hydrolysis of dialkyl dichlorosilane were reported by Hyde and Delong[133] in work which was originally planned to determine the effects of the introduction of organic radicals into silicate structures of a vitreous nature. From the hydrolysis of dichlorodiethylsilane, a cyclic trimer was isolated. Similarly, from dichlorodimethylsilane a corresponding trimer in an impure state was obtained.

The first workers to prepare the cyclic dimethylsiloxane oligomers in a highly purified form were Hunter et al[134]. In 1946 they prepared and characterised cyclic dimethyl siloxanes of three to eight repeat units by depolymerization of the higher molecular weight linear polymer.

At the same time, though independently, Patnode and Wilcock[135] prepared cyclic dimethyl siloxanes of three to nine repeat units by hydrolysis of dimethyldichlorosilane in various solvents. The linear trimethyl-terminated dimethyl siloxane oligomers were also synthesised by catalytic rearrangement of a mixture of the cyclic species and separated by vacuum distillation.

In 1965, Brown and Slusarczuk[136] demonstrated that ring-chain equilibriates of poly(dimethyl siloxane) may contain a range of cyclic molecules $[(CH_3)_2SiO]_x$ with values of x from 3 to $x > 200$. However, it was not until 1977 that Semlyen[45] first separated narrow molecular weight fractions of these cyclic dimethyl siloxanes for x upto 225, together with the linear polymers of equivalent chain length. These poly(dimethyl siloxane) fractions were the first high molecular weight synthetic cyclic polymers to be fully characterised and to have various physical properties (e.g. viscosity, light scattering, low-angle neutron scattering, photon correlation spectroscopy) compared with those of the equivalent open chains.

In addition to work on the siloxanes investigations have also been conducted by the author into the dependence of the tacticity of poly (N-vinyl carbazole) (P.V.K.) on the mode of synthesis. The monomer N-vinyl carbazole was first synthesised[137] in 1924, but the commercialisation awaited Reppe's development in 1935 of an industrial process for the vinylation of carbazole with acetylene at elevated temperatures and pressures[138]. Stimulated by the availability of this monomer a German company commenced the production of a vinyl carbazole polymer called Luvican[139].

Initially, scientific investigations of P.V.K. focused upon its interesting and useful dielectric properties. Indeed one of the first

large scale uses of P.V.K. was as a replacement for mica in capacitors. More recently, however, P.V.K. has been the subject of great interest because it possesses unusual conductive and photoconductive properties when doped with small amounts of electron-acceptor molecules such as 2, 4, 7 - trinitrofluorenone. Hoegl et at[23] first reported the photoconductive properties of P.V.K. and pointed out its possible application in electro-photography. The commerical use of doped P.V.K. in photocopying devices is now well established.

A complete understanding of the electronic properties of this material depends upon a knowledge of the interactions between the π electron systems of the large carbazole pendant groups. The intra and interchain π system interactions are in turn dependent on the chain tacticity and conformation and on the degree of ordering of the chain. There has, therefore, been interest in the structure of P.V.K. and the possibility of influencing its tacticity by changing the synthetic route. Though still in dispute, it now appears that synthetic procedure can effect the tacticity of the resulting polymer. The extent of stereoregularity may be determined by nuclear magnetic resonance spectroscopy[140-142].

In this chapter the methods used for the preparation of cyclic and linear dimethyl siloxane oligomers and poly(dimethyl siloxanes) are described, together with their characterisation using gas-liquid chromatography. Later chapters will describe how these cyclic and linear products were used in a comparative study of their dielectric properties. Three different synthetic methods used to prepare poly (N-vinyl carbazole) are also described, as well as the use of carbon-13 nuclear magnetic resonance to determine the tacticities of the individual products. The P.V.K. samples were used in a study of their dielectric and electro-optical properties.

3.02 Synthesis of Cylic Dimethyl Siloxane Oligomers

Cyclic dimethyl siloxane oligomers were prepared by a carefully controlled hyrolysis of dimethyldichlorosilane[135]. The procedure was as follows:-

A solution of dimethyldichlorosilane ($100cm^3$) in diethyl ether ($200cm^3$), in a dropping funnel, was slowly added with stirring, to $200cm^3$ of distilled water in a 1 litre beaker. Small pieces of ice were added from time-to-time to maintain a temperature in the range 283-293K. The aqueous layer was separated and eventually discarded. The organic layer was washed with distilled water, followed by a saturated solution of sodium bicarbonate, washed once more with water and then finally dried by standing over a molecular sieve (grade 3A). The total yield of the organic layer was approximately quantitative. The most volatile cyclics were removed by distilling the hydrolyzate at atmospheric pressure to yield distillate A. The remaining oily residue was subjected to pyrolysis to further increase the yield of low molecular weight cyclics.

The pyrolysis (a thermally-induced molecular rearrangement) was carried out using the apparatus shown in Figure 3.01. The involatile siloxane mixture placed in a round-bottomed flask ($100cm^3$), was heated electrically by means of wire-wrapped beakers connected to a variac. The temperature, indicated by a thermometer placed close to the wall of the flask, was increased slowly to 553K. When this temperature was attained it was observed that a high proportion of the involatile mixture could be converted into volatile cyclic siloxanes to give a distillate B. The remaining siloxane, probably highly crosslinked polymer, was discarded.

Distillates A and B were combined and fractionally distilled.

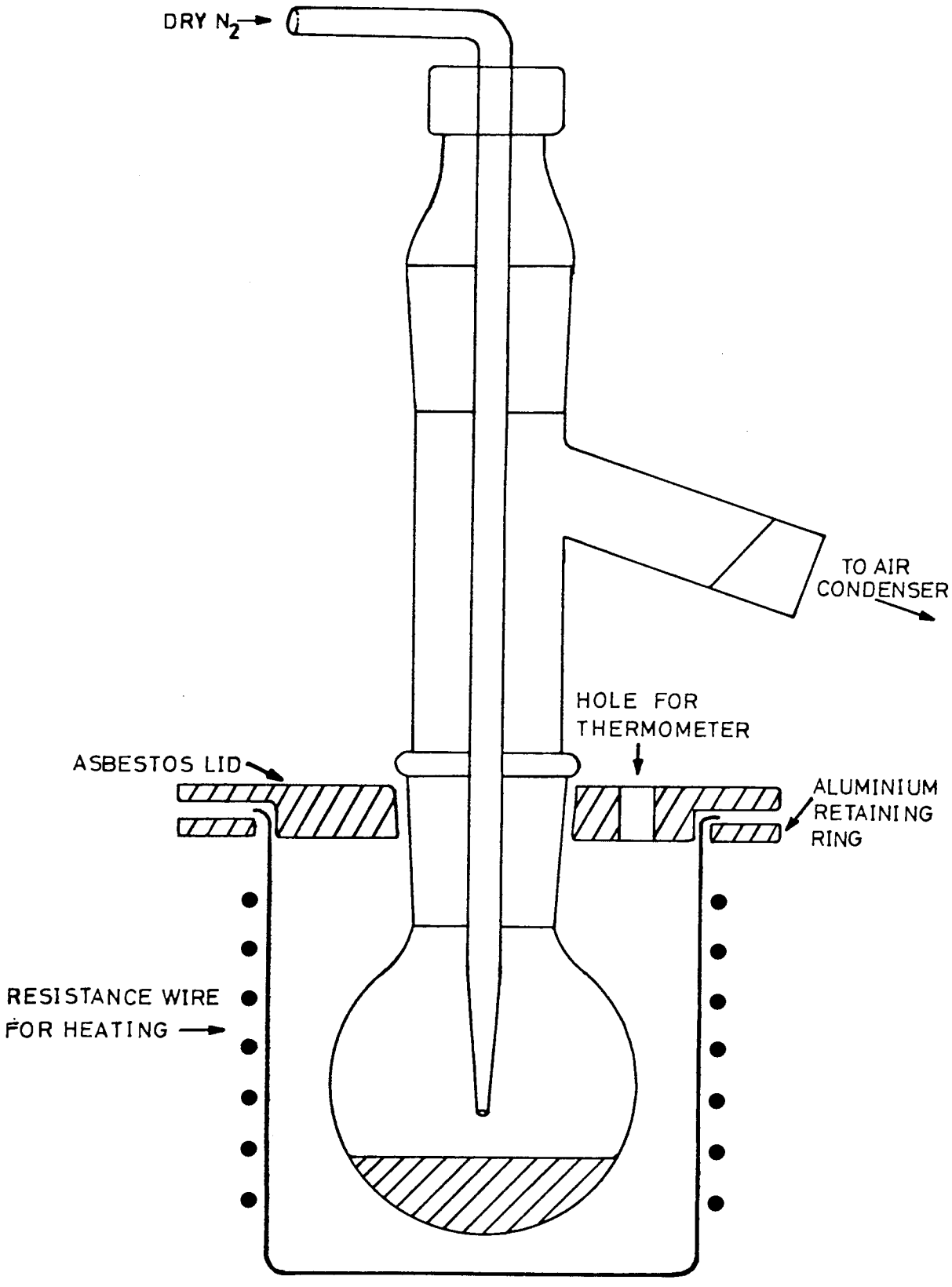

Figure 3.01 Pyrolysis apparatus

The Pyrex distillation column (approx. 280 x 30mm) was packed with single-turn glass helices and enclosed in an electrically-heated jacket. For cyclic dimethyl siloxanes with n = 12 and n = 14 backbone bonds (n) it was necessary to distil under reduced pressure (~10mmHg) using a rotary vacuum pump. Difficulties were experienced in obtaining pure high-boiling fractions, even under reduced pressure, since the cyclic tetramer was readily formed as a consequence of the thermal rearrangement of higher molecular weight cyclic oligomers. No distillation temperatures were recorded since the rate of through-put of the distillate was too slow to allow reliable readings to be taken.

3.03 Synthesis of Hexamethyldisiloxane

A quantity (200cm^3) of distilled water was placed in a three-necked flask equipped with a stirrer and an outlet port (for HCl). The inlet port was fitted with a dropping funnel containing trimethylchlorosilane (200cm^3). The silane was slowly added to the water with constant stirring. The temperature of the hydrolyzate was maintained at approximately room temperature by means of a large beaker of chilled water. The reaction mixture was then refluxed for about 30 minutes, cooled and transfered to a separating funnel. The lower, faint yellow, aqueous layer was discarded. The upper, water-white, organic layer was washed twice with a solution of sodium bicarbonate, followed by distilled water and was then dried over anhydrous calcium chloride. The product was then distilled through a Pyrex column (approx. 280 x 30mm) of single-turn glass helices and one fraction was collected at 372-373K (1 atmosphere). This fraction was analysed by gas-liquid chromatography and a single peak was observed. The purity was estimated to be greater than 99%.

3.04 Synthesis of Linear Dimethyl Siloxane Oligomers

Low molecular weight linear dimethyl siloxane oligomers terminated with trimethyl silyl groups were prepared by an acid catalysed ring-opening reaction of a mixture of cyclic dimethyl siloxanes with hexamethlydisiloxane[135]. The procedure was as follows:-

A mixture of hexamethyldisiloxane (200g) and cyclic tetramer (91.3g)(containing a small amount of other cyclic siloxanes), was shaken in a 500cm^3 round-bottomed flask with concentrated hydrochloric acid (12.5cm^3) for four hours at room temperature. Distilled water (30cm^3) was then added whilst shaking and the two-phase system allowed to stand. The lower aqueous layer was separated and discarded. The upper organic layer was washed twice with distilled water (30cm^3) and dried overnight using a molecular sieve (grade 3A). The filtered product was then fractionally distilled using the techniques previously described for the cyclic oligomers.

3.05 Packing of Columns for Gas-Liquid Chromatography

The presence of hydroxyl groups on the solid chromatographic support, which should ideally be totally inert, has been shown[143,144] to inhibit both speed and efficiency of the column and to cause band spreading. A quantity of chromosorb P (acid washed, mesh 60/80) was treated to convert surface active -OH groups to -OSi$(CH_3)_3$ groups, using the method of Bohemen et al[145]. The procedure was as follows:-

Chromosorb P (40g) was refluxed for one hour with hexamethyldi-siloxane (24cm^3) in a round-bottomed flask fitted with a condenser and a drying tube of calcium sulphate. A quantity (2cm^3) of n-propanol was then added to help wetting. (Although this material reacts with unchanged hexamethlydisiloxane to form $Si(CH_3)_3OPr$, this in turn reacts

with hydroxyl groups in the same way as the parent silazane. The mixture was left to stand overnight and then refluxed for a futher two hours. The treated chromosorb P was washed twice with 60-80 petroleum ether ($50cm^3$) andonce with n-propanol ($50cm^3$), followed by 60-80 petroleum ether ($50cm^3$). Finally, the treated material was dried on a steam-bath under nitrogen gas.

The silanolated chromosorb P was coated with 6% by weight of a high molecular weight silicone gum (E30, Jones Chromatography Ltd). The gum was dissolved in sufficient diethyl ether to cover the chromosorb P and the solvent was then removed by rotary evaporation. A length of glass column (180cm, I.D. 4mm, O.D. 6mm) was packed with the coated support and installed in a Pye chromatography (series 104).

3.06 Characterisation of Dimethyl Siloxane Oligomers using Gas-Liquid Chromatography

The purity of fractions of cyclic and linear dimethyl siloxane oligomers was determined using a Pye chromatography fitted with a Katharometer detector. Samples were injected either as 10% w/v solutions in toluene or as pure liquids. The operating conditions of the instrument were normally as follows:-

Oven temperature	= 413K
Detector oven temperature	= 433K
Katharometer current	= 75mA
Carrier gas (O_2 free N_2) flow speed	= $60cm^3min^{-1}$

Representative G.L.C. traces for cyclic and linear dimethyl siloxane oligomers are compared in Figure 3.02. These were produced by injecting 8µl sample volumes of pure liquids and employing the above chromatograph operating conditions. The retention times taken from

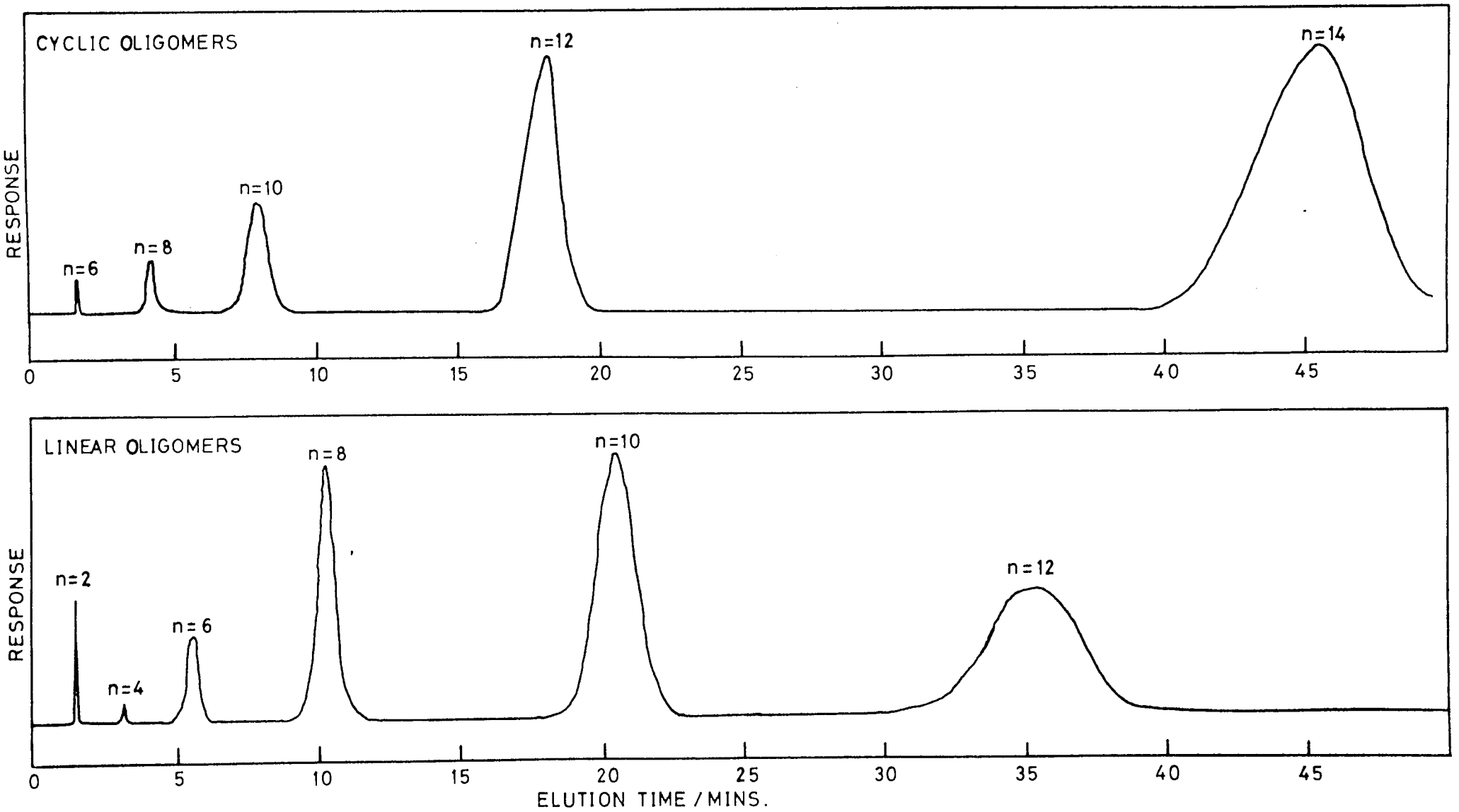

Figure 3.02 Comparison of gas-liquid chromatograms for cyclic and linear dimethyl siloxane oligomers.

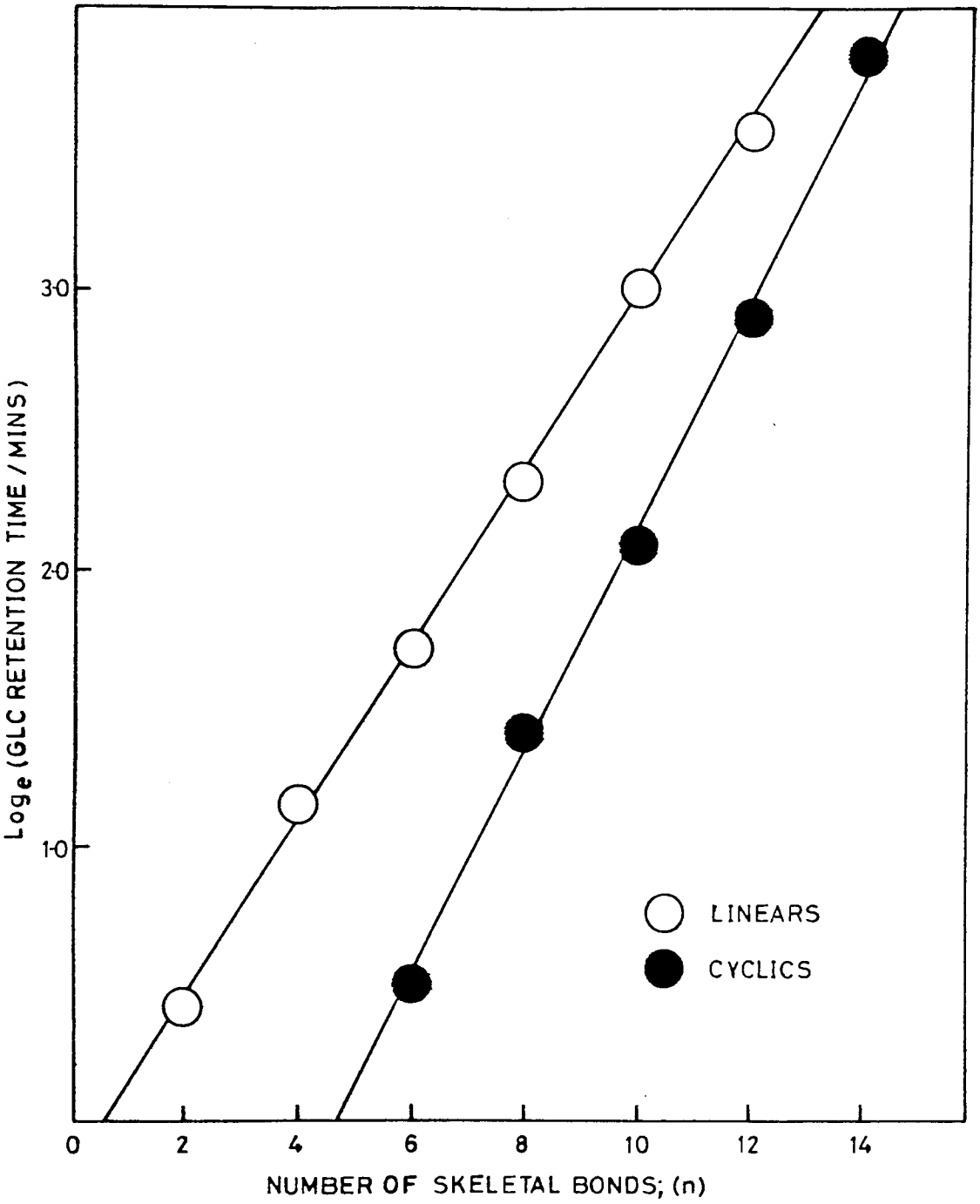

Figure 3.03 Log_e (G.L.C. retention times) of cyclic dimethyl siloxanes (●) and linear dimethyl siloxanes (○).

these traces for cyclic and linear oligomers containing n skeletal bonds are plotted in Figure 3.03. The retention times, T, were found to be reproducible to within ±1.0%. The best straight line through the experimental data was obtained using the method of least-mean squares. The equations for the lines were found to be

$$\ln T = 0.316n - 0.174 \qquad (3.1)$$

for the linear siloxanes, and

$$\ln T = 0.403n - 1.894 \qquad (3.2)$$

for the cyclic siloxanes. These straight lines reflected the typical behaviour of homologous series.

Mixtures of cyclic oligomers prepared according to the methods described above were analysed by G.L.C. and found to contain the proportions given in Table 3.01. The constitution of the distilled and pyrolyzed fractions, corresponding to distillates A and B respectively, are also indicated, together with literature[135] values of these proportions. The rather large differences between the literature values and those found in this study for the composition of distillate B are thought to be due to the pyrolysis being conducted at a lower temperature, 553K, in this work, compared with 623K to 673K in the reference quoted. Table 3.02 lists the percentage composition of a number of fractions of cyclic oligomers obtained by fractional distillation of the mixture of distillate A and distillate B. Sample 3 was used in the preparation of siloxane chains.

The percentage composition of the reaction mixture containing linear dimethyl siloxanes is shown in Table 3.03. The composition of individual fractions of linear dimethyl siloxanes are given in Table 3.04.

Table 3.01 Composition of distillates A and B obtained from hydrolysis of dimethyldichlorosilane in the preparation of cyclic dimethyl siloxane oligomers.

Number of Bonds, n	Distillate A (%)		Distillate B (%)		Total (%)
	Found	Lit.[135]	Found.	Lit.[135]	
6	0.0	1.0	1.2	44.0	0.3
8	91.6	82.0	77.0	24.0	88.8
10	10.1	12.0	7.0	9.0	9.4
12	0.9	3.0	2.7	10.0	1.3
>14	0.3	2.0	1.6	13.0	0.6

Table 3.02 Composition of fractions of cyclic oligomers resulting from fractional distillation of the combined distillates A and B.

Sample Number	Proportions of Cyclic Oligomers					Total Volume
	n = 6 (%)	n = 8 (%)	n = 10 (%)	n = 12 (%)	n = 14 (%)	
1	22.1	45.2	32.7			5
2		99+				280
3		95.4	4.6			88
4		5.0	95.0			12
5			99+			20
6		1.1	37.0	60.0	1.9	3
7			1.1	96.5	2.4	5
8					~55[a]	2

[a] Higher members not eluted from G.L.C.

Table 3.03 Composition of the purified product of the acid catalysed ring-opening reaction between cyclic dimethylsiloxanes and hexamethyldisiloxane in the preparation of linear dimethyl siloxane oligomers before fractional distillation.

Numbers of Bonds, n	Composition of Mixture (%)
Cyclic n = 10	0.7
Linear n = 2	26.5
Linear n = 4	19.6
Linear n = 6	14.5
Linear n = 8	9.4
Linear n = 10	10.9
Linear n = 12	4.0
Linear n = 14	14.4

Table 3.04 Composition of fractions of mainly linear oligomers obtained from the product of the acid catalysed ring-opening reaction.

Sample Number	Proportions of Linear Oligomers							Total Volume (cm^3)
	n = 2	n = 4	n = 6	n = 8	n = 10	n = 12	n = 10[a]	
1	93.2							40
2	99+							20
3	97.8	2.2						4
4	91.1	8.9						15
5		99+						45
6		92.3	3.8				3.9	10
7			90.7				9.3	12
8			97.2				2.8	10
9			99+					20
10			1.8	98.2				12
11				61.6	38.4			22
12				1.8	98.2			10
13					76.8	23.2		10
14					3.2	96.8		10
POT						~40[b]		45

[a] Cyclic oligomer

[b] Higher members not eluted from G.L.C.

3.07 Synthesis and Characterisation of High Molecular Weight Poly(Dimethyl Siloxane) Fractions

High molecular weight cyclic and linear poly(dimethyl siloxanes) were prepared and characterised by Dr J.A. Semlyen and his research group at the University of York, using methods described in detail elsewhere[45,46]. For the sake of completeness a brief summary of the preparative procedures will be given here.

The cyclic poly(dimethyl siloxanes) were prepared from the cyclic oligomers with n = 8 and n = 10 skeletal bonds by a ring-chain equilibrium reaction in solution in toluene at 383K, using a method similar to that recommended by Brown and Slusarczuk[136]. Cyclic oligomers with n = 6 to n = 12 were removed from the quenched equilibriate by fractional distillation under reduced pressure. The cyclics and linear high molecular weight polymer in the residue were separated by precipitating the linear polymer from a hot solution of the residue in acetone by allowing it to cool to room temperature and to stand for 24 hours. The supernatant solution containing the cyclic polymer was decanted from the linear polymer, and the acetone removed by distillation under reduced pressure. Cyclic polymer fractions were obtained from the residue by distillation and fractional precipitation. The fractions were purified by reprecipitation. They were dried and residual solvent was removed by heating the samples under vacuum.

High molecular weight fractions of linear poly(dimethyl siloxanes) were obtained by fractional distillation and precipitation of Dow Corning DC 200/10, DC 200/20 and DC 200/200 Dimethicone.

The dispersities of both the cyclic and linear fractions of poly(dimethyl siloxanes) were improved by the use of preparative gel permeation chromatography[46]. All fractions were characterised by analytical G.L.C. and/or G.P.C. to produce values for the average

molecular weights, $\bar{M}_w$ and $\bar{M}_n$, and hence the dispersity index, $\bar{M}_w/\bar{M}_n$.

3.08 Measurement of Densities

The densities of all the samples of cyclic and linear dimethyl siloxane oligomers and poly(dimethyl siloxanes) were measured by the research group of Dr Semlyen at the University of York, using instrumentation based at the University of Stathclyde. The density of each sample was measured at several different temperatures using an Anton Paar D.M. 610 densitimeter in conjunction with a D.M. 601 measuring cell. The temperature of the cell was maintained to within ±0.01K of the set temperature. The densities, ρ, at 298K, of the cyclic and linear dimethyl siloxanes are quoted in Tables 3.05 and 3.06, respectively, to five significant figures, together with the corresponding coefficients of volume expansion, β.

3.09 Preparation of Poly(N-Vinyl Carbazole)

Solutions of N-vinyl carbazole were polymerized using a variety of initiators in order to produce samples of polymers with different stereostructures. The polymerizations were performed in purpose built glass reaction vessels (approx. 250cm^3) fitted with gas-tight P.T.F.E./glass seals and Suba seals. All solvents were distilled, dried over alumina (Al_2O_3) and redistilled before use. The monomer (Fluka Ltd, purum grade) was used without futher purification. The concentration of monomer in all polymerizations was 0.5M (14.49g in 150cm of solvent).

a) Initiation by Aluminium Chloride

The monomer was placed in the reaction flask into which was distilled 130cm^3 of toluene under nitrogen. The monomer dissolved quickly upon shaking. The resulting solution was allowed to thermally equilibriate in a water-bath at 298K. The initiator, Aluminium

Table 3.05 Number-average number of backbone bonds, $\bar{n}$, heterogeneity indices $\bar{M}_w/\bar{M}_n$, densities ρ and temperature coefficients of volume expansion β for undiluted cyclic dimethyl siloxanes at 298K.

Fraction	$\bar{n}$	$\bar{M}_w/\bar{M}_n$	ρ $(/kgm^{-3})$	β $(X10^3/K^{-1})$
R1[a]	8.0	1.00	950.56	1.2023
R2[a]	10.0	1.00	953.47	1.1790[b]
R3[a]	12.0	1.00	962.87	1.0344
R4	14.7	1.05	967.76	0.9867
R5	19.7	1.07	972.98	0.9382
R6	23.8	1.05	974.19	0.9274
R7	31.2	1.03	973.57	0.9156
R8	35.0	1.02	973.06	0.9181
R9	38.2	1.02	972.96	0.9197
R10	44.0	1.02	973.02	0.9224
R11	109.0	1.03	971.46	0.9183
R12	190.0	1.04	971.67	0.9222

[a] Single component

[b] Ref. 146

Table 3.06 Number-average number of backbone bonds $\bar{n}$, heterogeneity indices $\bar{M}_w/\bar{M}_n$, densities ρ and temperature coefficients of volume expansion β for undiluted linear dimethyl siloxanes at 298K.

Fraction	$\bar{n}$	$\bar{M}_w/\bar{M}_n$	ρ ($/kgm^{-3}$)	β ($X10^3/K^{-1}$)
L1[a]	2.0	1.00	758.45[b]	1.3212[b]
L2[a]	4.0	1.00	815.36	1.2415
L3[a]	6.0	1.00	850.63	1.1659
L4[a]	8.0	1.00	872.08	1.1116
L5[a]	10.0	1.00	885.70	1.0807
L6[a]	12.0	1.00	899.40	1.0397
L7	16.5	1.02	915.29	1.0446
L8	21.7	1.01	928.31	1.0176
L9	24.4	1.01	933.77	1.0030
L10	32.4	1.01	941.96	0.9755
L11	41.6	1.01	949.44	0.9699
L12	105	1.20	958.99	0.9538
L13	206	1.17	966.08	0.9276

[a] Single component

[b] Ref. 146

Chloride (0.20g), which had been purified by subliming twice under vacuum was added to the monomer solution as a suspension in toluene ($20cm^3$). The concentration of the initiator was 0.5 mole-percent of the monomer concentration (≡ 0.0025M). The polymerization was allowed to proceed for 18.5 hours at 298K under nitrogen gas. For convenience this polymer sample will be subsequently referred to as sample S1.

b) Initiation by Boron Trifluoride Etherate

The monomer was placed in the reaction flask into which was distilled $150cm^3$ of toluene under nitrogen. The monomer dissolved quickly upon shaking. The resulting solution was allowed to thermally equilibriate in a water-bath at 298K. A quantity ($0.17cm^3$ ≡ 0.276g) of the initiator, boron trifluoride etherate, was then injected into the reaction flask through a Suba seal using a gas-tight syringe. The concentration of the initiator was 0.5 mole-percent of the monomer concentration (≡ 0.0025M). The polymerization was allowed to proceed for 18.5 hours at 298K under nitrogen gas. The polymer sample produced will be subsequently referred to as sample S2.

c) Initiation by Azobisisobutyronitrile

The monomer was placed in the reaction flask into which was distilled $140cm^3$ of benzene under nitrogen. The monomer dissolved quickly upon shaking. The flask was then evacuated and the solution degased several times. The evacuated flask containing the monomer solution was allowed to thermally equilibriate in a water-bath at 343K. A quantity (0.1232g) of the initiator, azobisisobutyronitrile, as a solution in benzene ($6.16cm^3$), was then injected into the reaction flask through a Suba seal. The concentration of the initiator was 1.0 mole-percent of the monomer concentration (≡ 0.005M). The polymerization

was allowed to proceed for 7 hours at 343K under vacuum. The polymer sample produced will be referred to as sample S3.

All the above polymerizations were terminated by pouring the reaction mixtures into excess methanol. The polymers were purified by repeated (at least three) precipitations, by adding a 1% w/v solution of the polymer in toluene dropwise into a large volume of stirred methanol.

A further sample of poly(N-vinyl carbazole), was also used in the studies presented in this thesis. This was obtained from Polymer Consultants Ltd, London and the method of polymerization was not quoted. This sample was purified by repeated precipitations, as above, and will be referred to as sample S4.

3.10 Fractional Precipitation of Poly(N-Vinyl Carbazole)

The polymer samples (S1-S4) prepared by the above methods had broad distributions of molecular weight, as judged by gel permeation chromatography. They were, therefore, fractionated to produce several samples of a narrower molecular weight distribution. The polymer samples were individually dissolved in tolulene (1% w/v) and sufficient methanol added to saturate the solution at 333K. The temperature, controlled by means of a water-bath, was decreased slowly by a few degrees until a reasonable amount of polymer had precipitated. The temperature was then kept constant for several hours whilst the flask was shaken occasionally in a vigorous manner to allow the solution and precipitate to attain thermodynamic equilibrium. The precipitate was then separated by decanting off the upper polymer solution and was purified by repeated dissolving and precipitating processes using toluene and methanol. Further fractions were produced at lower temperatures by repeating the above procedure with the remaining polymer

solution. The final fraction was obtained at approximately 273K.

3.11 Characterisation of Poly(N-Vinyl Carbazole) Fractions using Gel Permeation Chromatography and Low-Angle Laser Light-Scattering

The fractions of poly(N-vinyl carbazole) obtained by methods described previously were characterised in terms of number-average and weight-average polystyrene equivalent molecular weights, ${}_{ps}\bar{M}_n$ and ${}_{ps}\bar{M}_w$, by gel permeation chromatography (G.P.C.). Four G.P.C. columns were used in the chromatograph having a range of pore sizes (10^5nm, 10^4nm, 10^3nm and 10^2nm). These columns produced a satisfactory separation for the majority of the poly(N-vinyl carbazole) factions. However, some of the highest molecular weight fractions were excluded from these columns. For these fractions no reliable values of molecular weight were obtained.

Low-angle laser light-scattering (LALLS) was used to derive the absolute weight-average molecular weights of original unfractionated samples S1, S2 and S4 and fractions S3/L1, S3/L2 and S3/L4. Figure 3.04 shows a plot of the absolute weight-average molecular weights, $\bar{M}_w$, against the weight-average polystyrene equivalent molecular weights, ${}_{ps}\bar{M}_w$, for these samples. The method of least squares produced the following equation of the line through this plot.

$$\bar{M}_w = (1.76 \pm 0.06)\ {}_{ps}\bar{M}_w - (95{,}000 \pm 49{,}000) \qquad (3.3)$$

Equation (3.3) was used to give values of the absolute weight-average molecular weight for all samples of poly(N-vinyl carbazole) not measured directly by LALLS.

Tables 3.07 to 3.10 list the number-average and weight-average polystyrene equivalent molecular weights, ${}_{ps}\bar{M}_n$ and ${}_{ps}\bar{M}_w$, the absolute weight-average molecular weights, $\bar{M}_w$, and the heterogeneity indices, ${}_{ps}\bar{M}_w/{}_{ps}\bar{M}_n$, for fractions of poly(N-vinyl carbazole) samples S1 to S4, respectively, which were not excluded from the G.P.C. columns. All these measurements were conducted at the Rubber and Plastics Research

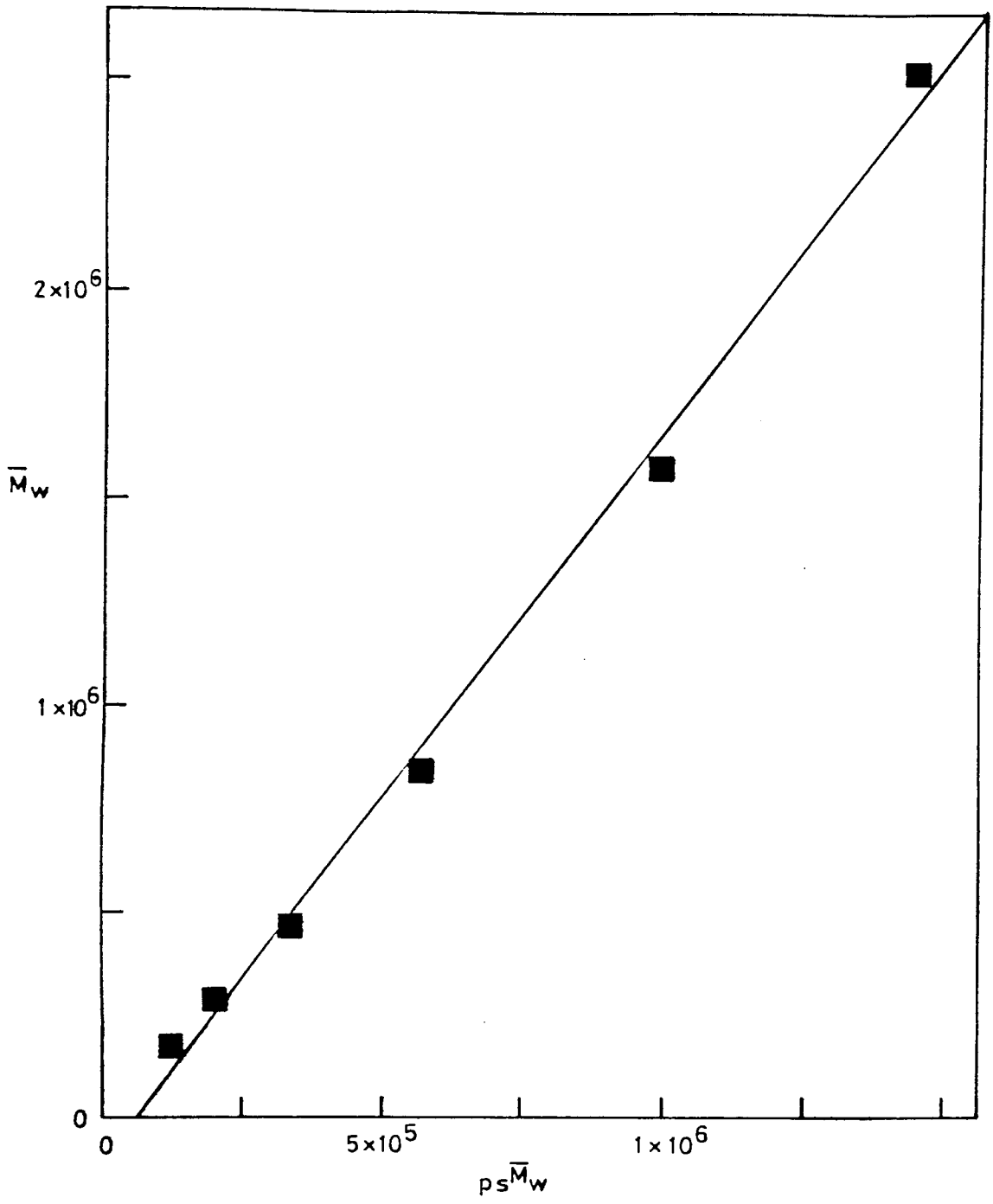

Figure 3.04 Absolute weight-average molecular weight, $\bar{M}_w$, against weight-average polystyrene equivalent molecular weight, $_{ps}\bar{M}_w$, for various samples of poly(N-vinyl carbazole).

Table 3.07 Number-average and weight-average polystyrene equivalent molecular weights, $_{ps}\bar{M}_n$ and $_{ps}\bar{M}_w$, the absolute weight-average molecular weights, $\bar{M}_w$, and the heterogeneity indices, $_{ps}\bar{M}_w/_{ps}\bar{M}_n$, for S1 fractions of poly(N-vinyl carbazole) not excluded by the G.P.C. columns.

Fraction	$_{ps}\bar{M}_n$	$_{ps}\bar{M}_w$	$\bar{M}_w$ [a]	$_{ps}M_w/_{ps}M_n$
H8	139,000	241,000	329,000	1.73
H10	340,000	603,000	966,000	1.77
H7	244,000	632,000	1,020,000	2.59
H6	193,000	1,170,000	1,960,000	6.08
H9	602,000	2,780,000	4,800,000	4.61
H5B	847,000	3,620,000	6,280,000	4.28
H5A	1,060,000	3,100,000	5,360,000	2.93

[a] Calculated using equation (3.3)

Table 3.08 Number-average and weight-average polystyrene equivalent molecular weights, $_{ps}\bar{M}_n$ and $_{ps}\bar{M}_w$, the absolute weight-average molecular weights, $\bar{M}_w$, and the heterogeneity indices, $_{ps}\bar{M}_w/_{ps}\bar{M}_n$, for S2 fractions of poly(N-vinyl carbazole) not excluded by the G.P.C. columns.

Fraction	$_{ps}\bar{M}_n$	$_{ps}\bar{M}_w$	$\bar{M}_w$ [a]	$_{ps}\bar{M}_w/_{ps}\bar{M}_n$
L4	8,780	18,000	-	2.13
L3	37,000	75,600	-	2.04
L2	66,800	185,000	231,000	2.76
L1	68,000	250,000	345,000	3.68
H5	258,000	1,690,000	2,880,000	6.56
H2	365,000	2,550,000	4,390,000	7.00
H4	564,000	4,060,000	7,050,000	7.20
H3	721,000	7,780,000	13,600,000	10.8

[a] Calculated using equation (3.3)

Table 3.09 Number-average and weight-average polystyrene equivalent molecular weights, $_{ps}\bar{M}_n$ and $_{ps}\bar{M}_w$, the absolute weight-average molecular weights, $\bar{M}_w$, and the heterogeneity indices, $_{ps}\bar{M}_w/_{ps}\bar{M}_n$, for S3 fractions of poly(N-vinyl carbazole) not excluded by the G.P.C. columns.

Fraction	$_{ps}\bar{M}_n$	$_{ps}\bar{M}_w$	$\bar{M}_w$ [a]	$_{ps}\bar{M}_w/_{ps}\bar{M}_n$
H6	9,340	41,100	-	4.39
H5	64,800	83,700	52,300	1.29
H4	80,000	102,000	84,500	1.27
H3	106,000	146,000	162,000	1.39
H2	116,000	181,000	224,000	1.56
H1	154,000	254,000	352,000	1.65

[a] Calculated using equation (3.3)

Table 3.10 Number-average and weight-average polystyrene equivalent molecular weights, $_{ps}\bar{M}_n$ and $_{ps}\bar{M}_w$, the absolute weight-average molecular weights, $\bar{M}_w$, and the heterogeneity indices, $_{ps}\bar{M}_w/_{ps}\bar{M}_n$, for S4 fractions of poly(N-vinyl carbazole).

Fraction	$_{ps}\bar{M}_n$	$_{ps}\bar{M}_w$	$\bar{M}_w$	$_{ps}\bar{M}_w/_{ps}\bar{M}_n$
L1	53,900	200,000	283,000[a]	3.71
L2	141,000	336,000	468,000[a]	2.38
L3	196,000	825,000	1,360,000[b]	4.21
L4	505,000	991,000	1,570,000[a]	1.96
L5	425,000	2,180,000	3,740,000[b]	5.13
L7	1,180,000	3,340,000	5,780,000[b]	2.82
L6	1,600,000	3,940,000	6,840,000[b]	2.47

[a] Measured directly by LALLS

[b] Calculated using equation (3.3).

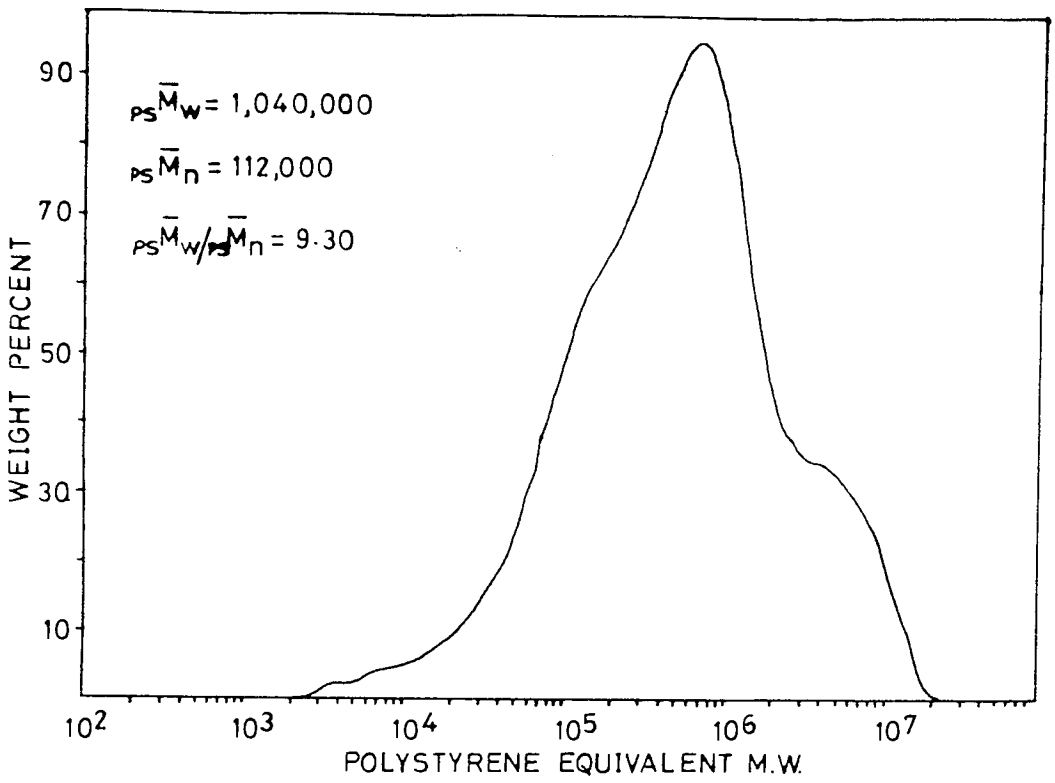

Figure 3.05 G.P.C. trace of sample S1. Poly(N-vinyl carbazole) prepared by initiation with $AlCl_3$.

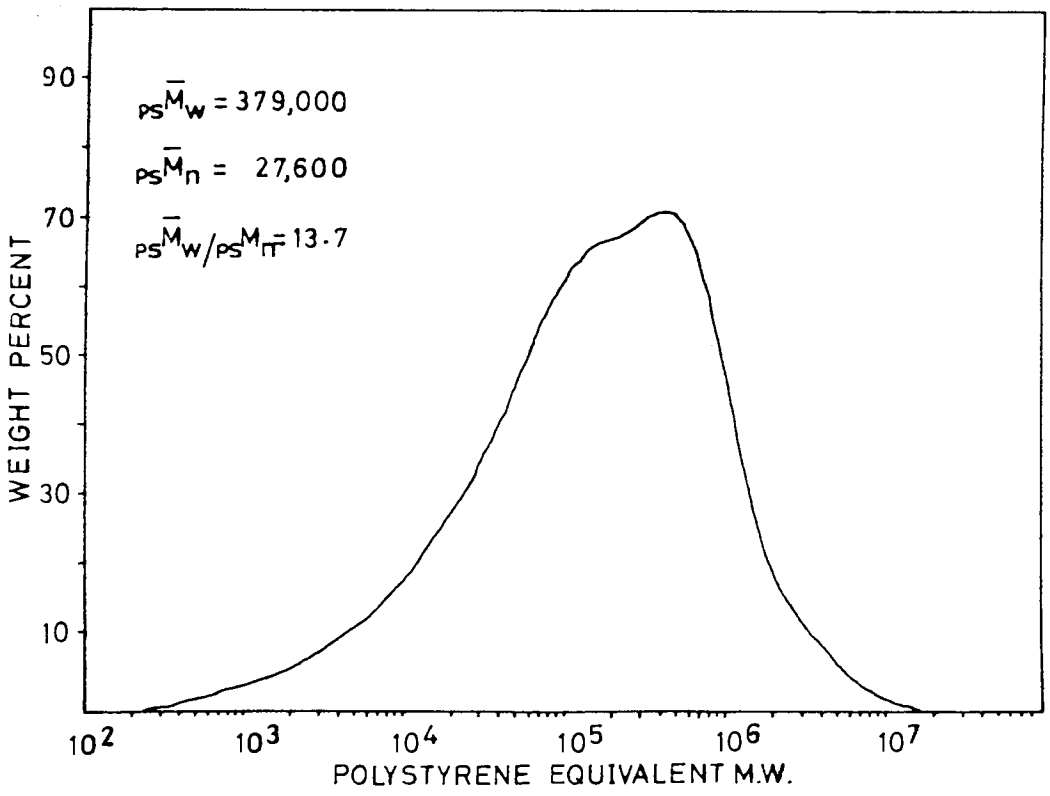

Figure 3.06 G.P.C. trace of sample S2. Poly(N-vinyl carbazole) prepared by initiation with BF_3 etherate.

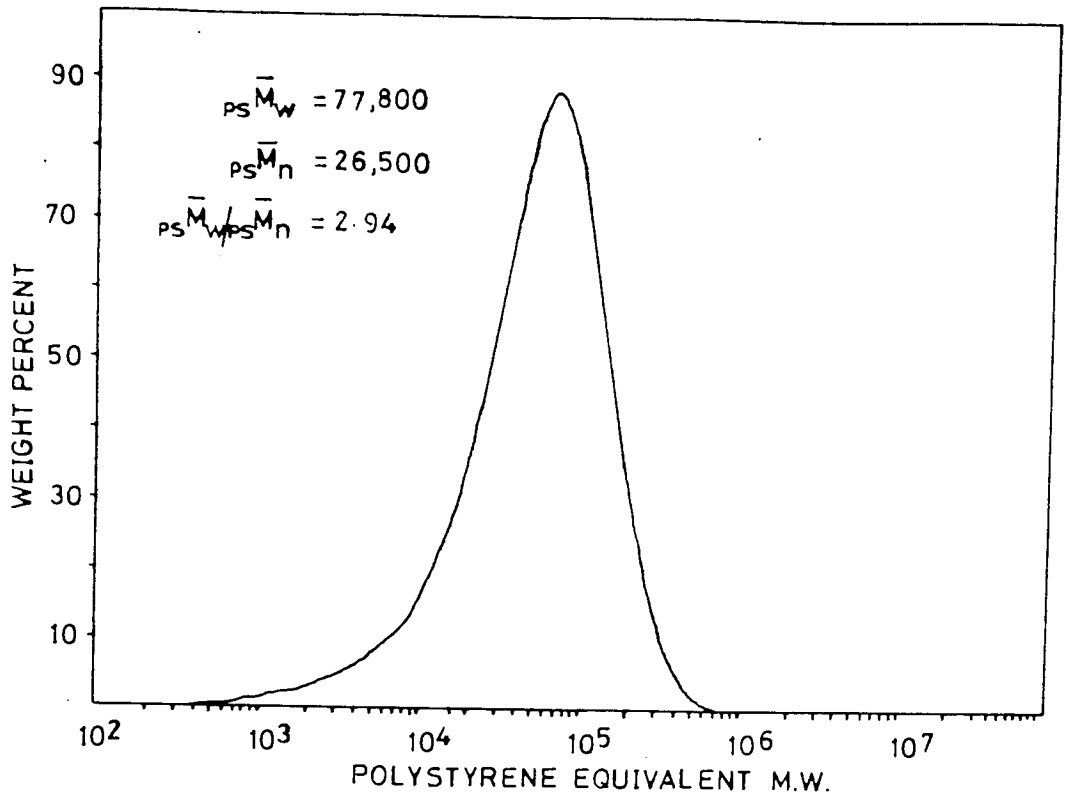

Figure 3.07 G.P.C. Trace of sample S3. Poly(N-vinyl carbazole) prepared by initiation with AZBN.

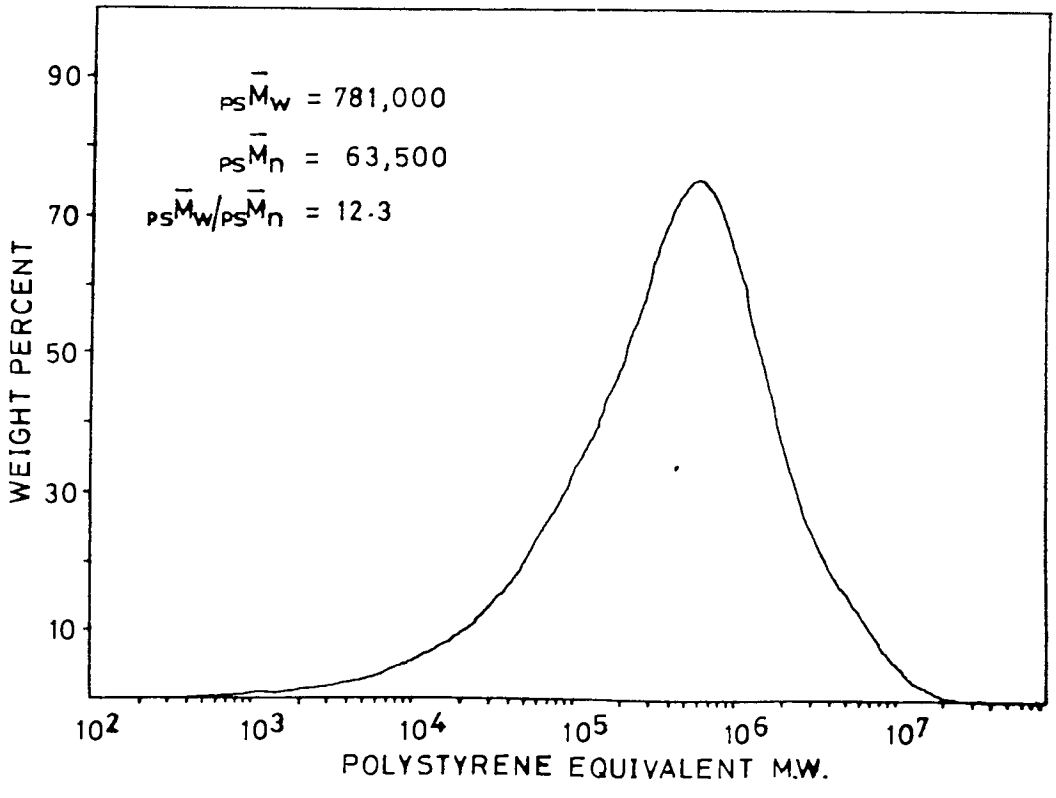

Figure 3.08 G.P.C. Trace of sample S4. Poly(N-vinyl carbazole) obtained from Polymer Consultants Ltd.

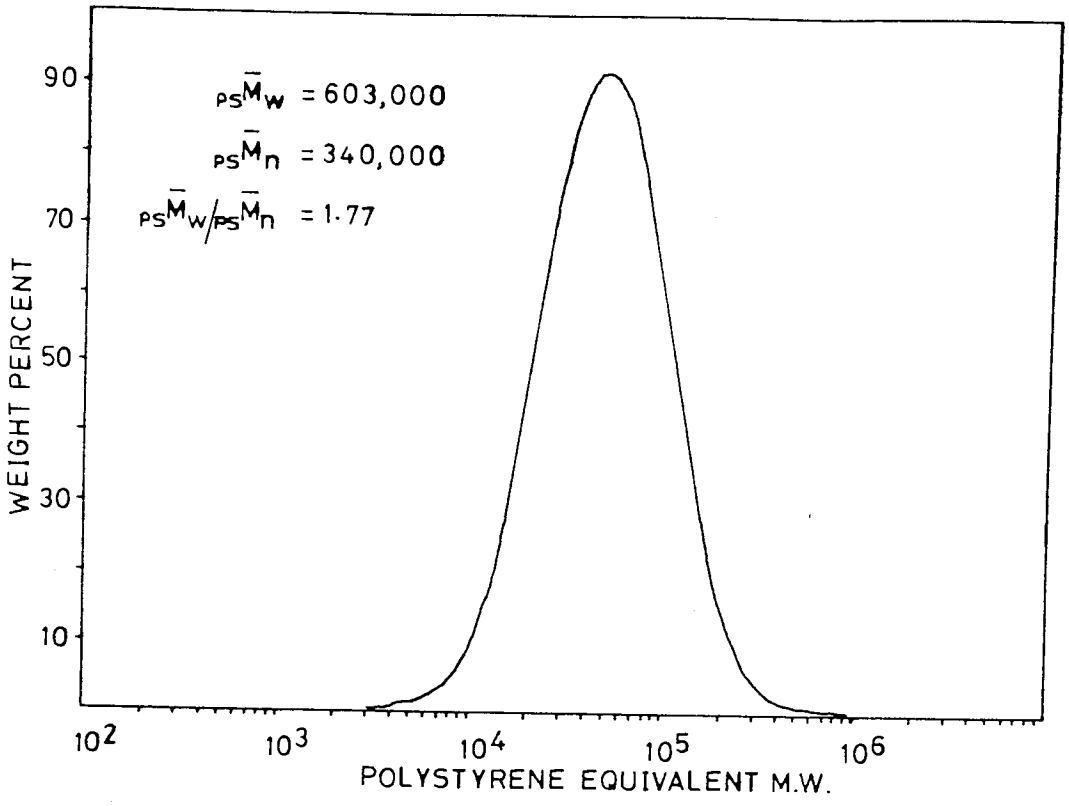

Figure 3.09 G.P.C. Trace of poly(N-vinyl carbazole) fraction S1/H10.

Association (R.A.P.R.A.).

The G.P.C. traces showing the molecular weight distributions of the unfractionated samples S1 to S4 are shown in Figures 3.05 to 3.08, respectively. The G.P.C. trace in Figure 3.05, corresponding to poly(N-vinyl carbazole) sample S1, may be seen to be showing exclusion of some of the highest molecular weight material from the G.P.C. columns. Figure 3.09 shows a typical G.P.C. trace of a fraction (S1/H10) prepared from this polymer sample, and serves to illustrate how the molecular weight distribution may be dramatically decreased by fractionation.

3.12 Characterisation of Poly(N-Vinyl Carbazole) Fractions using C-13 Nuclear Magnetic Resonance Spectroscopy.

The high resolution proton magnetic resonance spectrum of poly (N-vinyl carbazole) was first reported by Heller et al[147]. No differences between spectra of samples prepared by free radical, cationic or stereospecific Ziegler-type catalysts were observed. Heller et al concluded that only non-crystalline, atactic polymers were obtained because of the bulkiness of the carbazole side groups, or because of the non-stereospecific nature of the polymerization process.

Yoshimoto et al[148] reported the assignment of the proton N.M.R. peaks without showing the spectrum. They also reported that the relative intensities of the methine peaks (at 2.7 and 3.6ppm) differed between samples produced by thermal polymerization and cationic polymerization. It was concluded that the difference in the chemical shifts for the two methine peaks seemed too large to attribute it to changes in tacticity, and it was explained by the effect of neighbouring carbazolyl groups belonging to a chain molecule with restricted internal rotation.

Williams[149] suggested that the proton N.M.R. spectra of poly (N-vinyl carbazole) indicated the presence of hindered rotation of carbazole side groups with temperature dependent populations of

conformers. The tacticity of the polymer appeared to be fairly insensitive to the method of polymerization.

Clarification was provided by Okamoto et al[140], who showed that the stereoregularity depended on the polymerization method. Both methylene and methine protons of the polymers showed 'doublet' signals, and they assigned the peaks at higher fields to the isotatic sequence and the peaks at lower fields to the syndiotactic sequence. Thus, it was estimated that the cationic polymers had the largest amount of isotatic sequences (50%), and that the free-radical polymers had the smallest (25%).

Carbon-13 N.M.R. spectroscopy has been used extensively in recent years to obtain detailed information on the microstructure of polymers. The carbon-13 N.M.R. spectrum of poly(N-vinyl carbazole) was first shown by Tsuchihashi et al[150]. They assigned the majority of the peaks using N-ethylcarbazole as a monomeric model.

Kawamura and Matsuzaki[142] complete the assignment of the peaks in the C-13 N.M.R. spectrum and investigated the effect of varying the polymerization conditions. The methine and methylene regions of the carbon - 13 N.M.R. spectra recorded by these workers, for three different methods of polymerization, are reproduced in Figure 3.10. The absorption of the methylene and methine carbons may be seen to vary with the polymerization method. No temperature-dependent conformation effect was observed between 298K and 363K, and only peak resolution changed. The absorptions of the methine carbon of samples prepared by radical polymerization are split into a 'triplet', while those of the polymers obtained by cationic initiation are split into a 'doublet'. The relative intensities of the absorption of 'doublets' or 'triplets' of both the methylene and methine carbons may be seen to vary with synthetic procedure. It was tentatively assumed that the

polymers obtained by radical polymerization had syndiotactic-rich structures, that the polymers prepared with BF_3 etherate had isotactic-rich structures, and that the polymers prepared with $ALEtCl_2$ prossessed stereoblock structures.

Williams and Froix[141] have reported carbon-13 N.M.R. spectra of samples of low molecular weight poly(N-vinyl carbazole) prepared by synthetic methods similar to those described previously. The methine and methylene regions of the carbon-13 N.M.R. spectra recorded by these workers, for polymer samples produced by azobisisobutyronitrile (AZBN) and boron trifluoride etherate initiation, are reproduced in Figure 3.11. The spectrum of the AZBN initiated sample compares well with the corresponding spectrum reported by Kawamura and Matsuzaki[142] shown in Figure 3.10. However, the spectrum reported by Williams and Froix for the BF_3 etherate initiated sample resembles much more closely the spectrum of the $AlC_2H_5Cl_2$ initiated sample published by the Japanese workers.

Williams and Froix[141] analysed their spectra in a somewhat different manner than that of previous workers[140,142]. They regarded the methine peaks to be a 'triplet' corresponding to absorption of mr, rr and mm triads (where m = meso and r = racemic), whilst the methylene peaks were made up of absorptions due to rmr, mrm, rrr, mmr and mmm structures. By measuring the intensities of these peaks Williams and Froix were able to draw certain conclusions as to the spacial distribution of the carbazole groups. There appears to be a slight error in the text, as they state their findings show an increase in racemic content for cationically polymerized samples of poly(N-vinyl carbazole). Their results, however, show a clear decrease in racemic content for these samples, and are in agreement with those of

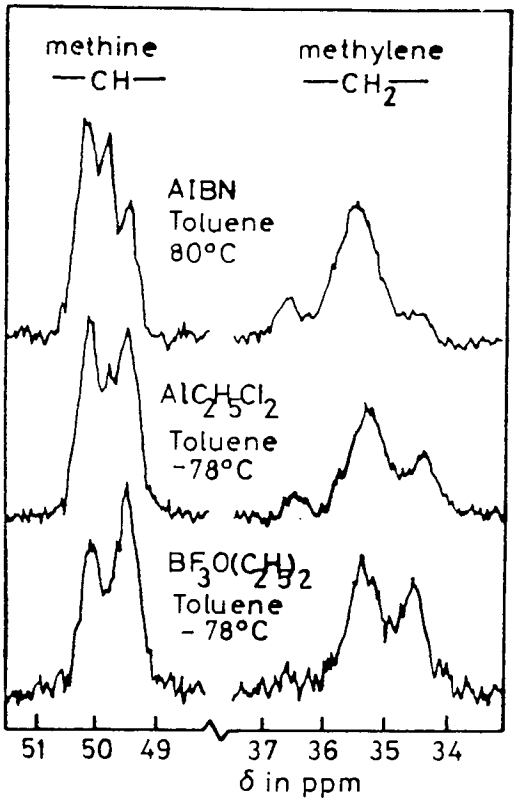

Figure 3.10 Carbon-13 N.M.R. spectra recorded by Kawamura and Matsuzaki[142] of poly (N-vinyl carbazole) prepared by three different synthetic routes.

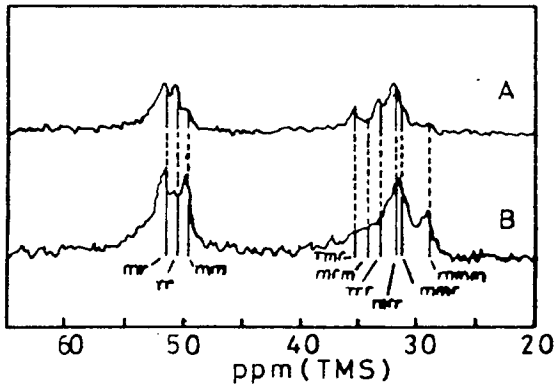

Figure 3.11 Carbon-13 N.M.R. spectra recorded by Williams and Froix[141] of poly(N-vinyl carbazole) reputedly prepared using AIBN(A) and BF_3 etherate (B) as initiators.

Okamoto et al[140]. Williams and Froix disagree with the notion that poly(N-vinyl carbazole) consists of either long chains of isotactic or syndiotactic sequences.

Therefore, in summary, it would seem that the synthetic route does effect the tacticity of the polymer produced, and this may be detected by either proton or carbon-13 N.M.R. However, there appears to be some doubt as to how the bulky carbazole side groups are ordered in these different structures.

The carbon-13 N.M.R. spectra of poly(N-vinyl carbazole) were recorded in this study with a Joel FX90Q Fourier transform spectrometer. The instrument was fitted with a spectrum computer having a memory capacity of 16,383 points (16k), and operated at 22.5MHz. The spectra were all broad band decoupled, to decouple directly bonded protons and all others. A pulse width of 15μs (approx 60^{o}) and a frequency range of 5,000Hz was employed. A trapezoidal exponential window was used, which although giving approximately 1Hz line broadening, gives an improved signal-to-noise ratio. The time domain signal was accumulated every 50 pulses in the memory of 8091 points (8k) after Fourier transformation. A total of approximately 200,000 pulses were used for each spectrum, requiring about 65 hours. When recording the peaks due to the methylene and methine carbon absorptions, all other peaks were allowed to off-scale (overflow). All measurements were carried out in glass N.M.R. tubes (10mm o.d.) at 332K without degasing. A capilliary containing D_2O was used as the deuterium internal lock. The solvent used was 1,4-dioxan and the concentration of solution was approximately 10% w/v. Hexamethyldisiloxane (H.M.D.S.) was used as an internal reference solvent. The chemical shifts are reported on the δ-scale in ppm with respect to tetramethylsilane (T.M.S.). The chemical shift of H.M.D.S. was 1.950 down field relative to T.M.S.

The complete carbon-13 N.M.R. spectrum recorded for poly(N-vinyl carbazole) fraction S1/H10 is shown in Figure 3.12. This spectrum is typical of that recorded for all the fractions of poly(N-vinyl carbazole) and compares well with the spectrum presented by Kawamura and Matsuzaki[142].

Figures 3.13 to 3.16 show the methine and methylene peaks from the carbon-13 N.M.R. spectra of poly(N-vinyl carbazole) fractions S1/H10, S2/H1, S3/H6 and S4/L1, respectively. The spectrum in Figure 3.15 of fraction S3/H6, which was initiated by AZBN, corresponds very closely to the spectrum presented in Figure 3.16 of fraction S4/L1, which was obtained from Polymer Consultants Ltd and whose method of polymerization was not quoted. The spectra of these two fractions also compare very well with the spectra of samples of polymer prepared by radical polymerization reported by Kawamura and Matsuzaki[142] and Williams and Froix[141] (see Figures 3.10 and 3.11). It would seem, therefore, that sample S4 was also prepared by a radical polymerization.

The spectra in Figure 3.13 and Figure 3.14 of poly(N-vinyl carbazole) fractions prepared by $AlCl_3$ and BF_3 etherate initiation, respectively, also compare well with the corresponding spectra reported by Kawamura and Matsuzaki (Figure 3.10)[142]. However, the spectrum reported by Williams and Froix (Figure 3.11)[141] of the sample reputedly prepared by BF_3 etherate initiation much more closely resembles the spectrum of the fraction (S1/H10) polymerized by $AlCl_3$ initiation. On the grounds of this evidence, and that presented above, we suspect the spectrum published by Williams and Froix[141] and purported to be of a sample of poly(N-vinyl carbazole) prepared by BF_3 etherate initiation, was in fact of an $AlCl_3$ initiated polymer sample.

The characterisation of the poly(N-vinyl carbazole) fractions by carbon-13 N.M.R. spectroscopy will be correlated later with the dielectric and electro-optical data also obtained for these fractions.

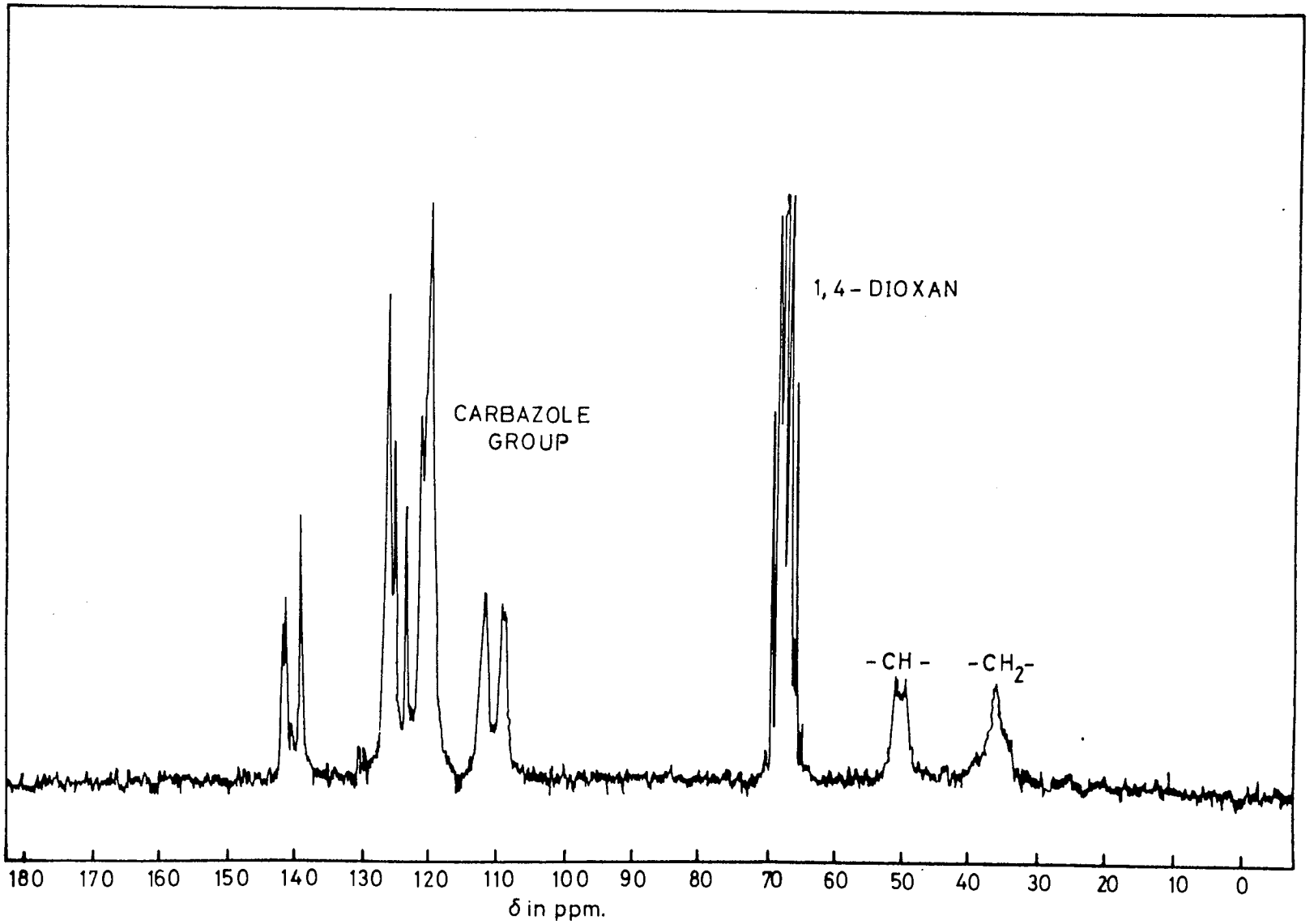

Figure 3.12 Carbon-13 N.M.R. spectrum recorded for poly(N-vinyl carbazole) fraction S1/H10 and typical of that recorded for all polymer fractions.

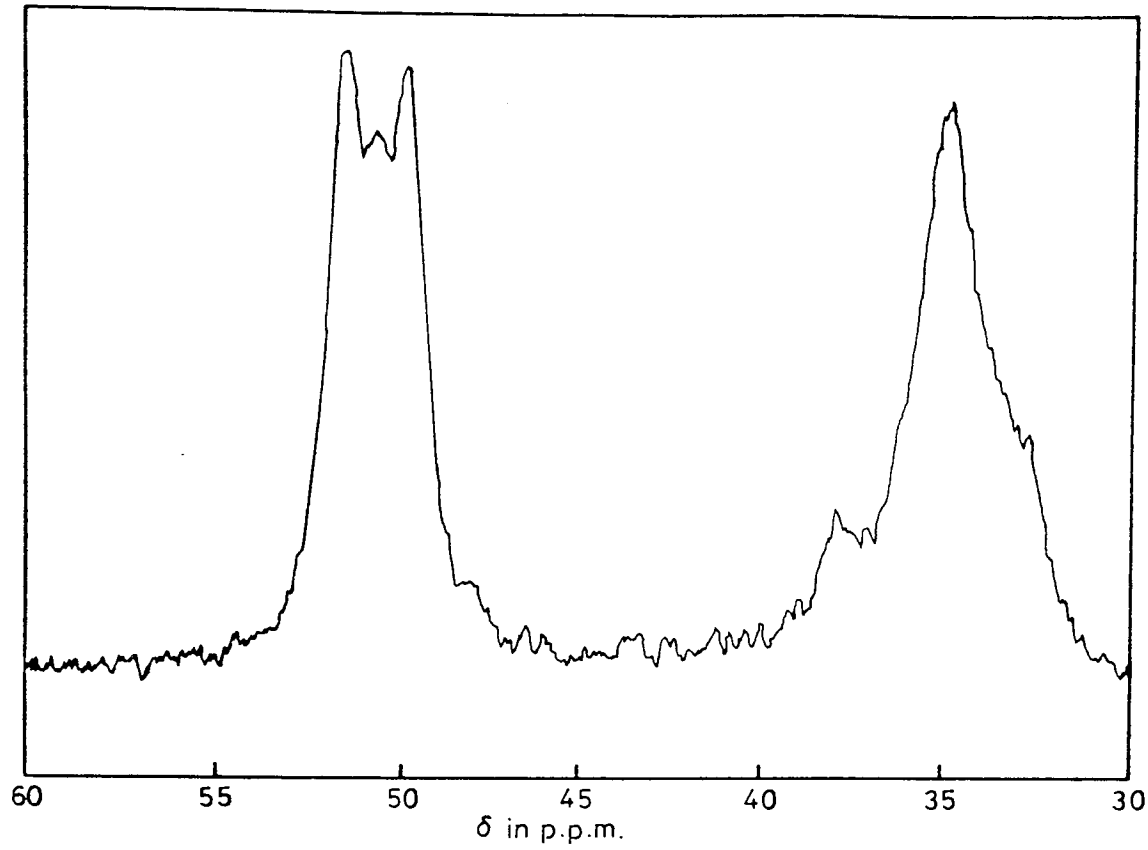

Figure 3.13 Methine and methylene peaks from C-13 N.M.R. spectrum of P.V.K. fraction S1/H10 (initiated by $AlCl_3$ at 298K).

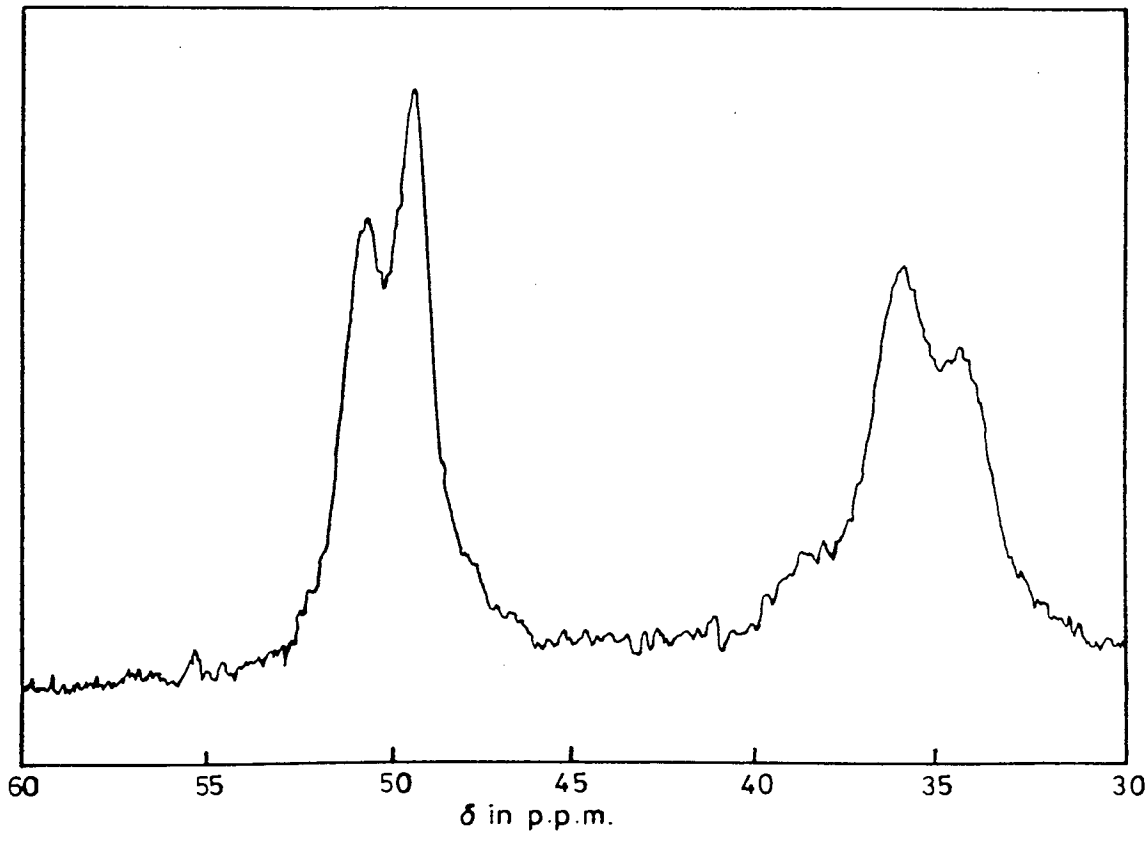

Figure 3.14 Methine and methylene peaks from C-13 N.M.R. spectrum of P.V.K. fraction S2/H1 (initiated by BF_3OEt at 298K).

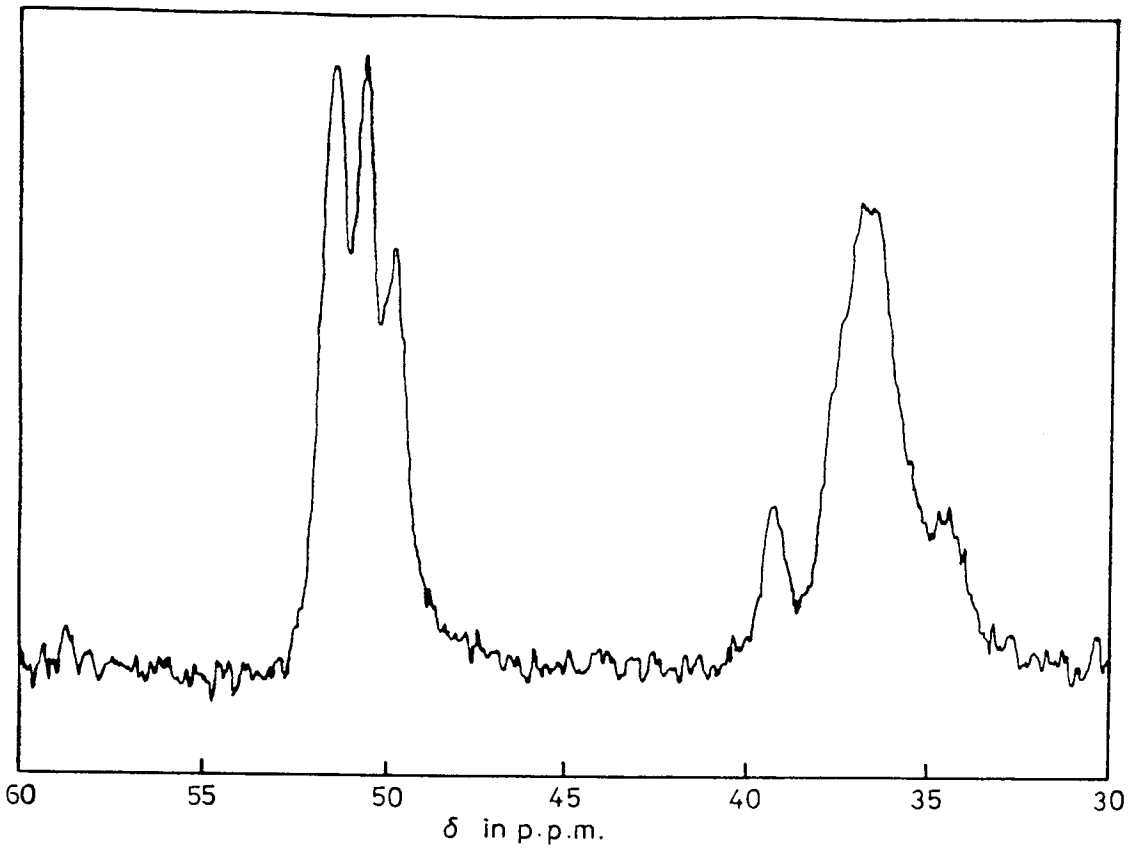

Figure 3.15 Methine and methylene peaks from C-13 N.M.R. spectrum of P.V.K. fraction S3/H6 (initiated by AZBN at 343K).

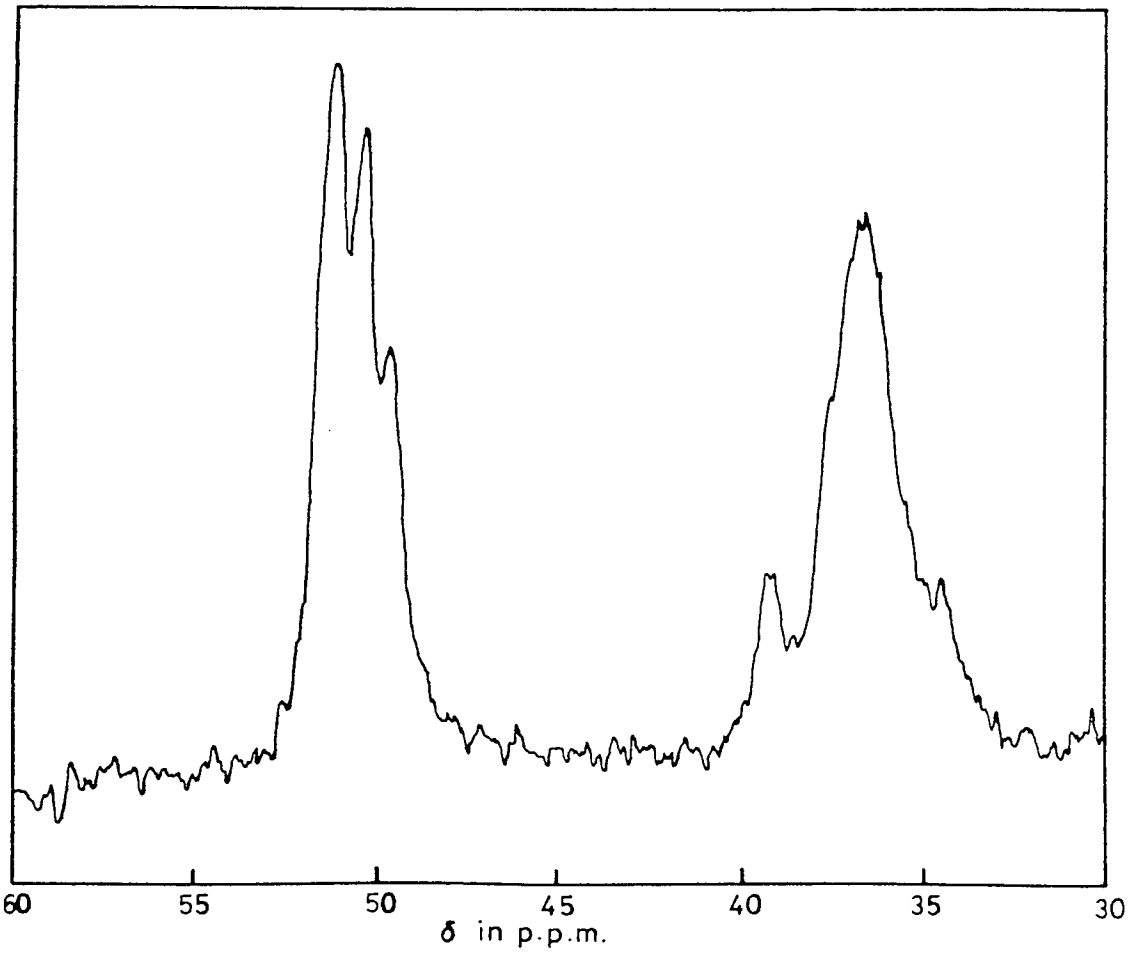

Figure 3.16 Methine and methylene peaks from C-13 N.M.R. spectrum of P.V.K. fraction S4/L1.

CHAPTER 4

EXPERIMENTAL INVESTIGATION OF THE DIELECTRIC PROPERTIES OF CYCLIC AND LINEAR DIMETHYL SILOXANES

4.01 Introduction

This chapter details the measurement, and results obtained, for the static dielectric permittivities and refractive indices of the cyclic and linear dimethyl siloxane oligomers and poly (dimethyl siloxanes). These are fundamental measured quantities and thus may be compared without relying upon the validity of any dielectric theory. However, a more useful quantity when comparing the dielectric properties of substances is the electric dipole moment. The electric dipole moment of a substance may be calculated provided that the static dielectric permittivity, refractive index, density and molecular weight are avaiable, and if one assumes a model for the dielectric behaviour of the substance either in the pure state or in solution. In the following chapter appropriate models will be outlined and the electric dipole moments calculated using experimentally derived quantities.

Since refractive index varies with wavelength, it is necessary to make measurements of refractive index at at least two wavelengths and extrapolate to a value at infinite wavelength. This infinite wavelength refractive index is then analogous to the respective zero frequency or static dielectric permittivity. The details of the measurement of these refractive indices and appropriate extrapolation using the Cauchy dispersion formula are presented in this chapter.

Previous studies concerned with the comparison of the dielectric properties of cyclic and linear dimethyl siloxanes have been restricted to low molecular weight samples containing less than 16 siloxane bonds[151-153, 64]. The fractions of cyclic and linear dimethyl siloxanes taken for the present comparative study are in the number-average molar mass range $160 < \bar{M}_n < 7700$ and have heterogeneity indices $\bar{M}_w/\bar{M}_n$ in the range 1.0 - 1.2. The dielectric behaviour of some cyclic and linear dimethyl siloxane oligomers and poly(dimethyl siloxanes) in solution in cyclohexane was also investigated.

4.02 Measurement of Static Dielectric Permittivities

The electrical capacitance of dielectric cell A was measured when empty and when filled with freshly distilled samples of cyclohexane, toluene, octamethylcyclotetrasiloxane and hexamethyldisiloxane using a Marconi Universal Bridge (Type T1313A) at a frequency of 10kHz. A substitution method described in section 2.05 was used to calculate the static dielectric permittivities of the liquids listed above, assuming a value of 2.0199 for the static dielectric permittivity of cyclohexane[37] at 298K. This value, in conjunction with the value of $-1.60 \times 10^{-3} K^{-1}$ for the temperature coefficient ($d\varepsilon/dT$) of cyclohexane[128], was used to calculate the static permittivities of the liquids at 313K.

Measured static dielectric permittivities of toluene (2.273), octamethylcyclotetrasiloxane (2.383) and hexamethyldisiloxane (2.170) at 298K were found to be close to the values quoted in the literature:- toluene (2.2725)[37], octamethylcyclotetrasiloxane (2.382 and 2.385)[151,154] and hexamethyldisiloxane (2.166 and 2.167)[151,154].

Static dielectric permittivities of the fractions of cyclic and linear dimethyl siloxanes at 298K and 313K were also obtained using the above procedure. These values are listed in Table 4.01 and Table 4.02 for the cyclic and linear fractions, respectively. The dielectric permittivities of the cyclic and chain fractions were estimated to have experimental errors of 0.05% and 0.1%, respectively.

For cyclic and linear dimethyl siloxane oligomers having n = 8 and n = 6 skeletal bonds, respectively, the static dielectric permittivities were measured at several different temperatures between 288K and 313K. These values are plotted in Figures 4.01 and 4.02 for the cyclic and linear members, respectively.

Table 4.01 Number - average number of backbone bonds, $\bar{n}$, and static dielectric permittivities, ε_0, for undiluted cyclic dimethyl siloxanes at 298K and 313K.

Fraction	$\bar{n}$	ε_0	
		298K	313K
R1[a]	8.0	2.383	2.343
R2[a]	10.0	2.491	2.457
R3[a]	12.0	2.606	2.557
R4	14.7	2.683	2.626
R5	19.7	2.745	2.689
R6	23.8	2.754	2.698
R7	31.2	3.755	2.699
R8	35.0	2.757	2.703
R9	38.2	2.765	2.709
R10	44.0	2.770	2.714
R11	109.0	2.763	2.706
R12	190.0	2.757	2.701

[a] single component

Table 4.02 Number - average number of backbone bonds, $\bar{n}$, and static dielectric permittivities, ε_0, for undiluted linear dimethyl siloxanes at 298K and 313K.

Fraction	$\bar{n}$	ε_0	
		298K	313K
L1[a]	2.0	2.170	2.145
L2[a]	4.0	2.297	2.255
L3[a]	6.0	2.390	2.344
L4[a]	8.0	2.456	2.407
L5[a]	10.0	2.499	2.450
L6[a]	12.0	2.550	2.490
L7	16.5	2.583	2.543
L8	21.7	2.628	2.579
L9	24.4	2.650	2.610
L10	32.4	2.673	2.621
L11	41.6	2.698	-
L12	105	-	-
L13	206	2.752	-

[a] single component

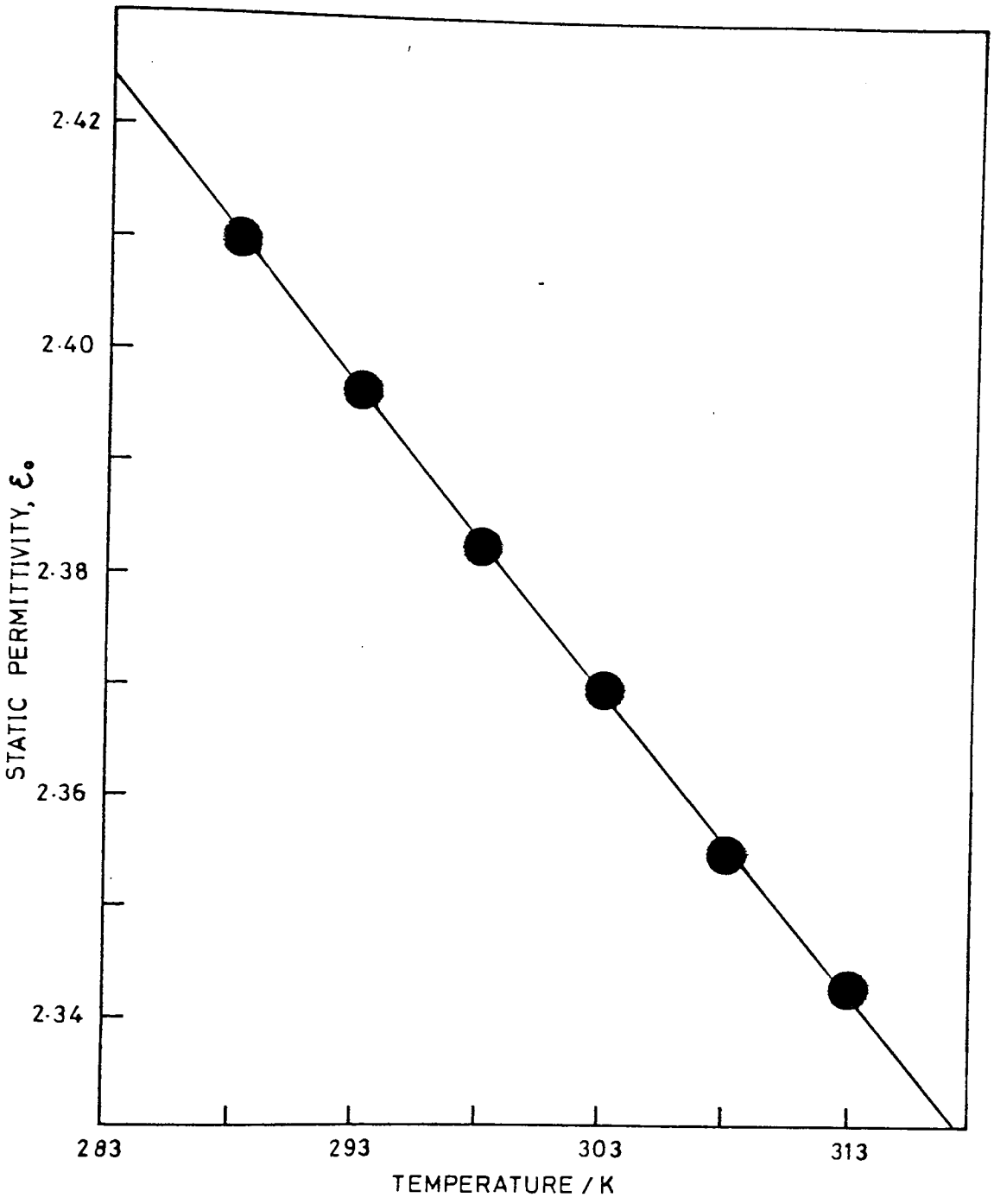

Fig. 4.01 Variation of static dielectric permittivity, ε_0, with temperature for octamethylcyclotetrasiloxane in the undiluted state.

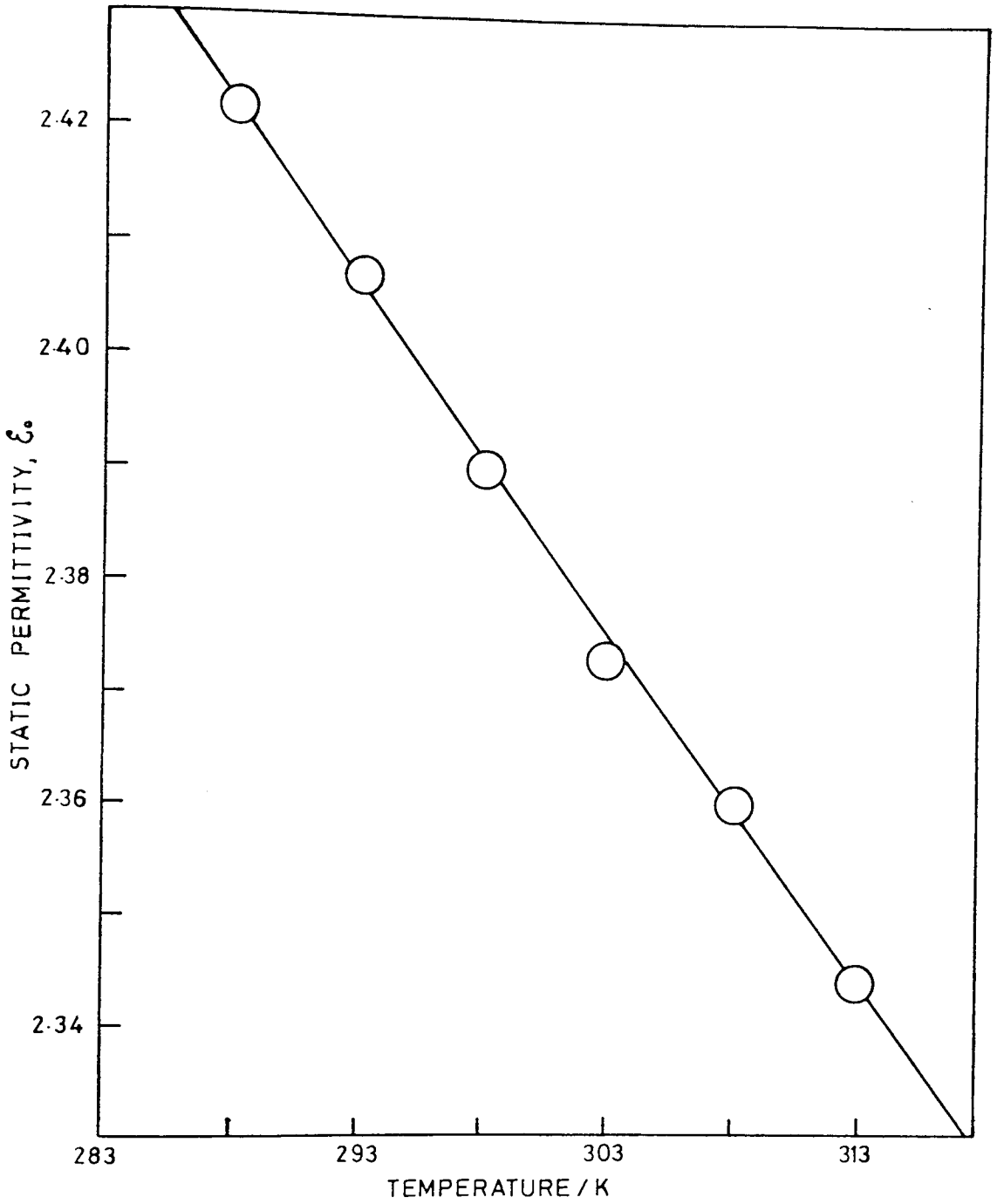

Fig. 4.02 Variation of static dielectric permittivity, ε_0, with temperature for decamethyltetrasiloxane in the undiluted state.

4.03 Comparison of Static Dielectric Permittivities of Cyclic and Linear Dimethyl Siloxanes

The static dielectric permittivities of the linear dimethyl siloxanes in the range n = 2 to 12 are generally in very good agreement with the values measured by other workers.[64,65,151,153,154] However, the permittivities obtained by Sutton and Mark[65] for the linear dimethyl siloxanes with n = 12, 16 and 20 are significantly larger than the corresponding values found in the present study. The static permittivities of several cyclic dimethyl siloxanes (n = 8-16) measured by Sauer and Mead[151] concurred with the values measured in the present study.

The dielectric behaviour of several fractions of cyclic and linear dimethyl siloxanes was also examined in solution in cyclohexane at 298K. Cyclohexane has been shown previously to be a 'good' solvent for poly(dimethyl siloxanes)[45]. The total solute dielectric polarizations, P_T, for the siloxanes in this solvent are shown in Table 4.03, together with the corresponding total polarizations found for the undiluted samples. The values of P_T found for the solutions were found to be independent of the concentration of solute over the concentration range 10 - 50% w/v. Similar differences between values of P_T for undiluted and diluted samples were found for the cyclic and linear siloxanes. This behaviour has been observed previously for linear dimethyl siloxanes[63] and has been attributed to specific solvent effects.[68]

Figure 4.03 shows the static dielectric permittivities at 298K plotted against the average number of skeletal bonds for undiluted cyclic and linear dimethyl siloxanes. For oligomers with less than ca. 50 skeletal bonds the permittivites of the cyclic siloxanes and the nearest equivalent (equal number of skeletal bonds) linear siloxanes differ quite markedly. These differences are a result of variations

in the densities of the samples of the cyclic and linear siloxanes, together with differences in their respective molecular dipole moments. For the cyclic dimethyl siloxanes the permittivity attains a maximum value of 2.77 in the region of 50 skeletal bonds and this is very close to the value of 2.76 obtained for a fraction of cyclic molecules with $\bar{n}$ = 190 (see Figure 4.03). The behaviour contrasts that exhibited by the linear dimethyl siloxanes and poly(dimethyl siloxanes). The dielectric permittivities of the low molecular weight linear oligomers ($\bar{n} \leq 5$) are significantly smaller than the nearest equivalent cyclic oligomers and they increase smoothly to the value of 2.75 obtained for the fraction of chains with $\bar{n}$ = 204.

Table 4.03 Solute dielectric polarizations, P_T, of cyclic and linear dimethyl siloxanes in solution in cyclohexane and in the undiluted state at 298K.

Fraction	$P_T(X10^6/m^3mol^{-1})$	
	Undiluted	Solution
L1[a]	60.07	59.67
L10	546.5	638.4
L13	2944	3569
R1[a]	98.41	108.0
R10	622.7	750.3
R11	1534	1863
R12	2673	3274

[a] single component (see Tables 4.01 and 4.02)

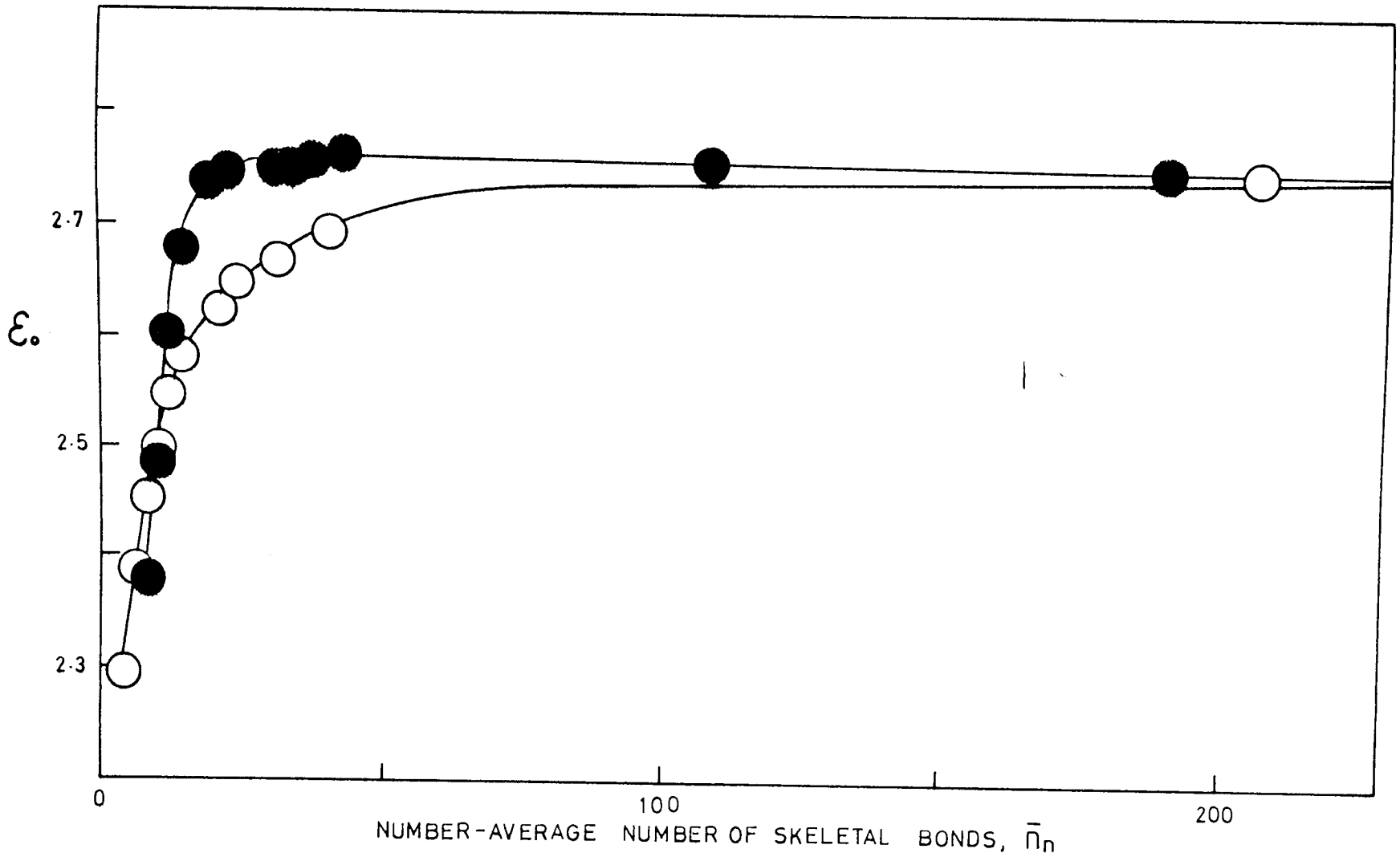

Fig. 4.03 Static dielectric permittivities, ε_0, of cyclic dimethyl siloxanes (●) and linear dimethyl siloxanes (○) in the undiluted state at 298K.

4.04 Measurement of Refractive Indices

Refractive indices of the samples of cyclic and linear dimethyl siloxanes were measured at wavelengths of 632.8nm (He/Ne laser) and 435.96nm (Hg discharge lamp) using a Zeiss Abbe refractometer (Model A Series 7). The temperature of the sample was 298 ± 0.01K. The refractive indices are quoted to five significant figures and were corrected for the dispersion characteristics of the refractometer. The relevant values for cyclic and linear dimethyl siloxanes are listed in Table 4.04 and Table 4.05, respectively.

4.05 Calculation of Infinite - Wavelength Refractive Indices

Classical dispersion theory of the frequency dependence of molecular polarizability may be described using the Cauchy dispersion equation[4] :-

$$n = a + \frac{b}{\lambda^2} + \frac{c}{\lambda^4} + \frac{d}{\lambda^6} + \cdots \qquad (4.1)$$

where a, b, c, etc are constants and n is the refractive index measured at wavelength λ. At infinite wavelength ($\lambda = \infty$),

$$n = a = n_{\lambda\to\infty} \qquad (4.2)$$

The refractive index at infinite wavelength, $n_{\lambda\to\infty}$, may be calculated with acceptable accuracy by using only the first term with λ in equation (4.1), that is,

$$n_{\lambda\to\infty} = n - \frac{b}{\lambda^2} \qquad (4.3)$$

Using the values of n_1 at λ_1 and n_2 at λ_2, we finally obtain, after rearrangement,

$$n_{\lambda\to\infty} = \frac{\lambda_1^2 n_1 - \lambda_2^2 n_2}{\lambda_1^2 - \lambda_2^2} \qquad (4.4)$$

The infinite - wavelength refractive indices, $n_{\lambda\to\infty}$, required for the calculation of the electronic polarizations, were obtained from the two term Cauchy expression in equation (4.4) using the refractive indices n_1 and n_2 measured at visible wavelengths λ_1 and λ_2, respectively (see above). The values of infinite - wavelength refractive index calculated in this manner for cyclic and linear dimethyl siloxanes are listed in Table 4.04 and Table 4.05, respectively.

Table 4.04 Refractive indices, n_1 and n_2, measured at wavelengths λ_1 and λ_2, and infinite - wavelength refractive indices, $n_{\lambda \to \infty}$, calculated using equation (4.4) for undiluted cyclic dimethyl siloxanes at 298K.

Fraction	n_1 λ_1 = 632.8nm	n_2 λ_2 = 436.0nm	$n_{\lambda \to \infty}$
R1[a]	1.3927	1.4040	1.3825
R2[a]	1.3947	1.4064	1.3841
R3[a]	1.3995	1.4120	1.3882
R4	1.4020	1.4138	1.3913
R5	1.4039	1.4155	1.3934
R6	1.4041	1.4157	1.3936
R7	1.4034	1.4153	1.3926
R8	1.4031	1.4150	1.3923
R9	1.4029	1.4147	1.3922
R10	1.4027	1.4143	1.3922
R11	1.4026	1.4139	1.3924
R12	1.4025	1.4140	1.3921

[a] single component (see Table 4.01)

Table 4.05 Refractive indices, n_1 and n_2, measured at wavelengths λ_1 and λ_2, and infinite - wavelength refractive indices, $n_{\lambda\to\infty}$, calculated using equation (4.4) for undiluted linear dimethyl siloxanes at 298K.

Fraction	n_1 λ_1 = 632.8nm	n_2 λ_2 = 436.0nm	$n_{\lambda\to\infty}$
L1[a]	1.3734	1.3856	1.3624
L2[a]	1.3809	1.3928	1.3701
L3[a]	1.3864	1.3978	1.3761
L4[a]	1.3897	1.4010	1.3795
L5[a]	1.3919	1.4032	1.3817
L6[a]	1.3931	1.4045	1.3828
L7	1.3954	1.4072	1.3847
L8	1.3970	1.4094	1.3858
L9	1.3980	1.4107	1.3865
L10	1.3985	1.4111	1.3871
L11	1.3997	1.4121	1.3885
L12	1.4011	1.4131	1.3903
L13	1.4015	1.4136	1.3906

[a] single component (see Table 4.02)

CHAPTER 5

DETERMINATION OF EXPERIMENTAL DIPOLE MOMENTS OF CYCLIC AND LINEAR DIMETHYL SILOXANES

5.01 Introduction

The mean - square end-to-end distance, $\langle r^2 \rangle$, is undoubtably the most commonly used property for describing the average conformations of polymer molecules. This is probably due to its relative ease of visualization, together with the relatively simple method of determination by viscosity measurements[30,31]. In general, however, $\langle r^2 \rangle$ can be determined reliably only in the case of relatively long chains. For this reason there is a growing interest in the characterization of polymer molecules through studies of their dipole moments[31,156], even though this approach is obviously restricted to molecules of significant polarity. The dipole moment of a polar polymer molecule can be readily determined over the entire range of chain length from monomer through to high molecular weight polymer, provided that they are soluble in a nonpolar solvent. In addition there is both theoretical[58-62] and experimental[63] evidence that dipole moments of many types of chain molecules are unaffected by excluded volume interactions. Such interactions are known to have a significant effect on chain dimensions and must be taken into account theoretically in order to obtain values of chain dimensions compatible with those obtained experimentally.

5.02 Dielectric Theory

The total polarization, P_T, of a molecule is comprised of three main terms. These are the electronic, P_E, atomic, P_A, and orientational, P_O, polarizations, which are additive. The total polarization is given by,

$$P_T = P_E + P_A + P_O \qquad (5.1)$$

If the dipole moment of a molecule is to be calculated from the total measured polarization then P_O must be isolated from this expression, since it is the orientation of the dipole moment in an electric field which gives rise to P_O. A method often employed to evaluate P_O is to measure P_T at different frequencies. The typical frequency dependence of P_T is illustrated in Figure 5.01. The total polarization can be obtained from measurements at radio frequencies, from which may be subtracted the electronic polarization calculated from refractive indices measured at optical frequencies. A value for the atomic polarization cannot be determined directly, and indirect methods are complex and difficult experimentally, though microwave measurements of dielectric permittivity have been used for this purpose. The total dielectric polarization of solids has also been used to obtain P_A. Consequently, many investigators have simply estimated P_A to be a fixed value somewhere in the region of 5 - 15% of P_E, or have neglected P_A completely. Since P_E is usually quite small, compared to P_O, this approach has normally been adequate. However, for the siloxanes this is not the case and the neglect of P_A may effect the dipole moment by a factor of two.

The present accepted interpretation of the dielectric constant, in terms of molecular dipole moments for electrically neutral materials is based upon the theory of Debye[2], who formed the equation:-

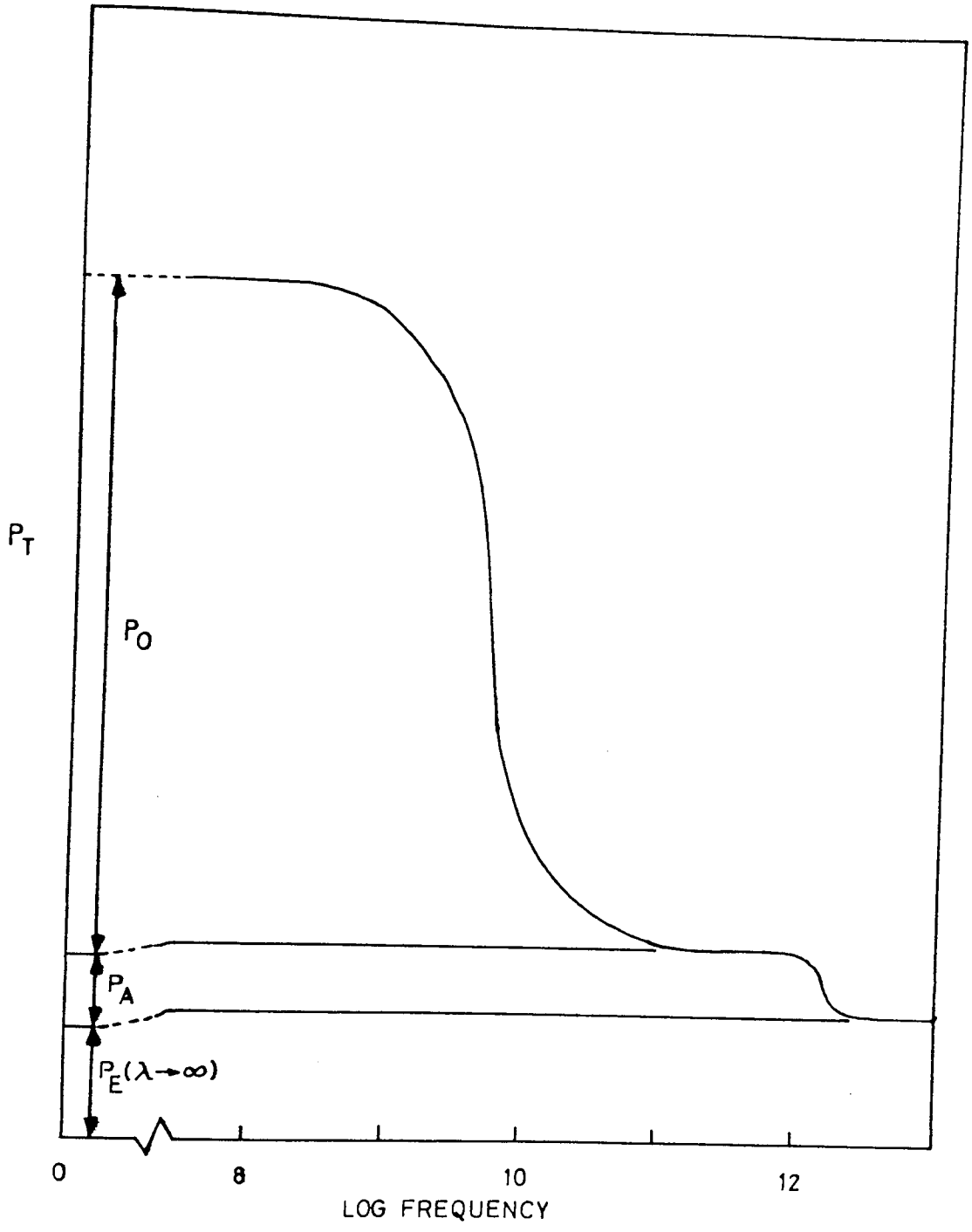

Figure 5.01 Typical frequency dependence of the total polarizations, P_T.

$$\mu_0^2 = \frac{9kT\varepsilon}{N} \quad \frac{M}{\rho}\left(\frac{\varepsilon_0 - 1}{\varepsilon_0 + 2} - \frac{\varepsilon_\infty - 1}{\varepsilon_\infty + 2}\right), \qquad (5.2)$$

where

μ_0 = dipole moment,

k = Boltzmann constant,

T = absolute temperature,

N = Avogadro's number,

M = molecular mass,

ρ = density,

ε = static dielectric permittivity of free space,

ε_0 = static dielectric permittivity of the medium,

and ε_∞ = dielectric permittivity measured at infinite frequency (optical wavelengths used).

Note that no allowance for atomic polarization is made in this equation.

Onsager[157] took account of the internal reaction field developed in a liquid, and effectively introduced a premultiplying term into Debye's equation:-

$$\mu_0^2 = \frac{9kT\varepsilon}{N}\frac{M}{\rho}\frac{(2\varepsilon_0 + \varepsilon_\infty)(\varepsilon_0 + 2)}{3\varepsilon_0(\varepsilon_\infty + 2)}\left(\frac{\varepsilon_0 - 1}{\varepsilon_0 + 2} - \frac{\varepsilon_\infty - 1}{\varepsilon_\infty + 2}\right) \qquad (5.3)$$

Again, no allowance for atomic polarization is made.

Many subsequent refinements to this theory and equation have since been published, but only the Guggenheim-Debye rearrangement[158] will be mentioned here. In this adaptation of the Debye equation, Guggenheim defines and applies a 'fictitious' atomic polarization,

$$P_A = \frac{3\varepsilon}{N}\left(\frac{\varepsilon_0 - 1}{\varepsilon_0 + 2} - \frac{N_0^2 - 1}{N_0^2 + 2}\right) \qquad (5.4)$$

Although this is only a disguised percentage estimate of P_A based on the value of P_0, if its presence is realised and understood it affords an improved description of the dielectric properties of 'typical' molecules, provided that P_A is relatively small compared to the total polarization. However, this approach is inadequate for the dimethyl

siloxanes, since they possess small dipole moments and relatively large atomic polarization.

5.03 Electric Dipole Moments of Dimethyl Siloxanes

Sauer and Mead[151] determined the dipole moments of cyclic and linear dimethyl siloxanes having n = 8 to 16 and n = 2 to 10 skeletal bonds, respectively. Their measurements were conducted on undiluted samples at 293K.

However, since these workers used the Onsager equation to interpret the dielectric data, the quantity P_A was totally neglected. Thus, the dipole moments obtained were substantially higher than the values found more recently. Dielectric measurements were repeated by Baker et al[155] on hexamethyldisiloxane in the bulk, and by Freiser et al[159] for the same compond in solution in benzene at 303K. Again, however, the atomic polarization term was not correctly represented. It was not until the publication by Kurita and Kondo[152] of their dielectric results for hexamethyldisiloxane, cyclic trimer and cyclic tetramer, measured at 293K on the pure liquids, that progress was made regarding the contribution of the atomic polarization to the total polarization. It was now known, from both electron diffraction[160] and X-ray diffraction[161], that the structure of the cyclic trimer was a strained planar ring. Thus it was reasonable to assume a zero permanent dipole moment for this first, anomalous, member of the homologous series of cyclic dimethyl siloxanes. The total polarization of the cyclic trimer could, therefore, be attributed to the atomic and electronic contributions only, and since P_E could be calculated (from refractive index measurements), P_A was easily found. This was the basis of the first means of estimating P_A for the higher members.

In 1955 Holland and Smyth[162] began, what was to become, a series of investigations[64,153,154] by Smyth and various coworkers, into the molecular structure of dimethyl siloxane oligomers using microwave techniques. They were able to measure the total distortion polarization ($P_D = P_E + P_A$) of cyclic and linear siloxanes having n = 6 and n = 8, and n = 2 to 8 and n = 12 skeletal bonds, respectively. By measuring static permittivities and refractive indices these authors were able to fully resolve the polarizations for the lower members. Sutton and Mark[65] used an extrapolation of the atomic polarization data, found by Smyth et al[64,154,162], to calculate the dipole moments of the higher chains. The straight line fitted to the atomic polarization data was accurate to a few tenths of a percent for the lower oligomers. Thus, providing the line did not deviate for the higher members, the problem of obtaining reliable atomic polarizations for the linear poly(dimethyl siloxanes) appeared to have been solved. Unfortunately, no similar data was available for the cyclic dimethyl siloxanes.

For all the siloxanes considered in the present study, the total dielectric polarizations were resolved into their electronic, atomic and orientational components and their dipole moments were then derived. The method of Debye[4] was used to obtain the total distorsion polarization, P_D, which in conjunction with a knowledge of the electronic polarization, was used to determine the atomic polarization. This method entails measuring the total polarization at at least two temperatures, and extrapolating to $1/T = 0$ to obtain P_D from the intercept on the P_T axis (see Figure 5.02). The dipole moments of the cyclic and linear oligomers and polymers obtained in this manner

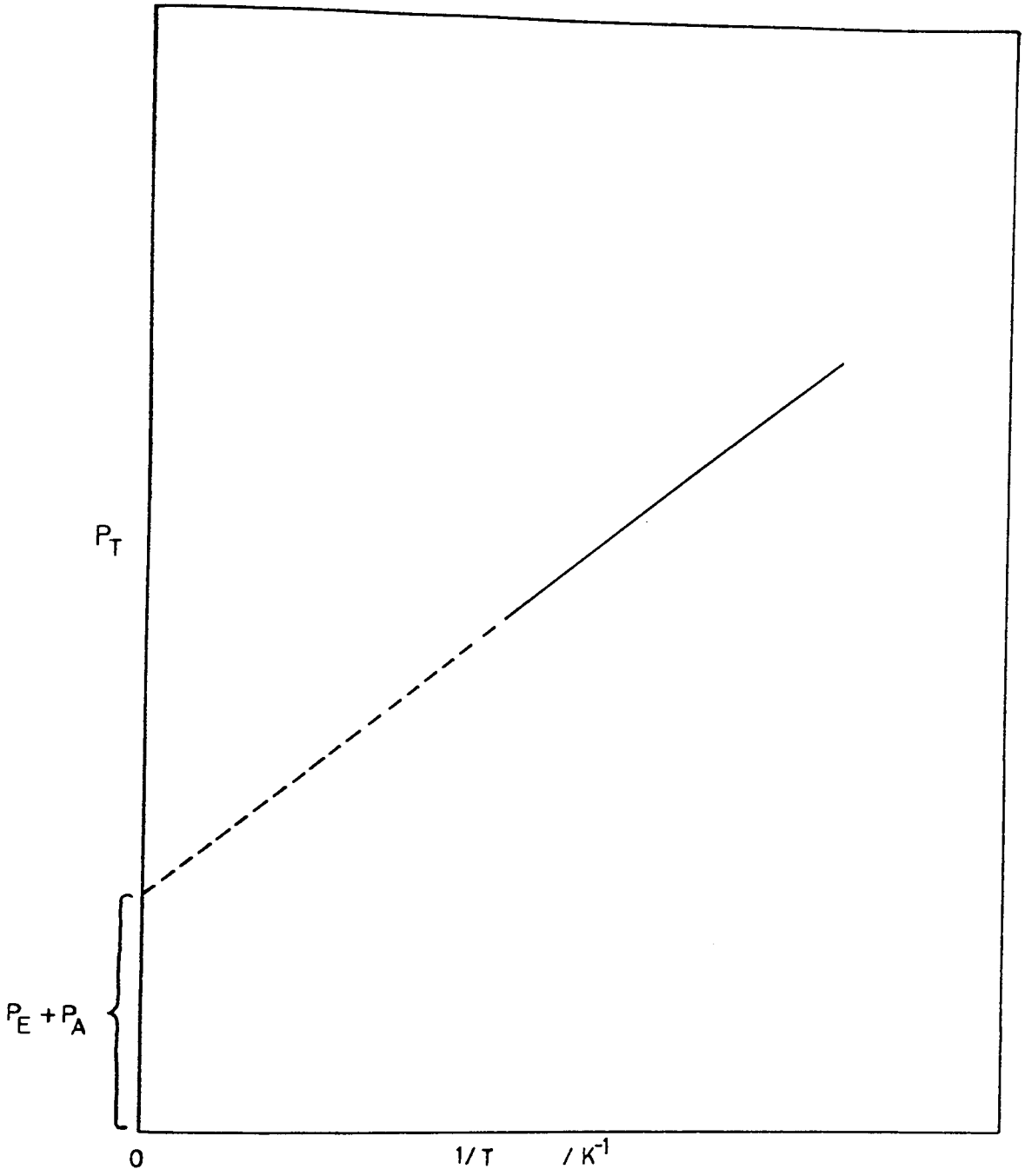

Figure 5.02 Debye method to obtain the distortion polarization ($P_D = P_E + P_A$). The solid line represents experimental points, whilst the broken line corresponds to an extrapolation to $1/T = 0$.

are compared with some values quoted in the literature for cyclic and linear oligomers.

One of the main purposes of this investigation was to discover whether or not there is any difference between the dipole moment of a polar cyclic polymer and the dipole moment of the corresponding linear polymer. Cyclic and linear poly(dimethyl siloxanes) containing up to 200 skeletal bonds were used for this purpose.

5.04 Results and Discussion

The total dielectric polarization, P_T, of each sample was calculated from the corresponding static dielectric permittivity using the familiar relationship[4] :-

$$P_T = \frac{(\varepsilon_0 - 1)}{(\varepsilon_0 + 2)} \frac{M}{\rho} \qquad (5.5)$$

where M is the mean molar mass and ρ is the density. Number average mean molar masses were measured by gas-liquid chromatography and/or gel permeation chromatography and the densities were measured as described in section 3.08. The contribution of the electronic polarization at the frequency of measurement of the static dielectric permittivity (effectively zero), $P_E(\lambda \to \infty)$, was obtained using the Lorentz-Lorenz relationship[4] :-

$$P_E(\lambda \to \infty) = \frac{(n^2_{\lambda \to \infty} - 1)}{(n^2_{\lambda \to \infty} + 2)} \frac{M}{\rho} \qquad (5.6)$$

The infinite wavelength refractive indices, $n_{\lambda \to \infty}$, required for the evaluation of P_E using equation (5.6) were obtained from the measurement of refractive indices at two wavelengths, in conjunction with the Cauchy two term expression, as described in section 4.04 and 4.05.

The total distorsion polarizations, P_D, were derived from measurements of P_T at 298K and 313K using the method of Debye[4] (see section 5.03) and the atomic polarizations calculated assuming:-

$$P_A = P_D - P_E(\lambda \to \infty) \qquad (5.7)$$

Since the value of P_T was determined at zero frequency and $P_E(\lambda \to \infty)$ is the electronic polarization extrapolated to infinite wavelength (zero frequency), it would be more rigorous to denote the atomic polarization by $P_A(\lambda \to \infty)$. This signifies that the atomic polarization may be frequency dependent and that the value of atomic polarization derived in the present study relates to that obtained indirectly by the measurement of P_T at zero frequency. Subsequent references to the atomic polarization will simply be denoted by P_A. However, it is noted that values of P_A obtained in this work may differ slightly from those measured by other techniques (e.g. microwaves).

In Figure 5.03 the experimental atomic polarizations of cyclic and linear dimethyl siloxanes are plotted against the average number of skeletal bonds. The atomic polarizations of the cyclic siloxanes were found to be well described by a single line of regression (see Table 5.01). The atomic polarizations of linear siloxanes are slightly larger than the nearest equivalent cyclic siloxanes and were also found to be reasonably well described by a single line of regression, assuming the same gradient as that found for the cyclic data. The two lines of regression were used to obtain atomic polarizations that were either not available or where it was evident that the experimental value of P_A was associated with an atypically large error. The fractions of linear siloxanes L8, L11 and L13 and the fractions of cyclic siloxanes R4 and R8 were the only samples

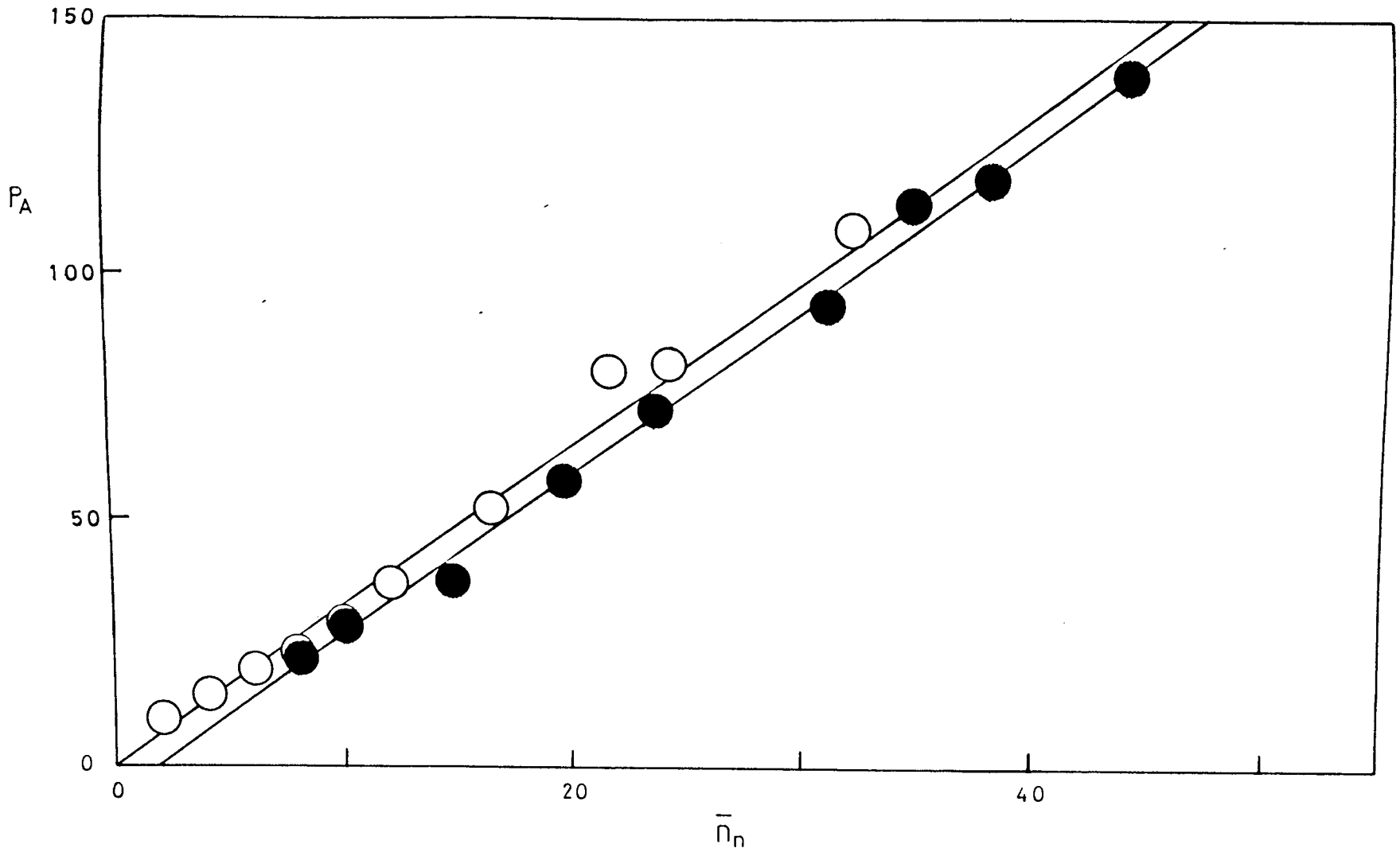

Figure 5.03 Experimental atomic polarizations $P_A(X10^6/m^3mol^{-1})$ of cyclic dimethyl siloxanes (●) and linear dimethyl siloxanes (○).

affected by this procedure in the subsequent calculations of the root-mean-square dipole moments. The atomic polarizations of the linear siloxanes were also calculated using the relationship:-

$$P_A = 2.15 + 2.827\bar{n} \qquad (5.8)$$

derived by Sutton and Mark[65] for the P_A values obtained by Dasgupta and Smyth[64] for linear dimethyl siloxanes with numbers of skeletal bonds in the range $2 \leq \bar{n} \leq 16$. Also, it seems reasonable to assume that for sufficiently large cyclic dimethyl siloxanes their atomic polarizations may be estimated using the similar relationship:-

$$P_A = 2.827\bar{n}$$

The various polarization components obtained using the methods described above are listed in Table 5.01 and in Table 5.02 for the cyclic and linear siloxanes, respectively. The contributions of the orientation polarization, P_O, to the total polarizations were obtained assuming

$$P_O = P_T - P_D, \qquad (5.10)$$

and the root-mean-square dipole moments calculated using the relationship:-

$$\langle\mu^2\rangle^{\frac{1}{2}} = \left(\frac{9P_O kT\varepsilon}{N}\right)^{\frac{1}{2}} \qquad (5.11)$$

$(\varepsilon = 8.854 \times 10^{-12}\ Fm^{-1})$.

In Figure 5.04 the experimental mean-square dipole moments are shown plotted against the mean number of skeletal bonds, $\bar{n}$, for cyclic and linear dimethyl siloxanes at 298K. For cyclic and linear siloxanes with a mean number of skeletal bonds not exceeding ca. 15 there are significant differences between their dipole moments, with the chains possessing the higher values. As the number of skeletal bonds increases the mean-square dipole moments of cyclic and linear siloxanes converge and become identical within experimental error for $\bar{n} \geq 20$.

Table 5.01 Polarizations P_T, P_E, P_A (I. This study; II. Dasgupta and Smyth[64] (see text) and P_0, and root-mean-square dipole moments $\langle\mu^2\rangle^{\frac{1}{2}}$ for cyclic dimethyl siloxanes at 298K.

$\bar{n}$	$10^6 P_T$ ($/m^3mol^{-1}$)		$10^6 P_E$ ($/m^3mol^{-1}$)	$10^6 P_A$ ($/m^3mol^{-1}$)		$10^6 P_0$ ($/m^3mol^{-1}$)	$10^{30}\langle\mu^2\rangle^{\frac{1}{2}}$ (/Cm)
	298K	313K		I	II		
8[a]	98.5	98.2	72.7	21.6[b]	22.6	4.2	1.50
10[a]	129.0	128.5	90.9	27.8	28.3	10.3	2.37
12[a]	164.5	163.7	111.4	36.6	33.9	16.5	3.00
14.7	203.0	201.5	134.3	37.3[c]	41.5	31.4	3.80
19.7	276.6	274.7	179.6	57.4	55.7	39.6	4.64
23.8	334.4	332.2	216.6	71.8	67.2	46.0	5.00
31.2	439.1	436.1	283.7	92.8	88.2	62.6	5.84
35.0	491.7	488.7	317.2	107.8[c]	98.7	66.7	6.03
38.2	538.8	535.2	346.5	117.7	107.9	74.6	6.37
44.0	622.7	618.6	399.8	137.0	124.4	85.9	6.84
109.0	1534	1524	987.9	324.8	308.1	221.3	11.0
190.0	2673	2655	1724	574.7	537.1	374.3	14.3

[a] Single component

[b] From five point plot of P_T vs 1/T (see Figure 4.01)

[c] Calculated using $10^6 P_A = 3.24\bar{n} - 5.46$ (see Figure 5.03)

Table 5.02 Polarizations P_T, P_E, P_A (I. This study; II. Dasgupta and Smyth [64] (see text) and P_O, and root-mean-square dipole moments, $\langle\mu^2\rangle^{\frac{1}{2}}$ for linear dimethyl siloxanes at 298K.

$\bar{n}$	$10^6 P_T$ ($/m^3 mol^{-1}$)		$10^6 P_E$ ($/m^3 mol^{-1}$)	$10^6 P_A$ ($/m^3 mol^{-1}$)		$10^6 P_O$ ($/m^3 mol^{-1}$)	$10^{30}\langle\mu^2\rangle^{\frac{1}{2}}$ (/Cm)
	298K	313K		I	II		
2[a]	60.07	59.91	47.53	9.44	7.80	3.1	1.30
4[a]	87.6	87.18	65.7	14.0	13.5	7.9	2.07
6[a]	115.6	115.0	84.0	19.2[b]	19.1	12.4	2.60
8[a]	144.2	143.3	102.3	23.1	24.8	18.8	3.21
10[a]	172.7	171.6	120.5	29.2	30.4	23.0	3.54
12[a]	201.9	200.6	138.2	36.8	36.0	26.9	3.83
16.5	321.6	263.1	218.1	52.2	48.9	51.3	4.24
21.7	395.3	335.8	263.9	69.4[c]	63.5	62.0	4.83
24.4	432.7	373.9	286.8	81.3	71.1	64.6	4.98
32.4	546.5	488.4	359.4	107.9	93.7	79.2	5.73
41.6	677.1	-	442.6	134.0[c]	119.7	100.5	6.66
105	-	-	980.9	338.8[c]	298.9	-	-
206	2944	-	1896	667.3[c]	584.5	380.7	14.4

[a] Single component

[b] From five point plot of P_T vs 1/T (see Figure 4.02)

[c] Calculated using $P_A = 3.24\bar{n} - 0.962$ (see Figure 5.03)

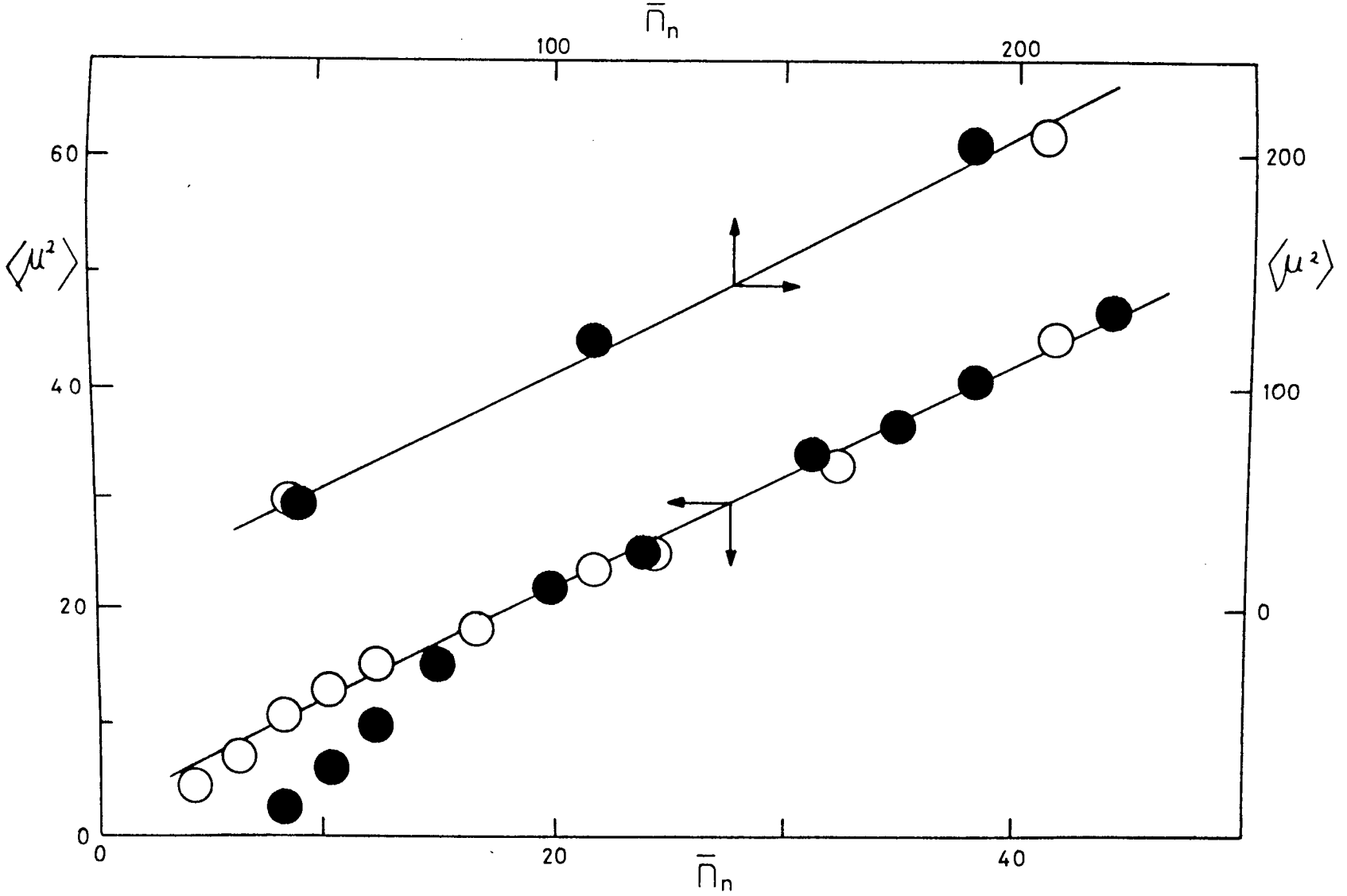

Figure 5.04 Mean square dipole moments $\langle\mu^2\rangle$ ($X10^{60}$/Cm) for cyclic dimethyl siloxanes (●) and linear dimethyl siloxanes (○).

It is important to appreciate the limitations of the Debye method when it is used to measure the atomic and orientation polarizations of flexible, polar molecules. The validity of this approach rests upon two main assumptions. The first assumption concerns the constancy of the mean-square dipole moment, $\langle\mu^2\rangle$, of the materials over the range of temperature in which P_T is measured. For the poly(dimethyl siloxanes) in the undiluted state the temperature coefficient $d\ln\langle\mu^2\rangle/dT$ has been shown to be quite small[64,67] although it is predicted to vary with chain length[67]. The second assumption relates to the neglect of internal reaction fields in the dielectric theory and to the neglect of directional correlation between the dipole moment vectors in addition to the directional correlation imposed by the molecular structure. Dipole moments, corrected for the effects of reaction fields, may be obtained using the relationship:-

$$\langle\mu^2\rangle_{corr} = \frac{(2\varepsilon_0 + \varepsilon_\infty)(\varepsilon_0 + 2)}{3\varepsilon_0\,(\varepsilon_\infty + 2)} \langle\mu^2\rangle \qquad (5.12)$$

based on the theory of Onsager[157](see equation (5.3)). The calculated ratios $\langle\mu^2\rangle_{corr}/\langle\mu^2\rangle$ were found to be less than 1.04 for all of the samples of cyclic and linear siloxanes considered in the present study and reflect the small dipole moment of the Si -O bond (2.0×10^{-30} Cm)[65,154]. It is noted that the Debye method will not be applicable for the determination of P_A and P_0 for 'flexible' polar molecules which possess large link dipole moments, and/or large temperature coefficients $d\ln\langle\mu^2\rangle/dT$, over the temperature range used to measure P_T.

The main conclusion of the present investigation is that in this first comparison of the dipole moments of a synthetic polar cyclic and linear polymer, the dipole moments are found to increase with the number of skeletal bonds but cyclic and linear polymers containing the same number of skeletal bonds have identical dipole moments within experimental error.

CHAPTER 6

ELECTRIC DIPOLE MOMENTS OF DIMETHYL SILOXANES

6.01 Introduction

Simple freely-jointed and free-rotating models are unable to describe the conformations of real polymer chains. By constrast, rotational isomeric-state models have achieved conspicuous success in interpreting the statistical conformations of many unperturbed linear macromolecules. In the rotational isomeric-state representation of a chain molecule, each skeletal bonds is assigned to one of a small number of discrete rotational states[32,163]. Since, the accessibility of such states almost invariably depends on the rotational states of neighbouring bonds, theoretical methods have been developed to take into account this interdependence[32,87,164-168]. The rotational isomeric-state model has been used in the study of random-coil dimensions[169-171], dipole moments[71,84,172], helix-coil transitions[173], ring-chain equilibria[174], stereochemical equilibria[175], the Kerr effect[176] and strain birefringence[177,178].

Studies on α, ω - dibromo-n-alkanes[84], poly(ethylene oxide)[71], and poly(tetramethylene oxide)[72,79] have demonstrated that conformational energies, or statistical weights, obtained from analyses of the random-coil dimensions of chain molecules of high molecular weight give predicted values of dipole moments and their temperature coefficients in good agreement with experiment over a wide range of molecular weight. Conformational energies have been determined for poly(dimethyl siloxane) and their applicability to dimethyl siloxane chains of any length has

been demonstrated by the successful calculation of ring-chain equilibrium constants for dimethyl siloxane molecules having degrees of polymerization ranging from 15-200[174].

In this study the electric dipole moments and temperature coefficients ($d\ln\langle\mu^2\rangle_0/dT$) of the linear poly(dimethyl siloxanes) are calculated using the rotational isomeric-state model of Flory, Crescenzi, and Mark[68]. As part of the development of computer programs for the calculation of the electric dipole moments of cyclic dimethyl siloxanes it was convenient to calculate the electric dipole moments of their linear counterparts; the equivalent open chains. This approach enabled the major aspects of the computer programs to be developed in a rapid, logical fashion and, perhaps more importantly, allowed checks to be made on the calculated dipole moments and their temperature coefficients by comparing the values obtained for the chains with those previously found by Mark[67]. Calculated electric dipole moments are then compared with the experimentally determined values. Temperature coefficients were not determined experimentally in the present study.

6.02 Rotational Isomeric-State Model of Dimethyl Siloxane Chains

In the Flory, Crescenzi and Mark[68] model of poly (dimethyl siloxane), each skeletal bond is assigned to one of three rotational isomeric-states; trans ($\phi = 0^o$), gauche + ($\phi = 120^o$) or gauche - ($\phi = 240^o$).

Generation of the partition function and the average values of conformational-dependent properties requires statistical weight matrices[87,168], the elements of which are the statistical weights for pairs of bond conformations. These matrices have been established for dimethyl siloxanes chains by the analysis of the random-coil

dimensions of the high molecular weight polymer[68]; they should of course, apply to dimethyl siloxane chains of any molecular weight[174]. For pairs of skeletal bonds flanking a silicon atom, the matrix is[68]

$$\underset{\sim}{U}' = \begin{array}{c} \\ t_i \\ g_i^+ \\ g_i^- \end{array} \begin{array}{c} \begin{array}{ccc} t_{i+1} & g_{i+1}^+ & g_{i+1}^- \end{array} \\ \begin{bmatrix} 1 & \sigma & \sigma \\ 1 & \psi\sigma & 0 \\ 1 & 0 & \psi\sigma \end{bmatrix} \end{array} \qquad (6.1)$$

where rows are associated with the states of the O-Si bond, and columns are associated with the following Si-O bond. The statistical weight ψ appearing in equation (6.1) takes into account the possibility of significant interactions occuring in $g^{\pm}g^{\pm}$ states (about O-Si-O bond pairs) which are not present in t $g^{\pm}$ states. Gauche pairs $g^{\pm}g^{\pm}$ of opposite sign must be assigned statistical weights of zero because of the presence of severe steric repulsions between pendant methyl groups in these conformations[68]. The corresponding matrix for conformations about pairs of skeletal bonds flanking an oxygen atom is[68]

$$\underset{\sim}{U}'' = \begin{array}{c} \\ t_{i-1} \\ g_{i-1}^+ \\ g_{i-1}^- \end{array} \begin{array}{c} \begin{array}{ccc} t_i & g_i^+ & g_i^- \end{array} \\ \begin{bmatrix} 1 & \sigma & \sigma \\ 1 & \sigma & \omega\sigma \\ 1 & \omega\sigma & \sigma \end{bmatrix} \end{array} \qquad (6.2)$$

The quantity σ is the statistical weight assigned to t $g^{\pm}$ and $g^{\pm}g^{\pm}$ bond pairs relative to an assignment of unity to tt and $g^{\pm}t$ pairs[68].

The factor ω is included to account for interactions in $g^{\pm}g^{\mp}$ conformations not present in t $g^{\pm}$ and $g^{\pm}g^{\pm}$ states.

The statistical weights may be represented by the following Boltzmann factors:-

$$\sigma = \exp(-E_{\sigma}/RT), \qquad (6.3)$$

$$\omega = \exp(-E_{\omega}/RT), \qquad (6.4)$$

$$\text{and} \quad \psi = \exp(-E_{\psi}/RT), \qquad (6.5)$$

where R is the gas constant, T the absolute temperature and E is the energy, associated with the pair of bonds in a particular conformation, relative to the trans conformation. Analysis of the chain dimensions of poly (dimethyl siloxanes) gave $E_{\sigma} = 3.56 kJmole^{-1}$, a positive energy arising from the disruption of favourable methyl-methyl interactions by transitions $t \rightarrow g^{\pm}$ about either Si - O or O-Si bonds[68]. The value of the energy E_{ω}, which characterizes interactions between O atoms engendered in $g^{\pm}g^{\mp}$ conformations about Si-O-Si bonds, was found[68] to be $4.39 kJmole^{-1}$. The energy E_{ψ} was assumed to be zero on the basis of careful consideration of the interactions involved ($\psi = 1$)[68]; this assumption was shown to be of little importance because of the relative insensitivity of the chain dimensions to this parameter[68].

6.03 Calculation of Dipole Moments of Dimethyl Siloxane Chains

Long range intramolecular interactions are believed to be of little consequence in determining the statistical conformations of undiluted oligomers and polymers in the liquid or amorphous state[30,179]; and, in accordance with accepted practice, mean-square dipole moments, $\langle \mu^2 \rangle_0$, are given the subscript zero to denote reference to chains

unperturbed by excluded volume effects. The angle brackets are used to denote the statistical mechanical average of the mean-square dipole moment over all conformations of the chain.

Calculation of $\langle\mu^2\rangle_0$ requires construction of right-handed Cartesian coordinate systems about each bond in the chain backbone[30]. If the x-axis is taken along bond i and the positive y axis in the plane determined by bonds i and i-1 and making an acute angle with bond i-1, then matrix $\underset{\sim}{T}_i$, which transforms a vector in coordinate system i+1 into that of system i, is[87,168]

$$\underset{\sim}{T}_i = \begin{bmatrix} \cos\theta & \sin\theta & 0 \\ \sin\theta\cos\phi & -\cos\theta\cos\phi & \sin\phi \\ \sin\theta\sin\phi & -\cos\theta\sin\phi & -\cos\phi \end{bmatrix}_i \qquad (6.6)$$

where the bond angle supplement, θ, and the rotational angle ϕ are illustrated in Figure 6.01. The bond angle supplements at oxygen and silicon atoms were taken to be $\theta = 37^o$ and 70^o, respectively[68]. The mean-square dipole moment may then be calculated from[30,87,168]

$$\langle\mu^2\rangle_0 = 2Z^{-1}\ \underset{\sim}{J}^*\ \underset{\sim}{G}_1(\underset{\sim}{G}''\ \underset{\sim}{G}')^X\ \underset{\sim}{G}''\ \underset{\sim}{J} \qquad (6.7)$$

where $\underset{\sim}{J}^*$ is the row vector, [100 ... 000], consisting of a single unity followed by fourteen zeros and $\underset{\sim}{J}$ is the column vector, [000...111], consisting of twelve zeros followed by three unities. The configurational partition function, Z, for the dimethyl siloxane chain is given by[68]

$$Z = \underset{\sim}{I}^*\ (\underset{\sim}{U}''\ \underset{\sim}{U}')^X\ \underset{\sim}{U}''\ \underset{\sim}{I} \qquad (6.8)$$

where $\underset{\sim}{I}^*$ = [100] and $\underset{\sim}{I}$ is the transpose of [111]. The number of repeat units, x, is related to the number of siloxane bonds, n, by n = 2x + 2. The generator matrix, $\underset{\sim}{G}_i$ has the form[168]

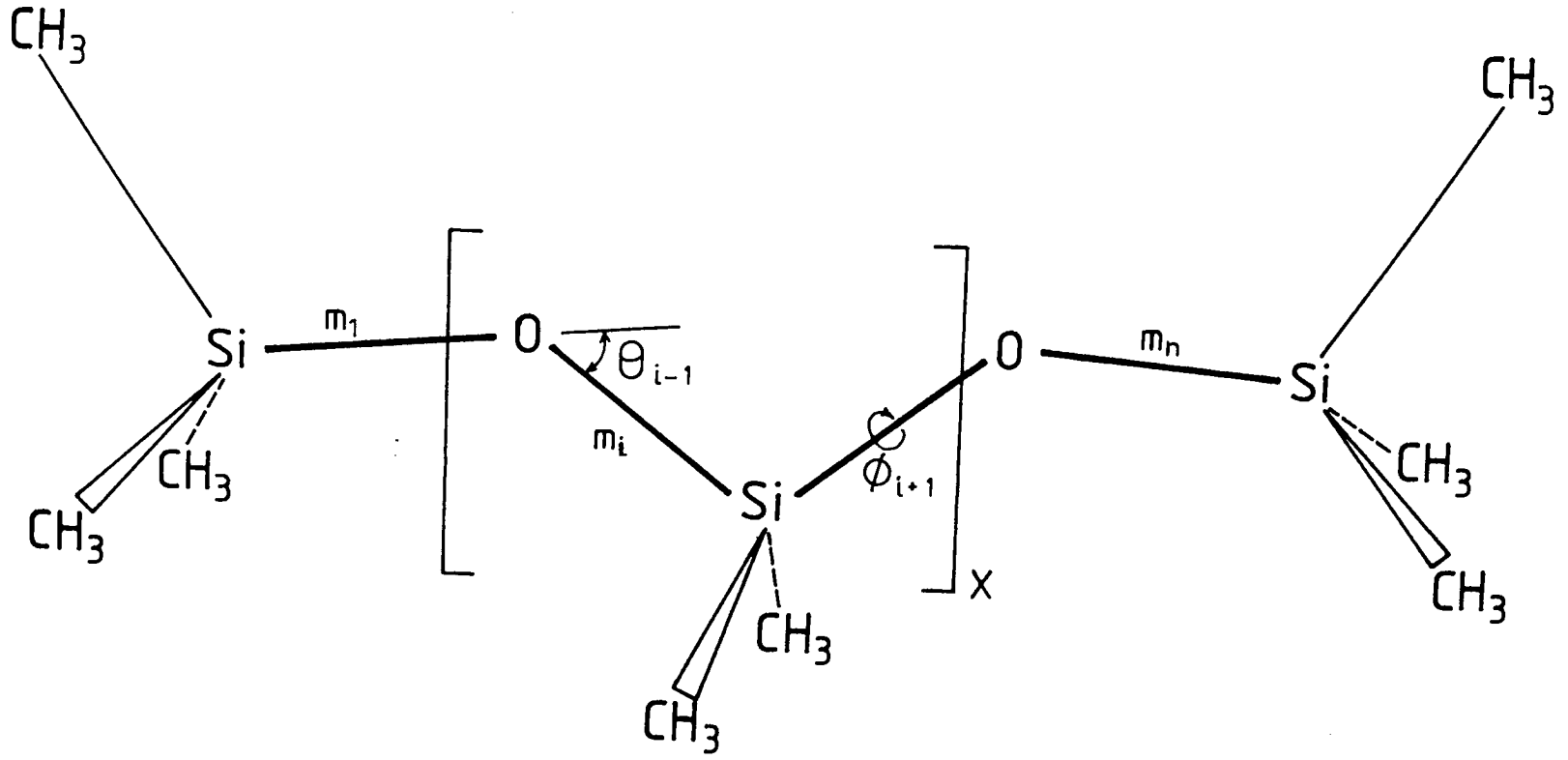

Figure 6.01 Schematic representation of the all-trans conformation of dimethyl siloxane chain of degree of polymerization x + 1(n = 2x + 2). Solid, heavy lines represent bond dipole moments.

$$\underset{\sim}{G}_i = \begin{bmatrix} \underset{\sim}{u} & (\underset{\sim}{u} \otimes \underset{\sim}{m}^T)||\underset{\sim}{I}|| & (\tfrac{1}{2}m^2)\ \underset{\sim}{u} \\ \underset{\sim}{0} & (\underset{\sim}{u} \otimes \underset{\sim}{E}_3)||\underset{\sim}{I}|| & \underset{\sim}{u} \otimes \underset{\sim}{m} \\ \underset{\sim}{0} & \underset{\sim}{0} & \underset{\sim}{u} \end{bmatrix}_i \qquad (6.9)$$

where $\underset{\sim}{0}$ denotes a block of zeros of the appropriate size and the subscript i on the bracket refers to all quantities contained therein; $\underset{\sim}{U}_1$ required in $\underset{\sim}{G}_1$ is simply the unit matrix $\underset{\sim}{E}_3$ of order three. The symbol $\otimes$ denotes the matrix direct product[87,168] (or Kronecker product), and $\underset{\sim}{m}$ is the bond moment vector,

$$\underset{\sim}{m} = \begin{bmatrix} m \\ 0 \\ 0 \end{bmatrix} , \qquad (6.10)$$

with $\underset{\sim}{m}^T$ its transpose. The link dipole moment was taken to be 2.0×10^{-30} Cm in the calculations presented here. This value is obtained from the experimental dipole moment of hexamethyldisiloxane (1.30×10^{-30}Cm) by assuming a supplementary bond angle of 37^o at the oxygen atom. The supermatrices, $||\underset{\sim}{I}_i||$, are defined by[87,168]

$$||\underset{\sim}{I}_i|| = \begin{bmatrix} \underset{\sim}{I}_i(\phi = 0^o) & \underset{\sim}{0} & \underset{\sim}{0} \\ \underset{\sim}{0} & \underset{\sim}{I}_i(\phi = 120^o) & \underset{\sim}{0} \\ \underset{\sim}{0} & \underset{\sim}{0} & \underset{\sim}{I}_i(\phi = 240^o) \end{bmatrix} \qquad (6.11)$$

6.04 Comparison of Calculated and Experimentally Determined Dipole Moments of Dimethyl Siloxane Chains

The mean-square dipole moments calculated for the dimethyl siloxane chains by means of equation (6.7) are plotted in Figure 6.02. The values obtained were found to be in very good agreement with those of Mark[67]. It may be seen from this plot that after some initial curvature of the line, the values of $\langle\mu^2\rangle_0$ are predicted to rise monotonically

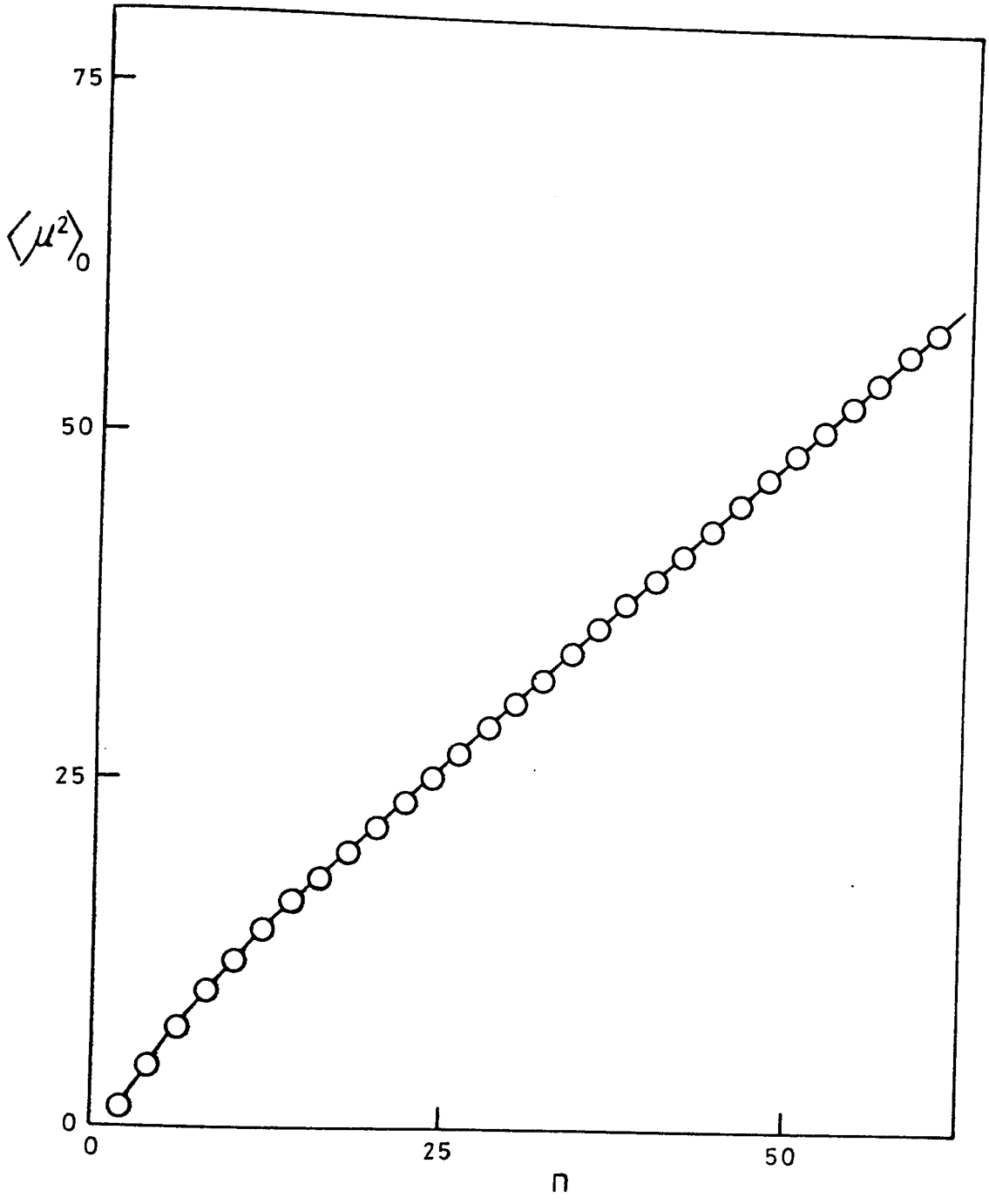

Figure 6.02 Calculated mean-square dipole moments, $\langle\mu^2\rangle_0 (X10^{60}/C^2m^2)$, of dimethyl siloxane chains.

Table 6.01 Number-average number of backbone bonds, $\bar{n}$, and root-mean-square dipole moments, $\langle\mu^2\rangle_0^{\frac{1}{2}}$, at 298K (I. Experimentally determined (see Chapter 5); II. Calculated using equation (6.7)).

$\bar{n}$	$\langle\mu^2\rangle_0^{\frac{1}{2}}$	
	I ($X10^{30}$/Cm)	II ($X10^{30}$/Cm)
2	1.30	1.27
4	2.07	2.07
6	2.60	2.67
8	3.21	3.14
10	3.54	3.46
12	3.83	3.77
16.5	4.24	4.23 (n = 16)
21.7	4.83	4.84 (n = 22)
24.4	4.98	5.04 (n = 24)
32.4	5.73	5.70 (n = 32)
41.6	6.66	6.47 (n = 42)
105	-	9.95 (n = 106)
206	14.4	13.9 (n = 206)

with increasing chain length.

Experimentally determined root-mean-square dipole moments of fractions of dimethyl siloxane chains are listed in Table 6.01, together with the corresponding values calculated for the nearest equivalent chain molecules. Good correlation between experiment and theory may be observed over the entire range of molecular weight.

6.05 Comparison of Calculated and Experimentally Determined Dipole Moment Ratios for Dimethyl Siloxanes

A quantity which is very sensitive to the conformational properties of flexible polymer molecules is the dipole moment ratio[57], $\langle\mu^2\rangle_0/nm^2$, where m is the link dipole moment. Experimental values of this ratio for cyclic and linear dimethyl siloxane oligomers and poly(dimethyl siloxanes) calculated using $m = 2.0 \times 10^{-30}$ Cm are plotted in Figure 6.03 and are compared with values found by Dasgupta, Garg and Smyth[154]; Dasgupta and Smyth[64] and Sutton and Mark[65]. Included in this comparison are theoretical values of $\langle\mu^2\rangle_0/nm^2$ calculated for chains of poly(dimethyl siloxane) at 298K using the rotational isomeric state model of Flory, Crescenzi and Mark[68]. For the small cyclic molecules ($\bar{n} < 20$) the dependence of the dipole moment ratio on the number of skeletal bonds is quite different to that observed for the corresponding linear molecules. The dipole moment ratio has a maximum value at $\bar{n} = 8$ for linear siloxanes whereas for the cyclic siloxanes the ratio simply increases steadily with increasing ring size and approaches the value (~ 0.26) found for the long chain molecules of dimethyl siloxane. The very small values of the dipole moment ratio obtained for the low molecular weight cyclic dimethyl siloxanes support the view[57] that the mean-square dipole

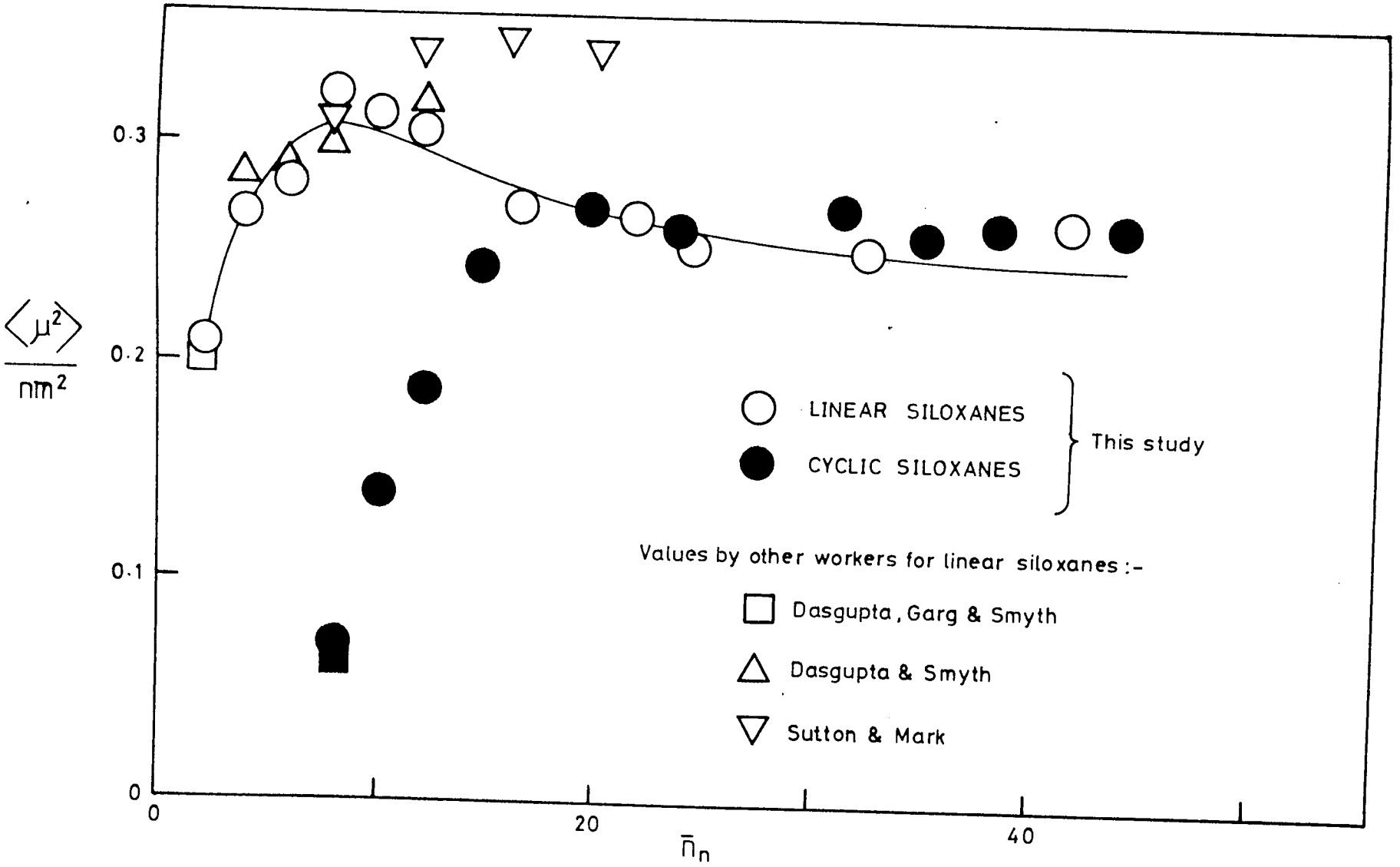

Figure 6.03 Comparison of dipole moment ratios, $\langle\mu^2\rangle_0/nm$, of cyclic and linear dimethyl siloxanes as found in this study and by other workers. The unbroken line was calculated for linear siloxanes using the theory of Flory, Crescenzi and Mark at 298K.

moment ratio of linear dimethyl siloxanes decreases rapidly after $\bar{n} = 8$ because of the alternating skeletal bond angles and statistically favoured all-trans conformation. For cyclic dimethyl siloxanes the intramolecular cancellation of the link dipole moments is expected to be enhanced since the cyclic molecules are constrained to be more centrosymmetric than the nearest equivalent linear molecules. There is a very good agreement between the experimental and theoretical values of $\langle\mu^2\rangle_0/nm^2$ for the linear dimethyl siloxanes over the entire range of $\bar{n}$ considered in the present study.

The small differences between the dipole moment ratios obtained for the linear siloxanes in the present study (see Figure 6.03) and those found in earlier studies are mainly due to the various methods used to estimate or measure the atomic polarization, P_A. Thus, the values of P_A quoted by Sutton and Mark[65] for the linear dimethyl siloxanes in the undiluted state were obtained from a linear extrapolation of a relationship derived by these authors based on values of P_A measured for low molecular weight linear dimethyl siloxanes with $\bar{n} \leq 14$ (see Section 5.03). In Figure 6.04 are plotted the atomic polarizations of the linear dimethyl siloxanes measured in this study and those measured by Dasgupta and Smyth[64]. The unbroken line represents the line of regression fitted to the atomic polarizations obtained in this investigation. The broken line is the line of regression fitted to the atomic polarizations measured by Dasgupta and Smyth[64], which was extrapolated by Sutton and Mark[177] to obtain atomic polarizations for the higher molecular weight members. A diversion of the lines with increasing molecular weight is apparent. Thus, the extrapolation of the line by Sutton and Mark[177] to obtain atomic polarizations of the linear dimethyl siloxanes for which n considerably exceeds 14 would seem invalid.

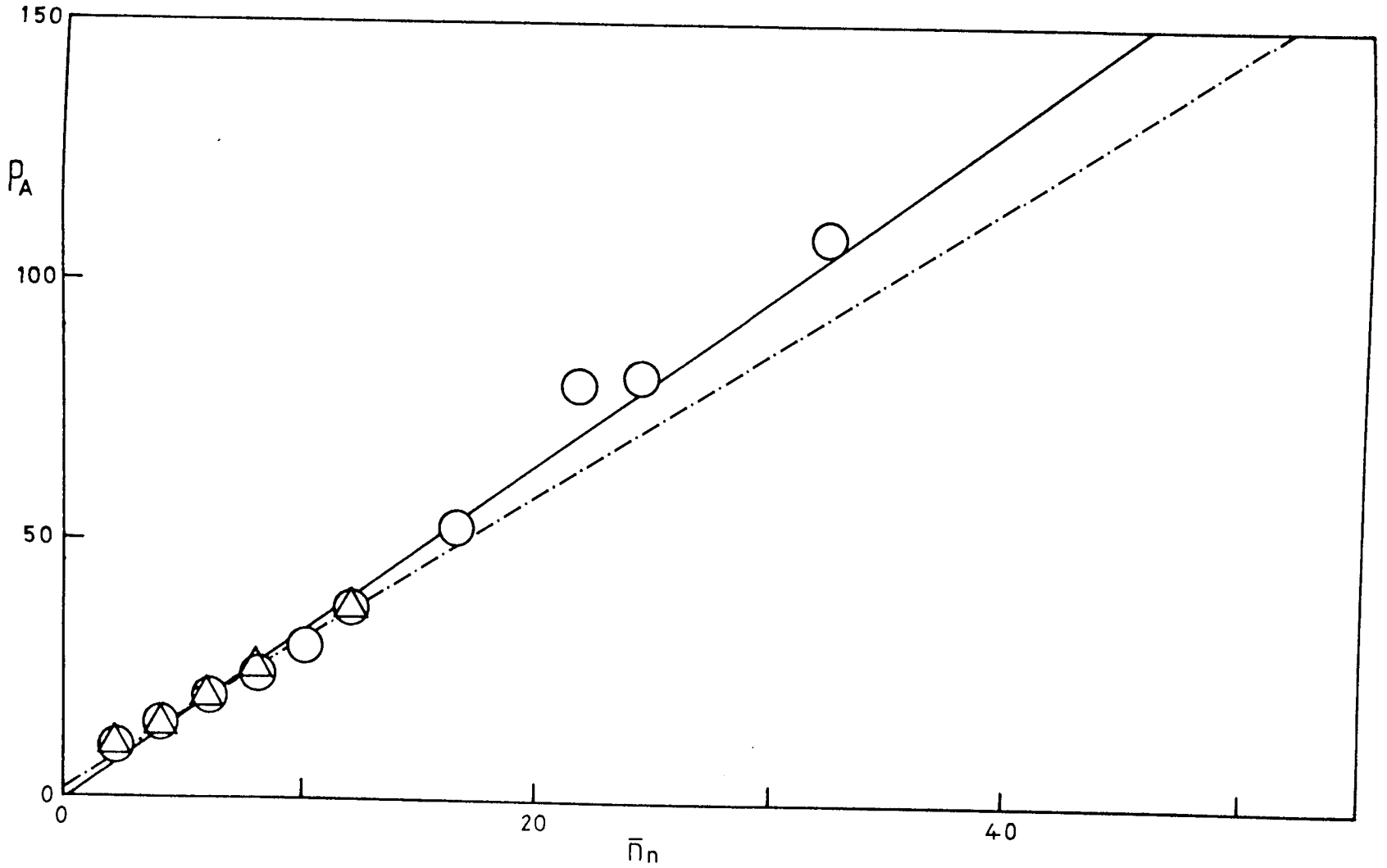

Figure 6.04 Experimental atomic polarizations, $P_A(X10^6/m^3mol^{-1})$ of linear dimethyl siloxanes as measured in this study (○) and by Dasgupta and Smyth (△).

6.06 Calculation of the Temperature Coefficients of the Mean-Square Dipole Moment of Dimethyl Siloxane Chains

Temperature coefficients of the mean-square dipole moment of dimethyl siloxane chains at 298K were calculated using [68]

$$\frac{d\ln\langle\mu^2\rangle_0}{dT} = T^{-1}\left(\frac{l_n\,\sigma\,\partial\ln\langle\mu^2\rangle_0}{\partial l_n\sigma} + \frac{l_n\,\omega\,\partial\ln\langle\mu^2\rangle_0}{\partial l_n\omega}\right) \qquad (6.12)$$

and entries of columns 2 and 3 of Table 6.02. The results are given in the final column of Table 6.02. The predicted temperature coefficent is negative for small values of n, reaching a maximum magnitude at n = 8, thereafter, it increases monotonically, reaching a moderately large, positive value in the limit of large n. Unfortunately. in the range of molecular weight under investigation in this study the values of temperature coefficient were too small to be verified experimentally.

Values of the temperature coefficients of the mean-square dipole moment calculated here for the dimethyl siloxane chains will be compared, in the following chapter, with those calculated for the cyclic dimethyl siloxanes.

Table 6.02 Partial derivatives $\partial \ln \langle \mu^2 \rangle_0 / \partial \ln \sigma$ and $\partial \ln \langle \mu^2 \rangle_0 / \partial \ln \omega$, and temperature coefficients of the mean square dipole moment of linear dimethyl siloxanes calculated at 298K using the F.C.M. model.

n	$\frac{\partial \ln \langle \mu^2 \rangle_0}{\partial \ln \sigma}$	$\frac{\partial \ln \langle \mu^2 \rangle_0}{\partial \ln \omega}$	$\frac{10^3 d \ln \langle \mu^2 \rangle_0}{dT}$
2	0.000	0.000	0.00
4	-0.234	-0.004	-1.15
6	-0.317	-0.007	-1.57
8	-0.335	-0.008	-1.66
10	-0.312	-0.009	-1.56
12	-0.268	-0.008	-1.34
14	-0.218	-0.008	-1.10
16	-0.173	-0.008	-0.88
18	-0.136	-0.007	-0.70
20	-0.106	-0.006	-0.55
22	-0.083	-0.005	-0.43
24	-0.065	-0.004	-0.34
26	-0.050	-0.003	-0.26
28	-0.038	-0.003	-0.20
30	-0.027	-0.002	-0.14
40	0.011	0.000	0.05
50	0.052	0.002	0.26
100	0.087	0.004	0.44
150	0.105	0.005	0.54
200	0.114	0.005	0.58

CHAPTER 7

THEORETICAL INVESTIGATION OF THE DIPOLE MOMENTS AND STATISTICAL CONFORMATIONS OF CYCLIC DIMETHYL SILOXANE OLIGOMERS

7.01 Introduction

In this chapter the calculation of the dipole moments of some cyclic dimethyl siloxanes with n = 8 - 20 is detailed. The method used employs a modified form of the rotational isomeric state model (RISM) of Flory, Crescenzi and Mark[68], which was utilised in the previous chapter for the calculation of the dipole moments of poly(dimethyl siloxane) chains. The matrix representation of this model, which uses a single generator matrix to describe the geometrical and energetic properties associated with each skeletal bond, cannot be used directly to calculate the properties of cyclic molecules since it is not known at the outset which conformations of the equivalent open chain correspond to those adopted by a cyclic molecule. However, the FCM model may still be utilized provided that one or two modifications are implemented. Essentially, all possible conformations, defined by a three-state RISM, of the equivalent open chains are generated using a computer program and the relative positions and orientations of the terminal skeletal bonds of the chains are carefully examined. If certain geometrical criteria are satisfied then the conformations are accepted to be those adopted

by a cyclic molecule and their statistical weights and dipole moments are calculated. The latter quantities may then be compared with values determined experimentally.

7.02 Cyclic Conformations of Equivalent Open Chains

The generation of cyclic conformations, using the concept of an equivalent open chain, raises an important question concerning the criteria used for the selection of the conformations of chains that approximate to conformations which could be adopted by the corresponding cyclic molecules. In a previous study it has been suggested that for unperturbed polymer chains a single test, involving only the end-to-end distance of the chains, may be used for this purpose[180,181]. Thus, for example, if the ends of the chains are separated by less than 0.3nm (say) then the chain conformations are assumed to be approximately the same as those of the corresponding cyclic molecules. Admittedly this is a subjective approach since it is necessary to choose an apparently arbitary value for the maximum acceptable end-to-end distance between the terminal atoms of the chains. Nevertheless this simple selection procedure appears to be satisfactory for the calculation of the mean-square radii of gyration[54] and equilibrium cyclization constants[181-184] of cyclic dimethyl siloxanes. It seems that in these types of calculations it is sufficient to specify the relative positions of the terminal atoms or groups of the open chains soley in terms of the scalar part of the displacement vector of the terminal pair of atoms. However, this approach is not expected to be satisfactory for the calculation of the dipole moments of the cyclic oligomers of dimethyl siloxanes. This is because the model employed in the calculation of the dipole moments is based on the concept of an equivalent open chain and the relative orientations

and rotational states of the terminal bonds of the chain must be accurately defined to permit evaluation of the molecular dipole moment. Consequently, a number of geometrical and conformational constraints must be imposed on the terminal skeletal bonds of the equivalent open chains which have to be satisfied before conformations are accepted to be those adopted by a cyclic molecule. The structure and nomenclature used in the present calculations are depicted in Figure 7.01. In order to simplify certain aspects of the calculations the exact equivalent open chain of a cyclic x-mer $\{(CH_3)_2\ SiO\}_x$ was extended by an extra silicon atom, Si_N. Thus, the equivalent chain used in the present calculations may be represented by $\{(CH_3)_2\ SiO\}_x Si$-. The important geometrical parameters are the angle $\theta_{N'}$, which may be regarded as the bond angle supplement associated with the closing bond denoted by N', the end-to-end distance r separating the terminal atoms Si_0 and Si_N of the equivalent open chain and the angle $\phi_{N'}$; the latter being defined by the relative orientations of the first and (N - 1)th skeletal bonds. It may be seen that for perfect closure to form a cyclic structure the skeletal atom Si_N must be exactly superimposed on the skeletal atom Si_0 and the vector corresponding to the virtual bond denoted by N' must coincide with the N^{th} bond vector (ie. r equals zero). The supplementary bond angles were fixed at 37^o for the oxygen atoms and at 70^o for the silicon atoms (except $\theta_{N'}$ which is to be calculated). The end-to-end distance r and angles $\theta_{N'}$ and $\phi_{N'}$ were calculated for each conformation generated by successively setting skeletal bonds i = 1, 2, ... N - 1 in all possible combinations of rotational states defined by trans ($\phi_i = 0^o$) and gauche ($\phi_i = \pm 120^o$) conformations. The principal criteria used for the selection of cyclic conformations were that angle $\theta_{N'}$ should lie within the range

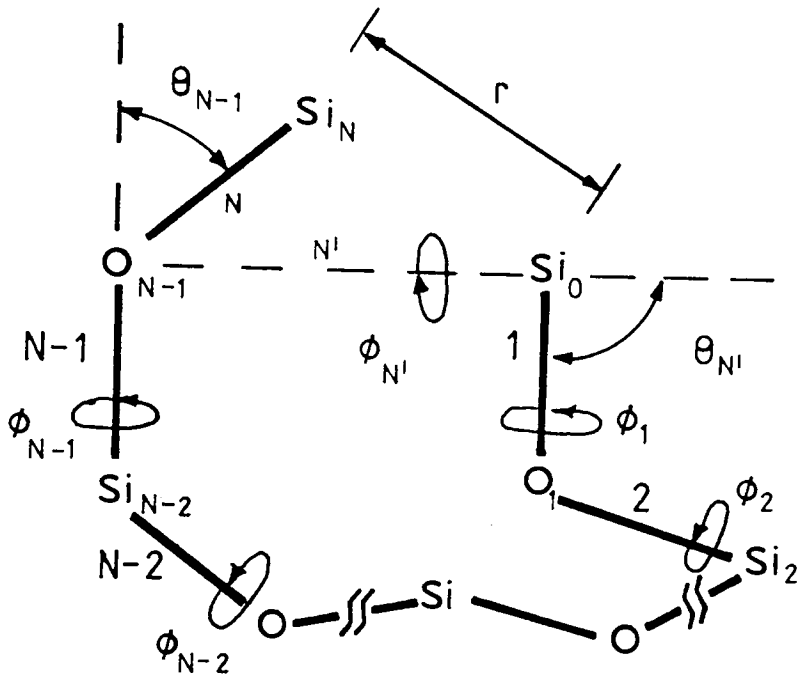

Figure 7.01 Equivalent open chain of a cyclic dimethyl siloxane $[(CH_3)_2\ SiO]_X$ (n = 2x) showing terminal skeletal bonds juxtaposed for a trail cyclic conformation.

$70^{o} \pm 15^{o}$ and that angle $\phi_{N'}$ should be close to the values used in the FCM RISM ($0^{o} \pm 15^{o}$ or $\pm 120^{o} \pm 15^{o}$)[68]. To avoid geometrical ambiguities arising from the position of skeletal atom O_{N-1} a check was made to ensure that its y-coordinate, expressed in the coordinate system centred on Si_{o}[68], was negative and that its z-coordinate was not greater than ± 0.05nm. The end-to-end distance, r, should be zero for perfect cyclic formation, but this restriction excludes almost all of the generated conformations, many of which require only a small adjustment of the bond rotational angles to complete the closure of the ring. In a later section of this chapter it will be demonstrated that fairly minor changes in the rotational states of the skeletal bonds can have a significant effect on the end-to-end distance of the chains without greatly modifying any other calculated parameters. Thus, conformations adopted by the equivalent chains were accepted to be cyclic conformations if their end-to-end distances were less than or equal to 0.35nm, provided that they possessed a non-zero statistical weight and that they satisfied the angular restrictions discussed above. The bond rotational angle $\phi_{N'}$ was evaluated and used (equation 6.1 and 7.1) in the calculation of the statistical weights of the resultant cyclic conformations.

In Figure 7.02 the number, n(x, r), of cyclic conformations accepted as a function of the end-to-end distance of the equivalent open chain are given for x = 4 - 10. For x = 4 - 7 the imposition of a three-state rotational isomeric model results in a rather discontinuous functional form for n(x, r) which rapidly becomes effectively continuous (subject to the incremental difference in r used to classify the end-to-end distances) for x = 8, 9 and 10. For x = 10 a statistical weight cut-off procedure was used to reduce computing times by excluding conformations associated with statistical weights of less than 10^{-7}. The effect of this procedure on the calculated dipole moments will be

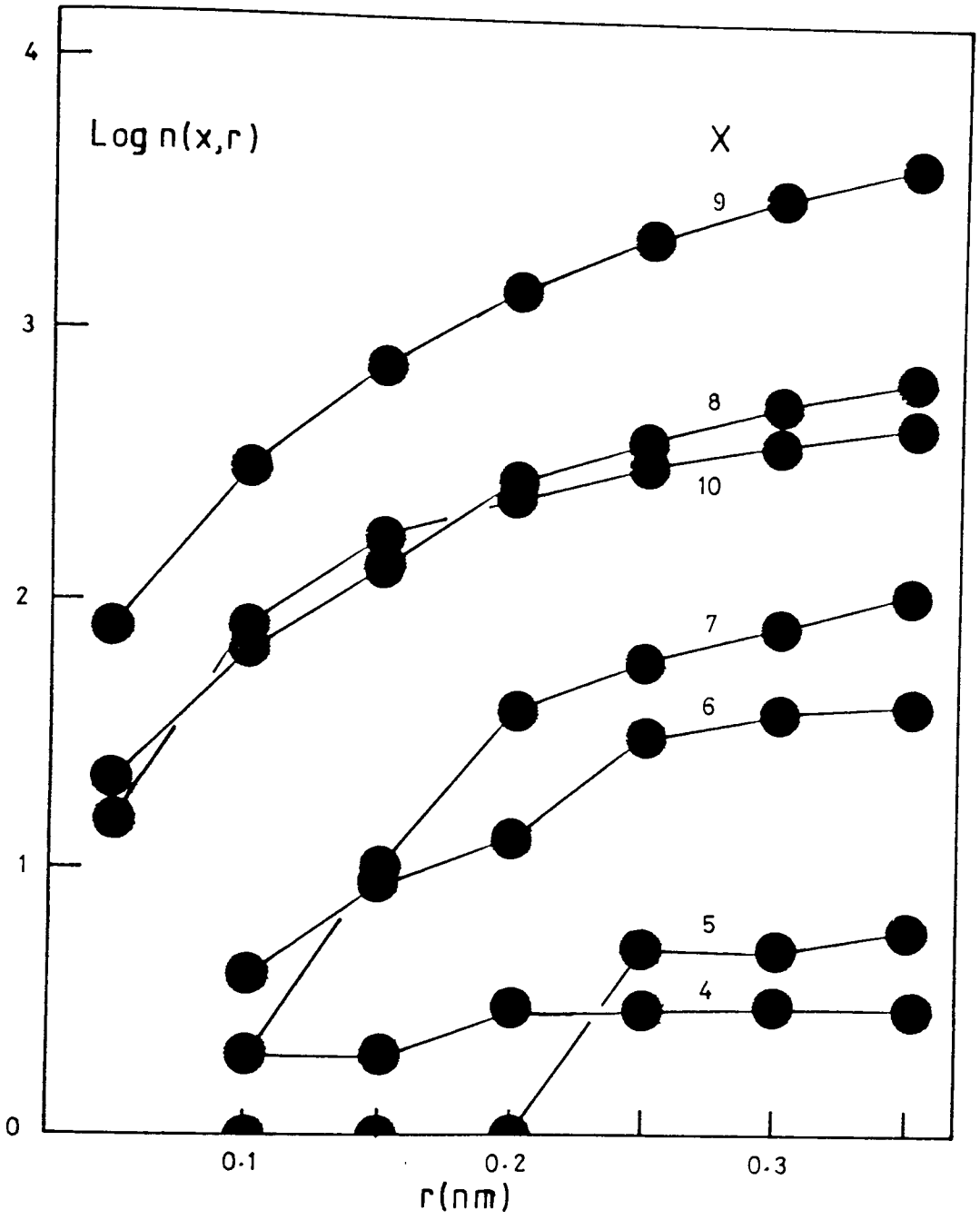

Figure 7.02 Numbers, n(x, r), of cyclic conformations vs end-to-end distance r for x = 4-10.

discussed subsequently.

7.03 Rotational Statistical Weight Matrices

The scheme of statistical weight matrices described in Section 6.02 for the linear dimethyl siloxanes requires modification before it can be used to assign statistical weights to conformations of cyclic dimethyl siloxanes. This is necessary because it is known that there are no severe steric conflicts between non-bonded atoms or groups for the sequence of bond rotational states $g^{\mp}g^{\pm}g^{\mp}g^{\pm}$ centred about a silicon atom, whereas the FCM model would accord a statistical weight of zero for such combinations of bond rotational states[181,183]. For the calculation of the dipole moments of long poly(dimethyl siloxane) chains this observation is of little consequence, but it becomes relatively important when considering the very small fraction of chain conformations which correspond to cyclic conformations. In the present calculations this problem was taken into account by employing two types of statistical weight matrices $\underset{\sim}{U}'$; one matrix corresponding to the form already given in equation (6.1) which was used to determine the statistical weight associated with sequences of rotational states $tg^{\pm}g^{\mp}t$ and $g^{\pm}g^{\pm}g^{\mp}g^{\mp}$, the other matrix being

$$\underset{\sim}{U}' = \begin{array}{c} \\ t_{i-1} \\ g^{+}_{i-1} \\ g^{-}_{i-1} \end{array} \begin{array}{c} \begin{array}{ccc} t_i & g^{+}_i & g^{-}_i \end{array} \\ \begin{bmatrix} 1 & \sigma & \sigma \\ 1 & \sigma & \sigma \\ 1 & \sigma & \sigma \end{bmatrix} \end{array} \qquad (7.1)$$

which was used to calculate the statistical weight of conformations containing sequences of bond rotational states $g^{\mp}g^{\pm}g^{\mp}g^{\pm}$ centred about a silicon atom. This amended statistical weight scheme was employed in all the calculations involving cyclic conformations of the open

chains, but as anticipated proved to be an unnecessary refinement for calculating the properties of the linear dimethyl siloxanes free to adopt all possible conformations specified by the FCM model.

7.04 Calculation of the Dipole Moments

The statistical weight, Ω, and the dipole moment, μ, of each of of the cyclic conformations was calculated assuming a value of 2.0×10^{-30} Cm for the silicon-oxygen bond and zero dipole moments for all other bonds. After examination of all the 3^{N-1} $(= 3^{2X-1})$ conformations generated for the equivalent open chain of a cyclic x-mer the mean-square dipole moment of the cyclic conformations with end-to-end distances in the range 0-r, was calculated using the expression

$$\langle \mu^2 \rangle_0 = \frac{\overset{\Sigma\Omega\mu^2}{\{\emptyset\}_r}}{Z_r} \qquad (7.2)$$

where Z_r is the configurational partition function of the cyclic conformations of the equivalent open chain with end-to-end distances in the range 0-r and is defined by

$$Z_r = \overset{\Sigma\Omega}{\{\emptyset\}_r} \qquad (7.3)$$

and $\{\emptyset\}_r$ denotes summation over all conformations possessing end-to-end distances in the range 0-r.

Table 7.01 lists values of Z_r for x = 4-10 calculated using the FCM model and the hard-sphere model ($\sigma = \omega = 1$). The entries in the final column of Table 7.01 are the total configurational partition functions calculated for the equivalent open chains described by the FCM model. It is noteworthy that the configurational partition function associated with the cyclic conformations of any particular x-mer is several orders of magnitude less than the total configurational partition function of the corresponding equivalent open chain. In

Table 7.01 Configurational partition function, Zr, for cyclic conformations of the equivalent open chain dimethyl siloxanes $[(CH_3)_2SiO]_xSi-$ with end-to-end distance in the range 0 to r nm calculated using the amended FCM RISM at 298K and the hard-sphere RISM.

n		r(nm)							Z_r chain
		0.05	0.10	0.15	0.20	0.25	0.30	0.35	
8	$10^8 Z_r$ =	0	0.86	0.86	0.89	0.89	0.89	0.89	8.22
8		(0)[a]	(2)	(2)	(3)	(3)	(3)	(3)	
10	$10^6 Z_r$ =	0	0.152	0.152	0.152	1.27	1.27	1.27	16.4
10		(0)	(1)	(1)	(1)	(5)	(5)	(6)	
12	$10^5 Z_r$=	0	0.179	0.794	0.884	0.981	1.70	1.70	32.7
12		(0)	(4)	(9)	(13)	(31)	(38)	(41)	
14	$10^4 Z_r$=	0	0.927	0.936	1.09	2.06	2.08	2.20	65.2
14		(0)	(2)	(10)	(39)	(60)	(81)	(110)	
16	$10^4 Z_r$=	0	0.928	7.62	39.7	41.2	41.5	41.5	130.1
16		(21)	(66)	(137)	(279)	(411)	(558)	(695)	
18	$10^4 Z_r$=	0.011	0.078	0.193	0.219	0.286	0.700	1.55	259.6
18		(74)	(289)	(745)	(1472)	(2277)	(3246)	(4333)	
20[b]	$10^3 Z_r$=	0.518	4.82	13.6	46.8	61.2	122.0	133.0	517.8
20		(15)	(81)	(169)	(246)	(325)	(402)	(468)	

[a] Quantities in parentheses indicate hard-sphere model ($\sigma = \omega = 1$).

[b] Conformations with statistical weights < 10^{-7} are excluded.

Table 7.02 the root-mean-square dipole moments for cyclics with x = 4-10 calculated using the FCM model at 298K, are listed as a function of the end-to-end distance, r, of the corresponding equivalent open chains. Included in this table are the experimental values of $\langle\mu^2\rangle_0^{\frac{1}{2}}$ measured for cyclics with x = 4, 5, 6, 7 and 10 in the undiluted state at 298K.

In a rigorously applied RISM the root-mean-square dipole moment should be calculated using only those conformations which possess a zero end-to-end distance, fixed bond angles and a non-zero statistical weight. In practice this rigid approach proved not to be very successful because it excluded many potential cyclic conformations. This is a consequence of using a model in which discrete rotational states are assigned to each rotatable skeletal bond. An alternative approach is to consider how Z_r and $\langle\mu^2\rangle_0^{\frac{1}{2}}$ vary as a function of the accepted end-to-end distance of the equivalent open chains. Referring to Table 7.02 it can be seen that if the end-to-end distance is greater than about 0.15nm then for a given value of x the calculated root-mean-square dipole moment is reasonably constant for different values of end-to-end distance up to a value of at least 0.35nm (approximately twice the length of the skeletal bond). For end-to-end distances less than 0.15nm the number of accepted cyclic conformations decreases dramatically (Figure 7.02) and values of $\langle\mu^2\rangle_0^{\frac{1}{2}}$ become either inaccurate and/or indeterminate. A more realistic approach would be to generate conformations using bond rotational states additional to those already specified by the FCM model, but such an approach would demand a great deal more detail concerning the conformational energies of the skeletal bonds.

Table 7.02 Calculated root-mean-square dipole moments ($x10^{30}$/Cm) of the cyclic conformations of the equivalent open chain $[(CH_3)_2SiO]_x$ Si- with end-to-end distances in the range 0 to r and experimental dipole moments for cyclic dimethyl siloxanes in the undiluted state at 298K.

n	r(nm)							EXPT.
	0.05	0.10	0.15	0.20	0.25	0.30	0.35	
8	-	0.13	0.13	0.33	0.33	0.33	0.33	1.50
10	-	3.95	3.95	3.95	2.41	2.41	2.41	2.37
12	-	4.10	2.75	2.71	2.83	2.81	2.81	3.00
14	-	3.94	3.96	3.90	3.92	3.92	3.89	3.79
16	1.73	4.07	4.86	5.25	5.24	5.24	5.24	-
18	6.26	6.14	5.68	5.72	5.46	4.69	4.11	-
20	5.39	4.67	4.21	4.57	4.79	4.90	4.81	4.64

7.05 Adjustment of the Bond Rotational States

The number of accepted cyclic conformations with end-to-end distances close to zero can be considerably increased by allowing the rotational states of the skeletal bonds to depart slightly from the rigidly defined states used in the FCM model. Provided that the bond rotational angles do not depart too much from those values used in the FCM RISM then the FCM statistical weight scheme may still be applied without serious loss of rigour since it is known that the rotational potential energy functions for poly(dimethyl siloxane) are slowly changing functions with respect to the various bond rotational angles[68]. Each of the cyclic conformations of the equivalent open chain, defined by the FCM model, may be used as a starting point for the generation of an additional 3^{2X-1} conformations by permitting each rotatable skeletal bond to adopt nine rotational states instead of the more usual three states. Thus, if a conformation, described by the FCM model, is represented by the sequence of rotational states

$$\phi_1 , \phi_2, \ldots \phi_{N-1} \qquad (7.4)$$

then the additional 3^{2X-1} conformations of the equivalent open chain may be represented by the set of bond rotational states.

$$\begin{aligned}
\phi_1 &= \phi_1, \phi_1 \pm \Delta\phi_1 \\
\phi_2 &= \phi_2, \phi_2 \pm \Delta\phi_2 \\
&\cdot \quad \cdot \quad \cdot \quad \cdot \\
&\cdot \quad \cdot \quad \cdot \quad \cdot \\
&\cdot \quad \cdot \quad \cdot \quad \cdot \\
\phi_{N-1} &= \phi_{N-1}, \phi_{N-1} \pm \Delta\phi_{N-1}
\end{aligned} \qquad (7.5)$$

Conformational populations, defined by equation (7.5) were generated for each of the previously accepted cyclic conformations of the equivalent open chains of the hexamer using a range of values for $\Delta\phi_i$. To prevent excessive computing times all $\Delta\phi_i$ were set

equal to one another, ie. $\Delta\emptyset_1 = \Delta\emptyset_2 = \ldots \Delta\emptyset_{N-1} = \Delta\emptyset$. The maximum value of $\Delta\emptyset$ was not allowed to exceed $\pm 15^o$ in order to retain the usage of the FCM statistical weight scheme. The magnitude of $\Delta\emptyset$ was gradually increased from 1^o through to 15^o, in steps of 1^o, and the end-to-end distance was calculated for each resultant conformation. In Figure 7.03 the end-to-end distances for x = 6, obtained after adjustment of the FCM conformations in the manner described above, are plotted against the initial end-to-end distances. It was found that over 75% of the starting conformations could be closed to within 0.04nm and that 45% of the conformations could be closed to within 0.01nm. Furthermore the dipole moments (Figure 7.04) of the majority (~ 83%) of the initial conformations were altered by less than ±10% as a consequence of this ring closing procedure. Thus, the root-mean-square dipole moment of $\sim 2.8 \times 10^{-30}$Cm, calculated for x = 6 using the FCM bond rotational states ($\emptyset_i = 0^o, \pm 120^o$) is only slightly below the value of 2.97×10^{-30}Cm calculated using the adjusted rotational bond angles and both of these values compare favourably with the experimentally determined value of 3.00×10^{-30}Cm. These calculations indicate that for the range of ring sizes considered in the present study the maximum acceptable end-to-end distance of the equivalent open chains may be taken to be approximately 0.25nm. If larger values of r are employed to select cyclic conformations then such conformations cannot be considered suitable for calculating root-mean-square dipole moments of cyclic dimethyl siloxanes using the FCM model, since it is not possible to effect ring closure by making small adjustments to the bond rotational angles of the equivalent open chains.

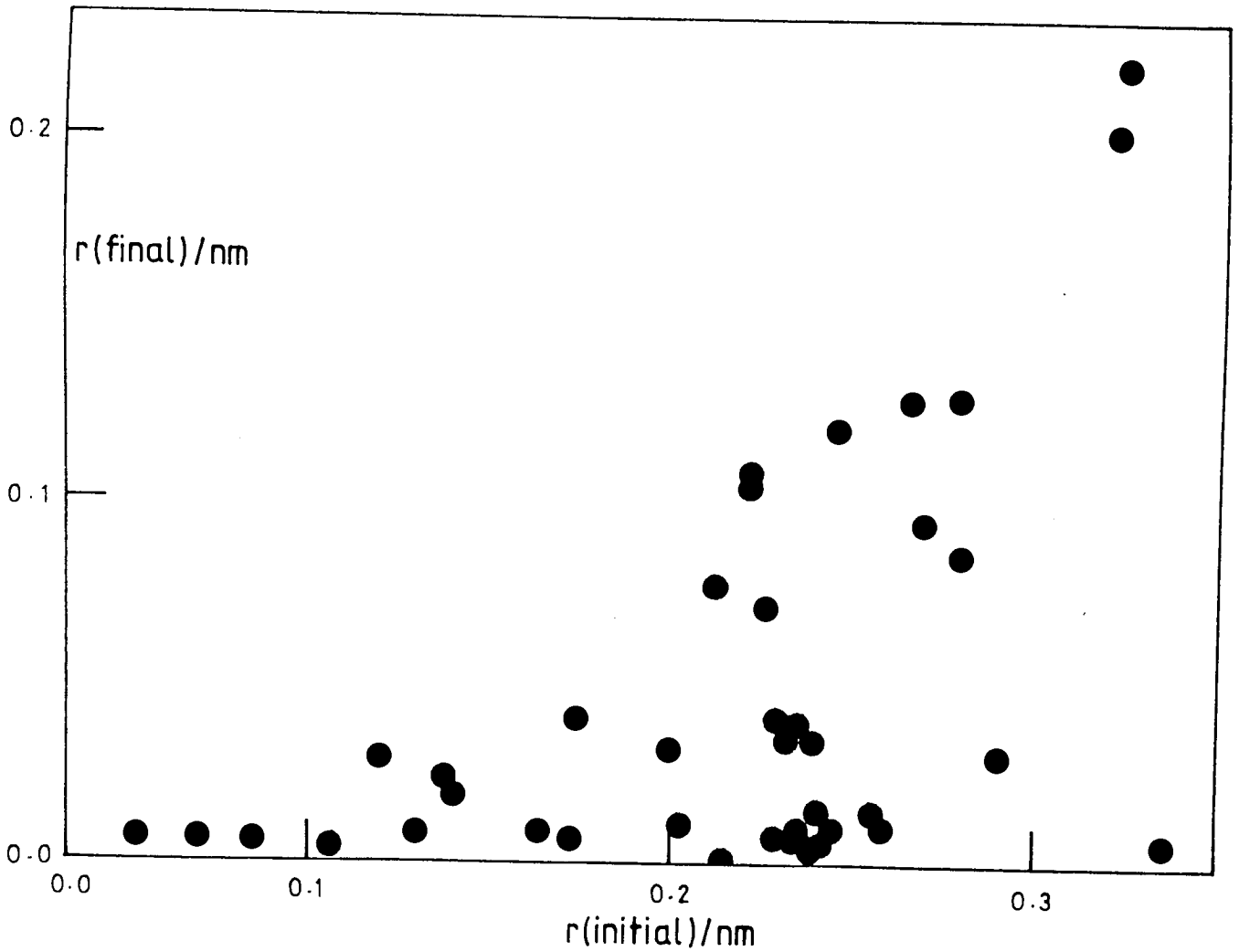

Figure 7.03 End-to-end distance, r, before and after adjustment of bond rotational angles for individual conformations of the equivalent open chain with x = 6.

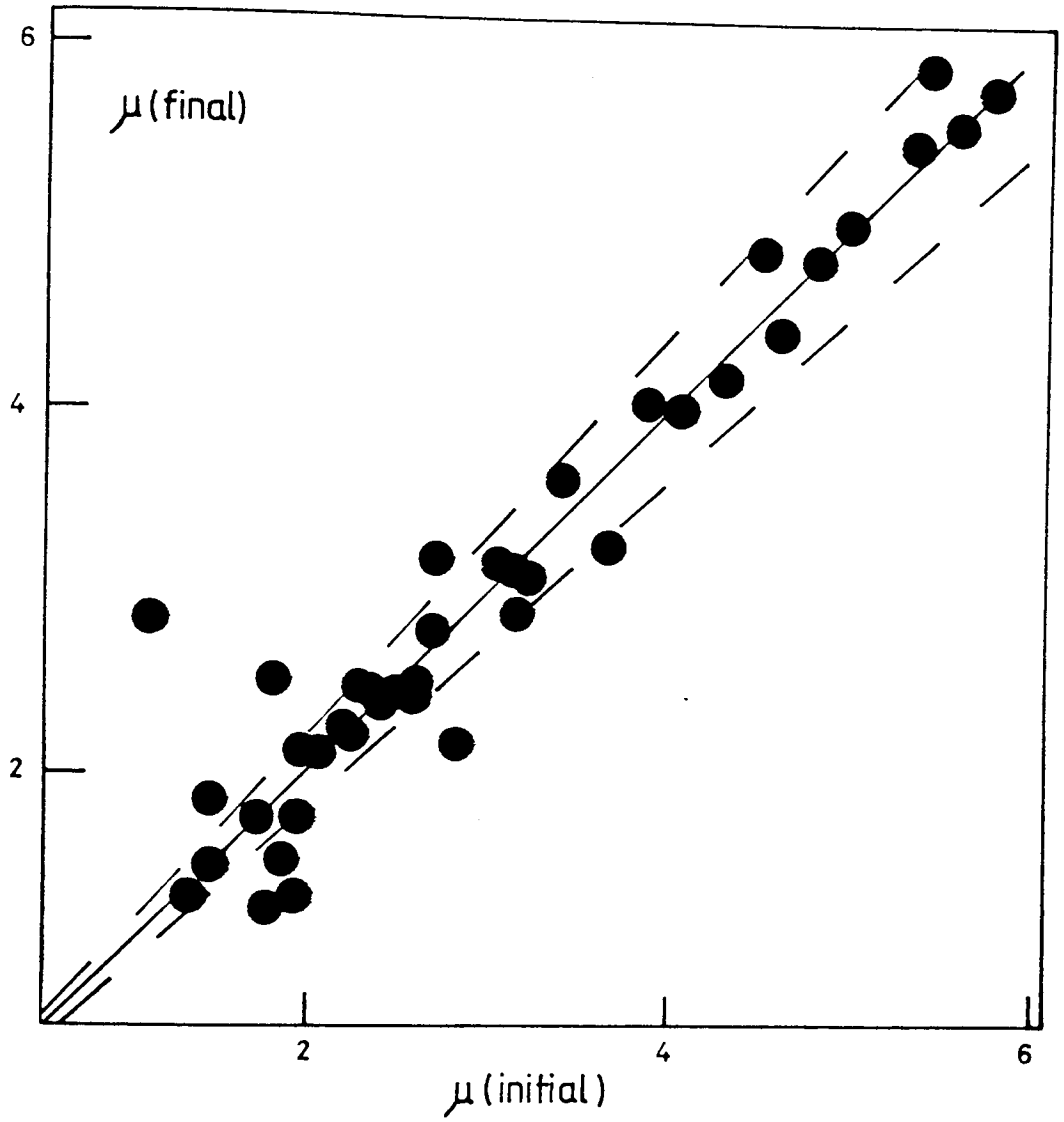

Figure 7.04 Calculated dipole moments ($X10^{30}$/Cm) before and after adjustment of bond rotational angles for individual conformations of the equivalent open chain with x = 6.

7.06 Statistical Weight Cut-Off Procedure

The combinational basis for the generation of the statistical weights of the cyclic conformations of the equivalent open chains results in a very wide range of values. This means that a large number of conformations will contribute very little to the calculated root-mean-square dipole moment and may therefore be disregarded without incurring serious loss of accuracy provided that the dipole moments of individual conformations are not large enough to offset the small statistical weights.

During the computations it is quite easy to calculate the statistical weight of the equivalent open chain before any elaborate, time consuming geometrical calculations have been pursued. By applying a minimum acceptable statistical weight, Ω_{min}, a large number of conformations may be rejected at an early stage in the calculations. Obviously, if the chosen minimum acceptable statistical weight is set too high then the accuracy of the calculated root-mean-square dipole moment will be reduced. The effect of this time saving device on the Z_r and $\langle\mu^2\rangle_0^{\frac{1}{2}}$ was studied for x = 7, 8 and 9 using various values for the minimum acceptable statistical weight. The results of these calculations are presented in Tables 7.03 and 7.04. For x = 7 the configurational partition function, Z_r (r = 0.35nm), is reduced by only 3% when Ω_{min} is changed from zero to 10^{-6}, but the number of cyclic conformations used to calculate $\langle\mu^2\rangle_0^{\frac{1}{2}}$ drops sharply from 110 to 7. This reduction is accompanied by a modest saving in the computing time. A similar effect is observed for x = 8 and x = 9. For the octamer the imposition of $\Omega_{min} = 5 \times 10^{-5}$ drastically reduces the number of cyclic conformations (with $r \leq 0.35$nm) from 695

Table 7.03 Configurational partition function $Z_r(x10^4)$, and number of cyclic conformations of the equivalent chain $[(CH_3)_2\ SiO]_x Si$- calculated using the amended FCM model at 298K for end-to-end distances in the range 0 to r and for various minimum statistical weights Ω_{min}.

x	Ω_{min}	r(nm) 0.05	0.10	0.15	0.20	0.25	0.30	0.35	CPU time[b] (min)
7	0	0.00	0.927	0.936	1.09	2.08	2.08	2.20	8.2
7		(0)[a]	(2)	(10)	(39)	(60)	(81)	(110)	
7	10^{-10}	0.00	0.927	0.936	1.09	2.08	2.08	2.20	8.1
7		(0)	(2)	(7)	(30)	(37)	(43)	(56)	
7	10^{-9}	0.00	0.927	0.936	1.09	2.08	2.08	2.20	7.9
7		(0)	(1)	(5)	(26)	(31)	(37)	(44)	
7	10^{-8}	0.00	0.927	0.936	1.09	2.08	2.08	2.20	7.0
7		(0)	(1)	(3)	(16)	(20)	(21)	(25)	
7	10^{-7}	0.00	0.927	0.936	1.09	2.07	2.07	2.20	6.0
7		(0)	(1)	(2)	(11)	(14)	(14)	(16)	
7	10^{-6}	0.00	0.927	0.927	1.03	2.01	2.01	2.14	5.0
7		(0)	(1)	(1)	(3)	(5)	(5)	(7)	
8	0	0.00	0.928	7.62	39.7	41.2	41.5	41.5	85
8		(21)	(66)	(137)	(279)	(411)	(558)	(695)	
8	10^{-6}	0.00	0.927	7.62	39.7	41.1	41.4	41.4	38
8		(0)	(1)	(4)	(15)	(23)	(24)	(25)	
8	10^{-5}	0.00	0.927	7.62	39.5	40.7	41.0	41.0	28
8		(0)	(1)	(4)	(9)	(11)	(12)	(12)	
8	$5x10^{-5}$	0.00	0.927	7.31	39.2	40.1	40.1	40.1	23
8		(0)	(1)	(3)	(8)	(9)	(9)	(9)	
9	0	0.011	0.078	0.193	0.219	0.286	0.700	1.55	761
9		(74)	(289)	(745)	(1472)	(2277)	(3246)	(4333)	
9	10^{-7}	0.010	0.068	0.164	0.180	0.228	0.623	1.45	342
9		(2)	(21)	(34)	(38)	(47)	(75)	(112)	
10	10^{-7}	5.18	48.2	136.0	468.0	612.0	1220	1330	3094
10		(15)	(81)	(169)	(246)	(325)	(402)	(468)	

[a] Entries in parentheses indicate number of accepted conformations.

[b] Central processing unit times for a CDC 7600 computer.

Table 7.04 Root-mean-square dipole moments $\langle\mu^2\rangle_0^{\frac{1}{2}}$ ($\times 10^{30}$/Cm) for cyclic conformations of the equivalent chain $[(CH_3)_2SiO]_xSi$ calculated using the amended FCM model at 298K for end-to-end distances in the range 0 to r for various minimum statistical weights Ω_{min}.

x	Ω_{min}	r(nm)						
		0.05	0.10	0.15	0.20	0.25	0.30	0.35
7	0	0.00	3.94	3.96	3.90	3.92	3.92	3.89
7	10^{-10}	0.00	3.93	3.96	3.91	3.92	3.92	3.89
7	10^{-9}	0.00	3.93	3.96	3.91	3.92	3.92	2.89
7	10^{-8}	0.00	3.93	3.96	3.91	3.92	3.92	3.89
7	10^{-7}	0.00	3.93	3.96	3.91	3.93	3.93	3.89
7	10^{-6}	0.00	3.93	3.93	3.80	3.87	3.87	3.83
8	0	1.73	4.07	4.86	5.25	5.24	5.24	5.24
8	10^{-6}	0.00	4.07	4.87	5.24	5.24	5.24	5.24
8	10^{-5}	0.00	4.07	4.87	5.24	5.24	5.24	5.24
8	$5X10^{-5}$	0.00	4.07	4.84	5.27	5.24	5.24	5.24
9	0	6.26	6.14	5.68	5.72	5.46	4.69	4.11
9	10^{-7}	6.29	6.41	5.92	6.02	5.76	4.77	4.12
10	10^{-7}	5.39	4.67	4.21	4.57	4.79	4.90	4.80

(Ω_{min} = 0) to 9 for only a small decrease (~3%) in the partition function. As x increases the savings in computing time become relatively more important. Thus for x = 9 the number of cyclic conformations with r ≤ 0.35nm was reduced from 4333 to 112 and the computing time was decreased by approximately 7 hours.

Since the range of values calculated for the dipole moments of the cyclic x-mers, for any given value of x, is not very great and the configurational partition function remains almost unaffected by the enrichment procedure described above it follows that the calculated values of $\langle\mu^2\rangle_0^{\frac{1}{2}}$ should be almost constant. The entries in Table 7.04 support this conclusion.

7.07 Examination of Selection Criteria for Cyclic Conformations

Since the angular criteria used for selecting acceptable cyclic conformations may appear to be arbitrary several checks were performed to test the dependence of the calculated root-mean-square dipole moments on the limits imposed on the bond angle supplement $\theta_{N'}$ and the bond rotational angle $\phi_{N'}$. The root-mean-square dipole moments for cyclic conformations of the equivalent open chains for x = 6 and x = 7 were calculated for the various ranges of end-to-end distances and for different combinations of $\theta_{N'}$ and $\phi_{N'}$. Values of $\langle\mu^2\rangle_0^{\frac{1}{2}}$ were found to be reasonably insensitive to the restrictions imposed on $\theta_{N'}$ and $\phi_{N'}$. Thus, for both x = 6 and x = 7 (Table 7.05) the dipole moments calculated for the cyclic conformations of the equivalent open chains were found to be approximately constant, for any given end-to-end distance, provided that the tolerances imposed on the angles $\theta_{N'}$ and $\phi_{N'}$ are not less than ±10%.

7.08 Dipole Moment of the Cyclic Tetramer

The conformations of the cyclic tetramer, x = 4, are not adequately described by the FCM RISM since it is known that this molecule exists

Table 7.05 Dependence of $\langle\mu^2\rangle_0^{\frac{1}{2}}$ ($\times 10^{30}$/Cm) on the bond angle supplement, θ_{N^1}, and bond rotational angle, ϕ_{N^1}, for the cyclic conformations of the equivalent chain $[(CH_3)_2SiO]_x$ Si- with x = 6 and x = 7 having end-to-end distances in the range 0 to r.

	$\Delta\theta_{N^1}$	$\Delta\phi_{N^1}$	r(nm)						
			0.05	0.10	0.15	0.20	0.25	0.30	0.35
x=6	$\pm 10^o$	$\pm 15^o$	-	4.10	2.77	2.70	2.80	2.80	2.80
	$\pm 15^o$	$\pm 15^o$	-	4.10	2.77	2.70	2.84	2.80	2.80
	$\pm 20^o$	$\pm 15^o$	-	4.10	2.77	2.74	2.84	2.80	2.80
	$\pm 15^o$	$\pm 10^o$	-	4.10	2.54	2.50	2.67	2.70	2.70
	$\pm 15^o$	$\pm 20^o$	-	4.10	2.77	2.70	2.84	2.80	2.80
x=7	$\pm 10^o$	$\pm 15^o$	-	3.94	3.97	3.87	3.87	3.87	3.87
	$\pm 15^o$	$\pm 15^o$	-	3.94	3.97	3.90	3.94	3.94	3.90
	$\pm 20^o$	$\pm 15^o$	2.77	3.87	3.90	3.87	3.90	3.90	3.87
	$\pm 15^o$	$\pm 10^o$	-	3.40	2.90	4.64	3.97	3.97	3.97
	$\pm 15^o$	$\pm 20^o$	-	3.94	3.97	3.77	3.87	3.70	3.67

in conformations other than those defined by the bond rotational states of trans ($\phi_i = 0^o$) and gauche ($\phi_i = \pm 120^o$). Structures corresponding to the crystalline[185] and vapour phase[186] have been previously reported and discussed by Carmichael and Kinsinger[187] (structures B and E in Table 7.06). Additional conformers for the cyclic tetramer have also been proposed (A, C, D and F in Table 7.06)[152]. The bond rotational angles of these conformations depart substantially from the values (0^o, $\pm 120^o$) assigned by the FCM RISM for the linear dimethyl siloxanes. After making a visual estimate of the bond rotational angles an interactive computer program was used to adjust the bond rotational angles to obtain an exact ring closure while maintaining the same bond angle supplements as the open chain (θ (oxygen) = 37^o, θ(silicon) = 70^o). The conformation, E, corresponding to that found in the solid phase was analysed in a different manner. Since the relative positions of all the atoms in this conformer have been determined using x-ray crystallography[55] the bond rotational angles may be readily calculated. The results of these calculations for conformers A-F are presented in Table 7.06. Also included in this table are the corresponding molecular dipole moments for each of the conformers calculated assuming a Si-O bond dipole moment of 2.0×10^{-30} Cm and zero dipole moments for all other bonds. The calculation of the root-mean-square dipole moment of the cyclic tetramer in the liquid state requires a knowledge of the statistical weights of the various conformers, but this demands an analysis of the non-bonded interactions across the ring which is not available at the present time. Calculation of distances between pairs of non-bonded methyl group carbon atoms of the various

conformers of the cyclic tetramer have been carried out and the shortest distance for each conformation is listed in Table 7.06. These distances between non-bonded carbon atoms place the corresponding methyl groups of conformers A, B, E and F beyond the range of any significant interaction and, thus, suggest that the statistical weights of these conformers should be set approximately equal to one another. In the case of conformer C it is apparent that there is severe steric overlap of a pair of opposite methyl groups and, therefore, this conformation was assigned a zero statistical weight. The shortest distance between non-bonded carbon atoms of conformer D is 0.431nm; a distance at which interactions between methyl groups might be considered to be attractive, resulting in a higher statistical weight. However, in the absence of futher, more quantitative, information the statistical weight of this conformation was set equal to that of conformers A, B, E and F. The value of the root-mean-square dipole moment so obtained (1.93×10^{-30}Cm) compared favourably with the experimental value of 1.5×10^{-30}Cm measured for the cyclic tetramer in the liquid state at 298K. It might also be noted that the dipole moment squared ($0.64 \times 10^{-60} C^2m^2$) of conformer D is significantly lower than the mean-square dipole moment of the remaining accepted conformations ($4.61 \times 10^{-60} C^2m^2$). Thus, had conformer D been allocated a higher statistical weight due to its favourable methyl-methyl interaction, the resulting root-mean-square dipole moment predicted for the cyclic tetramer would have been somewhat lower than 1.93×10^{-30}Cm giving a better correspondence with the experimentally determined value.

Table 7.06 Conformations, calculated dipole moments ($x10^{30}$/Cm) and shortest distance between non-bonded methyl group carbon atoms, d_{CC}(/nm), for the cyclic tetramer of dimethyl siloxane.

	Bond n° i	Conformer					
		A	B	C	D	E	F
ϕ_i	1	247.5°	128.9°	214.7°	142.3°	127.1°	127.6°
	2	112.5°	231.1°	214.7°	260.1°	259.3°	232.4°
	3	247.5°	231.1°	145.3°	180.0°	120.2°	96.6°
	4	112.5°	128.9°	145.3°	142.3°	204.2°	232.4°
	5	247.5°	128.9°	214.7°	142.3°	233.1°	232.4°
	6	112.5°	231.1°	214.7°	260.1°	100.6°	127.6°
	7	247.5°	231.1°	145.3°	180.0°	240.0°	127.6°
	8	112.5°	128.9°	145.3°	142.3°	155.5°	263.4°
$\langle\mu^2\rangle_0^{\frac{1}{2}}$		3.80	0.00	0.00	0.80	0.03	2.00
d_{CC}		0.153	0.672	0.296	0.431	0.615	0.595

7.09 Average Bond Conformations

It is well known that as a consequence of the alternating bond angles the siloxane chain will close to form a cyclic structure when the backbone is placed in the all-trans conformation. Since the trans rotational states are energetically more favoured relative to the gauche states this behaviour leads to a maximum in the experimentally determined dipole moment ratio $\langle\mu^2\rangle_0/nm^2$ for the linear dimethyl siloxanes in the region of x = 8 (see Section 6.05). However, for the cyclic dimethyl siloxanes the functional form of $\langle\mu^2\rangle_0/nm^2$ is substantially modified because the backbone is constrained to be disc-like[55], when averaged over all possible conformations, and a maximal behaviour of the experimental dipole moment ratio is not observed.

For the conformation of the open chains described by the FCM RISM the fraction, f_{tr}, of skeletal bonds occupying trans states steadily increases with increasing chain length (Figure 7.05) and approaches the value of 0.74 calculated for the infinitely long chain. The behaviour of the corresponding cyclic conformations of the equivalent open chains is quite different. For the smaller cyclics (x = 4, 5 and 6) the statistically weighted fractions of skeletal bonds in trans states, calculated using the amended FCM model, are markedly less than those of the corresponding equivalent open chains. Furthermore, the rate of change of f_{tr} as x increases from x = 4 to x = 8 is very rapid for the cyclic conformations whereas for the chains f_{tr} changes by only about 10% over the same range of x. Prohibitively long computing times prevented the calculation of f_{tr} for values of x greater than 10 but it is anticipated that the fraction of bonds occupying trans states would be a maximum at x = 11 for reasons previously discussed.

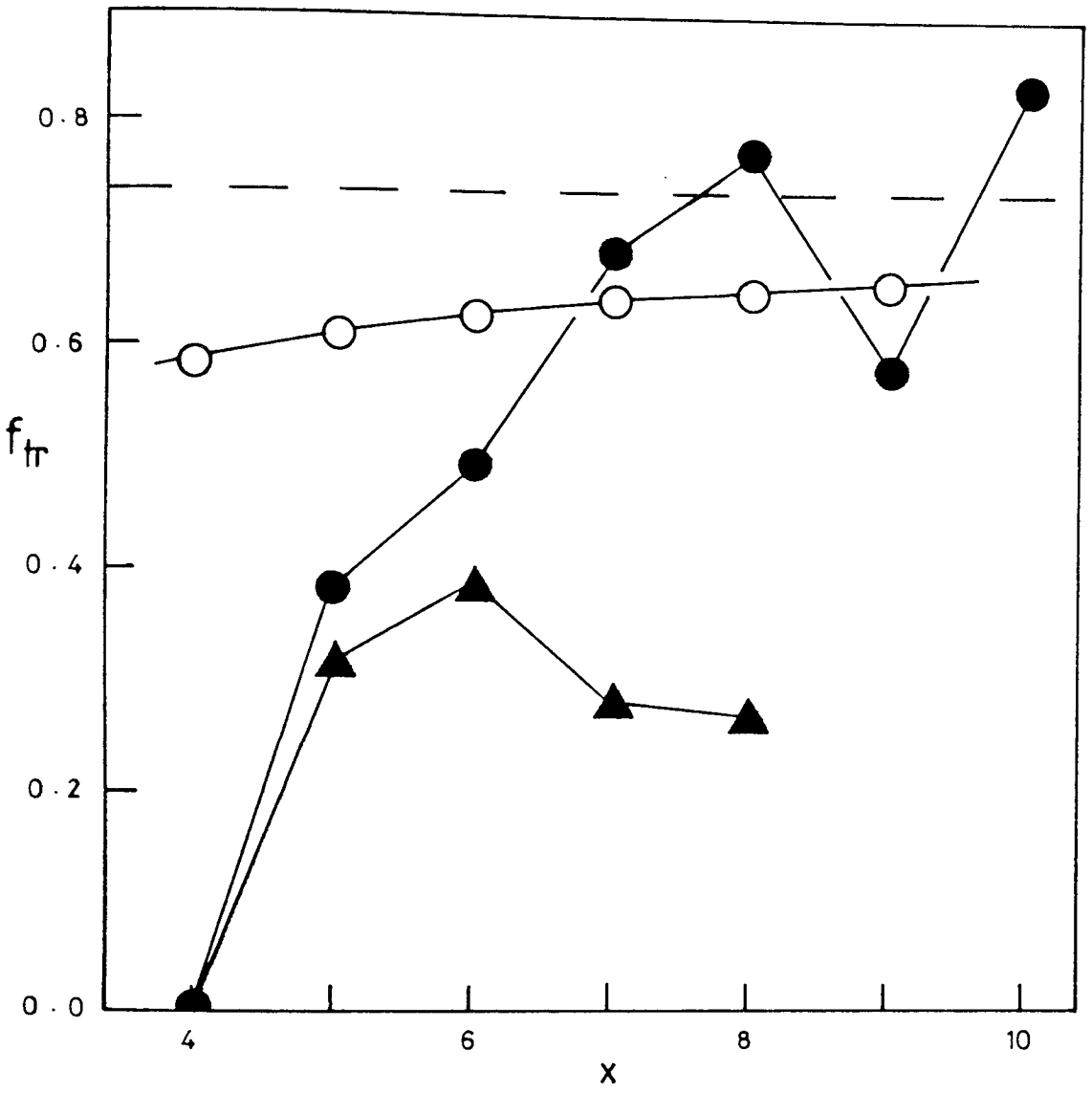

Figure 7.05 'Statistically weighted fraction of skeletal bonds occupying trans states, f_{tr}, for linear dimethyl siloxanes (○) and for cyclic conformations ($r \leq 0.35$nm) of the equivalent open chain calculated using the amended FCM model (●) and the hard-sphere model (▲) at 298K.

7.10 Temperature Coefficients of the Dipole Moments

The partial derivatives $\partial \ln \langle\mu^2\rangle_0/\partial \ln\sigma$ and $\partial \ln \langle\mu^2\rangle_0/\partial \ln\omega$ were calculated at 298K for the cyclic conformations of the equivalent open chains $[(CH_3)_2\ SiO]_x\ Si$ with x = 5-10 using the amended FCM statistical weight scheme. The temperature coefficients of the mean-square dipole moments were then obtained using equation (6.12). The calculated partial derivatives and temperature coefficients are listed in Table 7.07 for the cyclic conformations. It is noted that for the cyclic conformations the partial derivatives $\partial \ln\langle\mu^2\rangle_0/\partial \ln\sigma$ are generally smaller in magnitude than the values calculated for the corresponding equivalent open chains (see Section 6.06). The converse relationship was found for the partial derivative $\partial \ln\langle\mu^2\rangle_0/\partial \ln\omega$. Temperature coefficients $d \ln \langle\mu^2\rangle_0/dT$ (Figure 7.06) obtained for cyclic conformations with x = 5 and x = 6 were similar in magnitude to those calculated for the corresponding equivalent open chains but were opposite in sign. For x = 7 and x = 9 the temperature coefficients of the cyclic conformations were small and positive. Negative temperature coefficients, close in magnitude to those obtained for the open chains, were found for cyclic conformations with x = 8 and x = 10.

In Figure 7.07 the calculated temperature coefficients $d \ln\langle\mu^2\rangle_0/dT$ are plotted against the statistically weighted fraction, f_{tr}, of skeletal bonds occupying trans rotational states for cyclic and open chain conformations. For the cyclic conformations an approximately inverse relationship was found between $d \ln\langle\mu^2\rangle_0/dT$ and f_{tr} for x = 5-9; a functional dependence quite dissimilar to that found for the total conformational population of the corresponding equivalent open chains. The variation of the temperature coefficients with x for the cyclic conformations is quite irregular when compared to the very regular trend

exhibited by the chains, no doubt reflecting to some extent the drastic differences in the number of conformations taken for the averaging processes as well as reflecting the intrinsically different bond correlations of cyclic and linear molecules. However, the general dependence of the temperature coefficients of the cyclic conformations on x indicates that they are converging to a value similar to the asymptotic limit attained by the chain molecules.

Table 7.07 Partial derivatives $\partial \ln \langle \mu^2 \rangle_0 / \partial \ln \sigma$ and $\partial \ln \langle \mu^2 \rangle_0 / \partial \ln \omega$ and temperature coefficients of the mean-square dipole moments, $10^3 d\ln \langle \mu^2 \rangle_0 / dT$, for cyclic dimethyl siloxanes calculated at 298K using the amended FCM model.

n	$\frac{\partial \ln \langle \mu^2 \rangle_0}{\partial \ln \sigma}$	$\frac{\partial \ln \langle \mu^2 \rangle_0}{\partial \ln \omega}$	$10^3 \frac{d\ln \langle \mu^2 \rangle_0}{dT}$
10	0.038	0.438	2.79
12	0.009	0.347	2.11
14	-0.014	0.032	0.12
16	-0.188	-0.041	-1.15
18	-0.061	0.130	0.48
20	-0.048	-0.021	-0.36

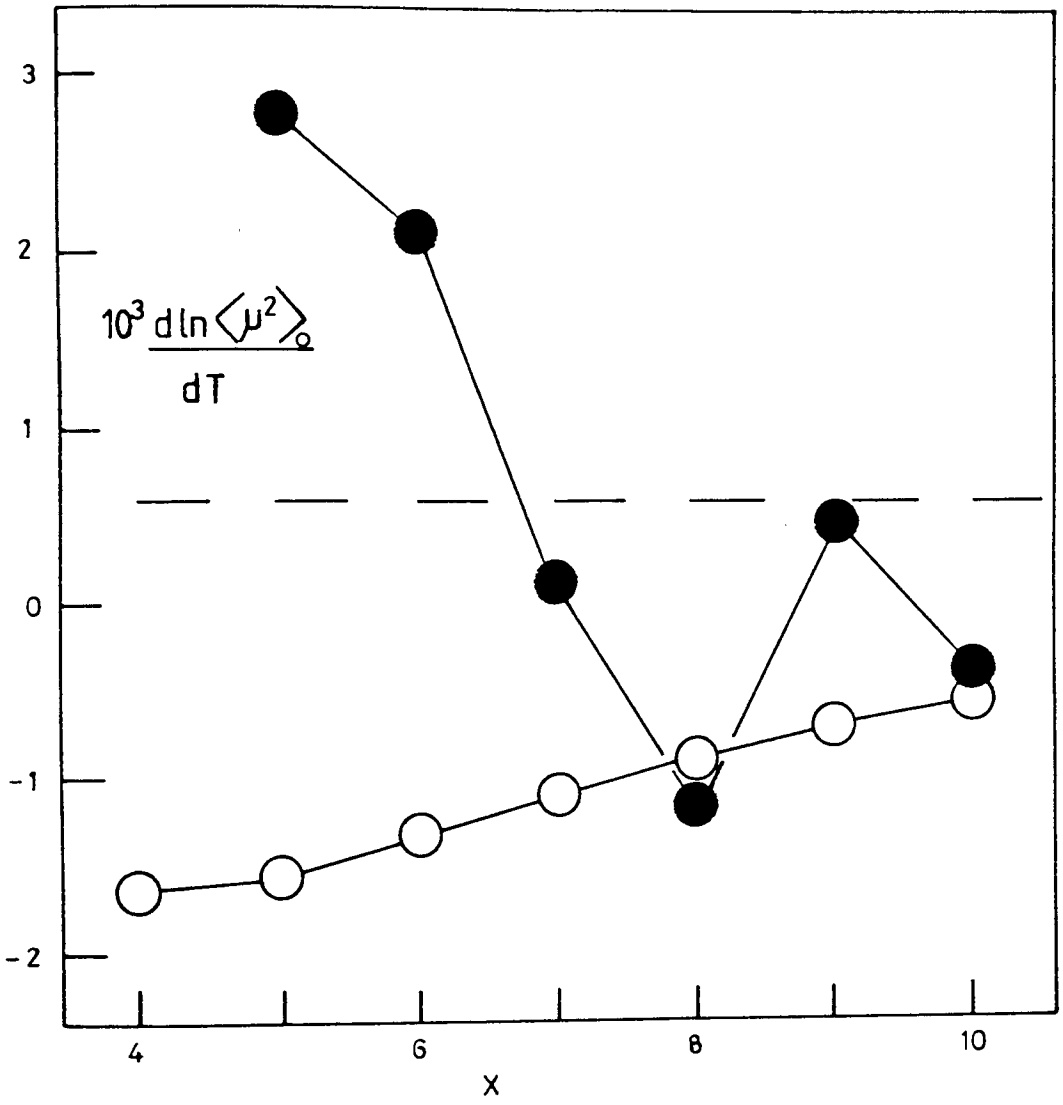

Figure 7.06 Calculated temperature coefficients for linear dimethyl siloxanes $(CH_3)_3SiO[(CH_3)_2SiO]_{X-1}Si(CH_3)_3$ (○) and cyclic conformations of the equivalent open chains $[(CH_3)_2SiO]_X$ Si - (●) at 298K based on the unamended and amended FCM models, respectively. The broken line is the value calculated for infinitely long chains.

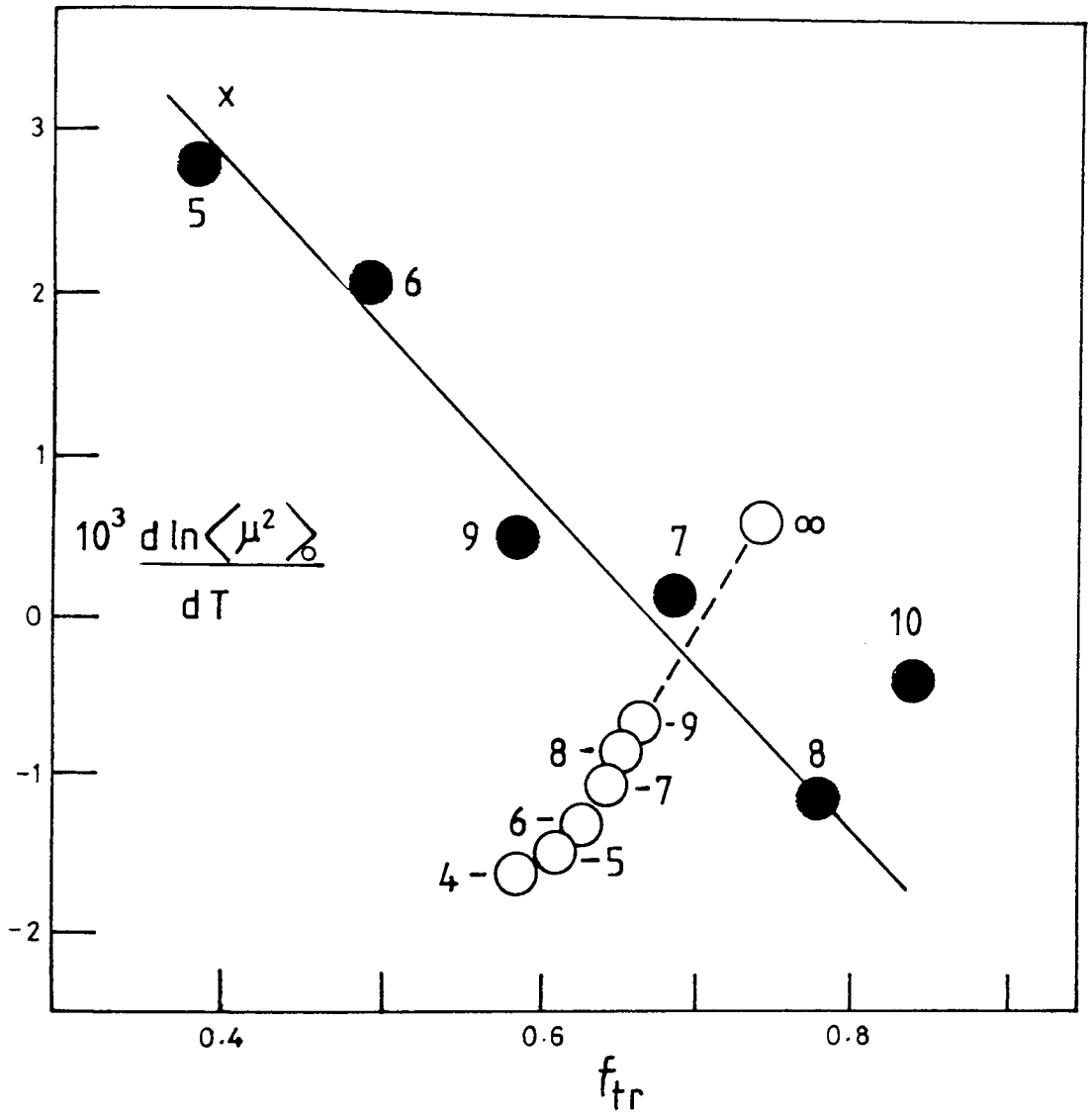

Figure 7.07 Calculated temperature coefficients of the mean-square dipole moments of linear dimethyl siloxanes $(CH_3)_3SiO[(CH_3)_2SiO]_{x-1}Si(CH_3)_3$ (○) and cyclic confomations (●) of the equivalent open chains $[(CH_3)_2SiO]_x$ Si - vs the statistically weighted fraction, f_{tr}, of skeletal bonds occupying trans states at 298K. The solid line was fitted to data obtained for x = 5-9.

CHAPTER 8

CALCULATION OF MEAN-SQUARE OPTICAL ANISOTROPIES AND MOLAR KERR CONSTANTS OF THE DIMETHYL SILOXANES

8.01 Introduction

Measurement of the optical and electro-optical properties of polymers in solution and in the pure state may be used as complementary techniques for the investigation of molecular conformations in addition to dielectric studies. The optical and electro-optical methods have the advantage that no permanent molecular dipole moment is required. However, in the case of the electro-optical Kerr effect if a substantial permanent dipole moment is present this usually forms the dominant term.

The total polarizability, $\underset{\sim}{\alpha}$, of a molecule may be regarded as the sum of the polarizability tensors, $\underset{\sim}{\alpha}_i$, of each of the bonds:

$$\underset{\sim}{\alpha} = \sum_i \underset{\sim}{\alpha}_i \qquad (8.1)$$

The bond polarizability tensors are considered to be invariant with changing conformations of the molecule. This additivity is often termed the valence-optical scheme. The validity of additivity of group dipole moments in flexible polymers has been accepted for many years. However, in the case of polarizability tensors it is only quite recently that their additivity has been verified[44]. The plethora of bond polarizabilities that have been suggested for common bond types has been responsible for much of the confusion about this principle. Proposed polarizabilities have not been derived for the conditions of ideal dilute polymer solutions. This problem was solved

by Patterson and Flory[44] who developed a procedure whereby the mean-square optical anisotropy, $\langle\gamma^2\rangle$, associated with isolated solute molecules can be obtained from measurements of the depolarized Rayleigh scattering by solutions of these molecules in optically isotropic and geometrically symmetric solvents. They also showed that the dependence of $\langle\gamma^2\rangle$ on chain length was well reproduced by calculations carried out using the valence optical scheme and rotational isomeric state theory. There is an alternative approach of combining atomic polarizabilities[188] and results for the alkanes have been presented by Ladanyi and Keyes[189]. However, this will not be mentioned further in this study.

In this Chapter calculations of the mean-square optical anisotropy of dimethyl siloxanes are presented and the results for the cyclic and linear species compared. The bond polarizabilities used in these calculations are those of Armstrong et al[190]. Calculations of electro-optical molar Kerr constants of the linear dimethyl siloxanes are also presented and comparison of these calculated values with limited experimental data discussed.

8.02 Calculation of the Mean-Square Optical Anisotropy of Polymer Chains

It has become usual[31,191] to describe the squared optical anisotropy of a molecule in terms of the traceless polarizability tensor, $\underset{\sim}{\beta}$, formed from $\underset{\sim}{\alpha}$ as follows

$$\underset{\sim}{\beta} = \sqrt{3/2}(\underset{\sim}{\alpha} - \bar{\alpha}\,\underset{\sim}{E}) \qquad (8.2)$$

If $\underset{\sim}{\alpha}$ is expressed in canonical (i.e. diagonal)form, then the squared optical anisotropy, γ^2, is the sum of the squares of the elements of $\underset{\sim}{\beta}$ and is defined by

$$\gamma^2 = (1/2)\left[(\alpha_1 - \alpha_2)^2 + (\alpha_1 - \alpha_3)^2 + (\alpha_2 - \alpha_3)^2 \right] \qquad (8.3)$$

where α_1, α_2, α_3 are the principal components of $\underset{\sim}{\alpha}$ being designated by a single index. This correspondence is expressed by

$$\gamma^2 = \text{trace}(\underset{\sim}{\beta}^T \underset{\sim}{\beta}) \tag{8.4}$$

where $\underset{\sim}{\beta}^T$ is the transpose of $\underset{\sim}{\beta}$. But the quantity on the right-hand side of this equation is an invariant for any second-order tensor $\underset{\sim}{\beta}$. In other words equation (8.2) must hold for $\underset{\sim}{\alpha}$ expressed in any reference frame related to the principal axes of $\underset{\sim}{\alpha}$ by a rotation. Since $\underset{\sim}{\beta}$, like $\underset{\sim}{\alpha}$, is symmetric, we have therefore

$$\gamma^2 = \text{trace}(\underset{\sim}{\beta}\underset{\sim}{\beta}) \tag{8.5}$$

It follows from equations (8.2) and (8.5) that[192,193]

$$\gamma^2 = (1/2)\left[(\alpha_{11} - \alpha_{22})^2 + (\alpha_{11} - \alpha_{33})^2 + (\alpha_{22} - \alpha_{33})^2\right] + 3(\alpha_{12}^2 + \alpha_{13}^2 + \alpha_{23}^2) \tag{8.6}$$

where $\underset{\sim}{\alpha}$ is expressed in an arbitary reference frame.

Exact matrix methods, analogous to those used in the calculation of mean-square dipole moments, have been developed[194] to calculate the mean-square optical anisotropy, $\langle\gamma^2\rangle_0$, of unperturbed polymer chains of any length and any specified structure. Thus, $\langle\gamma^2\rangle_0$ may be calculated by means of the equation

$$\langle\gamma^2\rangle_0 = 2Z^{-1}\ \underset{\sim}{J}^*\ \underset{\sim}{P}_1^{(n+1)}\ \underset{\sim}{J} \tag{8.7}$$

The configurational partition function, Z, is identical to that used in the calculation of the mean-square dipole moments (see equation (6.8)). $\underset{\sim}{J}^*$ is the row vector [100...000] consisting of a single unity followed by 32 zeros and $\underset{\sim}{J}$ is the column vector [000...111] consisting of 30 zeros followed by 3 unities. The generator matrix $\underset{\sim}{P}i$ has the form

$$\underset{\sim}{P}_i = \begin{bmatrix} \underset{\sim}{U} & (\underset{\sim}{U} \otimes \underset{\sim}{\gamma}^T)||\underset{\sim}{T} \otimes \underset{\sim}{T}|| & (1/2)\,\gamma^2 \underset{\sim}{U} \\ \underset{\sim}{0} & (\underset{\sim}{U} \otimes \underset{\sim}{E}_9)||\underset{\sim}{T} \otimes \underset{\sim}{T}|| & \underset{\sim}{U} \otimes \underset{\sim}{\gamma} \\ \underset{\sim}{0} & \underset{\sim}{0} & \underset{\sim}{U} \end{bmatrix}_i \qquad (8.8)$$

where $\underset{\sim}{U}$ is the statistical weight matrix, $\underset{\sim}{T}$ the transformation matrix and $\underset{\sim}{E}_9$ an identity matrix of order nine. The term $||\underset{\sim}{T} \otimes \underset{\sim}{T}||$ represents a pseudodiagonal matrix constructed from the matrices $\underset{\sim}{T}_i \otimes \underset{\sim}{T}_i$ for the various rotational states of bond i. The matrix $\underset{\sim}{\gamma}_i$ is simply the elements of $\underset{\sim}{\beta}_i$ rearranged in column form, the elements being ordered $\underset{\sim}{\gamma}_i = [\beta_{11}\ \beta_{12}\ \beta_{13}\ \beta_{21} \ldots\ \beta_{33}]$.

The serial product $\underset{\sim}{P}_1^{n+1}$ in equation (8.7) comprises n + 1 factors in order that it might take account of n + 1 group tensors, $\underset{\sim}{\gamma}_i$, including those for the two terminal groups (cf. seq.). Of course, $\underset{\sim}{T}_{n+1}$ is neither defined nor required inasmuch as only the final pseudocolumn of $\underset{\sim}{P}_{n+1}$ is used. The matrix $\underset{\sim}{U}_{n+1}$ is to be equated to an identity of order three. If the terminal groups are symmetric, as is the case for the dimethyl siloxane chain, then $\underset{\sim}{U}_1$ and $\underset{\sim}{U}_n$ may be also set equal to identities.

8.03 Traceless Optical Polarizability Tensors for Dimethyl Siloxanes

Polarizability tensors have been formulated for the end groups and two repeating units of the dimethyl siloxane chain from the bond anisotropies derived by Armstrong et al[190]. The method used in constructing these tensors closely follows that of Jernigan and Flory[194] who conducted calculations of the mean-square optical anisotropy of the n-alkanes. Although the final numerical results obtained by these workers were incorrect due to a programming error[44] the algebra is sound.

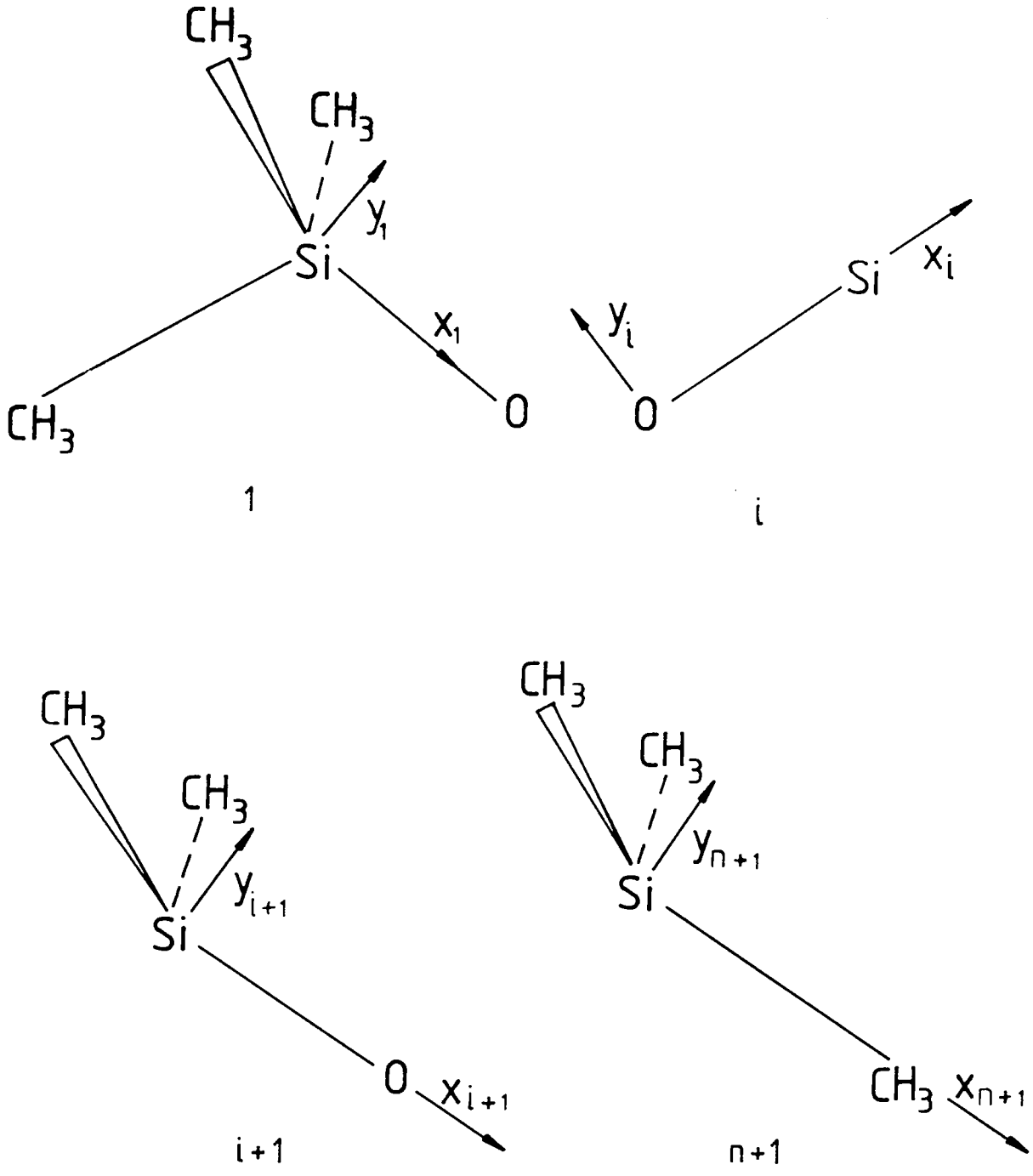

Figure 8.01 Schematic diagram of the moieties for which polarizability tensors were derived.

The groups for which polarizability tensors were derived in this study are shown in Figure 8.01. The supplementary bond angle, ϑ^1, at oxygen atoms was taken as 37^o, whilst angles at silicon atoms were all assumed to be tetrahedral. It is convenient to represent half the angle between methyl side groups by ψ.

Consider group i in Figure 8.01. If one fixs the principal axes for the polarizability tensor such that this Si-O bond lies along the x axis, then the traceless tensor, $\underset{\sim}{\beta}i$, (as defined in equation (8.2)) for this group is simply

$$\underset{\sim}{\beta}_i = \left(\frac{3}{2}\right)^{\frac{1}{2}} \begin{bmatrix} \frac{2}{3}\Delta\alpha_{SiO} & 0 & 0 \\ 0 & -\frac{1}{3}\Delta\alpha_{SiO} & 0 \\ 0 & 0 & -\frac{1}{3}\Delta\alpha_{SiO} \end{bmatrix} \qquad (8.9)$$

Here, $\Delta\alpha_{SiO}$ has been introduced to represent the difference between the polarizability components parallel, $\alpha_{\parallel}$, and perpendicular, $\alpha_{\perp}$, to the Si-O bond (i.e. $\Delta\alpha = \alpha_{\parallel} - \alpha_{\perp}$).

Consider group i + 1 in Figure 8.01. In this case the principal axes of the polarizability tensor are fixed as follows: an axis along the bisector of the angle between the methyl-silicon bonds, a second axis likewise in the plane of the silicon and oxygen atoms making an acute angle with the Si-O bond; and the third axis of the orthogonal set in the plane of the two Si-C bonds. The principal components of the polarizability tensor for the two $Si-CH_3$ groups alone are

$$\begin{aligned} &2(\alpha_{\perp SiCH_3} + \Delta\alpha_{SiCH_3}\cos^2\psi) \\ &2\alpha_{\perp SiCH_3} \\ &2(\alpha_{\perp SiCH_3} + \Delta\alpha_{SiCH_3}\sin^2\psi) \end{aligned} \qquad (8.10)$$

taken in the order in which the principal axes have been specified.

A traceless tensor $(\underset{\sim}{\beta}_{2SiCH_3})_{i+1}$ defined in accordance with equation (8.2), may be formed from the components of the polarizability tensor given by equation (8.10).

This tensor

$$(\underset{\sim}{\beta}_{2SiCH_3})_{i+1} = \left(\frac{3}{2}\right)^{\frac{1}{2}} \Delta\alpha_{SiCH_3} \begin{bmatrix} 2\cos^2\psi - \frac{2}{3} & 0 & 0 \\ 0 & -\frac{2}{3} & 0 \\ 0 & 0 & 2\sin^2\psi - \frac{2}{3} \end{bmatrix} \quad (8.11)$$

expresses the contribution of the two Si-CH_3 groups to the group tensor $\underset{\sim}{\beta}_{i+1}$, expressed in the coordinate system defined above.

As the two substituents (methyl groups) attached to the silicon atom are equivalent, the coordinate system in which equation (8.11) is expressed is related to the usual reference frame[31] of skeletal bond i by a single rotation. A rotation about the common z-axis by an angle ψ is required to bring the two frames into coincidence. Thus, the group tensor, $\underset{\sim}{\beta}_{i+1}$, of group i+1 in Figure 8.01, is obtained from equation (8.11) by first rotating the coordinate system through the angle ψ and then adding the tensor $\underset{\sim}{\beta}_i$ (see equation (8.9)) corresponding to the backbone bond. The result is

$$\underset{\sim}{\beta}_{i+1} = \left(\frac{3}{2}\right)^{\frac{1}{2}} \begin{bmatrix} \frac{2}{3}\Delta\alpha_{SiO} + 2(\cos^4\psi - \frac{1}{3})\Delta\alpha_{SiCH_3} & -2(\sin\psi\cos^3\psi)\Delta\alpha_{SiCH_3} & 0 \\ -2(\sin\psi\cos^3\psi)\Delta\alpha_{SiCH_3} & -\frac{1}{3}\Delta\alpha_{SiO} + 2(\sin^2\psi\cos^2\psi - \frac{1}{3})\Delta\alpha_{SiCH_3} & 0 \\ 0 & 0 & -\frac{1}{3}\Delta\alpha_{SiO} + 2(\sin^2\psi - \frac{1}{3})\Delta\alpha_{SiCH_3} \end{bmatrix}$$

(8.12)

Since all angles at silicon atoms are assumed to be tetrahedral; $\cos\psi = 1/\sqrt{3}$ and $\sin\psi = \sqrt{2/3}$. Thus, equation (8.12) may be simplified to give

$$\underset{\sim}{\beta}_{i+1} = \left(\frac{3}{2}\right)^{\frac{1}{2}} \begin{bmatrix} \frac{2}{3}\left(\Delta\alpha_{SiO} - \frac{2}{3}\Delta\alpha_{SiCH_3}\right) & -\frac{\sqrt{8}}{9}\Delta\alpha_{SiCH_3} & 0 \\ -\frac{\sqrt{8}}{9}\Delta\alpha_{SiCH_3} & -\frac{1}{3}\left(\Delta\alpha_{SiO} - \frac{2}{3}\Delta\alpha_{SiCH_3}\right) & 0 \\ 0 & 0 & -\frac{1}{3}(\Delta\alpha_{SiO} - 2\Delta\alpha_{SiCH_3}) \end{bmatrix} \tag{8.13}$$

In order to construct the traceless polarizability tensor $\underset{\sim}{\beta}_1$ for the first group in the dimethyl siloxane chain (see group 1 in Figure 8.01), the contribution of the additional Si-CH_3 group was introduced into $\underset{\sim}{\beta}_{i+1}$. This was achieved by fixing a set of axes to this additional Si-CH_3 group and resolving it into its principal polarizability components. This set of axes could then be rotated by an angle θ'', the tetrahedral bond angle supplement which is subtended at a silicon atom, to bring this coordinate system into coincidence with the coordinate system in which equation (8.13) is expressed. The two contributions to the traceless polarizability tensor of the first group were then simply added to give $\underset{\sim}{\beta}_1$:

$$\underset{\sim}{\beta}_1 = \underset{\sim}{\beta}_{i+1} + \left(\frac{3}{2}\right)^{\frac{1}{2}}\Delta\alpha_{SiCH_3} \begin{bmatrix} \cos^2\theta'' - \frac{1}{3} & \sin\theta''\cos\theta'' & 0 \\ \sin\theta''\cos\theta'' & \sin^2\theta'' - \frac{1}{3} & 0 \\ 0 & 0 & -\frac{1}{3} \end{bmatrix} \tag{8.14}$$

Since θ'' is taken to be tetrahedral, this may be simplified to

$$\underset{\sim}{\beta}_1 = \left(\frac{3}{2}\right)^{\frac{1}{2}} \begin{bmatrix} \frac{2}{3}(\Delta\alpha_{SiO} - \Delta\alpha_{SiCH_3}) & 0 & 0 \\ 0 & \frac{1}{3}(\Delta\alpha_{SiCH_3} - \Delta\alpha_{SiO}) & 0 \\ 0 & 0 & \frac{1}{3}(\Delta\alpha_{SiCH_3} - \Delta\alpha_{SiO}) \end{bmatrix} \tag{8.15}$$

The construction of the traceless polarizability tensor $\underset{\sim}{\beta}_{n+1}$ for the last group in the dimethyl siloxane chain requires the replacement of the Si-O bond in $\underset{\sim}{\beta}_{i+1}$ by a further $Si-CH_3$ group. Thus, one obtains

$$\underset{\sim}{\beta}_{n+1} = 6^{\frac{1}{2}}\Delta\alpha_{SiCH_3}\begin{bmatrix} \cos^4\psi & -\sin\psi\cos^3\psi & 0 \\ -\sin\psi\cos^3\psi & \sin^2\psi\cos^2\psi - \frac{1}{2} & 0 \\ 0 & 0 & \sin^2\psi - \frac{1}{2} \end{bmatrix} \quad (8.16)$$

Again assuming tetrahedral bond angles this becomes

$$\underset{\sim}{\beta}_{n+1} = \left(\frac{3}{2}\right)^{\frac{1}{2}}\Delta\alpha_{SiCH_3}\begin{bmatrix} \frac{2}{9} & -\frac{\sqrt{8}}{9} & 0 \\ -\frac{\sqrt{8}}{9} & -\frac{5}{9} & 0 \\ 0 & 0 & 0 \end{bmatrix} \quad (8.17)$$

Thus, the traceless optical polarizability tensors, $\underset{\sim}{\beta}_1$, $\underset{\sim}{\beta}_i$, $\underset{\sim}{\beta}_{i+1}$ and $\underset{\sim}{\beta}_{n+1}$ have been derived for dimethyl siloxane groups 1, i, i + 1 and n +1, respectively, shown in Figure 8.01. These tensors were used in the calculation of optical and electro-optical properties of dimethyl siloxane chain and cyclic molecules, to be described in the following sections of this chapter.

8.04 Calculation of the Mean-Square Optical Anisotropy of Dimethyl Siloxane Chains

Prior to calculating the mean-square optical anisotropy, $\langle\gamma^2\rangle_0$, of the dimethyl siloxane chains, the computer program was tested by calculating $\langle\gamma^2\rangle_0$ for the n-alkanes. Disparity between the results obtained for the n-alkanes and those published by Jernigan and Flory[194] has been noted earlier in this chapter. Values of $\langle\gamma^2\rangle_0/n$ obtained by these workers were substantially higher at low n (approx. 8% at n = 4) than those obtained in the present study, with the two sets of results asymptoting in the limit of n. However, the results obtained in the present study agree well with the values calculated

by Patterson and Flory[44]. These authors also pointed out the error in the former publication[194]. The values calculated in the present work for $\langle\gamma^2\rangle_0$ of the n-alkanes are listed in Appendix 2 as sample results from Program 8.

Mean-square optical anisotropies of the dimethyl siloxane chains were calculated using equation (8.7) in conjunction with the traceless polarizability tensors developed in the previous section and the bond anisotropies of Armstrong et al[190] ($\Delta\alpha_{SiO} = 0.460 \times 10^{-40} Cm^2V^{-1}$, $\Delta\alpha_{SiCH_3} = 1.265 \times 10^{-40} Cm^2V^{-1}$). The rotational isomeric-state model of Flory, Crescenzi and Mark[68] for dimethyl siloxanes was applied as detailed in Section 6.02. Results of these calculations are listed in Table 8.01. The mean-square optical anisotropy is plotted in Figure 8.02 against the number of skeletal bonds. It may be seen that after the first few members $\langle\gamma^2\rangle_0$ is predicted to rise monotonically with increasing chain length.

The quantity $\langle\gamma^2\rangle_0/n$, listed in the final column of Table 8.01 and plotted in Figure 8.03 against the number of skeletal bonds, may be regarded as being analogous to the characteristic ratio and dipole moment ratio. It is interesting to note that the plot of $\langle\gamma^2\rangle_0/n$ displays a maximum at n = 6. A similar plot of the characteristic ratio shows no maximum, whilst a plot of the dipole moment ratio shows a maximum at n = 8 which does not appear so pronounced. The presence of this maximum in the plot of dipole moment ratio, $\langle\mu^2\rangle_0/nm^2$ as a function of the number of siloxane bonds has been discussed by Mark[67] in terms of the statistically favoured all-trans conformation, the unequal bond angles and the resultant repeat unit dipole moment perpendicular to the chain axis. Figure 8.04 shows a section of dimethyl siloxane chain in the planar, all-trans conformation. Due to the unequal supplementary bond angles subtended at silicon and oxygen atoms, this chain does not generate a rectilinear axis. Instead,

Table 8.01 Calculated values of $\langle\gamma^2\rangle_0$ ($\times 10^{80}/C^2m^4V^{-2}$) and $\langle\gamma^2\rangle_0/n$ ($\times 10^{80}/C^2m^4V^{-2}$) for the linear dimethyl siloxanes.

n	$\langle\gamma^2\rangle_0$	$\langle\gamma^2\rangle_0/n$
2	1.890	0.9448
4	4.496	1.124
6	6.822	1.137
8	8.840	1.105
10	10.82	1.082
12	12.88	1.073
14	14.98	1.070
16	17.10	1.069
18	19.22	1.068
20	21.32	1.066
22	23.43	1.065
24	25.54	1.064
26	27.64	1.063
28	29.76	1.063
30	31.86	1.062
32	33.95	1.061
34	36.07	1.061
36	38.16	1.060
38	40.28	1.060
40	42.36	1.059
460	484.8	1.054
462	486.9	1.054
464	489.1	1.054
466	491.2	1.054
468	493.3	1.054
470	495.4	1.054
472	497.5	1.054

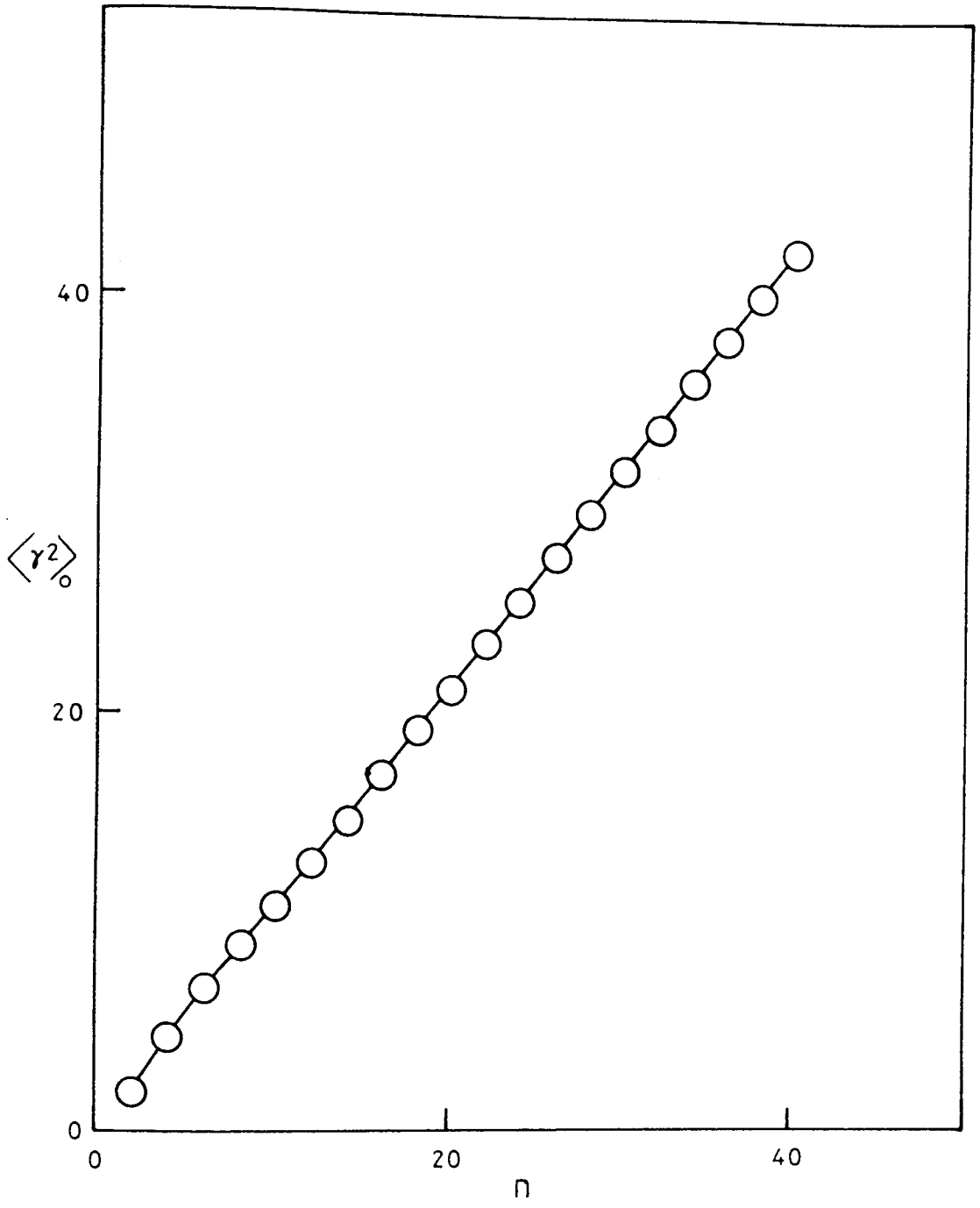

Figure 8.02 Calculated values of $\langle\gamma^2\rangle_0$ ($x10^{80}/C^2m^4V^{-2}$) for the linear dimethyl siloxanes.

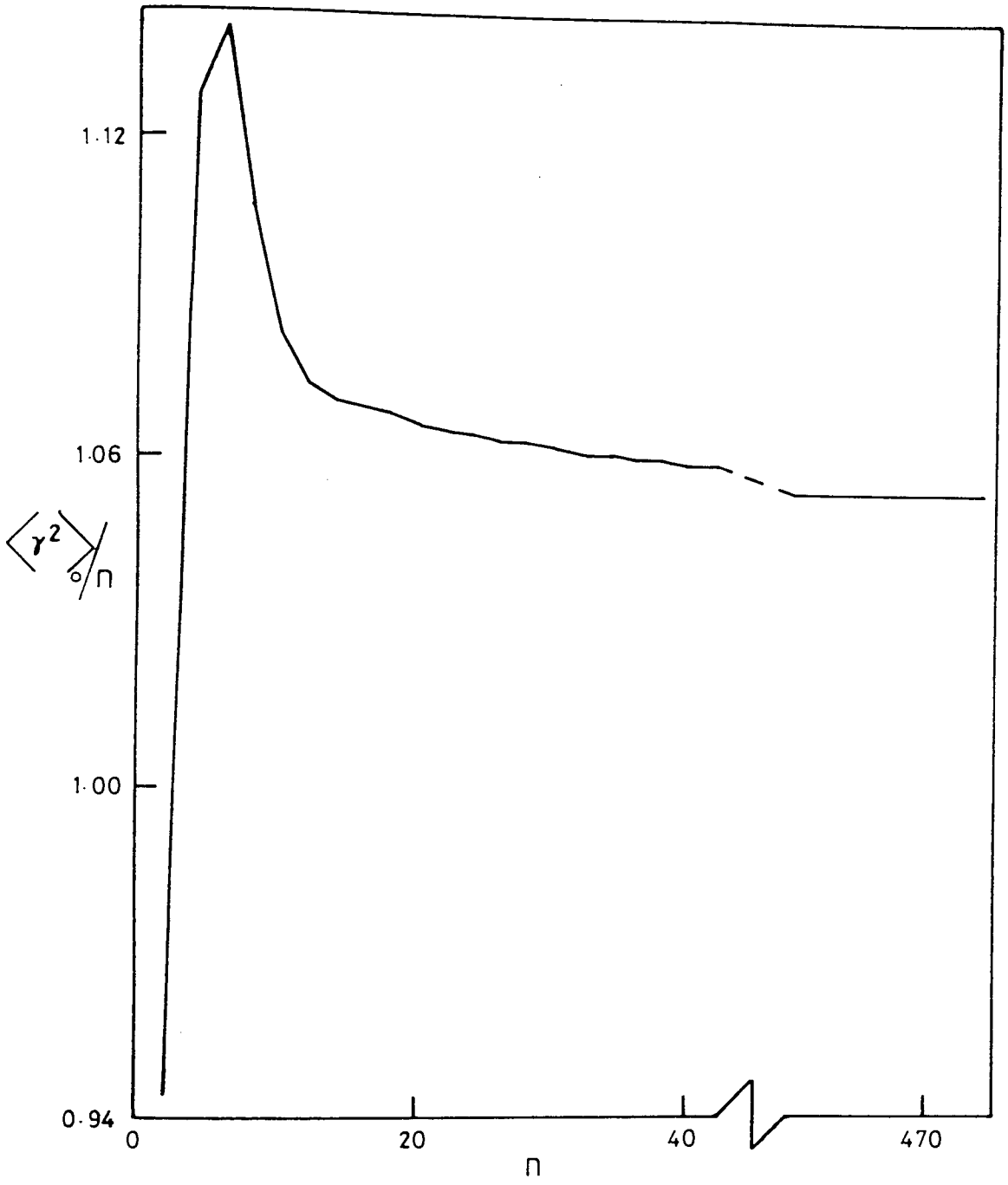

Figure 8.03 Calculated values of $\langle\gamma^2\rangle_0/n$ ($x10^{80}/C^2m^4V^{-2}$) for the linear dimethyl siloxanes

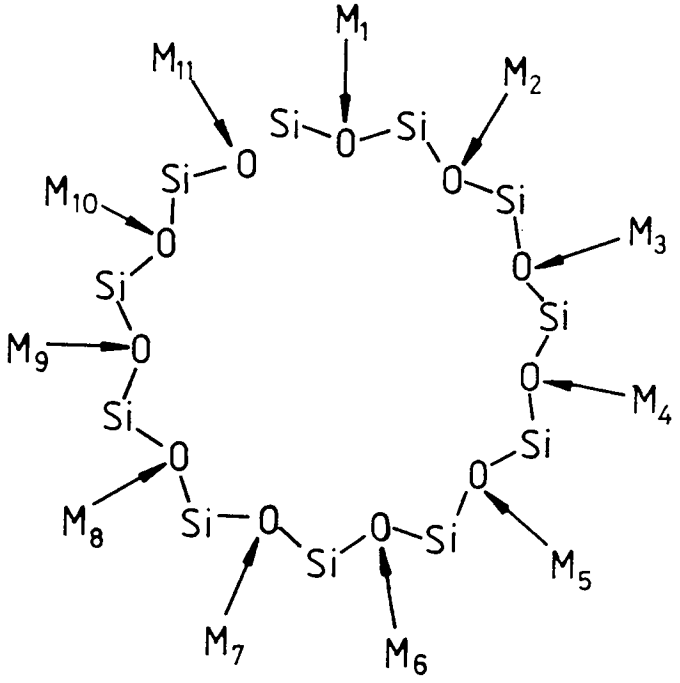

Figure 8.04 A segment of a dimethyl siloxane chain in its minimum energy, all-trans, planar conformation. The arrows represent group dipoles, M_i, for each $Si(CH_3)_2$-O-$Si(CH_3)_2$ pair of bonds.

it closes upon itself in the course of about eleven units. It may be seen by examination of Figure 8.04 that for the planar all-trans chain the dipole moment ratio may be expected to increase with n until the perpendicular resultant repeat unit dipole moments cease to be additive. After a certain value of n attenuation of the dipole vectors occurs, causing a decrease in the dipole moment ratio. Nonstatistical vectorial calculations for all-trans dimethyl siloxane chains of varying length have been conducted and the results are listed in the third and fourth columns of Table 8.02. It is apparent from these dipole moment ratios that attenuation of the dipole vectors begins after n = 8 and continues to a maximum at approximately chain closure (n = 22). This behaviour of the statistically favoured all-trans chain dominates in the statistical mechanical average over all conformations at short chain lengths. However, the effect of the all-trans conformation, which is statistically weighted unity for any chain length, upon $\langle\mu^2\rangle_0/nm^2$ diminishes as the partition function increases. Thus, although it is the all-trans conformation which is responsible for the maximum in the plot of $\langle\mu^2\rangle_0/nm^2$ against n, this conformation has a much reduced effect at longer chain lengths. Similar behaviour is also observed for plots of $\langle\gamma^2\rangle_0/n$ as a function of n, but is somewhat different due to γ^2 being a tensor property and as a consequence not displaying the same degree of attenuation. Indeed, whereas μ_0^2 for the all-trans dimethyl siloxane chain may be seen (Table 8.02) to rise to a maximum at n = 10, fall to a minimum at n = 22 (approximate ring closure) and then begin to rise again, γ_0^2 for the same type of chain merely increases steadily over the entire range of n. However, on inspection of the values of γ_0^2/n listed in the final column of Table 8.02, it does appear that it is the all-trans conformation of this chain which is responsible for the maximum at n = 6 in the $\langle\gamma^2\rangle_0/n$ plot. This phenomenon is illustrated more clearly

Table 8.02 Calculated values of the square of the dipole moment, $\mu_0^2 (x10^{60}/C^2m^2)$, dipole moment ratio, μ_0^2/nm^2, square of the optical anisotropy, $\gamma_0^2 (x10^{80}/C^2m^4V^{-2})$, and $\gamma_0^2/n (x10^{80}/C^2m^4V^{-2})$, for lengths of all-trans dimethyl siloxane chain, together with the configurational partition function, Z.

n	μ_0^2	μ_0^2/nm^2	γ_0^2	γ_0^2/n	Z
2	1.613	0.2014	1.890	0.9452	1.000
4	5.932	0.3703	6.046	1.512	2.065
6	11.56	0.4810	9.772	1.629	4.121
8	16.69	0.5208	12.48	1.560	8.221
10	19.66	0.4908	16.41	1.641	16.40
12	19.50	0.4058	23.89	1.991	32.71
14	16.29	0.2905	34.50	2.465	65.25
16	11.04	0.1723	45.59	2.850	130.1
18	5.460	0.0757	55.50	3.083	259.6
20	1.340	0.0167	65.60	3.280	517.8
22	0.01335	0.0002	78.61	3.573	1033
24	1.909	0.0199	95.28	3.970	2060
26	8.449	0.0811	113.5	4.365	4110
28	12.08	0.1077	130.8	4.671	8198

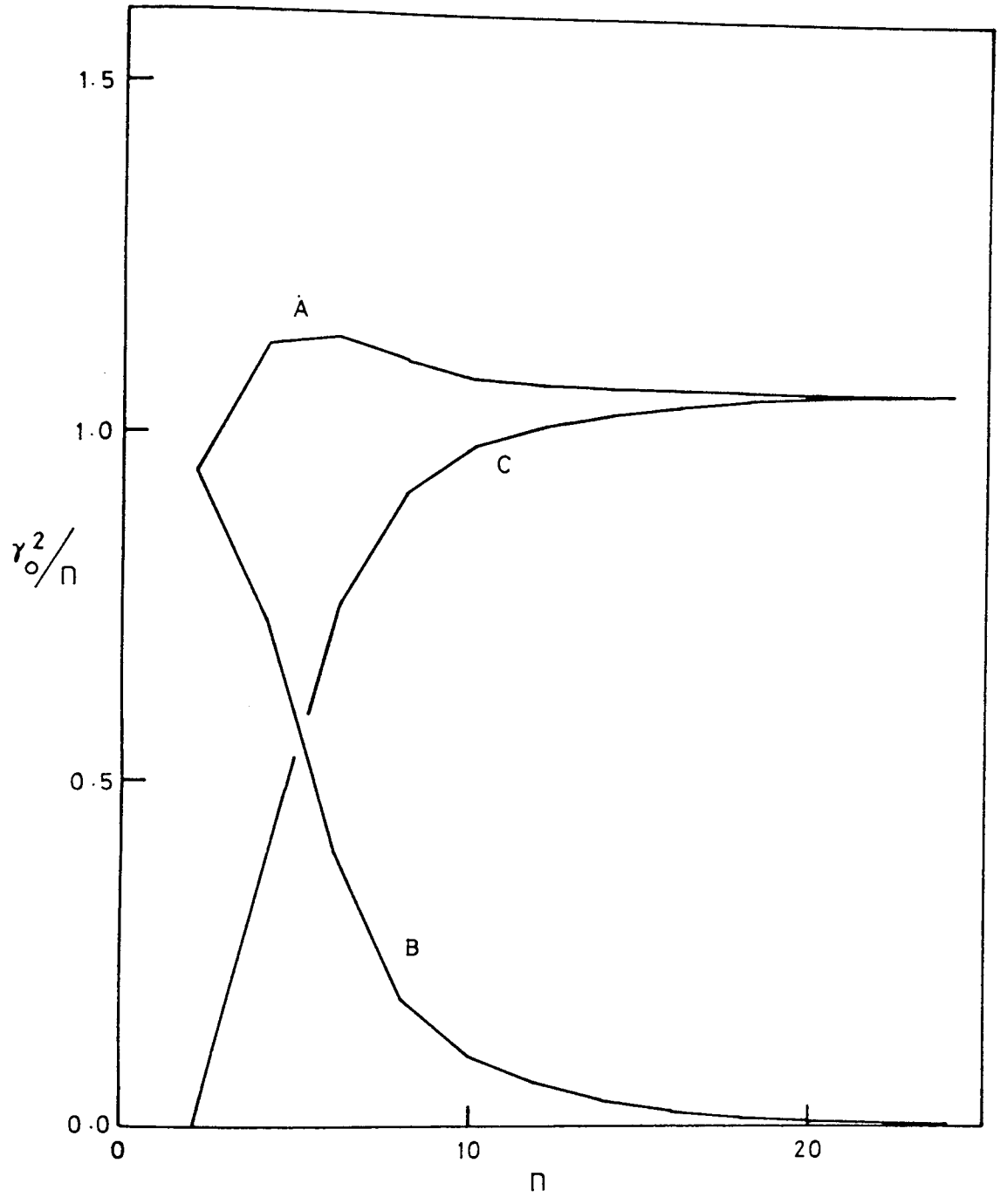

Figure 8.05 Calculated values of:

A. $\langle\gamma^2\rangle_0/n$,

B. Statistically weighted all-trans contribution, γ_0^2/nZ.

and C. Curve A - curve B,

for linear dimethyl siloxanes. All units are $(x10^{80}/C^2m^4V^{-2})$.

in Figure 8.05. In this diagram curve A represents the mean-square optical anisotropy averaged over all conformations and divided by n, $\langle\gamma^2\rangle_0/n$, as plotted in Figure 8.03, curve B represents the statistically weighted contribution of the square of the optical anisotropy, γ_0^2/nZ, of the all-trans conformation to $\langle\gamma^2\rangle_0/n$ and curve C represents the differences between curves A and B. It may be observed that if the contribution of the all-trans conformation (curve B) is subtracted from $\langle\gamma^2\rangle_0/n$ (curve A) no maximum is present in the resulting curve (c) as a function of n. Therefore, it may be concluded that it is the all-trans conformation which is responsible for the maximum in the plot of $\langle\gamma^2\rangle_0/n$ as a function of n. (Cf. origin of the maximum in the dipole moment ratio as discussed above).

8.05 Calculation of the Mean-Square Optical Anisotropy of Cyclic Dimethyl Siloxane Oligomers

Implicit matrix methods are not available to calculate average conformational properties of cyclic polymers such as the mean-square optical anisotropy, $\langle\gamma^2\rangle_0$. In order to calculate conformational dependant properties of cyclic polymers, using the rotational isomeric state model, each possible conformation of an equivalent length of polymer chain must be generated explicitly and tested to see if it satisfies the required constraints in order to be regarded as cyclic; rejecting it if it does not. Such acceptance/rejection procedures have already been conducted to generate cyclic populations for the calculation of the mean-square dipole moment of the cyclic dimethyl siloxane oligomers. Thus, the same conformational populations may be used to calculate $\langle\gamma^2\rangle_0$ for cyclic oligomers.

The equivalent open chain used in the calculation of $\langle\gamma^2\rangle_0$ for the cyclic dimethyl siloxane conformers is shown in Figure 8.06. The calculation is carried out by considering one conformation at a

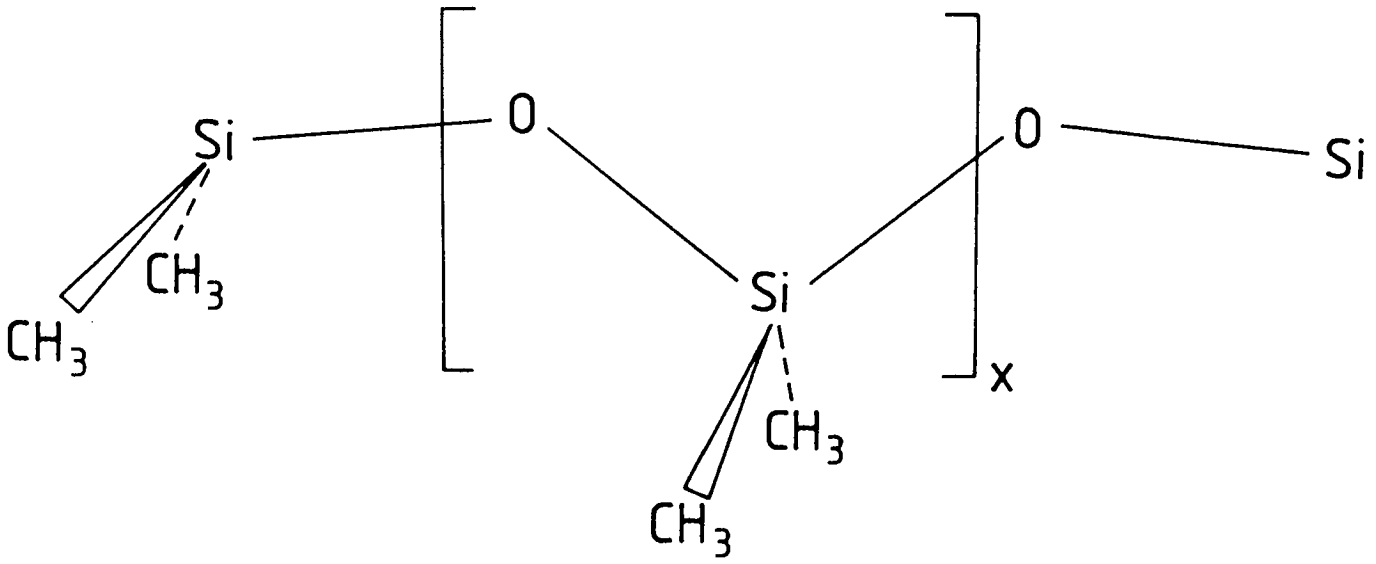

Figure 8.06 Schematic representation of the equivalent open chain used in the calculation of $\langle \gamma^2 \rangle_0$ for the cyclic dimethyl siloxanes.

time. The appropriate group polarizability tensors, formulated in Section 8.03, are transformed along the chain from their individual coordinate systems to the coordinate system of the first group. Once all the traceless group polarizability tensors of any particular conformer are expressed in the same coordinate system they may then be summed to produce the traceless polarizability tensor of the whole molecule, $\underset{\sim}{\beta}$, in the said conformation. The squared optical anisotropy, γ_0^2, of each conformation may then be obtained from $\underset{\sim}{\beta}$ using equation (8.5) and the result statistically weighted before summing over all cyclic conformations to produce $\langle\gamma^2\rangle_0$ for each oligomer.

Calculations of $\langle\gamma^2\rangle_0$ were carried out for cyclic dimethyl siloxane oligomers possessing n = 8 to n = 20 skeletal bonds. The values of $\langle\gamma^2\rangle_0$ and $\langle\gamma^2\rangle_0/n$ so produced are listed in Table 8.03 and classified in terms of the maximum end-to-end distance accepted. The conformations used in the calculation of $\langle\gamma^2\rangle_0$ for the cyclic with n = 20 skeletal bonds corresponds to a reduced population obtained by setting a maximum statistical weight of 10^{-7}. This is not expected to significantly effect the results obtained (see Chapter 7).

It was shown, in Chapter 7, that by slight adjustment of the bond rotational states the maximum acceptable end-to-end distance of the equivalent open chain may be taken to be approximately 0.25nm to calculate the mean-square dipole moment. However, since this choice of distance is somewhat arbitrary representative values of $\langle\gamma^2\rangle_0$ were calculated by averaging the entries in Table 8.03 corresponding to r = 0.20, 0.25, 0.30 and 0.35nm for each oligomer. These average values of $\langle\gamma^2\rangle_0$ are plotted in Figure 8.07 with error

Table 8.03 Calculated values of $\langle\gamma^2\rangle_0$ ($\times 10^{80}/C^2m^4V^{-2}$) and $\langle\gamma^2\rangle_0/n$ ($\times 10^{80}/C^2m^4V^{-2}$) for the cyclic conformations of the equivalent open chain $-[(CH_3)_2SiO]_x-Si$ with end-to-end distances in the range 0 to r.

n	r/nm							Chain
	0.05	0.10	0.15	0.20	0.25	0.30	0.35	
8	6.210	6.210	6.210	6.210	6.210	6.210	6.210	8.844
8	(0.7763)[a]	(0.7763)	(0.7763)	(0.7763)	(0.7763)	(0.7763)	(0.7763)	(1.106)
10	-	12.57	12.57	12.57	9.322	9.368	9.368	10.82
10	-	(1.256)	(1.256)	(1.256)	(0.9322)	(0.9368)	(0.9368)	(1.082)
12	-	18.90	15.25	15.98	16.00	16.63	16.63	12.88
12	-	(1.575)	(1.271)	(1.332)	(1.333)	(1.386)	(1.386)	(1.073)
14	-	28.39	28.35	27.54	28.38	28.38	27.74	14.99
14	-	(2.028)	(2.025)	(1.967)	(2.028)	(2.028)	(1.982)	(1.071)
16	7.231	36.95	31.74	30.36	30.44	30.42	30.42	17.12
16	(0.4519)	(2.310)	(1.984)	(1.898)	(1.903)	(1.901)	(1.901)	(1.070)
18	41.57	39.38	39.64	39.67	37.92	30.70	28.27	19.23
18	(2.310)	(2.189)	(2.202)	(2.205)	(2.107)	(1.706)	(1.571)	(1.069)
20	30.71	37.75	38.38	44.45	45.27	50.28	51.44	21.34
20	(1.536)	(1.888)	(1.919)	(2.222)	(2.264)	(2.514)	(2.572)	(1.067)

[a]Entries in parentheses are values of $\langle\gamma^2\rangle_0/n$.

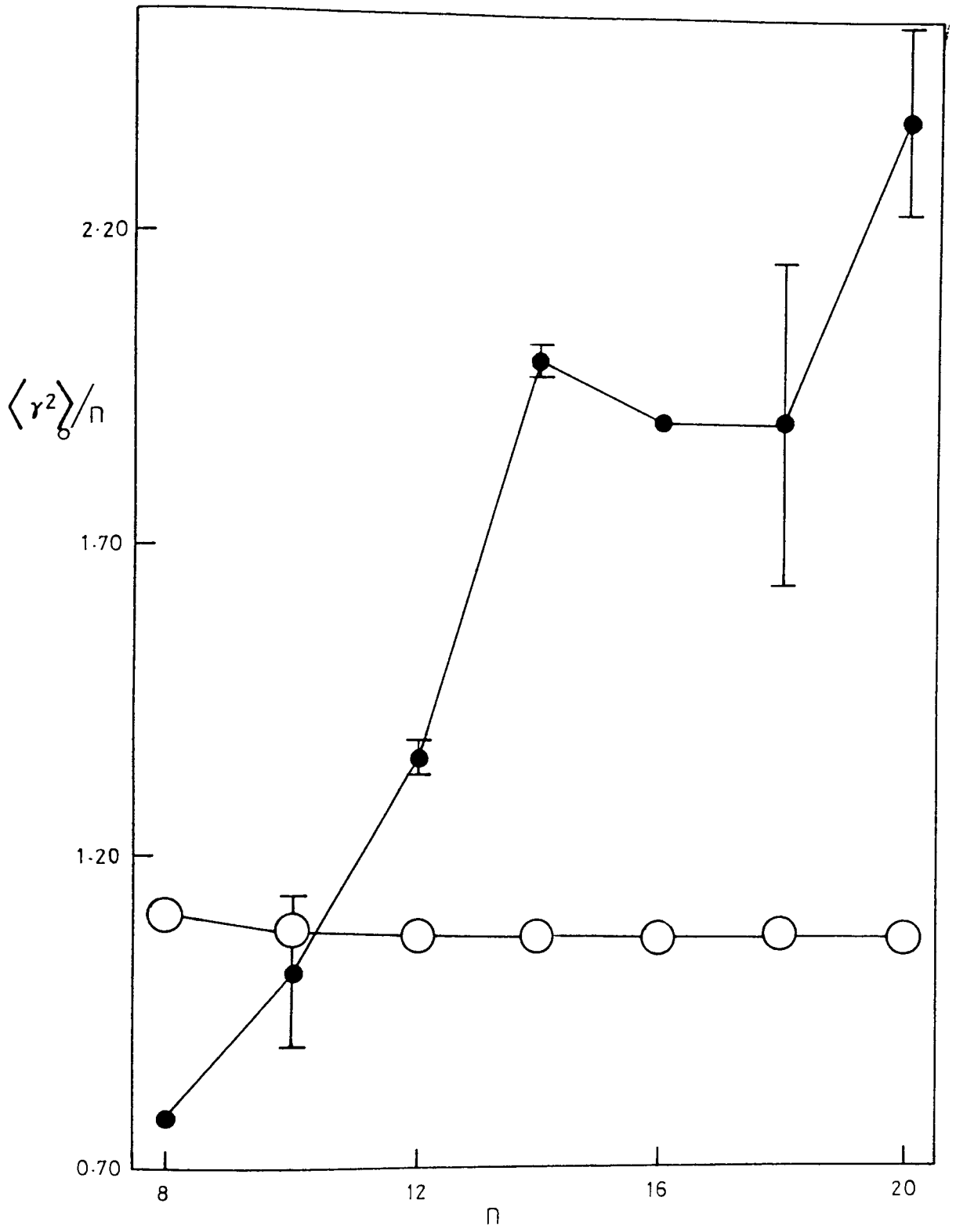

Figure 8.07 Calculated values of $\langle r^2 \rangle_0/n$ ($x10^{80}/C^2m^4V^{-2}$) for the cyclic and linear (○) dimethyl siloxanes.

bars representing the corresponding standard deviations. It may be seen from this diagram that above n = 12 the cyclic dimethyl siloxanes are predicted to have significantly higher values of $\langle\gamma^2\rangle_0/n$ than their open chain counterparts. The upward trend of $\langle\gamma^2\rangle_0/n$ exhibited by the cyclics in the range $8 \leq n \leq 20$ is not expected to continue since for much longer lengths of chain the conformations accessible to the molecule will be less internally correlated and closer to those adopted by a random flight polymer chain. As a consequence of this the optical anisotropy is expected to decrease with n. For n = 22, as noted earlier, the siloxane backbone closes upon itself when placed in the all-trans conformation. The corresponding γ_0^2/n for this conformation is calculated to be $3.5 \times 10^{-80} C^2 m^4 V^{-2}$, a value significantly larger than the average anisotropy ratio $\langle\gamma^2\rangle_0/n$ obtained for n = 20. If the configurational partition function, Z, was available for cyclic conformations of chains with n = 22 then the contribution of the all-trans conformation to $\langle\gamma^2\rangle_0/n$ for n = 22 could be calculated. This partition function is not available, however, some tentative suggestions may be made by recognising the special geometrical properties possessed by this length of chain. The ability to form a planar, highly weighted, cyclic structure implies that the all-trans conformation will dominate in the average quantity $\langle\gamma^2\rangle_0$. Other cyclic conformations will possess sequences of skeletal bonds with g^+ and g^- states and thus be allocated relatively small statistical weights. Therefore, in summary, it might be anticipated that the plot of $\langle\gamma^2\rangle_0/n$ for the cylic dimethyl siloxanes would rise to a maximum at n = 22 due to the contribution of the highly weighted all-trans conformation, and then fall to some asymptotic value with increasing n, having a value of $\langle\gamma^2\rangle_0/n$ closer to that predicted for the chain molecules.

8.06 Calculation of the Molar Kerr Constants of Polymer Chains[195]

Nagai and Ishikawa[176] have presented a rigorous treatment of the molar Kerr constant, ${}_mK$, for polymeric chain molecules, with due allowance for rotational hinderances and for the interdependence of neighbour rotations. Their result for unperturbed polymer chains is[176]

$$<{}_mK>_0 = (N_A/90\varepsilon kT)\left\{(3<\underset{\sim}{\mu}^T\,\underset{\sim}{\alpha}\underset{\sim}{\mu}> - T_r<\mu^2\underset{\sim}{\alpha}>)(kT)^{-1} + \left[3T_r<\underset{\sim}{\alpha}\underset{\sim}{\alpha}^1> - <(T_r\underset{\sim}{\alpha})(T_r\underset{\sim}{\alpha}^1)>\right]\right\} \qquad (8.18)$$

where N_A is Avogadro's number, ε is the static dielectric permittivity of free space, $\underset{\sim}{\mu}$ is the molecular dipole moment vector with $\mu = |\underset{\sim}{\mu}|$, and $\underset{\sim}{\alpha}$ and $\underset{\sim}{\alpha}^1$ are the optical and static polarizability tensors, respectively. Nagai and Ishikawa's result can be rearranged readily to

$$<{}_mK>_0 = (N_A/30\varepsilon kT)\left\{<\underset{\sim}{\mu}^T\hat{\underset{\sim}{\alpha}}\,\underset{\sim}{\mu}>(kT)^{-1} + <T_r(\hat{\underset{\sim}{\alpha}}\,\hat{\underset{\sim}{\alpha}}')>\right\} \qquad (8.19)$$

where $\hat{\underset{\sim}{\alpha}}$ and $\hat{\underset{\sim}{\alpha}}^1$ are traceless tensors $\underset{\sim}{\alpha} - \bar{\alpha}\underset{\sim}{E}_3$ and $\underset{\sim}{\alpha}^1 - \bar{\alpha}^1\underset{\sim}{E}_3$, respectively. It should be noted that $\hat{\underset{\sim}{\alpha}}$ is less than $\underset{\sim}{\beta}$ by a factor of $\sqrt{3/2}$.

It has been shown[178] that the first term in equation (8.19) may be evaluated for polymer chain molecules, using implicit matrix methods, by means of the equation

$$\sum_i^{n+1} <\underset{\sim}{\mu}^T\hat{\underset{\sim}{\alpha}}_i\underset{\sim}{\mu}>_0 = 2Z^{-1}\underset{\sim}{J}^*\,\underset{\sim}{Q}_1^{(n+1)}\,\underset{\sim}{J} \qquad (8.20)$$

where Z is the configurational partition function as defined by equation (6.8) and $\underset{\sim}{J}^*$ and $\underset{\sim}{J}$ are the appropriate row and column vectors discussed previously (see sections 6.03 and 8.02). The generator matrix $\underset{\sim}{Q}_i$ has the form as represented in equation (8.21).

Since $\hat{\underset{\sim}{\alpha}}$ and $\hat{\underset{\sim}{\alpha}}^1$ are symmetric, the second term in braces in equation (8.19) can be written[195]

$$<T_r(\hat{\underset{\sim}{\alpha}}\hat{\underset{\sim}{\alpha}}^1)> = <\hat{\underset{\sim}{\alpha}}^R\hat{\underset{\sim}{\alpha}}^{1C}> \qquad (8.22)$$

where R and C denote the row and column forms of these tensors, the one being the transpose of the other. Taking $\hat{\underset{\sim}{\alpha}}$ and $\hat{\underset{\sim}{\alpha}}^1$ to be the tensor

$$
\underset{\sim}{Q}_i = \begin{bmatrix}
\underset{\sim}{U} & (\underset{\sim}{U}\otimes\underset{\sim}{\mu}^T)||\underset{\sim}{T}|| & (\underset{\sim}{U}\otimes\hat{\underset{\sim}{\alpha}}^R)||\underset{\sim}{T}\otimes\underset{\sim}{T}|| & \tfrac{1}{2}(\underset{\sim}{U}\otimes\underset{\sim}{\mu}^T\otimes\underset{\sim}{\mu}^T)||\underset{\sim}{T}\otimes\underset{\sim}{T}\otimes\underset{\sim}{T}|| & \underset{\sim}{U}\otimes\left[\hat{\underset{\sim}{\alpha}}^R(\underset{\sim}{\mu}\otimes\underset{\sim}{E}_3)\right]||\underset{\sim}{T}|| & \tfrac{1}{2}\underset{\sim}{U}\left[\hat{\underset{\sim}{\alpha}}^R(\underset{\sim}{\mu}\otimes\underset{\sim}{\mu})\right] \\
\underset{\sim}{0} & (\underset{\sim}{U}\otimes\underset{\sim}{E}_3)||\underset{\sim}{T}|| & \underset{\sim}{0} & (\underset{\sim}{U}\otimes\underset{\sim}{E}_3\otimes\underset{\sim}{\mu}^T)||\underset{\sim}{T}\otimes\underset{\sim}{T}|| & (\underset{\sim}{U}\otimes\hat{\underset{\sim}{\alpha}})||\underset{\sim}{T}|| & \underset{\sim}{U}\otimes\left[(\underset{\sim}{E}_3\otimes\underset{\sim}{\mu}^T)\hat{\underset{\sim}{\alpha}}^C\right] \\
\underset{\sim}{0} & \underset{\sim}{0} & (\underset{\sim}{U}\otimes\underset{\sim}{E}_9)||\underset{\sim}{T}\otimes\underset{\sim}{T}|| & \underset{\sim}{0} & (\underset{\sim}{U}\otimes\underset{\sim}{\mu}\otimes\underset{\sim}{E}_3)||\underset{\sim}{T}|| & \tfrac{1}{2}(\underset{\sim}{U}\otimes\underset{\sim}{\mu}\otimes\underset{\sim}{\mu}) \\
\underset{\sim}{0} & \underset{\sim}{0} & \underset{\sim}{0} & (\underset{\sim}{U}\otimes\underset{\sim}{E}_9)||\underset{\sim}{T}\otimes\underset{\sim}{T}|| & \underset{\sim}{0} & \underset{\sim}{U}\otimes\hat{\underset{\sim}{\alpha}}^C \\
\underset{\sim}{0} & \underset{\sim}{0} & \underset{\sim}{0} & \underset{\sim}{0} & (\underset{\sim}{U}\otimes\underset{\sim}{E}_3)||\underset{\sim}{T}|| & \underset{\sim}{U}\otimes\underset{\sim}{\mu} \\
\underset{\sim}{0} & \underset{\sim}{0} & \underset{\sim}{0} & \underset{\sim}{0} & \underset{\sim}{0} & \underset{\sim}{U}
\end{bmatrix}_i \tag{8.21}
$$

sums of group contributions $\hat{\underset{\sim}{Q}}_i$ and $\hat{\underset{\sim}{Q}}_i^1$, respectively, the following equation has been obtained

$$\langle \hat{\underset{\sim}{Q}}^R \hat{\underset{\sim}{Q}}^{1C} \rangle = Z^{-1} \underset{\sim}{J}^* \underset{\sim}{A}_1^{n+1} \underset{\sim}{J} \qquad (8.23)$$

with

$$\underset{\sim}{A}i = \begin{bmatrix} \underset{\sim}{U} & (\underset{\sim}{U} \otimes \hat{\underset{\sim}{Q}}^R)||\underset{\sim}{T} \otimes \underset{\sim}{T}|| & (\underset{\sim}{U} \otimes \underset{\sim}{Q}^{1R})||\underset{\sim}{T} \otimes \underset{\sim}{T}|| & (\hat{\underset{\sim}{Q}}^R \hat{\underset{\sim}{Q}}^{1C})\underset{\sim}{U} \\ \underset{\sim}{0} & (\underset{\sim}{U} \otimes \underset{\sim}{E}_9)||\underset{\sim}{T} \otimes \underset{\sim}{T}|| & \underset{\sim}{0} & \underset{\sim}{U} \otimes \hat{\underset{\sim}{Q}}^{1C} \\ \underset{\sim}{0} & \underset{\sim}{0} & (\underset{\sim}{U} \otimes \underset{\sim}{E}_9)||\underset{\sim}{T} \otimes \underset{\sim}{T}|| & \underset{\sim}{U} \otimes \hat{\underset{\sim}{Q}}^C \\ \underset{\sim}{0} & \underset{\sim}{0} & \underset{\sim}{0} & \underset{\sim}{U} \end{bmatrix}_i \qquad (8.24)$$

Thus, by means of equations (8.19),(8.20), (8.21), (8.23) and (8.24) Kerr constants for polymer chains are readily calculable.

8.07 Calculation of the Molar Kerr Constants of Dimethyl Siloxane Chains

Prior to calculating the molar Kerr constant, ${}_mK$, of the dimethyl siloxane chains, the computer program (Program 10) was tested by calculating ${}_mK$ for the n-alkanes and the poly(oxyethylene glycols). The results obtained for both series of polymers were in good agreement with those calculated by Ishikawa and Nagai[198]. The values of ${}_mK$ obtained in the present study for the poly(oxyethylene glycols) are listed in Appendix 2 as sample output from Program 10.

Molar Kerr constants of dimethyl siloxane chains were calculated using the equations presented in the previous section, in conjunction with the traceless polarizability tensors developed in Section 8.03, after division by $\sqrt{3/2}$, and the bond anisotropies of Armstrong et al[190] ($\Delta\alpha_{SiO} = 0.460 \times 10^{-40} Cm^2V^{-1}$, $\Delta\alpha_{SiCH_3} = 1.265 \times 10^{-40} Cm^2V^{-1}$). The rotational isomeric-state model of Flory, Crescenzi and Mark[68] for dimethyl siloxanes as detailed in Section 6.02 was applied.

The bond anisotropies obtained by Armstrong et al[190] correspond to measurements made at optical wavelengths. Thus, substitution of these bond anisotropies into equation (8.9), (8.13), (8.15) and (8.17), after division by $\sqrt{3/2}$, will produce the optical traceless polarizability

tensor, $\underset{\sim}{\hat{\alpha}}$. In order to evaluate the second term appearing in equation (8.19) it is necessary to know the static polarizability tensor, $\underset{\sim}{\alpha}^1$. Gans suggested[122,196] that the half-axes of the static (a_1, a_2 and a_3) and optical (b_1, b_2 and b_3) polarizability ellipsoids could be assumed to be related by the following quotients.

$$\frac{a_1}{b_1} = \frac{a_2}{b_2} = \frac{a_3}{b_3} = \frac{(\varepsilon_0 - 1)}{(n^2 - 1)} \qquad (8.25)$$

However, it must be noted that Gans was working on non-polar gases and thus the static permittivity, ε_0, contained no contributions from orientational polarization. Le Fèvre[36], however, has obtained the same end by taking

$$\frac{a_i}{b_i} = \frac{P_D}{P_E} \qquad (8.26)$$

where P_D and P_E are the distortion (i.e. atomic and electronic) polarization and electronic polarization, respectively. It is convenient to measure the Kerr effect by using dilute solutions of solute molecules in a non-polar solvent. A value for the static polarizability ellipsoid (i.e. $P_D = P_E + P_A$) is still required, but the dielectric permittivity of the medium (solution) cannot be used to obtain P_D as was the case for a single-component non-polar gas. This is due to the fact that for a dilute solution the solvent contributes almost entirely to the electrostatic polarizability of the solution. In these circumstances the static dielectric permittivity of the solution cannot be used to calculate the atomic polarization of the solute molecules. Thus, P_D for the solute molecules must be obtained in a separate experiment. Values of P_D and P_E for the cyclic and linear dimethyl siloxanes have been measured by methods described previously and are tabulate in Chapter 5. The ratio P_D/P_E calculated from these measured polarizations of the linear dimethyl siloxanes

Table 8.04 Gans ratios (P_D/P_E) for linear dimethyl siloxanes calculated from the experimentally determined polarizations tabulated in Chapter 5.

$\bar{N}$	P_D/P_E
2	1.20
4	1.21
6	1.23
8	1.23
10	1.24
12	1.26
16.54	1.29
21.72	1.31
24.4	1.32
32.4	1.33
41.6	1.34
105	-
206	1.36

are listed in Table 8.04. It may be seen that the Gans ratios (~1.3) are considerably higher than those of 'typical' molecules which usually have values in the range 1.00 - 1.10. This difference reflects the anomalously high atomic polarizations of the dimethyl siloxanes.

By inspection of equation (8.19) it is apparent that the molar Kerr constant may be regarded as being composed of an anisotropy term, $\langle\theta_1\rangle_0$, and a dipole term, $\langle\theta_2\rangle_0$, such that

$$\langle {}_mK\rangle_0 = \langle\theta_1\rangle_0 + \langle\theta_2\rangle_0 \qquad (8.27)$$

The values of these terms have been calculated for dimethyl siloxane chains using a Gans ratio of 1.3 for the evaluation of $\langle\theta_1\rangle_0$. The terms $\langle\theta_1\rangle_0/n$, $\langle\theta_2\rangle_0/n$ and $\langle {}_mK\rangle_0/n$ as a function of the number of siloxane bonds, n, are plotted in Figure 8.08. The anisotropy term, $\langle\theta_1\rangle_0/n$, shows a maximum value at n = 6, but varies little over the entire range with n, and asymptotes quickly to a value of approximately $5.0 \times 10^{-27} m^5 V^{-2} mol^{-1}$ (S.I. units = $10^{-27} m^5 V^2 mol^{-1}$). By contrast the dipolar term, $\langle\theta_2\rangle_0/n$, has a pronounced maximum value at n = 4 of about 5.8 SI units and then falls rapidly to a shallow minimum of -5.2 SI units at n = 16, followed by a slow rise to an asymptotic value of approximately -4.2 SI units. The changes in the value of $\langle {}_mK\rangle_0/n$ with n naturally reflect those of the dominant dipolar term. At n = 4 $\langle {}_mK\rangle_0/n$ has a maximum value of 11.4 SI units, which falls rapidly with increasing n to become slightly negative at n = 16, rising slowly again to approach an asymptotic value close to 0.89 SI units. The induced term, $\langle\theta_1\rangle_0/n$, is the only term affected by the value of the Gans ratio. Since, this term is approximately constant throughout the whole range of n, a change in the value of the Gans ratio, which merely acts as a premultiplying factor for the anisotropy term, will simply cause a shift up or down the ordinate axis.

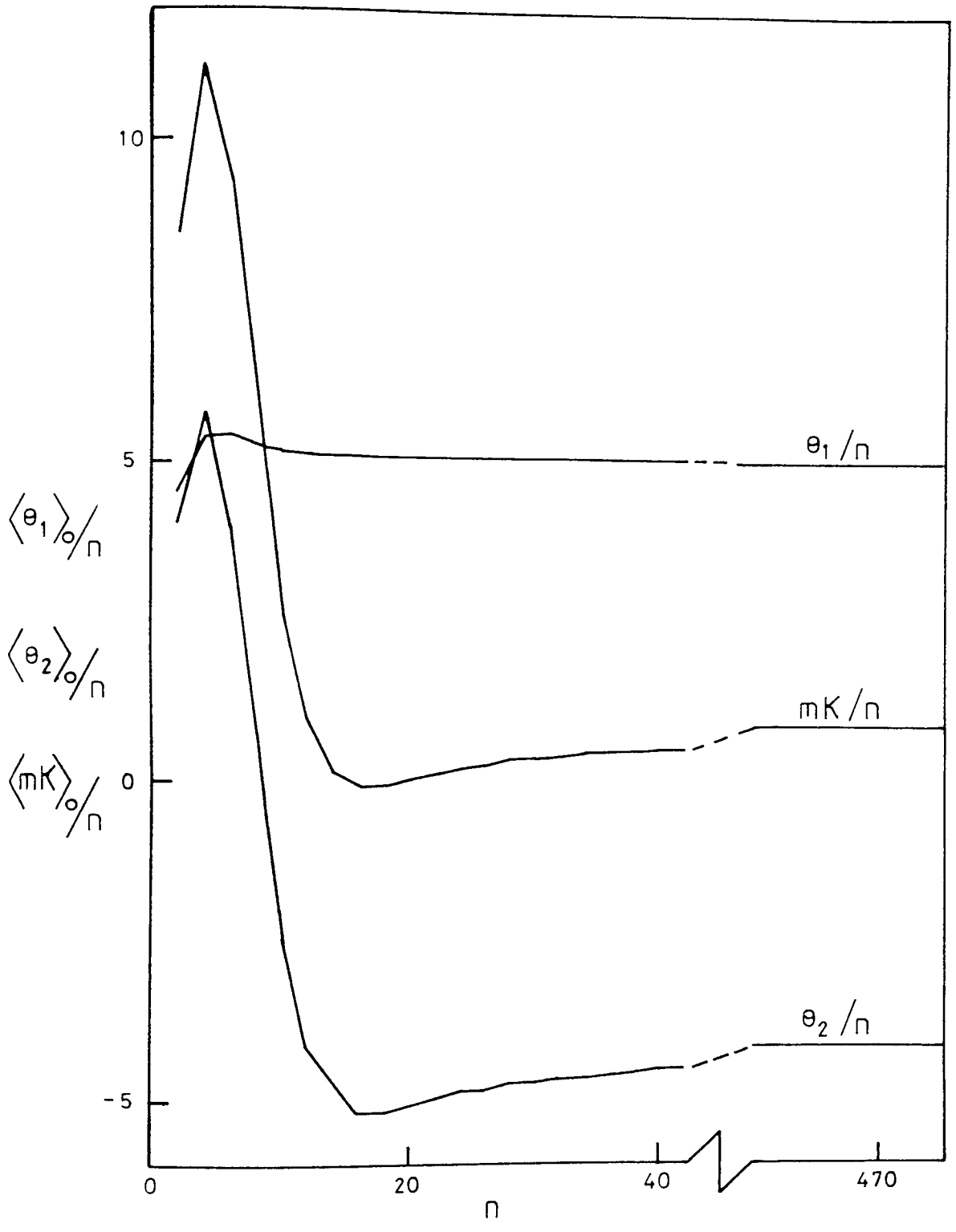

Figure 8.08 Calculated values of the anisotropy term, $\langle\theta_1\rangle_0/n$ ($x10^{27}/m^5V^{-1}\ mol^{-1}$), dipolar term, $\langle\theta_2\rangle_0/n$ ($x10^{27}/m^5V^{-1}mol^{-1}$), and the molar Kerr constant term, $\langle mK\rangle_0/n$ ($x10^{27}/m^5V^{-1}mol^{-1}$).

Consequently, this will be reflected by a similar shift in the value of $<_mK>_0/n$. Thus, the value of the Gans ratio has no significant effect upon the trend of the plot of $<_mK>_0/n$ with n as predicted by the valence optical scheme.

8.08 Comparison of Experimental and Calculated Molar Kerr Constants for Cyclic and Linear Dimethyl Siloxanes

Theoretical studies by Nagai and Ishikawa[61], and later by Doi[62] who added refinements, have shown that for polymer chains obeying certain symmetry conditions the mean-square dipole moment is unaffected by excluded-volume. The mean-square optical anisotropy, $<\gamma^2>$, has been shown by theory to be insensitive to excluded-volume[32,197]. Since $<\gamma^2>$ is related to the anisotropy term in the molar Kerr constant by

$$<\gamma^2> = (3/2)\,\text{trace}\,<\hat{\underset{\sim}{\alpha}}\,\hat{\underset{\sim}{\alpha}}>, \qquad (8.28)$$

the anisotropy term is also expected to be independant of excluded-volume effects. Thus, for polymer chains having the appropriate symmetry conditions the molar Kerr constant is expected to be unaffected by excluded-volume. One of the symmetry conditions described by Nagai and Ishikawa[61], pertinent to dimethyl siloxanes, is that there is no distinguishable direction along the chain contour (i.e. that the chain is not crystallographically polar). Therefore, experimental and theoretical values of $_mK$ for dimethyl siloxanes may be directly compared.

Preliminary experimental results of the Kerr effect of low molecular weight dimethyl siloxane oligomers measured in the undiluted state at 298K are shown in Table 8.05. The molar Kerr constant, $_mK$, was calculated from the experimental Kerr constant, B, by means of the equation[36]

$$_mK = \frac{6Bn_{\lambda\to\infty}\,\lambda M}{(\varepsilon_0 + 2)^2\,(n^2_{\lambda\to\infty} + 2)^2\rho}, \qquad (8.29)$$

Table 8.05 Experimental Kerr constants, $B(x10^{14}/mV^{-2})$, and molar Kerr constants, ${}_mK(x10^{27}/m^5V^{-2}mol^{-1})$, for some low molecular weight cyclic and linear dimethyl siloxane oligomers measured in the undiluted state at 298K.

Sample	B	${}_mK$	${}_mK/n$
I Chain n = 2	0.054	2.3[a]	1.15
II Chain residue[b]	0.067	~6.6[c]	~0.55[c]
III Cyclic n = 8	0.058	3.2	0.40
IV Cyclic n = 10	0.058	3.8	0.38

[a] In good agreement with the value ($2.51 \times 10^{-27} m^5V^{-2}mol^{-1}$) measured by Armstrong et al[190] in solution in carbon tetrachloride at 298K.

[b] Sample of chain residue after removing lower molecular weight material by fractional distillation (see Table 3.04).

[c] Approximate value of the molar Kerr constant calculated assuming $n \simeq 12$.

where all symbols have their usual meanings (see Chapter 4 and 5). The experimental value of ${}_mK(2.3 \times 10^{-27} m^5 V^{-2} mol^{-1})$(SI units = 10^{-27} $m^5 V^{-2} mol^{-1}$) for neat hexamethyldisiloxane (I. Chain n = 2) may be seen to be considerably lower than that calculated theoretically (17.13SI units). An approximate value of ${}_mK$(6.6 SI units) for the chain residue sample (II) was calculated assuming n = 12, and using the relevant physical quantities recorded in Chapter 4 for this oligomer. This value corresponds more closely to that predicted theoretically (11.3 SI units) for the chain than in the case of hexamethyldisiloxane. It might also be tentatively pointed out that the falling trend in the experimentally determined ratio ${}_mK/n$, between sample I and sample II, appears to have been correctly predicted by the valence optical method. Although no change in the value of the experimental Kerr constant, B, was observed for cyclics with n = 8 and cyclics with n = 10, a difference does arise in the molar Kerr constant of these samples due to differences in their other physical properties.

Discrepancies between values of ${}_mK/n$ determined experimentally and those predicted by means of the valence optical scheme may have arisen from several sources. Bond anisotropies determined by Armstrong et al[190] were derived from measurements on several silanes and siloxanes, and it is unclear as to whether or not these values are applicable to the different chemical environment of the dimethyl siloxanes. Measurements of the experimental Kerr constant, B, were made in this study on neat liquids instead of dilute solutions in a non-polar solvent, which would have been preferable. Thus, errors may have arisen from three major sources, as detailed by Patterson and Flory[44]: (i) the internal field due to neighbouring molecules, (ii) intermolecular influences originating in geometrical or electrical (e.g. dipolar) asymmetries of neighbouring molecules and involving correlations between the axes of their polarizability tensors, and (iii) induced

optical anisotropy due to intermolecular collisions giving rise to transitory asymmetries in the molecules. Unfortunately due to the small magnitudes of the molar Kerr constants for these dimethyl siloxane oligomers, it was not possible to make measurements upon dilute solutions of these materials with the currently available apparatus. The aforegoing discussion details some of the most probable sources of discrepancy between experimentally determined and theoretically predicted values of the molar Kerr constant of the dimethyl siloxanes. However, further measurements are required before firm conclusions may be drawn and before an explanation may be advanced to account for the discrepancies observed between experimental and theoretical molar Kerr constants of dimethyl siloxane oligomers.

CHAPTER 9

EXPERIMENTAL INVESTIGATION OF THE DIELECTRIC AND ELECTRO-OPTICAL PROPERTIES OF POLY(N-VINYL CARBAZOLE) AND MODEL COMPOUNDS

9.01 Introduction

Recently a great deal of interest[22] has been shown in the photo-induced electrical conductivity of bulk poly(N-vinyl carbazole), PVK, and PVK systems doped with a variety of electron acceptor molecules. Since PVK possesses a chiral centre in its repeat unit an important question arises concerning the effect of tacticity on its various electrical and photo-electrical properties. Proton[140] and carbon-13 NMR[141,142] studies have indicated that the synthetic route used to prepare PVK has a marked effect on its stereoregularity. Thus radical based polymerizations are believed to lead to an increased racemic content[141] while cationic mechanisms result in the production of polymer containing varying amounts of racemic and meso groups[140-142] depending on the exact nature of the catalytic system. However, it is recognised that the interpretation of proton and carbon-13 NMR spectra is not completely unambiguous. Thus, additional complementary experimental data on these materials, using techniques sensitive to their conformations, are essential if meaningful correlations are to be made between electrical conductivities and stereostructure.

This chapter details the measurement, and results obtained, for the static dielectric permittivity, ε_{12}, and the static experimental Kerr constant, B_{12}, of several samples of PVK prepared by different

synthetic routes. Values of ε_{12} and B_{12} are also recorded for carbazole and 9-ethyl carbazole, which will be used as monomeric models. All measurements were conducted on solutions of the solutes in 1,4-dioxan. Both ε_{12} and B_{12} are fundamental measured quantities and, thus, may be compared without relying upon the validity of any dielectric theory. However, more useful quantities, when investigating the tacticities and conformations of polymers in solution, are the electric dipole moment, μ_2, and the electro-optical molar Kerr constant, ${}_mK_2$, of the solute molecules. Values of μ and ${}_mK$ will be calculated in the following chapter using the measured values of ε_{12} and B_{12} together with the other relevant physical properties.

Previous studies of the dielectric properties of PVK have focused either on dielectric relaxation or have been performed on poorly characterised polymer samples[199-204]. No electro-optical Kerr effect measurements have been previously published for PVK. In the present dielectric and electro-optical study three different synthetic routes were used to prepare samples (S1, S2 and S3) of PVK with different stereostructures. Samples S1 and S2 were prepared by cationic polymerization using $AlCl_3$ and $BF_3(OC_2H_5)_2$ based systems, respectively, and sample S3 was obtained by radical polymerization using azobisisobutyronitrile, AZBN, as the initiator. (For further details of the preparation of these samples of PVK see Chapter 3). The fractions of polymer taken for the present study were in the number-average molar mass range $10^4 < \bar{M}_n < 10^7$.

9.02 Static Dielectric Permittivities of PVK Fractions and Model Compounds

Static dielectric permittivities, ε_{12}, of each of the different molecular weight fractions of PVK samples S1, S2, S3 and S4, and model

compounds, carbazole and 9-ethyl carbazole, were determined at 298K in solution in 1,4-dioxan. These measurements were made at several concentrations using the large sample volume dielectric apparatus in conjunction with dielectric cell B. The static dielectric permittivity of 1,4-dioxan at 298K was taken to be 2.209[131] and the frequency counter method of determining solution permittivities was employed (see Sections 2.06 and 2.07). Plots of ε_{12} against weight fraction of solute, w_2, for PVK samples S1-S4 are shown in Figures 9.01 to 9.04, respectively. For clarity in these Figures each of the lines corresponding to a different molecular weight fraction has been successively displaced up the ordinate axis. For all samples of PVK the plots of ε_{12} against w_2 are linear, and their gradients are independent of molecular weight and heterogeneity index. To aid comparison of the plots presented in Figures 9.01 to 9.04 an average gradient of each plot was calculated and these are shown in Figure 9.05. Gradients of plots corresponding to samples S1 and S2 are the same, within experimental error, as are those of samples S3 and S4. Although a least-mean squares analysis resulted in non-overlapping error bars for sample types S3 and S4, suggesting a slight difference in their dielectric behaviour, additional experimental data based on carbon-13 NMR indicated that the stereo-structure of these two polymers are identical to one another. However, it is quite apparent that there is a significant difference between the dielectric properties of samples S1-S2 and those found for S3-S4. It appears that the effective dipole moment associated with individual repeat units is greater for the polymers (S1-S2) prepared using cationic catalyst systems.

Plots of ε_{12} against w_2 for the model compounds, carbazole and

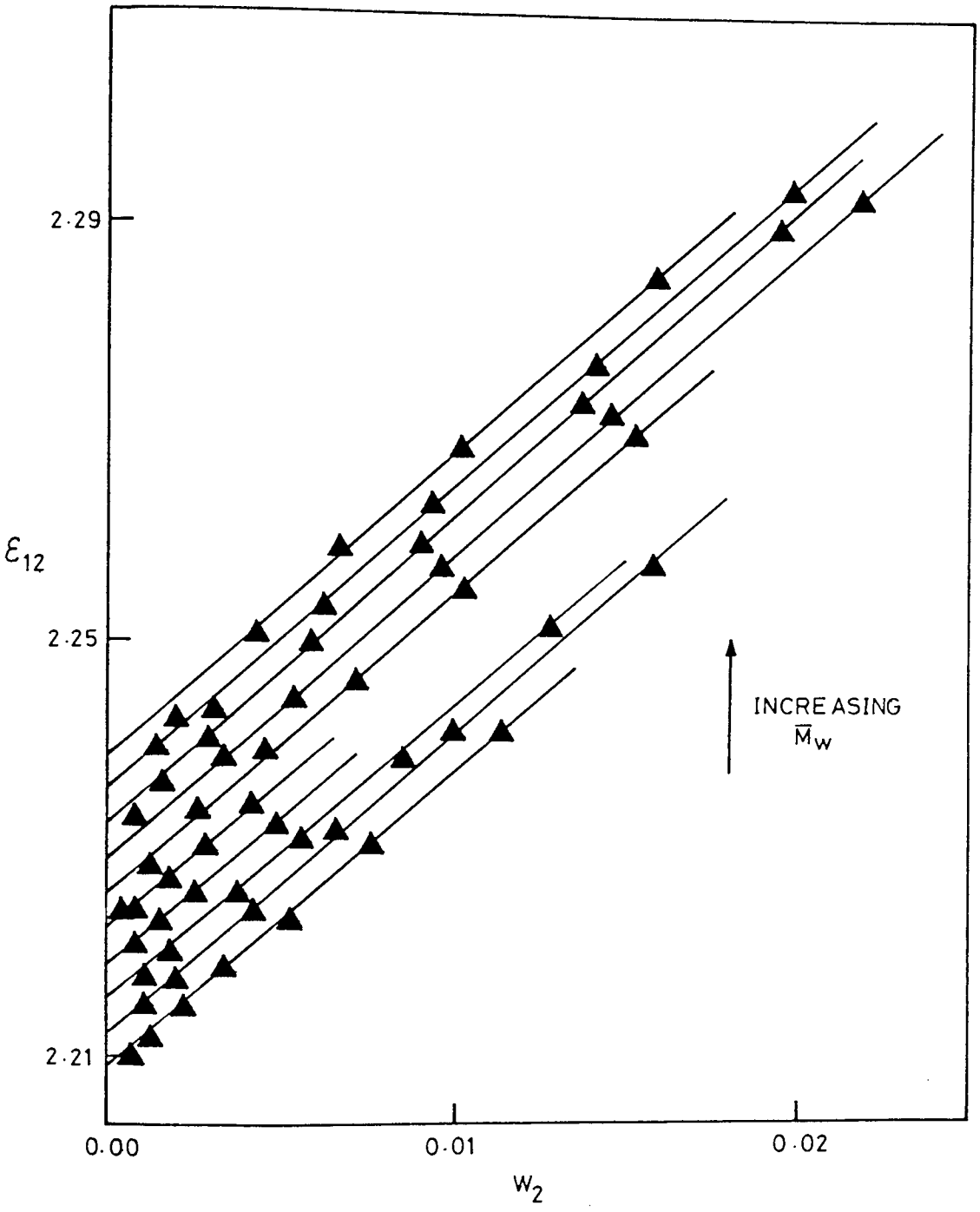

Figure 9.01 Static dielectric permittivity, ε_{12}, against weight fraction of solute, w_2, for fractions of PVK sample S1, in order of increasing weight-average molecular weight, $\bar{M}_w$, (see Table 3.07), in solution in 1,4-dioxan at 298K. The plots for each fraction are successively displaced for clarity.

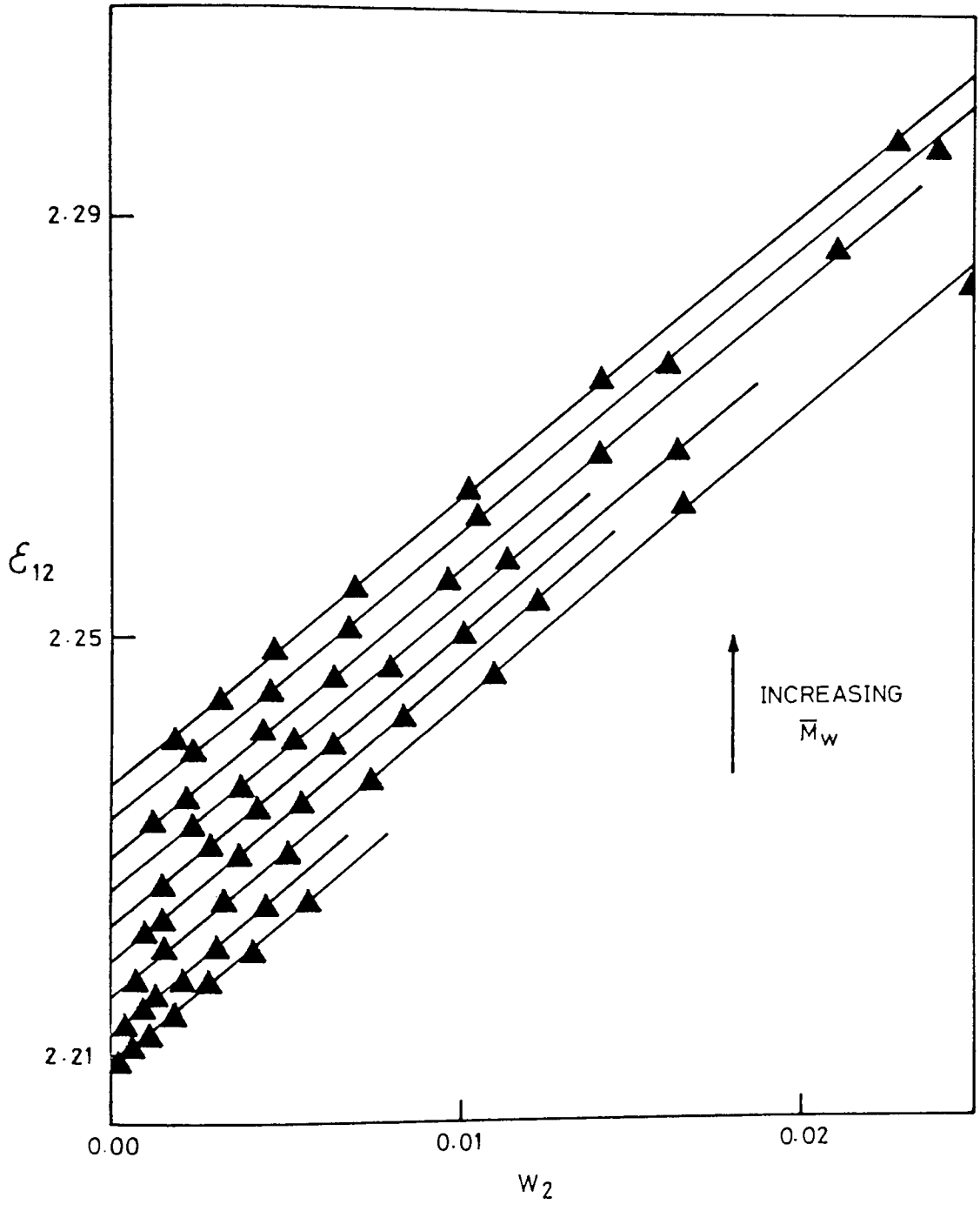

Figure 9.02 Static dielectric permittivity, ε_{12}, against weight fraction of solute, w_2, for fractions of PVK sample S2, in order of increasing weight-average molecular weight, $\bar{M}_w$, (see Table 3.08), in solution in 1,4-dioxan at 298K. The plots for each fraction are successively displaced for clarity.

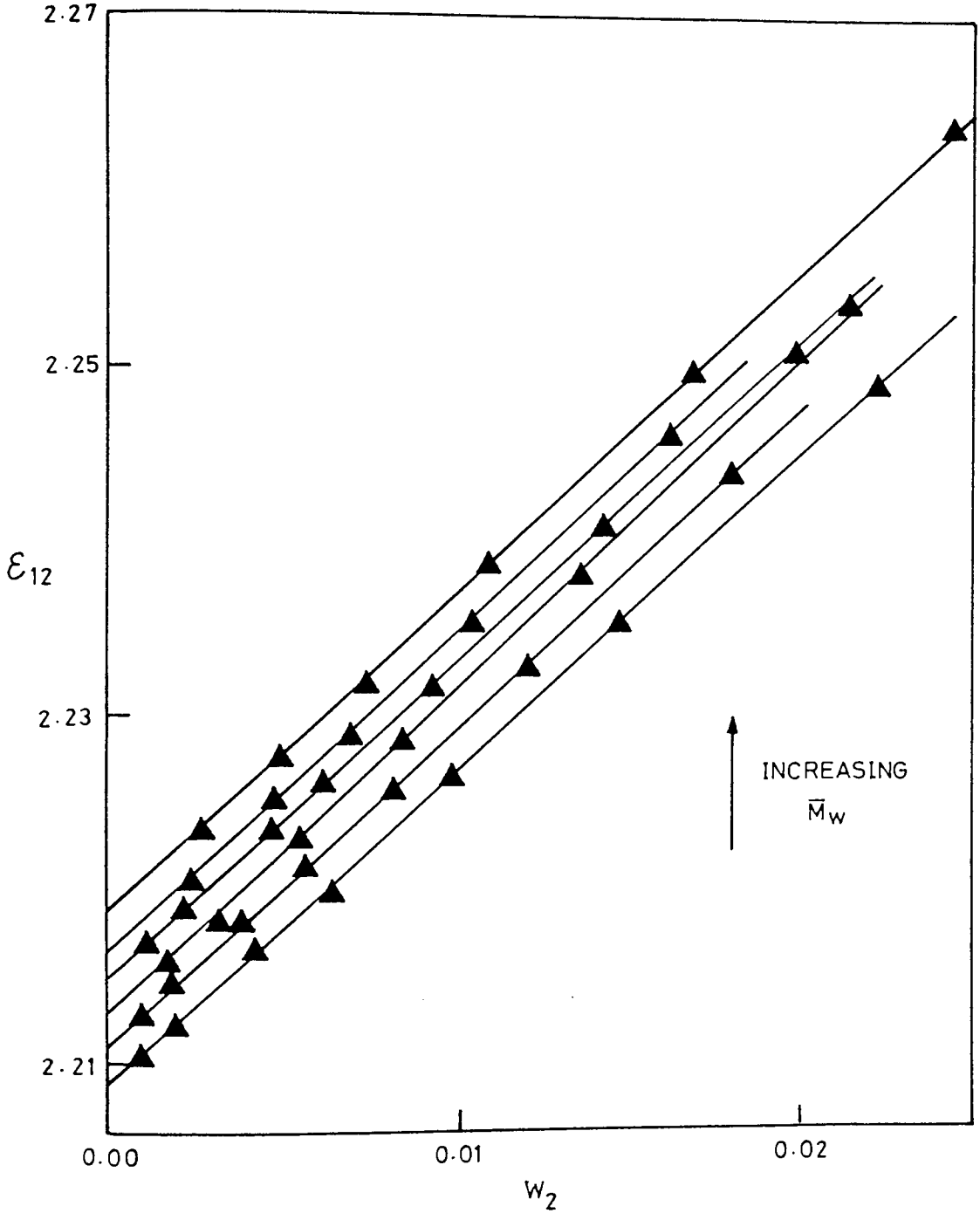

Figure 9.03 Static dielectric permittivity, ε_{12}, against weight fraction of solute, w_2, for fractions of PVK sample S3, in order of increasing weight-average molecular weight, $\bar{M}_w$, (see Table 3.09), in solution in 1,4-dioxan at 298K. The plots for each fraction are successively displaced for clarity.

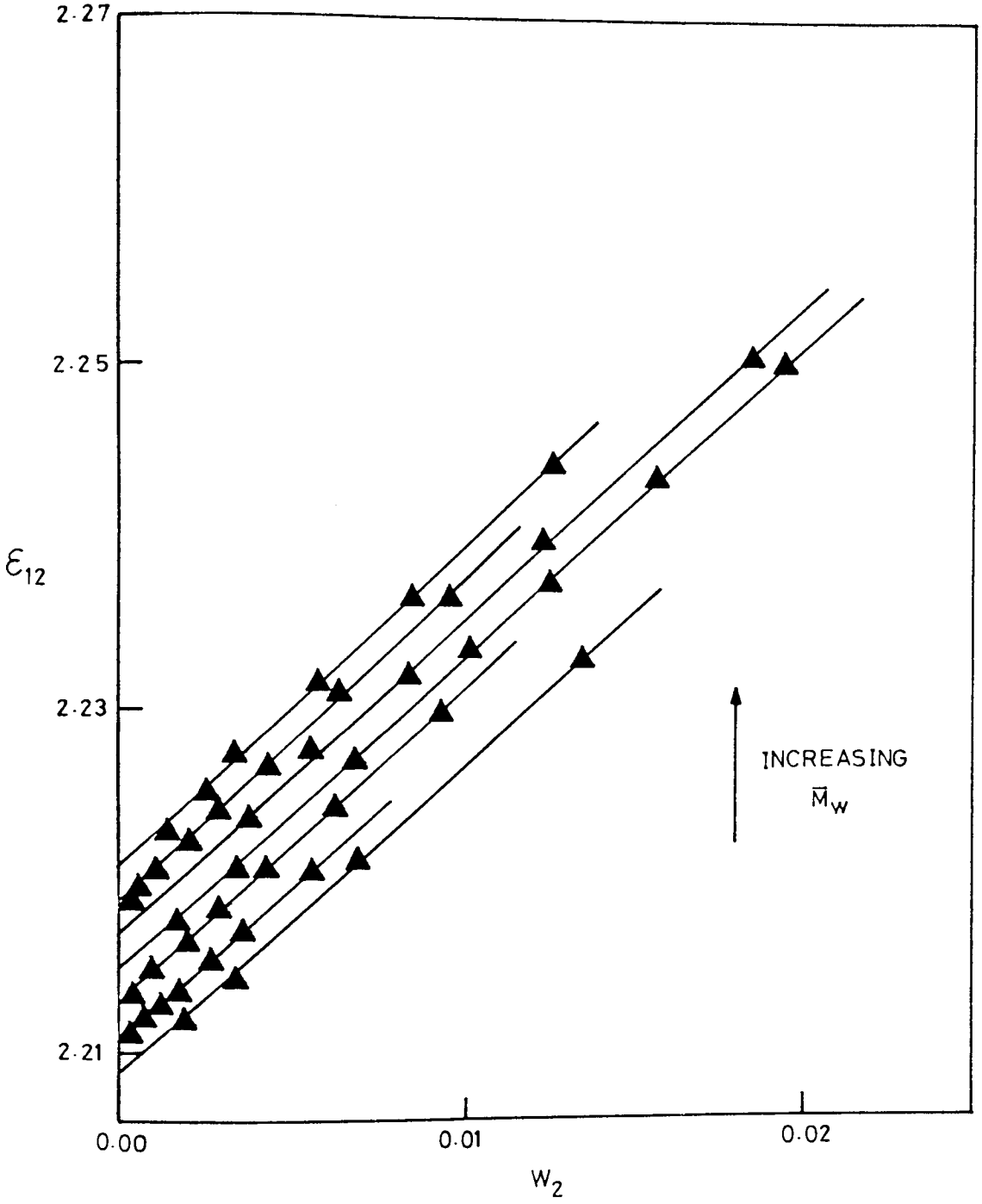

Figure 9.04 Static dielectric permittivity, ε_{12}, against weight fraction of solute, w_2, for fractions of PVK sample S4, in order of increasing weight-average molecular weight, $\bar{M}_w$, (see Table 3.10), in solution in 1,4-dioxan at 298K. The plots for each fraction are successively displaced for clarity.

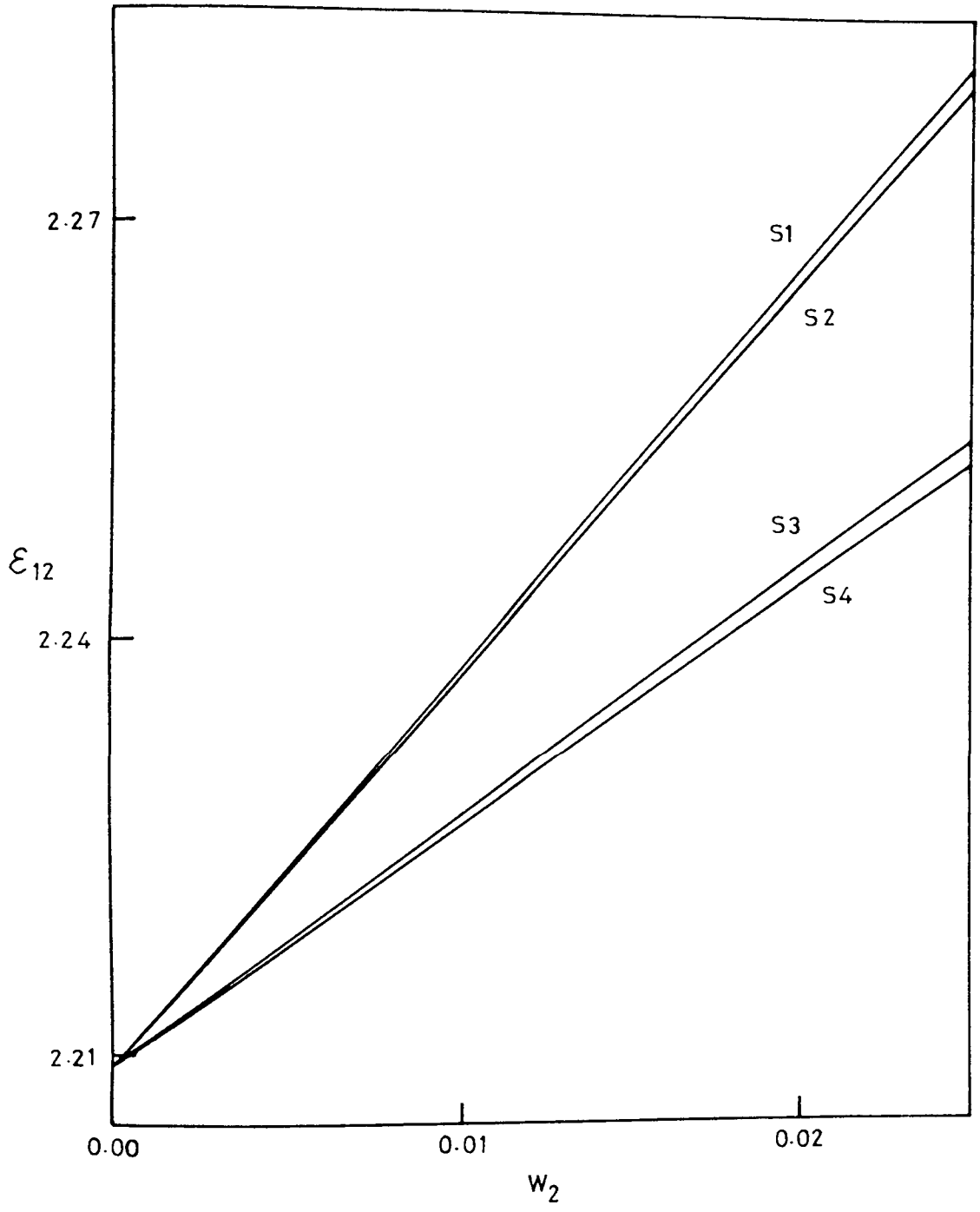

Figure 9.05 Comparison of the gradients of the plots of static dielectric permittivity, ε_{12}, against weight fraction of solute, w_2, for PVK samples S1, S2, S3 and S4 in solution in 1,4-dioxan at 298K.

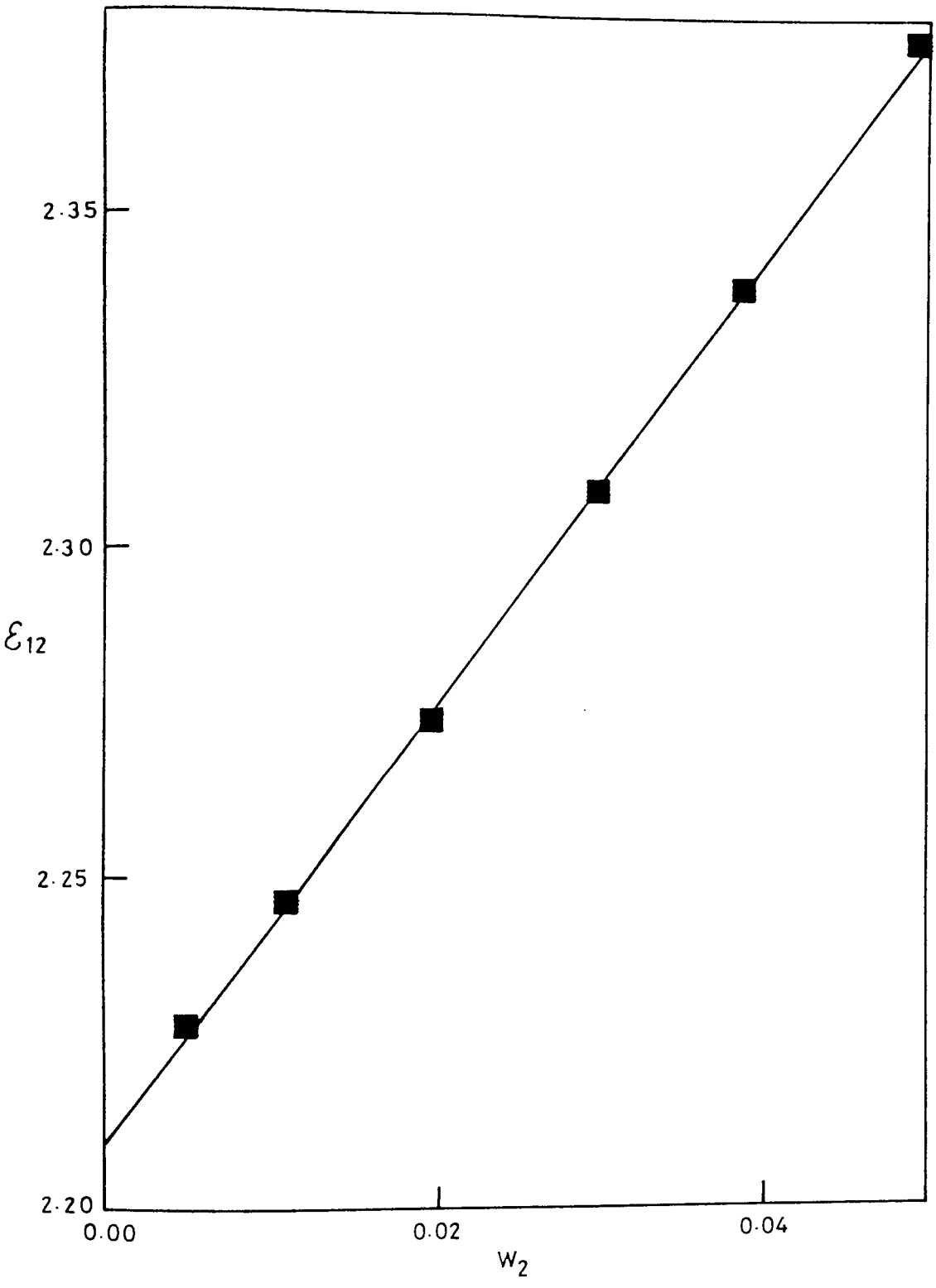

Figure 9.06 Static dielectric permittivity, ε_{12}, against weight fraction of solute, w_2, for carbazole in solution in 1,4-dioxan at 298K.

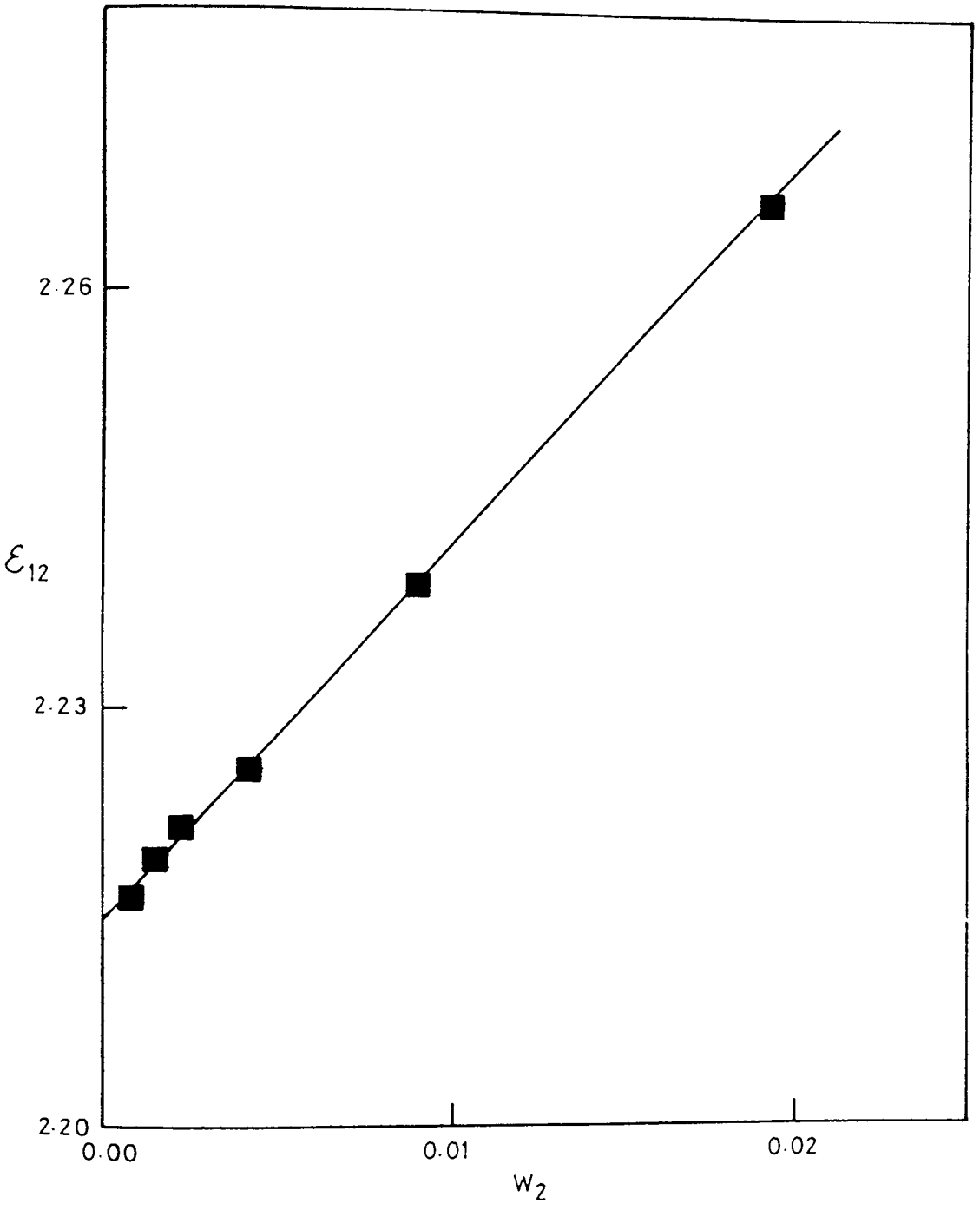

Figure 9.07 Static dielectric permittivity, ε_{12}, against weight fraction of solute, w_2, for 9-ethyl carbazole in solution in 1,4-dioxan at 298K.

9-ethyl carbazole, are shown in Figure 9.06 and Figure 9.07, respectively. The calculation of the effective dipole moments of the repeat units of the various PVK samples, and those of the model compounds are presented in the following chapter along with a detailed discussion.

9.03 Experimental Kerr Constants of PVK Fractions and Model Compounds

Experimental Kerr constants, B_{12}, of each of the different molecular weight fractions of PVK samples S1,S2,S3 and S4, and model compounds, carbazole and 9-ethyl carbazole, were determined at 298K in solution in 1,4-dioxan. These values of B_{12} were obtained by making measurements of analyser rotation, α^1, and plotting them against the square of the applied voltage, V^2. The gradient of such a plot was then compared to the gradient of a similar plot for pure toluene. By assuming a value ($B = 0.81 \times 10^{-14} mV^{-2}$)[131] for the experimental Kerr constant of toluene the unknown B_{12} of the solution could then be calculated (see Section 2.14). Measurements were made at several concentrations using the small sample volume Kerr cell (Kerr cell A). Plots of B_{12} against weight fraction of solute, w_2, for PVK samples S1-S4 are shown in Figures 9.08 to 9.11, respectively. For clarity in these Figures each of the lines corresponding to a different molecular weight fraction has been successively displaced down the ordinate axis. For all samples of PVK the plots of B_{12} against w_2 are linear, their gradients are negative and independent of molecular weight and heterogeneity index. To aid comparison of the plots presented in Figures 9.08 to 9.11 an average gradient of each plot was calculated and these are shown in Figure 9.12. In contrast to the two types of stereostructure suggested by the dielectric data, three different gradients are observed in Figure 9.12, suggesting three different types of stereostructure. Gradients of the lines

corresponding to samples S3 and S4 are the same, within experimental error.

Plots of B_{12} against w_2 for the model compounds, carbazole and 9-ethyl carbazole, are shown in Figure 9.13 and Figure 9.14, respectively. It is interesting to note that although the gradients of similar plots for the PVK samples are negative, those for the model compounds are positive. Calculation of the relevant values of specific and molar Kerr constants are presented in the following chapter together with a detailed discussion.

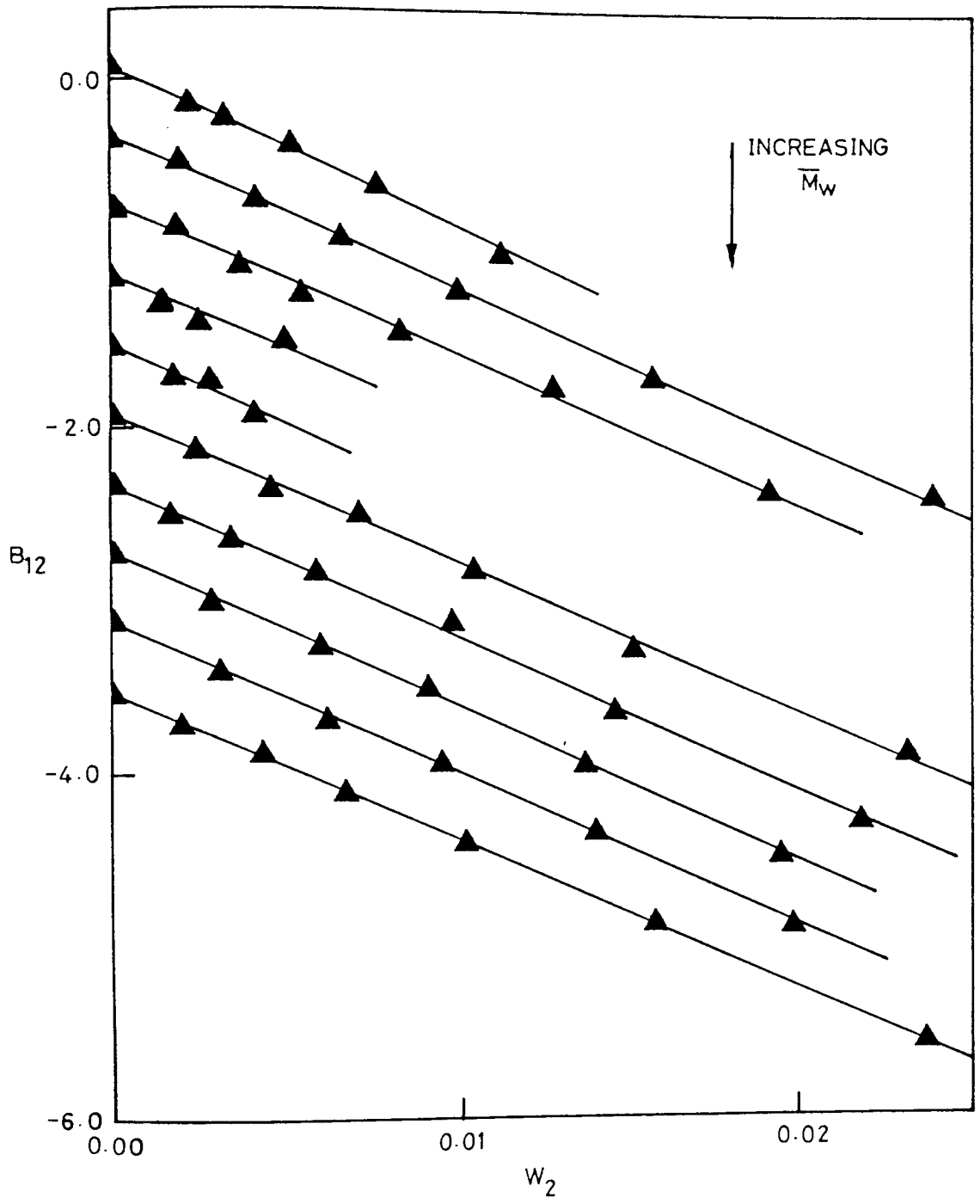

Figure 9.08 Experimental Kerr constant, $B_{12}(x10^{14}/mV^{-2})$, against weight fraction of solute, w_2, for fractions of PVK sample S1, in order of increasing weight-average molecular weight, $\bar{M}_w$, (see Table 3.07), in solution in 1,4-dioxan at 298K. The plots for each fraction are successively displaced for clarity.

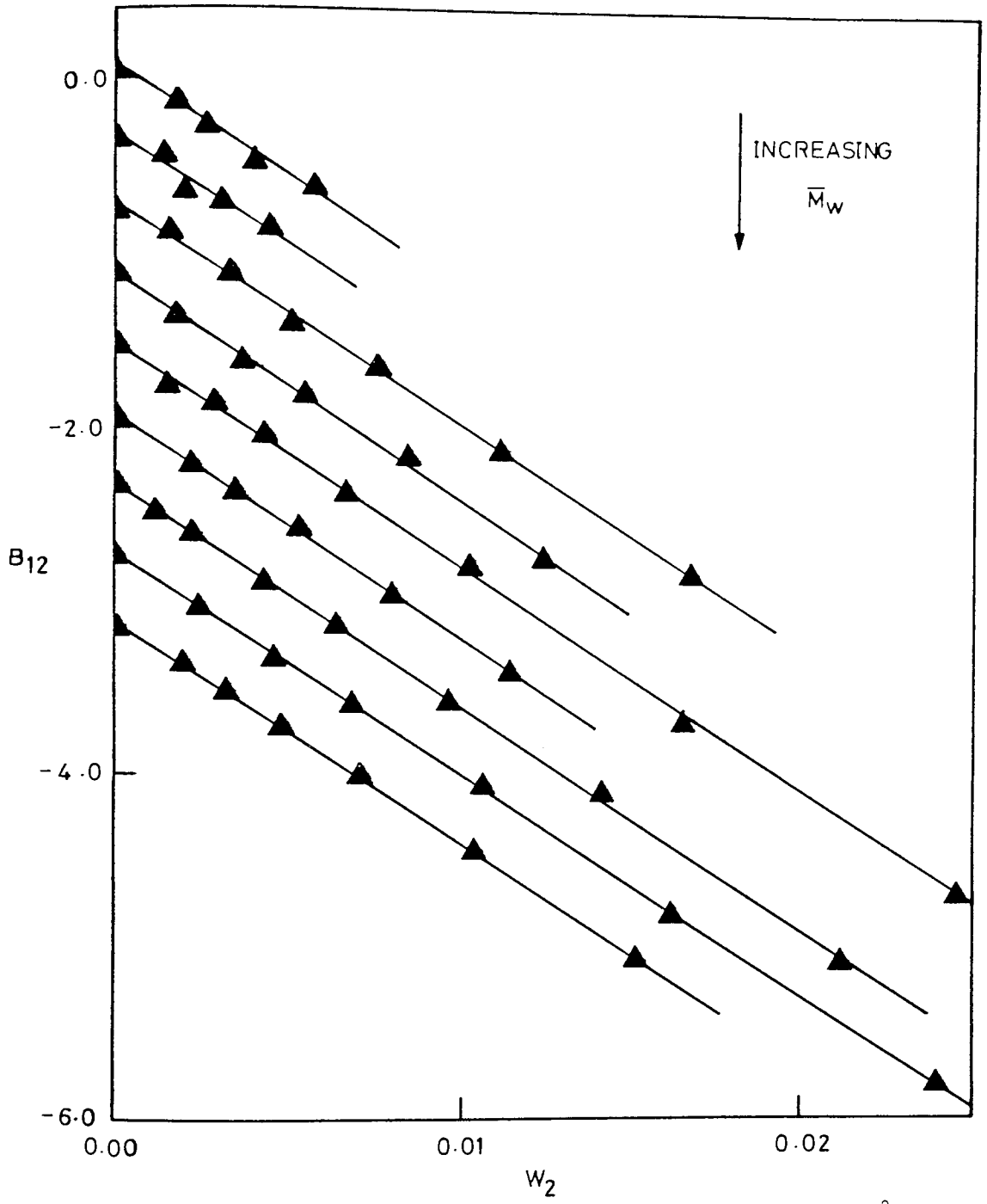

Figure 9.09 Experimental Kerr constant, $B_{12}(x10^{14}/mV^{-2})$, against weight fraction of solute, w_2, for fractions of PVK sample S2 in order of increasing weight-average molecular weight, $\bar{M}_w$, (see Table 3.08), in solution in 1,4-dioxan at 298K. The plots for each fraction are successively displaced for clarity.

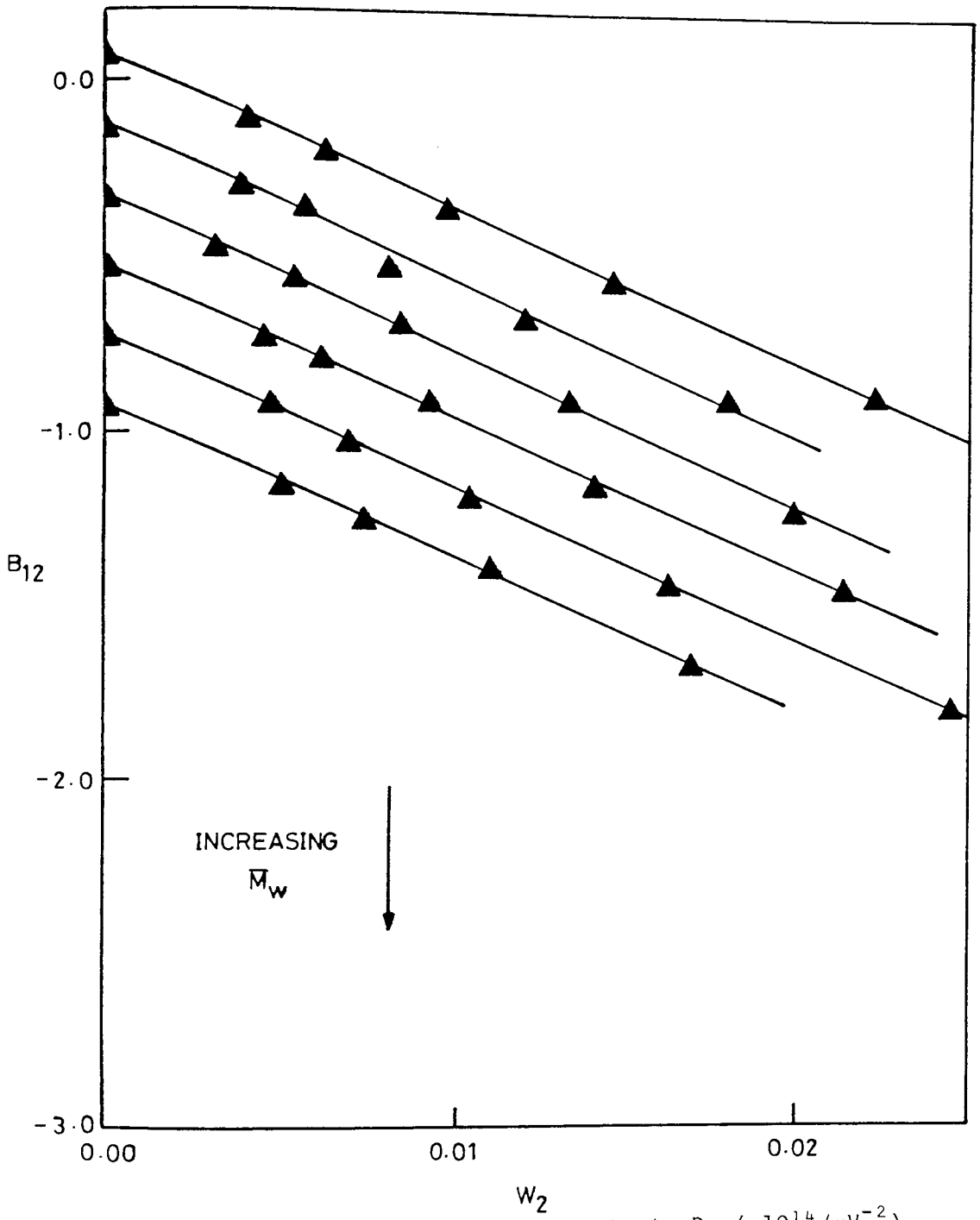

Figure 9.10 Experimental Kerr constant, $B_{12}(x10^{14}/mV^{-2})$, against weight fraction of solute, w_2, for fractions of PVK sample S3, in order of increasing weight-average molecular weight, $\bar{M}_w$, (see Table 3.09), in solution in 1,4-dioxan at 298K. The plots for each fraction are successively displaced for clarity.

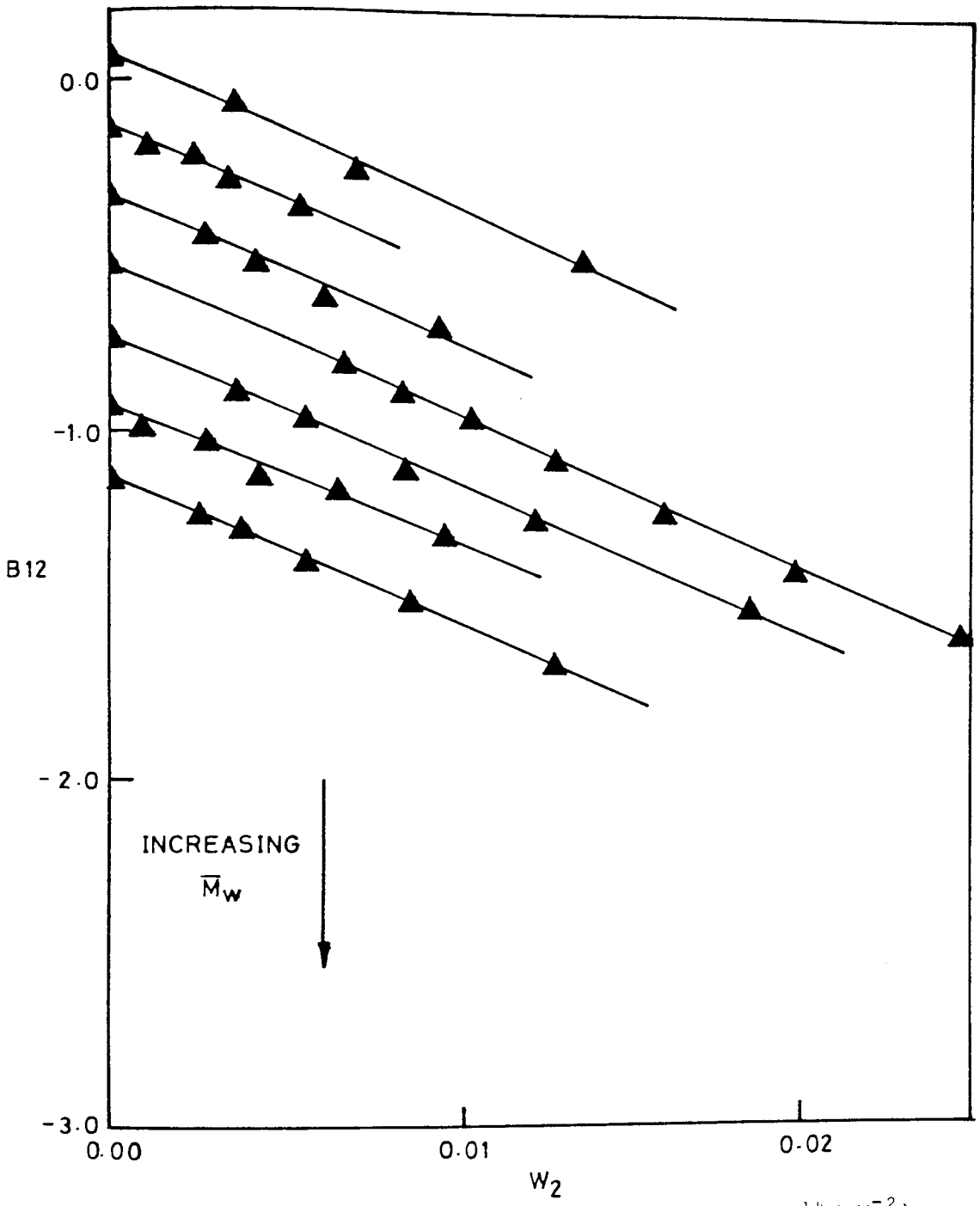

Figure 9.11 Experimental Kerr constant, $B_{12}(x10^{14}/mV^{-2})$, against weight fraction of solute, w_2, for fractions of PVK sample S4, in order of increasing weight-average molecular weight, $\bar{M}_w$, (see Table 3.10), in solution in 1,4-dioxan at 298K. The plots for each fraction are successively displaced for clarity.

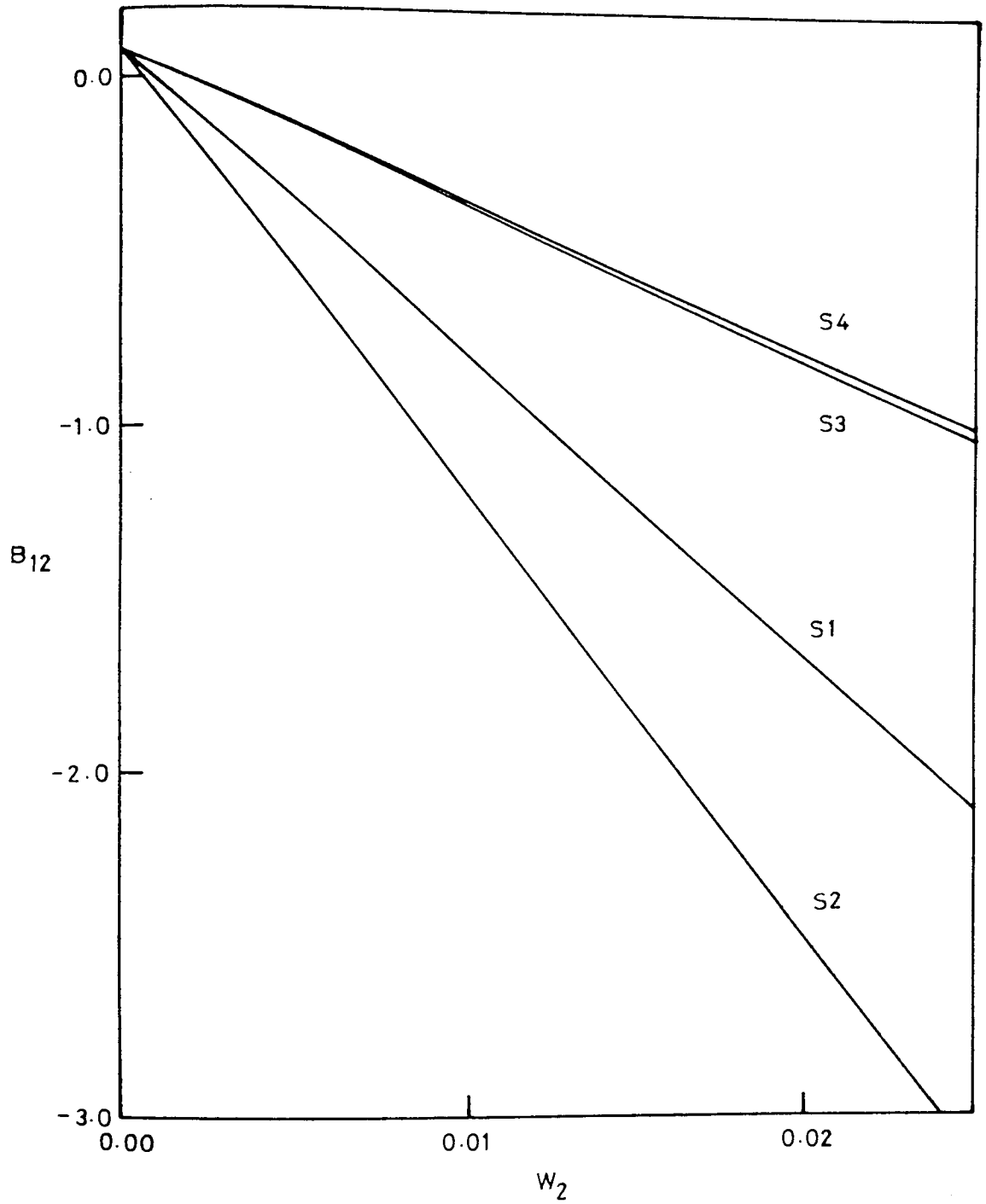

Figure 9.12 Comparison of the gradients of the plots of experimental Kerr constant, $B_{12}(x10^{14}/mV^{-2})$, against weight fraction of solute, w_2, for PVK samples S1, S2, S3 and S4 in solution in 1,4-dioxan at 298K.

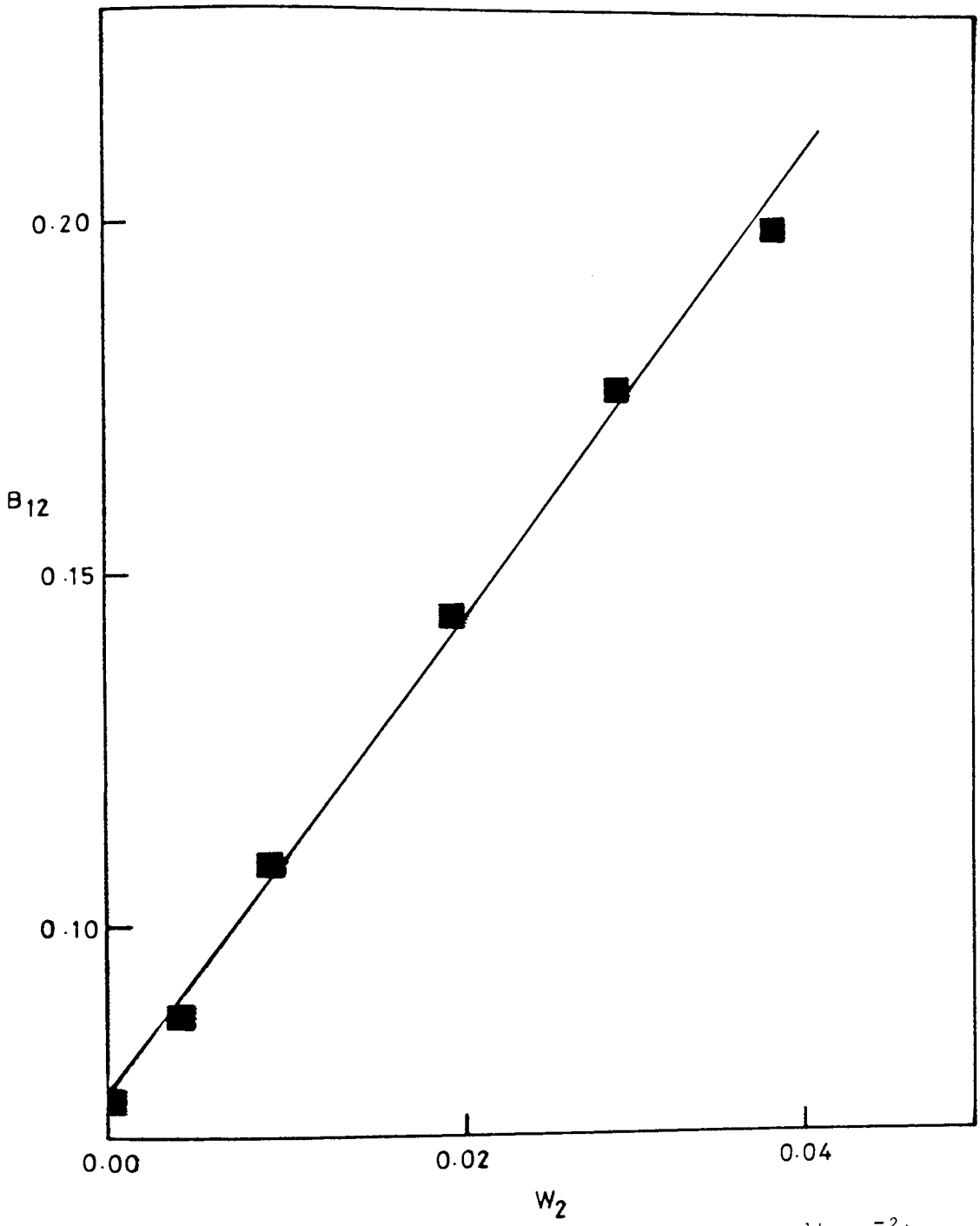

Figure 9.13 Experimental Kerr constant, $B_{12}(x10^{14}/mV^{-2})$, against weight fraction of solute, w_2, for carbazole in solution in 1,4-dioxan at 298K.

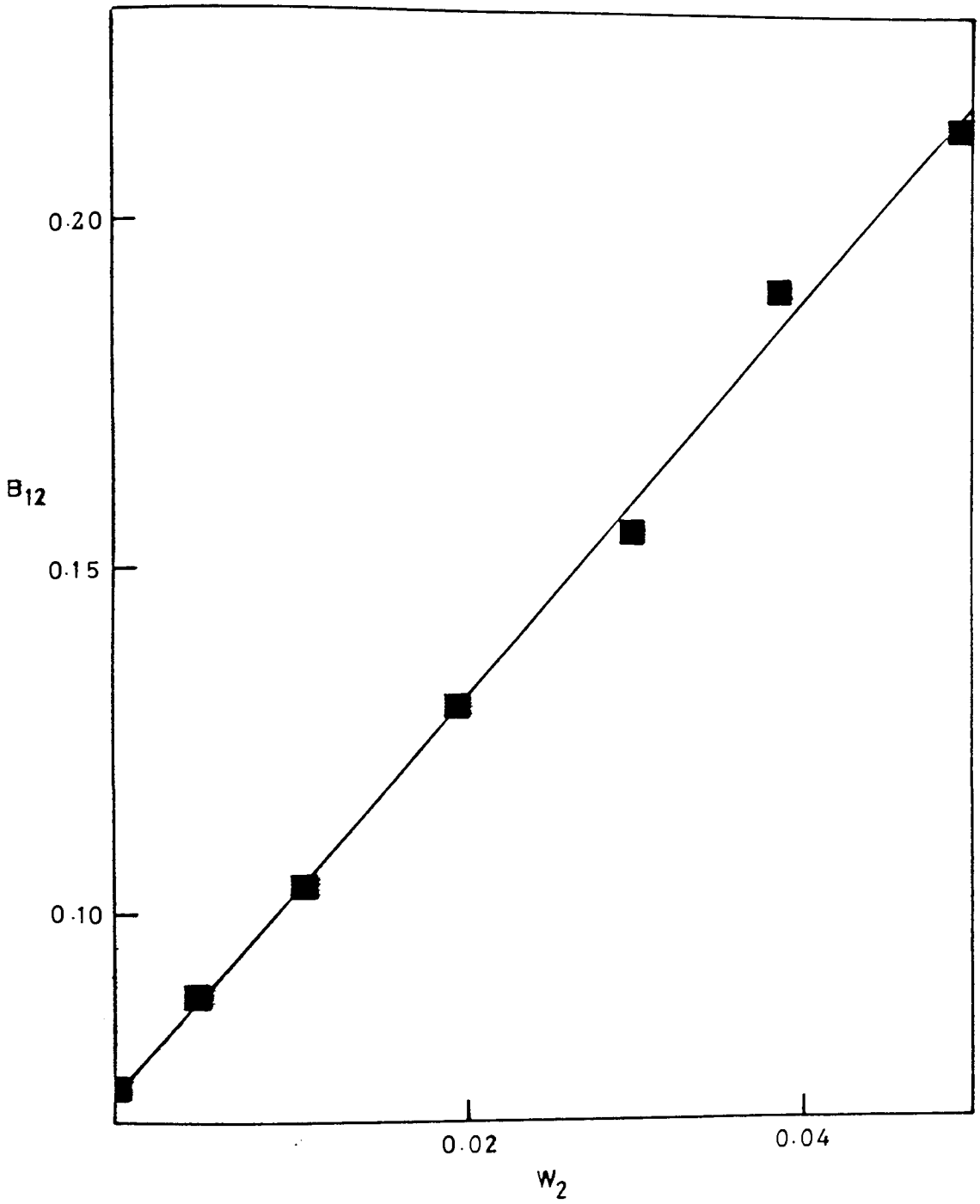

Figure 9.14 Experimental Kerr constant, $B_{12}(x10^{14}/mV^{-2})$, against weight fraction of solute, w_2, for 9-ethyl carbazole in solution in 1,4-dioxan at 298K.

CHAPTER 10

DETERMINATION OF EXPERIMENTAL DIPOLE MOMENTS AND KERR CONSTANTS OF POLY(N-VINYL CARBAZOLE) AND MODEL COMPOUNDS

10.01 Introduction

Since alternate carbon atoms in vinyl polymers are asymmetrically substituted, the conformational behaviour of the chains will be sensitive to the stereochemical composition. This has been demonstrated experimentally and theoretically for several conformationally dependent properties of vinyl polymers such as end-to-end distance[205], NMR chemical shifts[206], electric dipole moments[57], depolarized Rayleigh scattering[98] and the electro-optical Kerr effect[99,100,105,207]. Extensive calculations of end-to-end distances and dipole moments, and their dependence upon composition and stereoregularity, have been presented for several polymers by Mark[57]. The possibility of extending measurements into the region of very short chain length and the absence of any excluded volume effect on the dipole moments of most chain molecules were noted as being major advantages associated with the use of dipole moments, as opposed to end-to-end distances, for the characterisation of linear polymers. However, although mean-square dipole moments were found[57] to vary by up to factors of approximately 4 or 5 for different stereostructures of vinyl polymers, they were often either multivalued or nearly constant over a substantial range of tacticity, for polymers containing varying proportions of isotactic and syndiotactic blocks. By

comparison, the Kerr constant appears to be a parameter very sensitive to the conformational properties of flexible polymers, as demonstrated recently by calculation[99,100] and experiment[99,105,207]. In the majority of studies reported to date the electro-optical Kerr effect has been shown to provide a very sensitive means of investigating the stereostructure of polymer molecules in solution. Consequently, in the present study, concerning the effect of synthetic route upon the stereostructure of poly(N-vinyl carbazole), PVK, the electro-optical Kerr effect has been employed in addition to dielectric and carbon-13 NMR measurements.

Theoretical developments[61,62] in the early 1970's, using arguments based on symmetry, suggested the mean-square dipole moment would be independent of excluded volume for many types of polymer chains. However, recent studies[102-104] have shown these predictions to be falacious for certain structures in which the side chain/group contributes to the dipole moment. There are believed to be profound implications for monosubstituted vinyl polymers, poly(CH_2CHX) such as PVK, in which the dipole moment is dominated by the contribution from the C-X bonds. The effect of excluded volume on Kerr constants of similar chains is uncertain at the present time[104]. Consequently, it would seem unwise to directly compare the measured dipole moments and Kerr constants with the corresponding quantities calculated assuming freedom from excluded volume effects, unless the measurements have been performed under theta point conditions.

The present chapter details the calculation of mean-square dipole moments and Kerr constants, of the samples of PVK and model compounds, from the measured values of ε_{12} and B_{12}. The results are compared

and discussed along with the carbon-13 NMR data presented in Section 3.12.

10.02 Determination of Dipole Moments for Poly(N-Vinyl Carbazole) and Model Compounds

The Guggenheim rearrangement of the Debye equation for the calculation of solute dipole moments, μ_2, may be written as[157]

$$\mu_2^2 = \frac{27\varepsilon kT10^6}{N(\varepsilon_1 + 2)(n_1^2 + 2)} \left(\frac{\Delta}{c}\right)_{c\to 0} \qquad (10.1)$$

where:- ε = permittivity of free space ($8.85416 \times 10^{-12} Fm^{-1}$),

k = Boltzmann's constant ($1.38062 \times 10^{-23} JK^{-1}$),

T = absolute temperature

N = Avogadro's number ($6.02217 \times 10^{23} mol^{-1}$),

ε_1 = relative permittivity of the solvent,

n_1 = refractive index of the solvent,

c = concentration of solute ($mol\ m^{-3}$)

and $\Delta = (\varepsilon_{12} - n_{12}^2) - (\varepsilon_1 - n_1^2)$

$\simeq (\varepsilon_{12} - \varepsilon_1)$ for dilute solutions.

However, by inspection,

$$\left(\frac{\Delta}{c}\right)_{c\to 0} = \left(\frac{d\varepsilon_{12}}{d\omega_2}\right)_{w\to 0} \times \frac{M_2}{\rho_1} \qquad (10.2)$$

where:- ε_{12} = relative permittivity of the solution,

ω_2 = weight fraction of the solute,

M_2 = relative molecular mass of the solute

and ρ_1 = density of the solvent (kgm^{-3})

then the 'Guggenheim-Debye' equation may be re-expressed as

$$\mu_2^2 = \frac{27\varepsilon kT10^6}{N(\varepsilon_1 + 2)(n_1^2 + 2)} \left(\frac{d\varepsilon_{12}}{d\omega_2}\right)_{\omega_2\to 0} \times \frac{M_2}{\rho_1} \qquad (10.3)$$

Equation (10.3) was used to calculate the dipole moments of PVK and the model compounds. The gradient of the plots of ε_{12} against ω_2 (all observed to be straight line plots), presented in the previous chapter,

were substituted for $(d\varepsilon_{12}/d\omega_2)_{\omega_2 \to 0}$ in the latter equation. For PVK samples S1 to S4 the mean-square dipole moment calculated corresponded to that of the repeat unit, and was obtained after substituting the relative molecular mass of the repeat unit (193 for PVK) into Equation (10.3). The dipole moment per repeat unit for samples S1 to S4 of PVK and molecular dipole moments found for the two model compounds are listed in Table 10.01. The dipole moment obtained for carbazole (7.04×10^{-30}Cm) compares favourably with the values obtained by Cowley and Partington[208] (6.97×10^{-30}Cm) and by Liptay et al[209] ($6.7 \pm 0.3 \times 10^{-30}$Cm) for this material, all measurements being on solutions in 1,4 - dioxan. The repeat unit dipole moment found for sample S3(5.73×10^{-30}Cm) is some 16% lower than that measured by North and Philips (6.84×10^{-30}Cm)[199,201] for polymer samples prepared using the same initiator. However, the dielectric data recorded by North and Philips[199,201] was made on solutions containing 10% by weight of PVK in toluene; conditions considerably different to those used in the present investigation. North and Philips[199,201] also prepared two samples of PVK having lower molecular weights ($M_n = 1.66 \times 10^3$ and 4.72×10^3) by charge-transfer polymerization using auric chloride ($AuCl_3$) as the initiator. These samples were found to have repeat unit dipole moments of 5.14×10^{-30}Cm and 5.80×10^{-30}Cm, respectively. The lower repeat unit dipole moments obtained for these lower molecular weight samples was regarded as evidence for rod-like behaviour at molecular weights below 4×10^3. However, in the present study we have shown that the stereostructure of PVK is dependent upon initiator, the conclusions drawn by North and Philips[199,201] regarding rod-like behaviour may therefore be questioned.

Table 10.01 Polymerization initiator, polymerization temperature (/K), gradients, $(d\varepsilon_{12}/d\omega_2)_{\omega_2 \to 0}$, of the plots of solution permittivity against weight fraction, repeat unit dipole moment of PVK samples S1 to S4 and molecular dipole moments of model compounds carbazole and 9-ethyl carbazole. All dipole moments expressed as $\mu(x10^{30}/Cm)$ at 298K.

Sample	Initiator	Polym. temp	$\left(\frac{d\varepsilon_{12}}{d\omega_2}\right)_{\omega_2 \to 0}$	μ
S1	$AlCl_3$	298	2.89	7.24
S2	$BF_3(OC_2H_5)_2$	298	2.83	7.16
S3	AZBN	343	1.81	5.73
S4	AZBN(?)	-	1.75[a]	5.63
Carbazole	-	-	3.16	7.04
9-E-Carbazole	-	-	2.63	6.94

[a] $(d\varepsilon_{12}/d\omega_2)_{\omega_2 \to 0}$ was found to be 1.71 for sample S4 measured in solution in benzene at 298K.

In addition to the extensive dielectric measurements at 100kHz, measurements of dielectric permittivity were also made in the range 0.3kHz to 100kHz on solutions of PVK in 1,4 - dioxan at 298K. Dielectric cell A and a variable frequency bridge were used for this purpose. The dielectric constant of the solutions, ε_{12}, was found to be independant of frequency in this range for number-average molecular weights 10^4 - 10^7. This observation is consistent with more extensive work conducted by North and Philips[199,201].

10.03 Determination of Kerr Constants for Poly(N-Vinyl Carbazole) and Model Compounds

Le Fèvre[37] has shown the importance of extrapolating measurements to infinite dilution before calculating the Kerr constant of a solute. A set of equations have been presented to facilitate the required extrapolation. The following relationships are assumed to apply at high dilutions for the permittivity, density, refractive index and experimental Kerr constant, respectively

$$\varepsilon_{12} = \varepsilon_1(1 + \alpha\omega_2) \qquad (10.4)$$

$$d_{12} = d_1(1 + \beta\omega_2) \qquad (10.5)$$

$$n_{12} = n_1(1 + \gamma\omega_2) \qquad (10.6)$$

$$B_{12} = B_1(1 + \delta\omega_2) \qquad (10.7)$$

Thus, by making measurements at several concentrations the values of α, β, γ and δ may be found. These are then substituted into Equation (10.8) to find the specific Kerr constant of the solute at infinite dilution, ${}_\infty({}_sK_2)$

$${}_\infty({}_sK_2) = \left[(1 - \beta + \gamma + \delta - H\gamma - J\alpha\varepsilon_1)\right] {}_sK_1 \qquad (10.8)$$

where $H = 4n_1^2/(n_1^2 + 2)$ (10.9)

and $J = 2/(\varepsilon_1 + 2)$. (10.10)

In practice, β and γ are usually very small, relative to the other terms in Equation (10.8), and in the present study were neglected.

Table 10.02 Polymerization initiator, coefficients $\alpha\varepsilon_1$ and δ, and specific Kerr constants at infinite dilution, ${}_\infty({}_sK_2)(x10^{25}/m^5V^{-2}kg^{-1})$, measured at 298K in 1,4 dioxan.

Sample	Initiator	$\alpha\varepsilon_1$	δ	${}_\infty({}_sK_2)$
S1	$AlCl_3$	6.384	-86.75	-12.3
S2	$BF_3(OC_2H_5)_2$	6.251	-128.5	-18.1
S3	AZBN	3.998	-43.3	-6.14
S4	AZBN(?)	3.866	-43.3[a]	-6.14
Carbazole	-	3.320	37.5	5.13
9-E-Carbazole	-	2.660	43.4	5.99

[a] δ was found to be -45.7 for sample S4 measured in solution in benzene at 298K.

Thus, Equation (10.8) reduces to

$$_{\infty}(_{S}K_2) = \left[(1 + \delta - J\alpha\varepsilon_1)\right]_{S}K_1 \qquad (10.11)$$

The permittivity of 1,4 - dioxan was taken to be 2.209 and the specific Kerr constant as 13.9 x $10^{-27}m^5V^{-2}kg^{-1}$ (ref. 17).

The coefficients α and δ and the specific Kerr constants at infinite dilution, $_{\infty}(_{S}K_2)$, of the various PVK samples and model compounds are listed in Table 10.02.

10.04 Discussion of the Dipole Moments, Kerr Constants and Carbon-13 NMR Spectra Pertaining to Poly(N-Vinyl Carbazole)

Although it is not possible to obtain reliable numerical values for the Markov probabilities of the meso-racemic traids, from the carbon-13 NMR spectra of PVK samples S1 to S4 shown in Figures 3.13 to 3.16, it is possible to make a few qualitative statements as to the extent of meso or racemic groups in each of the samples. Williams and Froix[141] have tentatively assigned the peaks in the carbon-13 NMR spectrum of PVK associated with the methine and methylene carbons of the meso-racemic triads. Applying these assignments to each of the spectra obtained for PVK samples S1 to S4 it may be observed that sample S2, which was initiated by $BF_3(OC_2H_5)_2$, contains the highest proportion of meso groups, followed by sample S1, which was initiated by $AlCl_3$. Samples S3 and S4 have almost identical carbon-13 NMR spectra, and the smallest proportion of meso groups (ie. the highest racemic content). Sample S3 was polymerized by a radical mechanism using AZBN as the initiator. The sample S4 was obtained commercially and its polymerization conditions are unknown. However, in the light of the evidence (dielectric, Kerr effect and NMR) presented it would appear that PVK sample S4 was also prepared by free radical initiation.

The higher values of the effective repeat unit dipole moment and specific Kerr constant for PVK sample S2 support the carbon-13 NMR evidence, since dipole moments of consecutive repeat units related in a meso manner would be expected to be additive in a direction approximately perpendicular to the backbone of the chain. Conversely, the dipole moments of consecutive repeat units related in a racemic fashion would be expected, on average, to have a cancelling effect. In a similar manner, the observations made about the carbon-13 NMR spectrum of S1 are supported by the Kerr effect results. However, any differences in the stereostructure of samples S1 and S2 could not be distinguished by dielectric measurements. This would appear to be experimental evidence in support of the typical trend calculated for vinyl polymers by Mark[57], who showed that the dipole moment may remain nearly constant over a substantial range of mixtures of sequences of different tacticity.

The specific Kerr constant of the solute at infinite dilution, ${}_{\infty}({}_{S}K_2)$, may be regarded as being due to the term θ_2 involving the permanent dipole moment, μ, and the term θ_1 due only to induced dipole moments such that[36]

$$ {}_{\infty}({}_{S}K_2) = \frac{N(\theta_1 + \theta_2)}{18M_2\varepsilon} \qquad (10.12) $$

where N = Avogadro's number,

M_2 = solute relative molecular mass

and ε = permittivity of free space.

The anisotropy term, θ_1, is expanded as

$$ 45kT\theta_1 = \left[(a_1 - a_2)(b_1 - b_2) + (a_2 - a_3)(b_2 - b_3) + (a_3 - a_1)(b_3 - b_1)\right] \qquad (10.3) $$

and the dipolar term, θ_2, is expanded as

$$45k^2T^2\theta_2 = \left[(\mu_1^2 - \mu_2^2)(b_1 - b_2) + (\mu_2^2 - \mu_3^2)(b_2 - b_3) + (\mu_3^2 - \mu_1^2)(b_3 - b_1)\right] \quad (10.14)$$

Equation (10.13) contains electrostatic polarizabilities, a_1, a_2 and a_3, and electro-optical polarizabilities, b_1, b_2 and b_3. These two sets of polarizabilities may be related by[36] (see Section 8.07)

$$\frac{a_i}{b_i} = \frac{D^P}{E^P} \quad (10.15)$$

Thus, equation (10.13) reduces to

$$45kT\ {}_E P = {}_D P \left[(b_1 - b_2)^2 + (b_2 - b_3)^2 + (b_3 - b_1)^2\right] \quad (10.16)$$

The algebraic sign of the Kerr constant gives information concerning the disposition within the molecular framework of the resultant molecular dipole moment with respect to the principal axes of polarizability. This may be illustrated by a simplified case. Assume that the resultant dipole moment of the molecule lies in the plane made by the axes b_1 and b_2 and makes an angle β with the former. Then, in equation (10.14), μ_3 is zero, $\mu_1 = \mu\cos\beta$ and $\mu_2 = \mu\sin\beta$. The part of equation (10.14) in square brackets then becomes

$$\mu^2 \left[3\cos^2\beta(b_1 - b_2) + 2b_2 - b_1 - b_3\right] \quad (10.17)$$

This, for an ellipsoid of rotation in which $b_2 = b_3$, reduces to

$$\mu^2 \left[(3\cos^2\beta - 1)(b_1 - b_2)\right] \quad (10.18)$$

When $\beta = 0^o$, $\cos\beta = 1$ and the sign of θ_2 is controlled by $(b_1 - b_2)$. If b_1 is the axis of maximum polarizability, then θ_2 is positive. If, on the other hand, β is 90^o, then $\cos\beta = 0$ and θ_2 is negative. The algerbraic sign of θ_2 changes from positive to negative when $3\cos^2\beta = 1$, ie. when the angle β is 54.7^o. It is interesting to note that whilst the specific Kerr constants of the monomeric model compounds, carbazole and 9-ethyl carbazole, are positive the values of ${}_\infty({}_S K_2)$ for all the polymer samples are negative. These facts may be discussed in

simplistic terms. The positive Kerr constants of the model compounds show that any angular displacement of the resultant molecular dipole moment vector from the principal axis of maximum polarizability is small. However, since rotations about backbone bonds in PVK are severely sterically restricted it is believed that there is a strong tendency for the polymer to exist as a series of straight rigid helical sections[210-212]. Thus, the axis of maximum polarizability will be concurrent with the chain axis, where the tendency for the individual group polarizabilities to be additive is greatest. However, the resultant repeat unit dipole moment is approximately perpendicular to the chain axis for PVK, and will tend to add in a root-mean-square fashion along any direction taken perpendicular to the long axis of the rod. Consequently, the nett effect is that the resultant dipole moment of the molecule tends to be approximately perpendicular to the principal axis of polarizability, resulting in a negative Kerr constant. This situation for PVK may be contrasted with that for a similar polymer polystyrene. There are two major differences between polystyrene and PVK. The first is that rotations about skeletal bonds are not so severely restricted in polystyrene as they are in PVK and thus the tendency for the polarizability to increase along the chain axis is diminished. The second difference concerns the magnitude of the repeat unit dipole moment. The dipole moment of the monomeric model for polystyrene, ethyl benzene (1.96×10^{-30})[128], is considerably smaller than the dipole moments found for either carbazole (7.04×10^{-30}Cm) or 9-ethyl carbazole (6.94×10^{-30}Cm). Thus, the resultant dipole moment of the polymer perpendicular to the chain axis does not dominate to the same extent as in PVK. The final consequence of all these factorsis that polystyrene is found to have a small positive Kerr constant[213]. A vinyl polymer which has a negative Kerr constant is poly(vinyl chloride)[101]. Although this polymer is able to undergo rotations about its backbond bonds with considerable ease

compared with PVK, it does have a reasonably large dipole moment perpendicular to the chain axis. The specific Kerr constant found by Khanarian et al[101] for a low molecular weight (M_w = 42,000) sample of poly(vinyl chloride) in solution in 1,4-dioxan was negative ($-0.256 \times 10^{-27} m^5 V^{-2} kg^{-1}$), but was considerably smaller than values found for the various samples of PVK.

Significant differences in the carbon-13 NMR spectra of PVK samples S1 and S2 were observed. These differences were consistent with a higher proportion of meso groups in S2. However, no differences were observed in the dielectric properties of the samples S1 and S2 in solution in 1,4 dioxan at 298K. However, these two samples of PVK could be distinguished by the electro-optical Kerr effect and had specific Kerr constants differing by a factor of approximately 1.5. The ability of the Kerr effect to discriminate between closely related stereostructures in cases where dielectric measurements fail to do so, arises from the difference terms present in equations (10.13) and (10.14), and demonstrates the value of using complementary experimental techniques. By measuring the molar refraction and depolarization ratio of solutions of carbazole in 1,4-dioxan, in addition to the dipole moment and molar Kerr constant, the semi-axes of the electro-optical polarizability elipsoid, b_1, b_2 and b_3, may then be calculated for this molecule. These polarizabilities, together with the carbazole group dipole moment, may then be used, in conjunction with a computer program, to calculate the molecular dipole moment and molar Kerr constant of several model (trial) PVK chains representing different stereostructures. Thus, an attempt could be made to combine all the informaton gained about the different stereo-structures of this polymer, using carbon-13 NMR in conjunction with dielectric and Kerr effect measurements in order to produce a model chain for each structurally different form of PVK which is quantitatively compatible with the experimental results.

APPENDIX 1

OPTICAL THEORY OF THE KERR EFFECT

A1-I The Use of a Quarter Wave Retarder

The diagram in Figure A1-1 of the electric vectors of the light before entering, and after leaving, the various optical components, serves to illustrate the use of a quarter wave plate. The parallel beam of incident light, whose electric vectors are randomly oriented, is plane polarized at an angle of 45^{o} to the direction of the applied electric field, E, by the polarizer. The electric vector,

$$\bar{V}_{45} = a \sin\omega t, \qquad \text{(A1-1)}$$

may be resolved into the parallel and perpendicular components

$$\bar{V}_{\perp} = a \sin\omega t \sin 45^{o} \qquad \text{(A1-2)}$$

and

$$\bar{V}_{\parallel} = a \sin\omega t \cos 45^{o} \qquad \text{(A1-3)}$$

respectively. On passing through a birefringent sample the parallel component is retarded relative to the perpendicular component by a phase difference, δ, and the resultant waveform becomes

$$\bar{V}'_{\parallel} = a \sin(\omega t - \delta)\sin 45^{o}. \qquad \text{(A1-4)}$$

The parallel and perpendicular components of the electric vector may each be further resolved into two components at 45^{o} to the direction of the applied electric field. These components are

$$\bar{V}'_{45} = a \sin\omega t \cos^{2}45^{o} + a \sin(\omega t - \delta)\sin^{2}45^{o} \qquad \text{(A1-5)}$$

and

$$\bar{V}'_{135} = a \sin\omega t \cos^{2}45^{o} \sin 45^{o} - a \sin(\omega t - \alpha)\sin 45^{o}\cos 45^{o}, \qquad \text{(A1-6)}$$

respectively. Component, $\bar{V}'_{45}$, suffers a relative phase retardation of $\pi/2$ (90^{o}) on passing through the quarter wave plate. The waveform emerging from the quarter wave plate may now be represented by the

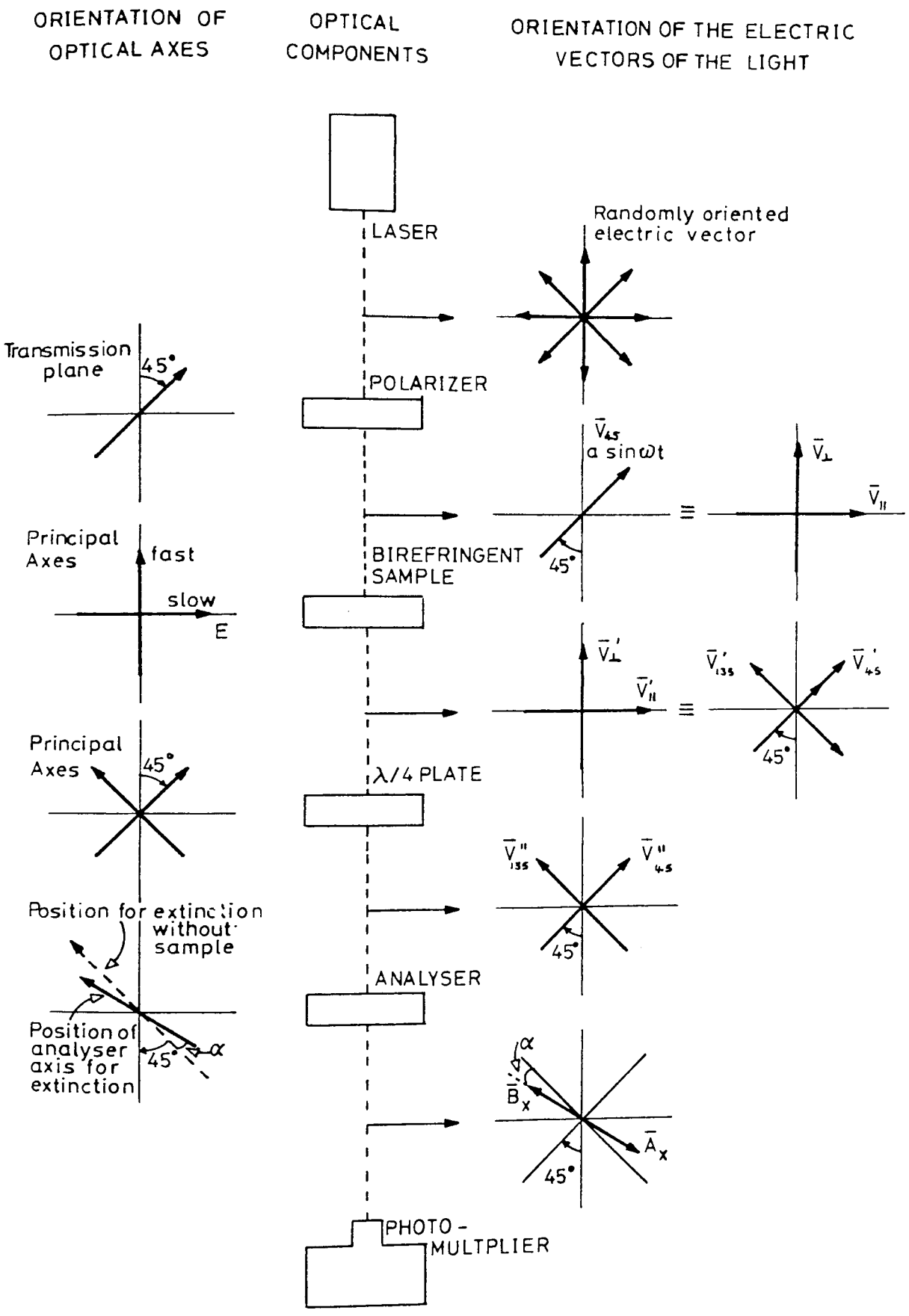

Figure A1-1 Electric vectors of light before entering, and after leaving, the various optical components of the electro-optical Kerr effect apparatus.

following orthogonal electric vectors

$$\bar{V}''_{45} = a \sin(\omega t - \pi/2) \cos^2 45^o + a \sin(\omega t - \delta - \pi/2) \sin^2 45^o \quad \text{(A1-7)}$$

and

$$\bar{V}''_{135} = a \sin\omega t \cos 45^o \sin 45^o - a \sin(\omega t - \delta) \sin 45^o \cos 45^o \quad \text{(A1-8)}$$

Since,

$$\sin 45^o = \cos 45^o$$

the two components may be simplified to give

$$\bar{V}''_{45} = a \cos^2 45^o \left[\sin(\omega t - \pi/2) + \sin(\omega t - \delta - \pi/2)\right] \quad \text{(A1-9)}$$

and

$$\bar{V}''_{135} = a \cos^2 45^o \left[\sin\omega t - \sin(\omega t - \delta)\right]. \quad \text{(A1-10)}$$

Applying the identity,

$$\sin x \pm \sin y = 2 \sin\tfrac{1}{2}(x \pm y) \cos(x \mp y),$$

enables equations (A1-9) and (A1-10) to be rewritten in the form

$$\bar{V}''_{45} = 2a \cos^2 45^o \left[\sin\tfrac{1}{2}(\omega t - \pi/2 + \omega t - \delta - \pi/2) \cos\tfrac{1}{2}(\omega t - \pi/2 - \omega t + \delta + \pi/2)\right] \quad \text{(A1-11)}$$

and $$\bar{V}''_{135} = 2a \cos^2 45^o \left[\sin\tfrac{1}{2}(\omega t - \omega t + \delta) \cos\tfrac{1}{2}(\omega t + \omega t - \delta)\right]. \quad \text{(A1-12)}$$

These further simplify to give

$$\bar{V}''_{45} = 2a \cos^2 45^o \cos \delta/2 \sin(\omega t - \pi/2 - \delta/2) \quad \text{(A1-13)}$$

and $$\bar{V}''_{135} = 2a \cos^2 45^o \sin \delta/2 \cos(\omega t - \delta/2). \quad \text{(A1-14)}$$

Since,

$$\sin(x - \pi/2) = -\cos x$$

equation (A1-13) may be written in the form

$$\bar{V}''_{45} = -2a \cos^2 45^o \cos \delta/2 \cos(\omega t - \delta/2). \quad \text{(A1-15)}$$

Thus, it can be seen that the two orthogonal components,

$$\bar{V}''_{45} = -2a \cos^2 45^o \cos \delta/2 \cos(\omega t - \delta/2) \quad \text{(A1-15)}$$

and $$\bar{V}''_{135} = 2a \cos^2 45^o \sin \delta/2 \cos(\omega t - \delta/2), \quad \text{(A1-14)}$$

have the same phase relationship, and differ only in their relative amplitudes. Therefore, the light emerging from the quarter wave plate is polarized and may thus be completely extinguished by the analyser when the latter is rotated by an amount ${}_s\alpha_n$ from its normally crossed

position. The above procedure corresponds to the measurement of the static electro-optical Kerr effect.

AL-II Measurement of Phase Difference, δ, Using Static Electric Fields

Consider the waveform of the light after having passed through the sample and the quarter wave plate. The two orthogonal components of the electric vector of the light are expressed by equations (A1-15) and (A1-14). These components, $\bar{V}''_{45}$ ($\equiv \bar{A}$) and $\bar{V}''_{135}$ ($\equiv \bar{B}$), may be resolved (see Figure A1-2(a)) into two pairs of components, $\bar{A}_x$ and $\bar{B}_x$, and $\bar{A}_y$ and $\bar{B}_y$, such that $\bar{A}_x$ and $\bar{B}_x$ cancel one another, and $\bar{A}_y$ and $\bar{B}_y$ augment each other. In other words $\bar{A}_y$ and $\bar{B}_y$, together, represent plane polarized light with the direction of the electric vector denoted by ${}_s\alpha_n$. Referring to Figure A1-2(a), it can be seen that

$$\frac{\sin {}_s\alpha_n}{\cos {}_s\alpha_n} = \frac{\bar{A}_x/\bar{A}}{\bar{B}_x/\bar{B}} = \frac{\bar{B}}{\bar{A}} \qquad \text{(A1-16)}$$

Substituting expressions for components $\bar{A}(\equiv \bar{V}''_{45})$ and $\bar{B}(\equiv \bar{V}''_{135})$, as defined by equations (A1-15) and (A1-14), into equation (A1-16) one obtains

$$\frac{\sin {}_s\alpha_n}{\cos {}_s\alpha_n} = \frac{2a\cos^2 45^o \sin \delta/2 \cos(\omega t - \delta/2)}{-2a\cos^2 45^o \cos \delta/2 \cos(\omega t - \delta/2)}, \qquad \text{(A1-17)}$$

which may be readily simplified to give

$$\frac{\sin {}_s\alpha_n}{\cos {}_s\alpha_n} = \frac{\sin \delta/2}{-\cos \delta/2} \qquad \text{(A1-18)}$$

Hence,

$$\tan {}_s\alpha_n = -\tan \delta/2 \qquad \text{(A1-19)}$$

and therefore,

$${}_s\alpha_n = -(\delta/2) \pm 2n\pi \qquad \text{(A1-20)}$$

Thus, for rotations of the analyser of less and 180^o the relation

$${}_s\alpha_n = -\delta/2 \qquad \text{(A1-21)}$$

may be employed to determine the electrically-induced phase retardation, δ.

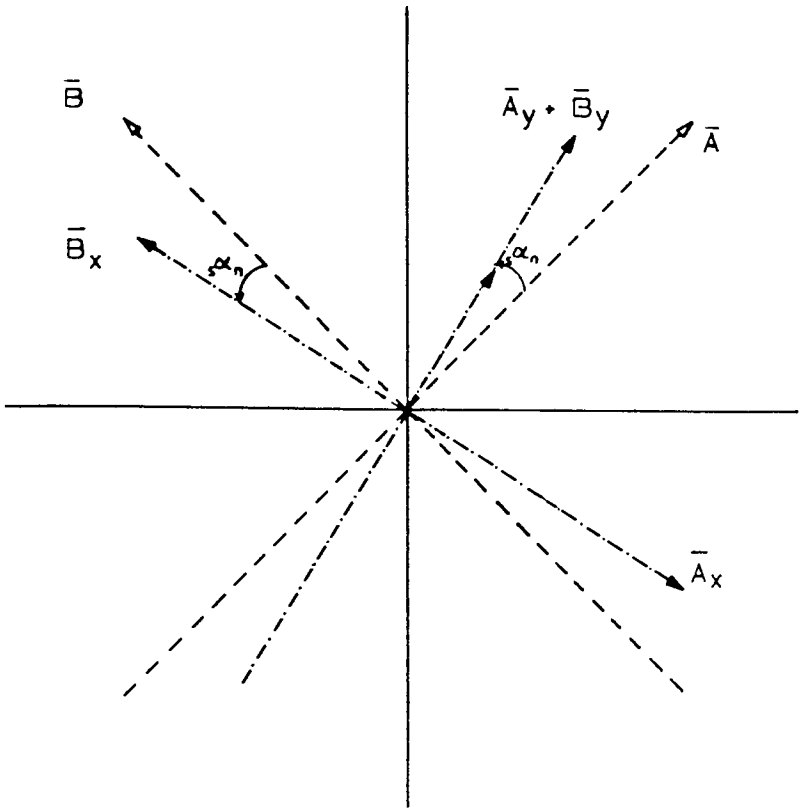

Figure A1-2(a) Resolved electric vector of light having passed through sample and quarter wave plate

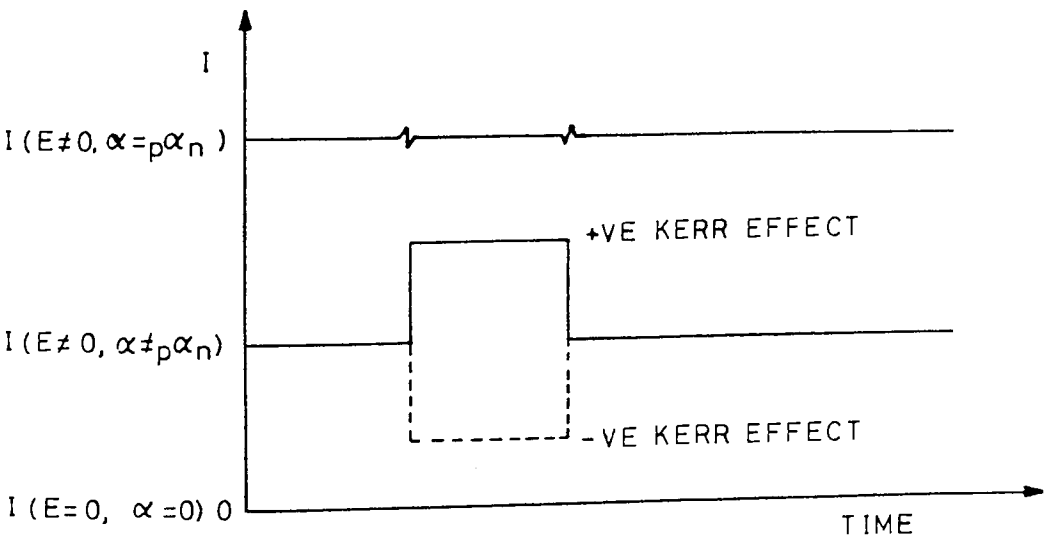

Figure A1 - 2(b) Optical pulse observed for different analyser rotations and electrical field conditions.

A1-III Measurement of the Phase Difference, δ, Using Pulsed Electric Fields

The symbol, ${}_p\alpha_n$, denotes the rotation of the analyser, from its normally crossed position, required to null the pulse of light transmitted through the sample during the application of a short duration pulse of high voltage to the Kerr cell. In practical terms the amplitude of the pulse viewed on the oscilloscope is reduced, by rotation of the analyser, to the level corresponding to the absence of the applied electric field. See Figure A1-2(b).

The relationship between the transmitted intensity, I, of a plane polarized beam of light, the initial intensity, I_0, and the rotation, α, of the analyser with respect to the nulled position is known as Malus' Law and may be expressed as

$$I = I_0 \sin^2\alpha$$

Applying Malus' Law, the intensity of light transmitted by the analyser, when the applied electric field, E, is zero, is given by

$$I_{E=0} = I_0 \sin^2\alpha. \qquad \text{(A1-22)}$$

However, upon application of an electric field to the sample, the light transmitted by the sample becomes

$$I_{E\neq 0} = I_0 \sin^2(\alpha + \delta/2) \qquad \text{(A1-23)}$$

If the electronically-induced pulse of light is nulled, by rotating the analyser, to the quiescent level then intensities $I_{E=0}$ and $I_{E\neq 0}$ become equal. Thus, from equations (A1-22) and (A1-23) we may write

$$I_0 \sin^2 {}_p\alpha_n = I_0 \sin^2({}_p\alpha_n + \delta/2).$$

Thus,

$$\sin^2 {}_p\alpha_n = \sin^2({}_p\alpha_n + \delta/2), \qquad \text{(A1-24)}$$

and for arguments corresponding to less than 20^0 a satisfactory approximation is given by

$${}_p\alpha_n^2 = ({}_p\alpha_n + \delta/2)^2. \qquad \text{(A1-25)}$$

Expanding and rearranging equation (A1-25) gives

$$_{p}\alpha_{n} = -\delta/4 \qquad \text{(A1-26)}$$

Thus, for the pulsed mode of operation, expression (A1-26) describes the relationship between the angular rotation of the analyser, required to null the optical signal, and the electronically-induced phase retardation, δ.

On comparing equation (A1-26), with the corresponding relationship given by equation (A1-21) for the static d.c. method of operation, one would predict a higher signal-to-noise ratio in favour of the static method. This is indeed the case for birefringent samples which are not unduely perturbed by the application of a high voltage electric field. However, for samples which are somewhat electrically conductive, the signal-to-noise ratio is found to favour the pulsed electric field method, since the samples are less disturbed by the application of an electric pulse of short duration.

APPENDIX 2

The principal computer programs used in this thesis are presented here. Each program listing is preceded by a brief description of its functions and followed by a sample output. All programs were written in extended Fortran 4 and were run either on an ICL 1904S computer at the University of Aston in Birmingham, or on a CDC 7600 machine at the Regional Computer Centre (UMIST).

Program 1 Calculation of Dipole Moments and End-to-End Distances of Polymer Chains

The mean-square dipole moment or end-to-end distance of a polymer chain in any known conformation may be calculated by addition of the appropriate group vectors. This program reads the bond angle supplements, θ, dihedral angles, ϕ, and bond vectors. A series of transforming and summing procedures are then carried out producing the components of the molecular vector and its scalar. The coordinates of every atom in the chain are also output but these only have meaningful values if it is the end-to-end distance which is being calculated.

The sample output following this program is the result of a calculation of the end-to-end distance of the conformation of octamethylcyclotetrasiloxane (n = 8) corresponding to the crystallographic form[185] (see structure E in Table 7.06). Since this is a cyclic conformation the end-to-end distance should be zero within the limits of accuracy, and this may be seen to be the case. This calculation was carried out as one check that the dihedral angles, ϕ, produced by Program 6 from the atom coordinates[185] were able to reproduce the correct atom coordinates. All distances are expressed in Angstroms.

```
      MASTER DIPOLE
C
C     COMPUTES THE MOLECULAR DIPOLE MOMENT VECTOR FOR A LINEAR CHAIN
C     MOLECULE OF N SKELETAL BONDS. CONFORMATIONS ARE GENERATED EXPLICITLY
C     AND ARE DEFINED BY BOND ANGLE SUPPLEMENTS THETA AND DIHEDRAL
C     ANGLES PHI.
C
C     NCONF IS THE NUMBER OF CONFORMATIONS TO BE GENERATED.
C     NUBV,NUTHET,NUPHI MAY ALL BE EITHER ZERO OR ONE.
C     IF ZERO THEN INITIAL VALUES OF BOND VECTORS,THETAS AND PHIS
C     RESPECTIVELY ARE USED FOR ALL CONFORMATIONS. IF UNITY THEN NEW
C     VALUES ARE READ WITH EACH CONFORMATION.
C
C      *** DATA INPUT ORDER ***
C     (1) NCONF
C     (2) N,NUBV,NUTHET,NUPHI
C     (3) BOND VECTORS
C     (4) THETAS
C     (5) PHIS
C
C     *** COMMON TO THE SUBROUTINE VECTOR ***
C     COMMON NCONF.
C
      COMMON NCONF
      READ(1,1090)NCONF
 1090 FORMAT(I0)
      WRITE(2,100)
  100 FORMAT(/,10X,'DATA',/,10X,'----')
      WRITE(2,150)NCONF
  150 FORMAT(/,10X,'NCONF =',I6)
      CALL VECTOR
      STOP
      END
C
      SUBROUTINE VECTOR
C
C     THIS SUBROUTINE FORMS A MOLECULAR VECTOR 'SUM' FOR A LINEAR CHAIN
C     MOLECULE HAVING N SKELETAL BONDS. THE CONFORMATIONS ARE
C     GENERATED EXPLICITLY ONE AT A TIME AND ARE DEFINED BY BOND
C     ANGLE SUPPLEMENTS THETA AND BY BOND DIHEDRAL ANGLES PHI.
C     EACH SKELETAL BOND IS ASSOCIATED WITH A VECTOR QUANTITY AND IT IS
C     ASSUMED THESE VECTORS ARE ADDITIVE AND INVARIANT WITH CONFORMATION.
C
      COMMON NCONF
      INTEGER N,NUBV,NUTHET,NUPHI
C
C     IF NUMBER OF SKELETAL BONDS IS GREATER THAN 101 THEN THE STATEMENT
C     BELOW MUST BE RE-DIMENSIONED THETAS(N-1), PHIS(N-1) AND STORE(3,N).
C
      DIMENSION TEMP(3,3),PROD(3,3),TR(3,3),SUM(3,1),BOND(3,1),
     2 TEMPU(3,1),THETAS(100),PHIS(100),STORE(3,101),COORDS(3,102)
C
C     EXTERNAL STATEMENT LISTS SUBROUTINES TO BE CALLED TO
C     SUBROUTINE 'VECTOR'.
```

```
C
      EXTERNAL MATSET,FILLTR,MATMUL,MATADD,MATEQU
C
C     MAIN DO LOOP STARTS HERE.
C
      DO 99 K=1,NCONF
C
C     READ IN N,NUBV,NUTHET,AND NUPHI AS APPROPRIATE.
C
      READ(1,1095)N,NUBV,NUTHET,NUPHI
 1095 FORMAT(4I0)
      WRITE(2,200)N
  200 FORMAT(/,10X,'N =',I6)
      WRITE(2,205)NUBV,NUTHET,NUPHI
  205 FORMAT(/,10X,'NUBV, NUTHET AND NUPHI ARE RESPECTIVELY',3I6)
      IF(NUBV.EQ.0) GO TO 33
C
C     READ BOND VECTORS.
C
      DO 13 J=1,N
   13 READ(1,1093) (STORE(I,J),I=1,3)
 1093 FORMAT(3F0.0)
      WRITE(2,210)
  210 FORMAT(//,10X,'BOND VECTORS')
      WRITE(2,230)
  230 FORMAT(/,10X,'BOND NO.',7X,'X',14X,'Y',14X,'Z')
      DO 260 J=1,N
  260 WRITE(2,300)J,(STORE(I,J),I=1,3)
  300 FORMAT(10X,I5,1X,3F15.5)
   33 CONTINUE
      IF(NUTHET.EQ.0) GO TO 44
C
C     READ THETAS AND CONVERT INTO RADIANS
C
C     IF NUMBER OF SKELETAL BONDS IS GREATER THAN 101 THEN FORMAT
C     STATEMENTS 1094 AND 1096 MUST BE REDIMENSIONED.
C
      NLESS1=N-1
      NPLUS1 = N+1
      RAD=0.0174533
      READ(1,1094) (THETAS(I),I=1,NLESS1)
 1094 FORMAT(100F0.0)
      WRITE(2,350) (THETAS(I),I=1,NLESS1)
  350 FORMAT(//,10X,'THETAS =',100F9.2)
      DO 6 I=1,NLESS1
    6 THETAS(I)=THETAS(I)*RAD
   44 CONTINUE
      IF(NUPHI.EQ.0) GO TO 55
C
C     READ PHIS AND CONVERT INTO RADIANS
C
      READ(1,1096) (PHIS(I),I=1,NLESS1)
 1096 FORMAT(100F0.0)
      WRITE(2,400) (PHIS(I),I=1,NLESS1)
```

```
 400 FORMAT(/,10X,'PHIS =',100F9.2)
     DO 9 I=1,NLESS1
   9 PHIS(I)=PHIS(I)*RAD
  55 CONTINUE
C
C     INITIALISE TEMPORARY MATRIX 'TEMP' PRIOR TO FORMING SERIAL
C     PRODUCT OF TRANSFORMATION MATRICES 'PROD'.
C
      CALL MATSET(TEMP,3,3,1)
      CALL MATSET(SUM,3,1,0)
      CALL MATSET(COORDS,3,102,0)
      DO 10 II=1,NLESS1
C
C     FORM PRE-MULTIPLYING TRANSFORMATION PRODUCT 'PROD'.
C
      CALL FILLTR(THETAS(II),PHIS(II),TR)
      DO 11 J=1,3
      CALL MATMUL(TEMP,TR,PROD,3,3,3,3)
C
C     FILL BOND VECTOR BOND FOR (II+1)TH SKELETAL BOND FROM 'STORE'.
C
  11 BOND(J,1) = STORE(J,II+1)
C
C     TRANSFORM (II)TH BOND VECTOR INTO COORDINATE SYSTEM ATTACHED
C     TO THE FIRST BOND IN THE CHAIN.
C
      CALL MATMUL(PROD,BOND,TEMPU,3,3,3,1)
      CALL MATADD(SUM,TEMPU,SUM,3,1)
      DO 450 J=1,3
 450 COORDS(J,II+2) = SUM(J,1)
C
C     REINITIALISE ARRAY TEMP.
C
      CALL MATEQU(TEMP,PROD,3,3)
  10 CONTINUE
C
C     THE CONSTRUCTION OF DO LOOP NUMBER 10 IS SUCH THAT THE VECTOR
C     ASSOCIATED WITH THE FIRST BOND IN THE CHAIN MUST BE ADDED
C     TO SUM OUTSIDE OF THE LOOP.
C
      DO 12 I=1,3
  12 SUM(I,1) = SUM(I,1)+STORE(I,1)
      DO 500 J=2,NPLUS1
      DO 500 I=1,3
 500 COORDS(I,J) = COORDS(I,J) + STORE(I,1)
C
C     MOLECULAR VECTOR IS NOW COMPLETE.
C     COMPUTE SCALAR PART OF THE MOLECULAR VECTOR.
C
      X=SUM(1,1)
      Y=SUM(2,1)
      Z=SUM(3,1)
      SCALAR=SQRT(X*X + Y*Y + Z*Z)
C
```

```
C     WRITE COMPONENTS OF THE MOLECULAR VECTOR ALONG WITH THE SCALAR.
C
      WRITE(2,250Ø)
  250Ø FORMAT(////,1ØX,'RESULTS',/,1ØX,'-------')
      WRITE(2,550Ø)
  550Ø FORMAT(/,1ØX,'ATOM COORDINATES',/)
      WRITE(2,560Ø)
  560Ø FORMAT(1ØX,'(TO BE IGNORED IF THE MOLECULAR DIPOLE MOMENT IS BEING
     2 COMPUTED',/,11X,'SOONER THAN THE END-TO-END LENGTH.)')
      WRITE(2,600Ø)
  600Ø FORMAT(/,1ØX,'ATOM NO.',7X,'X',14X,'Y',14X,'Z')
      DO 650Ø J=1,NPLUS1
      JLESS1 = J-1
  650Ø WRITE(2,700Ø)JLESS1,(COORDS(I,J),I=1,3)
  700Ø FORMAT(1ØX,I5,1X,3F15.5)
      WRITE(2,1060Ø)
 1060Ø FORMAT(//,1ØX,'COMPONENTS OF MOLECULAR VECTOR',/)
      WRITE(2,1070Ø)X,Y,Z,SCALAR
 1070Ø FORMAT(1ØX,'X=',F1Ø.4,/1ØX,'Y=',F1Ø.4,
     1/1ØX,'Z=',F1Ø.4,//1ØX,'SCALAR=',F1Ø.4)
      WRITE(2,1020Ø)
 1020Ø FORMAT('1')
   99 CONTINUE
      RETURN
      END
C
      SUBROUTINE MATSET (ARRAYA,IA,JA,K)
C
C     IF K EQUALS Ø THEN ALL ELEMENTS SET TO ZERO ONLY.
C     IF K EQUALS 1 THEN IDENTITY IS FORMED
C
      DIMENSION ARRAYA(IA,JA)
      DO 1 I=1,IA
      DO 1 J=1,JA
    1 ARRAYA(I,J) = Ø.Ø
      IF (K.EQ.Ø) GO TO 3
      DO 2 I=1,IA
    2 ARRAYA(I,I) = 1.Ø
    3 CONTINUE
      RETURN
      END
C
      SUBROUTINE FILLTR(THETA,PHI,TR)
C
C     FILLS ORTHOGONAL MATRIX REQUIRED FOR TRANSFORMING VECTOR FROM
C     ONE CARTESIAN COORDINATE SYSTEM TO ANOTHER.
C     ANGLES THETA (BOND ANGLE SUPPLEMENTS) AND PHI (DIHEDRAL ANGLE)
C     MUST BE EXPRESSED IN RADIANS.
C
      DIMENSION TR(3,3)
      COST = COS(THETA)
      SINT = SIN(THETA)
      COSP = COS(PHI)
      SINP = SIN(PHI)
```

```
      TR(1,1) = COST
      TR(1,2) = SINT
      TR(1,3) = 0.0
      TR(2,1) = SINT*COSP
      TR(2,2) = -COST*COSP
      TR(2,3) = SINP
      TR(3,1) = SINT*SINP
      TR(3,2) = -COST*SINP
      TR(3,3) = -COSP
      RETURN
      END
C
      SUBROUTINE MATMUL(ARRAYA,ARRAYB,ARRAYC,IA,JA,IB,JB)
C
C     POSTMULTIPLICATION OF ARRAYA BY ARRAYB TO GIVE ARRAYC.
C
      DIMENSION ARRAYA(IA,JA),ARRAYB(JA,JB),ARRAYC(IA,JB)
      DO 1 I=1,IA
      DO 1 J=1,JB
      CIJ = 0.0
      DO 2 K=1,JA
    2 CIJ = CIJ + ARRAYA(I,K) * ARRAYB(K,J)
    1 ARRAYC(I,J) = CIJ
      RETURN
      END
C
      SUBROUTINE MATADD(ARRAYA,ARRAYB,ARRAYC,IA,JA)
C
C     ADDS TWO MATRICES ARRAYA AND ARRAYB TO GIVE ARRAYC.
C
      DIMENSION ARRAYA(IA,JA),ARRAYB(IA,JA),ARRAYC(IA,JA)
      DO 1 I=1,IA
      DO 1 J=1,JA
    1 ARRAYC(I,J) = ARRAYA(I,J) + ARRAYB(I,J)
      RETURN
      END
C
      SUBROUTINE MATEQU(ARRAYA,ARRAYB,IA,JA)
C
C     MATRIX A BECOMES EQUAL TO MATRIX B.
C
      DIMENSION ARRAYA(IA,JA),ARRAYB(IA,JA)
      DO 1 I=1,IA
      DO 1 J=1,JA
    1 ARRAYA(I,J) = ARRAYB(I,J)
      RETURN
      END
      FINISH
```

DATA

NCONF = 1

N = 8

NUBV, NUTHET AND NUPHI ARE RESPECTIVELY 1 1 1

BOND VECTORS

BOND NO.	X	Y	Z
1	1.66000	0.00000	0.00000
2	1.65500	0.00000	0.00000
3	1.65000	0.00000	0.00000
4	1.64000	0.00000	0.00000
5	1.66000	0.00000	0.00000
6	1.65500	0.00000	0.00000
7	1.65000	0.00000	0.00000
8	1.64000	0.00000	0.00000

THETAS = 37.75 67.61 37.88 66.66 37.00 67.57 38.12

PHIS = 0.00 259.34 120.21 204.16 233.14 100.63 239.99

RESULTS

ATOM COORDINATES

(TO BE IGNORED IF THE MOLECULAR DIPOLE MOMENT IS BEING COMPUTED SOONER THAN THE END-TO-END LENGTH.)

ATOM NO.	X	Y	Z
0	0.00000	0.00000	0.00000
1	1.66000	0.00000	0.00000
2	2.96859	1.01322	0.00000
3	3.29277	1.62114	1.49928
4	2.63124	2.51566	2.70419
5	0.97136	2.49596	2.70265
6	-0.33847	1.48434	2.70063
7	-0.66338	0.87806	1.20084
8	0.00146	-0.02004	0.00042

COMPONENTS OF MOLECULAR VECTOR

X= 0.0015

Y= -Ø.Ø2ØØ
Z= Ø.ØØØ4

SCALAR= Ø.Ø2Ø1

Program 2 Calculation of the Root-Mean-Square Average over all Conformations of Dipole Moments or End-to-End Distances of Siloxane Chains

Implicit matrix methods developed by Flory and Jernigan[31,87,168] are employed here to calculate root-mean-square dipole moments or end-to-end distances of siloxane chains averaged over all conformations. This computer program may be used to evaluate Equation 6.7 for siloxanes (see Chapter 6 for details of the matrices involved). However, with only slight adjustments the program could be used to calculate dipole moments or end-to-end distances for any type of polymer chain.

The sample output following this program is a calculation of the statistical mechanical average over all conformations of the end-to-end distances of various lengths of siloxane chain (n = 5 to 11). The chains start with a silicon atom and terminate with an oxygen atom. This calculation is used to model the equilibrium behaviour of these chains under reflux in toluene and, therefore, the temperature used to calculated the statistical weights (σ, ψ and ω) was 383K. All distances are expressed in Angstroms.

```
C
      MASTER MEANSQMOM
C
C     THIS PROGRAM CALCULATES THE MEAN-SQUARE MOMENT OF A SILOXANE
C     POLYMER MOLECULE OVER ALL CONFORMATIONS.
C     EACH CONFORMATION IS STATISTICALLY WEIGHTED BY READING IN THE
C     VALUES OF SIGMA, CAPITAL PHI AND OMEGA (THE STATISTICAL WEIGHTS
C     FOR THE INDEVIDUAL BOND CONFORMATIONS DEPENDANT UPON PHI) AND
C     APPLYING THESE THROUGH THE STATISTICAL WEIGHT MATRICES ARRAYU1 AND
C     ARRAYU2. THEY ARE DENOTED BY SIG, CPHI AND OMEG RESPECTIVELY.
C     FACILITIES ARE AVAILABLE FOR STARTING AND/OR FINISHING THE CHAIN
C     WITH EITHER SI-O OR O-SI BONDS.
C     NEAREST NEIGHBOUR INTERACTIONS ARE TAKEN INTO ACCOUNT.
C
C      *** DATA INPUT ORDER ***
C     (1) NSETS              NUMBER OF SETS OF DATA.
C     (2) NUN,NUBV,NUTHET,   MAY ALL BE EITHER ZERO OR UNITY.
C         NUPHI,NUSW         IF ZERO INITIAL CORRESPONDING VALUES ARE
C                            USED IN EACH CALCULATION.
C                            IF UNITY NEW VALUES ARE READ IN EACH TIME.
C     (3) N                  NUMBER OF SKELETAL BONDS IN CHAIN.
C     (4) INSI,OUTSI         MAY BOTH BE EITHER ZERO OR UNITY.
C                            IF BOTH UNITY CHAIN STARTS AND ENDS WITH
C                            SILICON ATOMS.
C                            IF BOTH ZERO CHAIN STARTS AND ENDS WITH
C                            OXYGEN ATOMS ETC.
C     (5) BOND VECTORS
C         INTO 'STORE'.
C     (6) THETAS             BOND ANGLE SUPPLEMENTS.
C     (7) PHIS               BOND DIHEDRAL ANGLES.
C     (8) SIG,CPHI,OMEG      STATISTICAL WEIGHTS RELATIVE
C                            TO TRANS TRANS CONFORMATION.
C
C      *** CALLS SUBROUTINES ***
C     FILLTR, MATSET, FILLTRDIAG, FILLMATU, MATRAN, DIRPROD, MATMUL,
C     SCALMUL, FILLMATG, FILLJS, MATEQU, FILLJUS
C
      DIMENSION STORE(3,2), THETA(2), PHIS(3), TRA(3,3), TRB(3,3),
     2 TRC(3,3), TRDIAG1(9,9), TRDIAG2(9,9), ARRAYU1(3,3), ARRAYU2(3,3),
     3 BOND1(3,1), BOND2(3,1), BOND1T(1,3), BOND2T(1,3), ARG12A(3,9),
     4 ARG12(3,9), ARG13(3,3), ARRAYE3(3,3), ARG22A(9,9), ARG22(9,9),
     5 ARG23(9,3), ARGSIO(15,15), ARGOSI(15,15), ARGOSI1(15,15),
     6 ARGSIO1(15,15), TEMP(15,15), ARRAYJJ(1,15), ARRAYJ(15,1),
     7 T1(1,15), T2(1,1), ARRAYU(3,3), ARRAYJJU(1,3), ARRAYJU(3,1),
     8 Z(1,1), TEMPU(1,3)
C
      REAL MSQU
      INTEGER OUTSI
C
C     READ NUMBER OF SETS OF DATA.
C
      READ(1,100)NSETS
  100 FORMAT(I0)
      ICOUNT = 0
```

```
    1 CONTINUE
C
C     READ NUN, NUBV, NUTHET, NUPHI AND NUSW.
C
      READ(1,200)NUN,NUBV,NUTHET,NUPHI,NUSW
  200 FORMAT(5I0)
      IF(NUN.EQ.0)GO TO 11
C
C     READ NUMBER OF BACKBONE BONDS.
C
      READ(1,300)N
  300 FORMAT(I0)
   11 CONTINUE
C
C     READ INSI AND OUTSI.
C
      READ(1,350)INSI,OUTSI
  350 FORMAT(2I0)
      IF(NUBV.EQ.0)GO TO 22
C
C     READ BOND VECTORS INTO 'STORE'.
C
      DO 2 J=1,2
      READ(1,400)(STORE(I,J),I=1,3)
  400 FORMAT(3F0.0)
    2 CONTINUE
   22 CONTINUE
      IF(NUTHET.EQ.0)GO TO 33
C
C     READ BOND ANGLE SUPPLEMENTS THETA.
C
      RAD = 0.0174533
      READ(1,500)(THETA(I),I=1,2)
  500 FORMAT(2F0.0)
      DO 3 I=1,2
    3 THETA(I) = THETA(I) * RAD
   33 CONTINUE
      IF(NUPHI.EQ.0)GO TO 44
C
C     READ DIHEDRAL ANGLES PHI.
C
      READ(1,600)(PHIS(I),I=1,3)
  600 FORMAT(3F0.0)
      DO 4 I=1,3
    4 PHIS(I) = PHIS(I) * RAD
   44 CONTINUE
      IF(NUSW.EQ.0)GO TO 55
C
C     READ STATISTICAL WEIGHTS SIG, CPHI AND OMEG FOR THE TWO TYPES OF
C     BOND; THE SI-O FORM FIRST.
C
      READ(1,700)SIG1,CPHI1,OMEG1,SIG2,CPHI2,OMEG2
  700 FORMAT(6F0.0)
   55 CONTINUE
```

```
C
C     WRITE OUT DATA.
C
      WRITE(2,800)
  800 FORMAT(/,10X,'DATA',/,10X,'----')
      WRITE(2,900)NSETS
  900 FORMAT(/10X,'NSETS =',I6)
      WRITE(2,1000)NUN,NUBV,NUTHET,NUPHI,NUSW
 1000 FORMAT(/,10X,'NUN, NUBV, NUTHET, NUPHI',/,10X,
     2 'AND NUSW ARE RESPECTIVELY',5I6)
      WRITE(2,1100)N
 1100 FORMAT(/10X,'N =',I6)
      WRITE(2,1200)INSI,OUTSI
 1200 FORMAT(/,10X,'INSI AND OUTSI ARE RESPECTIVELY',2I6)
      WRITE(2,1240)
 1240 FORMAT(//,10X,'BOND VECTORS')
      WRITE(2,1260)
 1260 FORMAT(19X,'X',14X,'Y',14X,'Z')
      DO 5 J=1,2
      WRITE(2,1300)(STORE(I,J),I=1,3)
 1300 FORMAT(10X,3F15.5)
    5 CONTINUE
      WRITE(2,1400)(THETA(I),I=1,2)
 1400 FORMAT(/,10X,'THETAS =',2F11.4)
      WRITE(2,1500)(PHIS(I),I=1,3)
 1500 FORMAT(/,10X,'PHIS =',3F11.4)
      WRITE(2,1600)SIG1,CPHI1,OMEG1
 1600 FORMAT(//,10X,'STATISTICAL WEIGHTS',/,18X,'SIG1',11X,'CPHI1',10X,
     2 'OMEG1',/,10X,3F15.5)
      WRITE(2,1650)SIG2,CPHI2,OMEG2
 1650 FORMAT(//,10X,'STATISTICAL WEIGHTS',/,18X,'SIG2',11X,'CPHI2',10X,
     2 'OMEG2',/,10X,3F15.5)
C
C     FILL THE TRANSFORMATION MATRIX FOR EACH VALUE OF PHI AND
C     FIRST VALUE OF THETA, CORRESPONDING TO SI-O BOND.
C
      CALL FILLTR(THETA(1),PHIS(1),TRA)
      CALL FILLTR(THETA(1),PHIS(2),TRB)
      CALL FILLTR(THETA(1),PHIS(3),TRC)
C
C     FILL THE PSEUDO-DIAGONAL TRANSFORMATION MATRIX TRDIAG1.
C
      CALL MATSET(TRDIAG1,9,9,0)
      CALL FILLTRDIAG(TRA,TRB,TRC,TRDIAG1)
C
C     SIMILARLY FOR SECOND VALUE OF THETA, CORRESPONDING TO O-SI BOND.
C
      CALL FILLTR(THETA(2),PHIS(1),TRA)
      CALL FILLTR(THETA(2),PHIS(2),TRB)
      CALL FILLTR(THETA(2),PHIS(3),TRC)
      CALL MATSET(TRDIAG2,9,9,0)
      CALL FILLTRDIAG(TRA,TRB,TRC,TRDIAG2)
C
C     FILL THE STATISTICAL WEIGHT ARRAYS FOR SI-O AND O-SI
```

```
C     BONDS RESPECTIVELY.
C
      CALL FILLMATU(SIG1,CPHI1,OMEG1,ARRAYU1)
      WRITE(2,901)
  901 FORMAT(//,10X,'STATISTICAL WEIGHT MATRIX ARRAYU1')
      DO 703 I=1,3
  703 WRITE(2,903)(ARRAYU1(I,J),J=1,3)
      CALL FILLMATU(SIG2,CPHI2,OMEG2,ARRAYU2)
      WRITE(2,902)
  902 FORMAT(//,10X,'STATISTICAL WEIGHT MATRIX ARRAYU2')
      DO 704 I=1,3
  704 WRITE(2,903)(ARRAYU2(I,J),J=1,3)
  903 FORMAT(/,10X,3F15.5)
C
C     FILL BOND VECTORS FROM STORE AND FIND TRANSPOSES.
C
      DO 6 I=1,3
      BOND1(I,1) = STORE(I,1)
    6 CONTINUE
      CALL MATRAN(BOND1,BOND1T,3,1)
      DO 7 I=1,3
      BOND2(I,1) = STORE(I,2)
    7 CONTINUE
      CALL MATRAN(BOND2,BOND2T,3,1)
C
C     FIND SCALAR OF BOND VECTORS.
C
      BL1 = SQRT ( BOND1(1,1)**2.0 + BOND1(2,1)**2.0 + BOND1(3,1)**2.0 )
      BL2 = SQRT ( BOND2(1,1)**2.0 + BOND2(2,1)**2.0 + BOND2(3,1)**2.0 )
C
C     MANIPULATE THESE MATRICES AND FILL THE G MATRIX ARGSIO FOR
C     THE SI-O BOND.
C
      CALL DIRPROD(ARRAYU1,BOND1T,ARG12A,3,3,1,3,3,9)
      CALL MATMUL(ARG12A,TRDIAG1,ARG12,3,9,9,9)
      BL1SQU = (BL1**2.0)/2.0
      CALL SCALMUL(ARRAYU1,BL1SQU,ARG13,3,3)
      CALL MATSET(ARRAYE3,3,3,1)
      CALL DIRPROD(ARRAYU1,ARRAYE3,ARG22A,3,3,3,3,9,9)
      CALL MATMUL(ARG22A,TRDIAG1,ARG22,9,9,9,9)
      CALL DIRPROD(ARRAYU1,BOND1,ARG23,3,3,3,1,9,3)
      CALL MATSET(ARGSIO,15,15,0)
      CALL FILLMATG(ARRAYU1,ARG12,ARG13,ARG22,ARG23,ARGSIO)
C
C     SIMILARLY FOR THE O-SI BOND FILL THE G MATRIX ARGOSI.
C
      CALL DIRPROD(ARRAYU2,BOND2T,ARG12A,3,3,1,3,3,9)
      CALL MATMUL(ARG12A,TRDIAG2,ARG12,3,9,9,9)
      BL2SQU = (BL2**2.0)/2.0
      CALL SCALMUL(ARRAYU2,BL2SQU,ARG13,3,3)
      CALL DIRPROD(ARRAYU2,ARRAYE3,ARG22A,3,3,3,3,9,9)
      CALL MATMUL(ARG22A,TRDIAG2,ARG22,9,9,9,9)
      CALL DIRPROD(ARRAYU2,BOND2,ARG23,3,3,3,1,9,3)
      CALL MATSET(ARGOSI,15,15,0)
```

```
      CALL FILLMATG(ARRAYU2,ARG12,ARG13,ARG22,ARG23,ARGOSI)
C
C     ALSO FILL THE G MATRIX FOR THE FIRST OR LAST BOND IN
C     THE CHAIN OF THE TYPE O-SI.
C
      CALL DIRPROD(ARRAYE3,BOND2T,ARG12A,3,3,1,3,3,9)
      CALL MATMUL (ARG12A,TRDIAG2,ARG12,3,9,9,9)
      CALL SCALMUL(ARRAYE3,BL2SQU,ARG13,3,3)
      CALL DIRPROD(ARRAYE3,ARRAYE3,ARG22A,3,3,3,3,9,9)
      CALL MATMUL(ARG22A,TRDIAG2,ARG22,9,9,9,9)
      CALL DIRPROD(ARRAYE3,BOND2,ARG23,3,3,3,1,9,3)
      CALL MATSET(ARGOSI1,15,15,0)
      CALL FILLMATG(ARRAYE3,ARG12,ARG13,ARG22,ARG23,ARGOSI1)
C
C     FILL THE G MATRIX FOR THE FIRST OR LAST BOND IN THE
C     CHAIN OF THE TYPE SI-O.
C
      CALL DIRPROD(ARRAYE3,BOND1T,ARG12A,3,3,1,3,3,9)
      CALL MATMUL(ARG12A,TRDIAG1,ARG12,3,9,9,9)
      CALL SCALMUL(ARRAYE3,BL1SQU,ARG13,3,3)
      CALL MATMUL(ARG22A,TRDIAG1,ARG22,9,9,9,9)
      CALL DIRPROD(ARRAYE3,BOND1,ARG23,3,3,3,1,9,3)
      CALL MATSET(ARGSIO1,15,15,0)
      CALL FILLMATG(ARRAYE3,ARG12,ARG13,ARG22,ARG23,ARGSIO1)
C
C     FORM THE SERIAL PRODUCT OF THE G MATRICES.
C
      KOUNT = NINT(FLOAT(N-4)/2.0)
      IF(INSI.EQ.0)GO TO 10
      CALL MATMUL(ARGSIO1,ARGOSI,TEMP,15,15,15,15)
      IF(KOUNT.EQ.0)GO TO 8
      DO 8 I=1,KOUNT
      CALL MATMUL(TEMP,ARGSIO,TEMP,15,15,15,15)
      CALL MATMUL(TEMP,ARGOSI,TEMP,15,15,15,15)
    8 CONTINUE
      IF(OUTSI.EQ.0)GO TO 9
      CALL MATMUL(TEMP,ARGSIO,TEMP,15,15,15,15)
      CALL MATMUL(TEMP,ARGOSI1,TEMP,15,15,15,15)
      GO TO 14
    9 CONTINUE
      CALL MATMUL(TEMP,ARGSIO1,TEMP,15,15,15,15)
   10 CONTINUE
      IF (INSI.NE.0)GO TO 14
      CALL MATMUL(ARGOSI1,ARGSIO,TEMP,15,15,15,15)
      IF(KOUNT.EQ.0)GO TO 12
      DO 12 I=1,KOUNT
      CALL MATMUL(TEMP,ARGOSI,TEMP,15,15,15,15)
      CALL MATMUL(TEMP,ARGSIO,TEMP,15,15,15,15)
   12 CONTINUE
      IF(OUTSI.EQ.1)GO TO 13
      CALL MATMUL(TEMP,ARGOSI,TEMP,15,15,15,15)
      CALL MATMUL(TEMP,ARGSIO1,TEMP,15,15,15,15)
      GO TO 14
   13 CONTINUE
```

```
      CALL MATMUL(TEMP,ARGOSI1,TEMP,15,15,15,15)
   14 CONTINUE
C
C     PRE- AND POST-MULTIPLY THE SERIAL PRODUCT OF THE G MATRICES BY THE
C     ROW AND COLUMN MATRICES ARRAYJJ AND ARRAYJ RESPECTIVELY.
C
      CALL FILLJS(ARRAYJJ,ARRAYJ,15,15)
      CALL MATMUL(ARRAYJJ,TEMP,T1,1,15,15,15)
      CALL MATMUL(T1,ARRAYJ,T2,1,15,15,1)
C
C     FORM NUMERATOR OF EXPRESSION.
C
      TOP = T2(1,1) * 2.Ø
C
C     FORM SERIAL PRODUCT OF STATISTICAL WEIGHT MATRICES.
C
      IF(INSI.EQ.Ø)GO TO 16
      CALL MATEQU(ARRAYU,ARRAYU2,3,3)
      IF(KOUNT.EQ.Ø)GO TO 15
      DO 15 I=1,KOUNT
      CALL MATMUL(ARRAYU,ARRAYU1,ARRAYU,3,3,3,3)
      CALL MATMUL(ARRAYU,ARRAYU2,ARRAYU,3,3,3,3)
   15 CONTINUE
      IF(OUTSI.EQ.Ø)GO TO 18
      CALL MATMUL(ARRAYU,ARRAYU1,ARRAYU,3,3,3,3)
      GO TO 18
   16 CONTINUE
      CALL MATEQU(ARRAYU,ARRAYU1,3,3)
      IF(KOUNT.EQ.Ø)GO TO 17
      DO 17 I=1,KOUNT
      CALL MATMUL(ARRAYU,ARRAYU2,ARRAYU,3,3,3,3)
      CALL MATMUL(ARRAYU,ARRAYU1,ARRAYU,3,3,3,3)
   17 CONTINUE
      IF(OUTSI.EQ.1)GO TO 18
      CALL MATMUL(ARRAYU,ARRAYU2,ARRAYU,3,3,3,3)
   18 CONTINUE
C
C     PRE- AND POST-MULTIPLY SERIAL PRODUCT OF STATISTICAL WEIGHT
C     MATRICES TO FORM PARTITION FUNCTION Z.
C
      CALL FILLJUS(ARRAYJJU,ARRAYJU,3,3)
      CALL MATMUL(ARRAYJJU,ARRAYU,TEMPU,1,3,3,3)
      CALL MATMUL(TEMPU,ARRAYJU,Z,1,3,3,1)
C
C     THUS, MEANSQUARE MOMENT OF MOLECULE.
C
      MSQU = TOP / Z(1,1)
C
      WRITE(2,17ØØ)
 17ØØ FORMAT(////,1ØX,'RESULTS',/,1ØX,'———————')
      WRITE(2,175Ø)Z(1,1)
 175Ø FORMAT(/,1ØX,'PARTITION FUNCTION OF MOLECULE =',E15.6,/)
      WRITE(2,18ØØ)MSQU
 18ØØ FORMAT(/1ØX,'MEAN SQUARE MOMENT OF MOLECULE = ',F15.4,/////)
```

```
      WRITE(2,1900)
 1900 FORMAT('1')
C
      ICOUNT = ICOUNT +1
      IF(ICOUNT.NE.NSETS)GO TO 1
C
      STOP
      END
C
      SUBROUTINE FILLTR (THETA,PHI,TR)
C
C     FILLS ORTHOGONAL MATRIX REQUIRED FOR TRANSFORMING VECTOR FROM
C     ONE CARTESIAN COORDINATE SYSTEM TO ANOTHER.
C     ANGLES THETA (BOND ANGLE SUPPLEMENT) AND PHI (DIHEDRAL ANGLE)
C     MUST BE EXPRESSED IN RADIANS.
C
      DIMENSION TR(3,3)
      COST = COS(THETA)
      SINT = SIN(THETA)
      COSP = COS(PHI)
      SINP = SIN(PHI)
      TR(1,1) = COST
      TR(1,2) = SINT
      TR(1,3) = 0.0
      TR(2,1) = SINT * COSP
      TR(2,2) = -COST * COSP
      TR(2,3) = SINP
      TR(3,1) = SINT * SINP
      TR(3,2) = -COST * SINP
      TR(3,3) = -COSP
      RETURN
      END
C
      SUBROUTINE MATSET (ARRAYA,IA,JA,K)
C
C     IF K EQUALS 0 THEN ALL ELEMENTS SET TO ZERO ONLY.
C     IF K EQUALS 1 THEN IDENTITY IS FORMED.
C
      DIMENSION ARRAYA(IA,JA)
      DO 1 I=1,IA
      DO 1 J=1,JA
    1 ARRAYA(I,J) = 0.0
      IF(K.EQ.0) GO TO 3
      DO 2 I=1,IA
    2 ARRAYA(I,I) = 1.0
    3 CONTINUE
      RETURN
      END
C
      SUBROUTINE FILLTRDIAG (TRA,TRB,TRC,TRDIAG)
C
C     FORMS DIAGONAL MATRIX CONSISTING OF SMALLER
C     MATRICES TRA, TRB, TRC.
C
```

```
      DIMENSION TRA(3,3), TRB(3,3), TRC(3,3), TRDIAG(9,9)
      DO 1 I=1,3
      DO 1 J=1,3
      TRDIAG(I,J) = TRA(I,J)
    1 CONTINUE
      DO 2 I=1,3
      DO 2 J=1,3
      II = I+3
      JJ = J+3
      TRDIAG(II,JJ) = TRB(I,J)
    2 CONTINUE
      DO 3 I = 1,3
      DO 3 J=1,3
      II = I+6
      JJ = J+6
      TRDIAG(II,JJ) = TRC(I,J)
    3 CONTINUE
      RETURN
      END
C
      SUBROUTINE FILLMATU (SIG, CPHI, OMEG, ARRAYU)
C
C     THIS SUBROUTINE FILLS THE STATISTICAL WEIGHT MATRIX U
C     WITH THE RELEVANT VALUES OF SIGMA, CAPITAL PHI AND OMEGA.
C
      DIMENSION ARRAYU(3,3)
      ARRAYU(1,1) = 1.Ø
      ARRAYU(1,2) = SIG
      ARRAYU(1,3) = SIG
      ARRAYU(2,1) = 1.Ø
      ARRAYU(2,2) = SIG * CPHI
      ARRAYU(2,3) = SIG * OMEG
      ARRAYU(3,1) = 1.Ø
      ARRAYU(3,2) = SIG * OMEG
      ARRAYU(3,3) = SIG * CPHI
      RETURN
      END
C
      SUBROUTINE MATRAN (ARRAYA, ARRAYB, IA, JA)
C
C     FINDS THE TRANSPOSE OF A RECTANGULAR MATRIX ARRAYA.
C     NOTE - IF ARRAY IS ORTHOGONAL THEN ITS TRANSPOSE IS ITS INVERSE.
C
      DIMENSION ARRAYA(IA,JA),ARRAYB(JA,IA)
      DO 1 I=1,IA
      DO 1 J=1,JA
    1 ARRAYB(J,I) = ARRAYA(I,J)
      RETURN
      END
C
      SUBROUTINE DIRPROD (ARRAYA,ARRAYB,ARRAYC,IA,JA,IB,JB,IC,JC)
C
C     FINDS DIRECT PRODUCT OF ARRAYA AND ARRAYB TO GIVE ARRAYC.
C     IA * IB MUST EQUAL IC AND JA * JB MUST EQUAL JC.
```

```
C
      DIMENSION ARRAYA(IA,JA), ARRAYB(IB,JB), ARRAYC(IC,JC)
      DO 1 I=1,IA
      DO 1 J=1,JA
      DO 1 K=1,IB
      DO 1 L=1,JB
      II = (I-1) * IB + K
      JJ = (J-1) * JB + L
      ARRAYC(II,JJ) = ARRAYA(I,J) * ARRAYB(K,L)
    1 CONTINUE
      RETURN
      END
C
      SUBROUTINE MATMUL (ARRAYA,ARRAYB,ARRAYC,IA,JA,IB,JB )
C
C     POST MULTIPLICATION OF ARRAYA BY ARRAYB TO GIVE ARRAYC.
C
      DIMENSION ARRAYA(IA,JA),ARRAYB(IB,JB),ARRAYC(IA,JB),TEMPRE(20,20)
      DO 3 I=1,IA
      DO 3 J=1,JA
      TEMPRE(I,J) =ARRAYA(I,J)
    3 CONTINUE
      DO 1 I=1,IA
      DO 1 J=1,JB
      CIJ = 0.0
      DO 2 K=1,JA
    2 CIJ = CIJ + TEMPRE(I,K) * ARRAYB(K,J)
    1 ARRAYC(I,J) = CIJ
      RETURN
      END
C
      SUBROUTINE SCALMUL (ARRAYA,S,ARRAYB,IA,JA)
C
C     MULTIPLIES ARRAYA BY A SCALAR S TO GIVE ARRAYB.
C
      DIMENSION ARRAYA(IA,JA),ARRAYB(IA,JA)
      DO 1 I=1,IA
      DO 1 J=1,JA
      ARRAYB(I,J) = S * ARRAYA(I,J)
    1 CONTINUE
      RETURN
      END
C
      SUBROUTINE FILLMATG (ARRAYU,ARG12,ARG13,ARG22,ARG23,ARG)
C
C     FILLS THE G MATRIX FROM THE OTHER RELEVANT MATRICES.
C
      DIMENSION ARRAYU(3,3), ARG12(3,9), ARG13(3,3), ARG22(9,9),
     2 ARG23(9,3), ARG(15,15)
C
      DO 1 I=1,3
      DO 1 J=1,3
      ARG(I,J) = ARRAYU(I,J)
    1 CONTINUE
```

```
      DO 2 I=1,3
      DO 2 J=1,9
      JJ = J+3
      ARG(I,JJ) = ARG12(I,J)
    2 CONTINUE
      DO 3 I=1,3
      DO 3 J=1,3
      JJ = J+12
      ARG(I,JJ) = ARG13(I,J)
    3 CONTINUE
      DO 4 I=1,9
      DO 4 J=1,9
      II = I+3
      JJ = J+3
      ARG(II,JJ) = ARG22(I,J)
    4 CONTINUE
      DO 5 I=1,9
      DO 5 J=1,3
      II = I+3
      JJ = J+12
      ARG(II,JJ) = ARG23(I,J)
    5 CONTINUE
      DO 6 I=1,3
      DO 6 J=1,3
      II = I+12
      JJ = J+12
      ARG(II,JJ) = ARRAYU(I,J)
    6 CONTINUE
      RETURN
      END
C
      SUBROUTINE MATEQU (ARRAYA,ARRAYB,IA,JA)
C
C     MATRIX A BECOMES EQUAL TO MATRIX B.
C
      DIMENSION ARRAYA(IA,JA), ARRAYB(IA,JA)
      DO 1 I=1,IA
      DO 1 J=1,JA
    1 ARRAYA(I,J) = ARRAYB(I,J)
      RETURN
      END
C
      SUBROUTINE FILLJS(ARRAYJJ,ARRAYJ,IA,JA)
C
C     FILLS THE PRE- AND POST-MULTIPLICATION ROW AND COLUMN ARRAYS
C     TO MULTIPLY THE SERIAL PRODUCT OF THE G MATRIX.
C
      DIMENSION ARRAYJJ(1,JA), ARRAYJ(IA,1)
      ARRAYJJ(1,1) = 1.Ø
      DO 1 J=2,JA
      ARRAYJJ(1,J) = Ø.Ø
    1 CONTINUE
      DO 2 I=1,12
      ARRAYJ(I,1) = Ø.Ø
```

```
    2 CONTINUE
      DO 3 I=13,IA
      ARRAYJ(I,1) = 1.Ø
    3 CONTINUE
      RETURN
      END
C
      SUBROUTINE FILLJUS (ARRAYJJU,ARRAYJU,IA,JA)
C
C     FILLS THE PRE- AND POST-MULTIPLICATION ROW AND COLUMN ARRAYS
C     TO MULTIPLY THE SERIAL PRODUCT OF THE STATISTICAL WEIGHT MATRIX.
C
      DIMENSION ARRAYJJU(1,JA), ARRAYJU(IA,1)
      ARRAYJJU(1,1) = 1.Ø
      DO 1 J=2,JA
      ARRAYJJU(1,J) = Ø.Ø
    1 CONTINUE
      DO 2 I=1,IA
      ARRAYJU(I,1) = 1.Ø
    2 CONTINUE
      RETURN
      END
      FINISH
```

DATA

NSETS = 4

NUN, NUBV, NUTHET, NUPHI
AND NUSW ARE RESPECTIVELY 1 1 1 1 1

N = 5

INSI AND OUTSI ARE RESPECTIVELY 1 Ø

BOND VECTORS

X	Y	Z
1.64ØØØ	Ø.ØØØØØ	Ø.ØØØØØ
1.64ØØØ	Ø.ØØØØØ	Ø.ØØØØØ

THETAS = Ø.6458 1.2217

PHIS = Ø.ØØØØ 2.Ø944 4.1888

STATISTICAL WEIGHTS

SIG1	CPHI1	OMEG1
Ø.327ØØ	1.ØØØØØ	Ø.ØØØØØ

STATISTICAL WEIGHTS

SIG2	CPHI2	OMEG2
Ø.327ØØ	1.ØØØØØ	Ø.25Ø8Ø

STATISTICAL WEIGHT MATRIX ARRAYU1

1.ØØØØØ	Ø.327ØØ	Ø.327ØØ
1.ØØØØØ	Ø.327ØØ	Ø.ØØØØØ
1.ØØØØØ	Ø.ØØØØØ	Ø.327ØØ

STATISTICAL WEIGHT MATRIX ARRAYU2

1.ØØØØØ	Ø.327ØØ	Ø.327ØØ
1.ØØØØØ	Ø.327ØØ	Ø.Ø82Ø1
1.ØØØØØ	Ø.Ø82Ø1	Ø.327ØØ

RESULTS

PARTITION FUNCTION OF MOLECULE = Ø.395854E Ø1

MEAN SQUARE MOMENT OF MOLECULE = 4Ø.7346

DATA

NSETS = 4

NUN, NUBV, NUTHET, NUPHI
AND NUSW ARE RESPECTIVELY 1 Ø Ø Ø Ø

N = 7

INSI AND OUTSI ARE RESPECTIVELY 1 Ø

BOND VECTORS

X	Y	Z
1.64ØØØ	Ø.ØØØØØ	Ø.ØØØØØ
1.64ØØØ	Ø.ØØØØØ	Ø.ØØØØØ

THETAS = Ø.6458 1.2217

PHIS = Ø.ØØØØ 2.Ø944 4.1888

STATISTICAL WEIGHTS

SIG1	CPHI1	OMEG1
Ø.327ØØ	1.ØØØØØ	Ø.ØØØØØ

STATISTICAL WEIGHTS

SIG2	CPHI2	OMEG2
Ø.327ØØ	1.ØØØØØ	Ø.25ØØØ

STATISTICAL WEIGHT MATRIX ARRAYU1

1.ØØØØØ	Ø.327ØØ	Ø.327ØØ
1.ØØØØØ	Ø.327ØØ	Ø.ØØØØØ
1.ØØØØØ	Ø.ØØØØØ	Ø.327ØØ

STATISTICAL WEIGHT MATRIX ARRAYU2

1.00000	Ø.32700	Ø.32700
1.00000	Ø.32700	Ø.08201
1.00000	Ø.08201	Ø.32700

RESULTS

PARTITION FUNCTION OF MOLECULE = Ø.953324E Ø1

MEAN SQUARE MOMENT OF MOLECULE = 69.7385

DATA

NSETS = 4

NUN, NUBV, NUTHET, NUPHI
AND NUSW ARE RESPECTIVELY 1 Ø Ø Ø Ø

N = 9

INSI AND OUTSI ARE RESPECTIVELY 1 Ø

BOND VECTORS

X	Y	Z
1.64000	Ø.00000	Ø.00000
1.64000	Ø.00000	Ø.00000

THETAS = Ø.6458 1.2217

PHIS = Ø.0000 2.0944 4.1888

STATISTICAL WEIGHTS

SIG1	CPHI1	OMEG1
Ø.32700	1.00000	Ø.00000

STATISTICAL WEIGHTS

SIG2	CPHI2	OMEG2
Ø.32700	1.00000	Ø.25080

STATISTICAL WEIGHT MATRIX ARRAYU1

1.00000	Ø.32700	Ø.32700
1.00000	Ø.32700	Ø.00000
1.00000	Ø.00000	Ø.32700

STATISTICAL WEIGHT MATRIX ARRAYU2

1.00000	Ø.32700	Ø.32700
1.00000	Ø.32700	Ø.08201
1.00000	Ø.08201	Ø.32700

RESULTS

PARTITION FUNCTION OF MOLECULE = Ø.229606E Ø2

MEAN SQUARE MOMENT OF MOLECULE = 101.5018

DATA

NSETS = 4

NUN, NUBV, NUTHET, NUPHI AND NUSW ARE RESPECTIVELY 1 Ø Ø Ø Ø

N = 11

INSI AND OUTSI ARE RESPECTIVELY 1 Ø

BOND VECTORS

X	Y	Z
1.64000	Ø.00000	Ø.00000

1.64000 0.00000 0.00000

THETAS = 0.6458 1.2217

PHIS = 0.0000 2.0944 4.1888

STATISTICAL WEIGHTS

SIG1	CPHI1	OMEG1
0.32700	1.00000	0.00000

STATISTICAL WEIGHTS

SIG2	CPHI2	OMEG2
0.32700	1.00000	0.25080

STATISTICAL WEIGHT MATRIX ARRAYU1

1.00000	0.32700	0.32700
1.00000	0.32700	0.00000
1.00000	0.00000	0.32700

STATISTICAL WEIGHT MATRIX ARRAYU2

1.00000	0.32700	0.32700
1.00000	0.32700	0.08201
1.00000	0.08201	0.32700

RESULTS

PARTITION FUNCTION OF MOLECULE = 0.553004E 02

MEAN SQUARE MOMENT OF MOLECULE = 134.6783

Program 3 Calculation of the Dipole Moment of a Siloxane Chain using an Amended FCM Model

It is known that there are no severe steric conflicts between non-bonded atoms or groups for the sequence of bond rotational states $g^{\mp}g^{\pm}g^{\mp}g^{\pm}$ centred about a silicon atom in the poly(dimethyl siloxane) chain. However, the FCM model would accord a statistical weight of zero for such combinations of bond rotational states[181,183]. This computer program may be used to generate all conformations of any particular chain length which contain these combinations of bond rotational states. The sum of the weighted squared dipole moments and partition function of these conformations may then be calculated, and combined with the original values of these terms obtained from Program 2 using the unamended FCM model. A corrected value of the mean-square dipole moment of any length of siloxane chain may thus be obtained.

The sample output following this program lists the sum of the weighted square of dipole moments and partition function of the additional conformations for a length of dimethyl siloxane chain having n = 14 skeletal bonds. On combining these values with those obtained from the unamended model it is found that there are no significant differences between the dipole moments predicted by the two types of model for the dimethyl siloxane chain. However, this is not expected to be the case when considering the very small fraction of chain conformations which correspond to cyclic conformations (see Chapter 7). All dipole moments are expressed in Debyes.

```
JOB :EADXX,MBMD6MX,CP76(P1000,T2400,SP)
FTN(L=0,OPT=2,ROUND)
ATTACH(LIB,\:EAAXX.PMICLLIBRARY\,ST=S4S,FO=ASIS)
LIBRARY(LIB)
LDSET(MAP=B/ZZZZMP,PRESET=NGINF)
LGO(PL=10000000)
CATALOG(MBR3,MBRES3,ST=S4S)
####S
      PROGRAM LINDIP(INPUT,OUTPUT,MBR3,TAPE1=INPUT,TAPE2=MBR3)
C
C     THIS PROGRAM CALCULATES THE MEAN SQUARE DIPOLE MOMENT OF THOSE
C     POLYMER CHAINS WHICH ARE EXCLUDED FROM FLORY'S IMPLICIT MATRIX
C     METHOD DUE TO FOUR-BOND INTERACTIONS WHICH ARE STRICTLY ACCEPTABLE.
C     THESE OCCUR WHEN BONDS ARE IN THE STATES G-G+G-G+ OR G+G-G+G- ABOUT
C     A SILICON ATOM. THE PARTITION FUNCTION AND SUM OF THE WEIGHTED
C     DIPOLE MOMENTS ARE ALSO PRODUCED. THESE RESULTS MAY THEN BE USED
C     ALONG WITH THOSE FROM THE MATRIX METHOD TO PRODUCE A MORE ACCURATE
C     DIPOLE MOMENT FOR THE SHORTER CHAINS.
C
C      *** CALLS SUBROUTINES ***
C     FILMATU, FILLTR, TRANSFM, MATMUL.
C
      DIMENSION THETAS(40), ARRAYU(3,3), TR(3,3), TRSTOR(9,6),
     2 TEMP(3,3), SUMDIP(3,1), PROD(3,3), REMEM(2)
      INTEGER ARPHI(1,40), SAVESW(1,40), SIGN
C
C     SET NUMBER OF CONFORMATIONS AND NUMBER OF BACKBONE BONDS.
C
      N = 14
      MULT = 9
      RAD = 0.0174532925199432957
C
C     SET THETAS.
C
      NLESS1 = N-1
      NLESS2 = N-2
      NLESS3 = N-3
      NLESS5 = N-5
      DO 2 I=1,NLESS1,2
    2 THETAS(I) = 37.0
      DO 3 I=2,NLESS2,2
    3 THETAS(I) = 70.0
C
C     SET STATISTICAL WEIGHTS AND FILL STATISTICAL WEIGHT MATRIX ARRAYU.
C
      SIG = 0.238
      CPHI = 1.0
      OMEG = 0.170
      CALL FILMATU(SIG,CPHI,OMEG,ARRAYU)
      SAVESW(1,N+1) = 0.0
C
C     FILL THE 9 BY 6 MATRIX TRSTOR WITH ALL THE TRANSFORMATION MATRICES
C     TO BE USED BY USING SUBROUTINE FILLTR.
C
```

```
      DO 26 I=1,7,3
      DO 26 J=1,4,3
      IF(J.EQ.1) T=37.Ø
      IF(J.EQ.4) T=7Ø.Ø
      IF(I.EQ.1) P=Ø.Ø
      IF(I.EQ.4) P=12Ø.Ø
      IF(I.EQ.7) P=24Ø.Ø
      CALL FILLTR(T,P,TR)
      DO 26 II=1,3
      DO 26 JJ=1,3
      K = II + (I-1)
      L = JJ + (J-1)
      TRSTOR(K,L) = TR(II,JJ)
   26 CONTINUE
C
C     READ IN STARTING VALUE OF MAIN DO LOOP COUNTER.
C
      READ(1,*)KOUNT
C
      WRITE(2,1ØØ)
  1ØØ FORMAT('1')
      NCONFS = Ø
      SUMWSDS = Ø.Ø
      Z = Ø.Ø
      KNOW = 1
C
C     MAIN DO LOOP STARTS HERE.
C
      DO 999 K=KOUNT,MULT
      KKK = (K-1)*59Ø49
      DO 99 KK=1,59Ø49
      KKK = KKK+1
      REMEM(1) = Ø.Ø
C
C     FILL ARRAY ARPHI WITH THE RELEVANT VALUES OF PHI.
C
      A = FLOAT(KKK-1)
      DO 1 I=1,NLESS2
      C = A/3.Ø
      A = AINT(C)
      II = N-I
      ARPHI(1,II) = (NINT(3.Ø*(C-A))) * 12Ø
    1 CONTINUE
      ARPHI(1,1) = Ø.Ø
      ARPHI(1,N) = Ø.Ø
C
C     DETECT AND ELIMINATE ANY CONFORMATIONS WHICH DO NOT HAVE AT LEAST
C     ONE SET OF BONDS ABOUT A SILICON ATOM IN EITHER G-G+G-G+ OR
C     G+G-G+G- STATES.
C
      NOTE = Ø
      DO 22 I=2,NLESS2,2
      IF((ARPHI(1,I).NE.12Ø).OR.(ARPHI(1,I+1).NE.24Ø))GO TO 11
      IF((ARPHI(1,I-1).NE.24Ø).OR.(ARPHI(1,I+2).NE.12Ø))GO TO 99
```

```
      NOTE = 1
      GO TO 22
   11 CONTINUE
      IF((ARPHI(1,I).NE.240).OR.(ARPHI(1,I+1).NE.120))GO TO 22
      IF((ARPHI(1,I-1).NE.120).OR.(ARPHI(1,I+2).NE.240))GO TO 99
      NOTE = 1
   22 CONTINUE
      IF(NOTE.NE.1)GO TO 99
C
C     INITIALISE TEMPORARY MATRIX 'TEMP' PRIOR TO FORMING THE SERIAL
C     PRODUCT OF THE TRANSFORMATION MATRICES 'PROD'.
C     DIPOLE MOMENT VECTORS ARE CONSIDERED AS UNITY AT THIS POINT.
C
      TEMP(1,1) = 1.0
      TEMP(2,2) = 1.0
      TEMP(3,3) = 1.0
      TEMP(1,2) = 0.0
      TEMP(1,3) = 0.0
      TEMP(2,1) = 0.0
      TEMP(2,3) = 0.0
      TEMP(3,1) = 0.0
      TEMP(3,2) = 0.0
      SUMDIP(1,1) = 1.0
      SUMDIP(2,1) = 0.0
      SUMDIP(3,1) = 0.0
      SIGN = 1
      DO 5 II=1,NLESS1
      SIGN = -SIGN
C
C     FORM PRE-MULTIPLYING TRANSFORMATION PRODUCT 'PROD'.
C
      CALL TRANSFM(THETAS(II),ARPHI(1,II),TR,TRSTOR)
      CALL MATMUL(TEMP,TR,PROD,3,3,3,3)
      SUMDIP(1,1) = SUMDIP(1,1) + (PROD(1,1)*SIGN)
      SUMDIP(2,1) = SUMDIP(2,1) + (PROD(2,1)*SIGN)
      SUMDIP(3,1) = SUMDIP(3,1) + (PROD(3,1)*SIGN)
C
C     REINITIALISE ARRAY 'TEMP'.
C
      TEMP(1,1) = PROD(1,1)
      TEMP(1,2) = PROD(1,2)
      TEMP(1,3) = PROD(1,3)
      TEMP(2,1) = PROD(2,1)
      TEMP(2,2) = PROD(2,2)
      TEMP(2,3) = PROD(2,3)
      TEMP(3,1) = PROD(3,1)
      TEMP(3,2) = PROD(3,2)
      TEMP(3,3) = PROD(3,3)
    5 CONTINUE
C
C     COMPUTE THE SQUARE OF THE SCALAR OF THIS MOLECULAR
C     DIPOLE MOMENT VECTOR.
C
      SCDSQ = (SUMDIP(1,1)**2.0 + SUMDIP(2,1)**2.0 +
```

```
     2 SUMDIP(3,1)**2.Ø) * (Ø.6**2.Ø)
C
C     CALCULATE STATISTICAL WEIGHT OF ACCEPTED CONFORMATION.
C
      DO 9 I=1,N
      IF(ARPHI(1,I).EQ.Ø) SAVESW(1,I)=1
      IF(ARPHI(1,I).EQ.12Ø) SAVESW(1,I)=2
      IF(ARPHI(1,I).EQ.24Ø) SAVESW(1,I)=3
    9 CONTINUE
      STATW = 1.Ø
      II = SAVESW(1,N)
      JJ = SAVESW(1,1)
      DO 15 I=1,N
      STATW = ARRAYU(II,JJ) * STATW
      II = SAVESW(1,I)
      JJ = SAVESW(1,I+1)
   15 CONTINUE
      REMEM(1) = STATW
      WSCDSQ = STATW * SCDSQ
      REMEM(2) = WSCDSQ
      Z = Z + REMEM(1)
      SUMWSDS = SUMWSDS + REMEM(2)
      NCONFS = NCONFS + 1
      KNOW = KNOW+1
   99 CONTINUE
  999 CONTINUE
      IF(REMEM(1).EQ.Ø.Ø) KNOW=KNOW-1
      WRITE(2,9ØØ)NCONFS
  9ØØ FORMAT(1ØX,'TOTAL NUMBER OF CONFORMATIONS =',I1Ø)
      IF(NCONFS.EQ.Ø)GO TO 9999
      WRITE(2,1ØØØ)SUMWSDS
 1ØØØ FORMAT(/,1ØX,'SUM OF WEIGHTED SQUARED DIPOLE MOMENTS =',E14.5)
      WRITE(2,11ØØ)Z
 11ØØ FORMAT(1ØX,'PARTITION FUNCTION =',E14.5)
      AVSQDIP = SUMWSDS / Z
      RMSDIP = SQRT(AVSQDIP)
      WRITE(2,12ØØ)RMSDIP
 12ØØ FORMAT(//,1ØX,'R.M.S. DIPOLE MOMENT =',E14.5)
 9999 CONTINUE
      STOP
      END
C
      SUBROUTINE FILMATU (SIG, CPHI, OMEG, ARRAYU)
C
C     THIS SUBROUTINE FILLS THE STATISTICAL WEIGHT MATRIX U WITH
C     THE RELEVANT VALUES OF SIGMA, CAPITAL PHI AND OMEGA.
C
      DIMENSION ARRAYU(3,3)
      ARRAYU(1,1) = 1.Ø
      ARRAYU(1,2) = SIG
      ARRAYU(1,3) = SIG
      ARRAYU(2,1) = 1.Ø
      ARRAYU(2,2) = SIG * CPHI
      ARRAYU(2,3) = SIG * OMEG
```

```
      ARRAYU(3,1) = 1.Ø
      ARRAYU(3,2) = SIG * OMEG
      ARRAYU(3,3) = SIG * CPHI
      RETURN
      END
C
      SUBROUTINE FILLTR (THETA, PHI, TR)
C
C     FILLS ORTHOGONAL MATRIX REQUIRED FOR TRANSFORMING A VECTOR
C     FROM ONE CARTESIAN COORDINATE SYSTEM TO ANOTHER.
C     ANGLES THETA (BOND ANGLE SUPPLEMENT) AND PHI (DIHEDRAL ANGLE)
C     MUST BE EXPRESSED IN RADIANS.
C
      DIMENSION TR(3,3)
      RAD = Ø.Ø1745329251994329 57
      THETA = THETA * RAD
      PHI = PHI * RAD
      COST = COS(THETA)
      SINT = SIN(THETA)
      COSP = COS(PHI)
      SINP = SIN(PHI)
      TR(1,1) = COST
      TR(1,2) = SINT
      TR(1,3) = Ø.Ø
      TR(2,1) = SINT * COSP
      TR(2,2) = -COST * COSP
      TR(2,3) = SINP
      TR(3,1) = SINT * SINP
      TR(3,2) = -COST * SINP
      TR(3,3) = -COSP
      RETURN
      END
C
      SUBROUTINE TRANSFM(T,P,TR,TRSTOR)
C
C     THIS SUBROUTINE IS CALLED MANY TIMES DURING THE CALCULATIONS.
C     IT PROVIDES THE PROGRAM WITH TRANSFORMATION MATRICES WICH HAVE
C     PREVIOUSLY BEEN FILLED. NO CALCULATIONS ARE PERFORMED OTHER THAN
C     THOSE NECESSARY TO TRANSFER THE CONTENTS OF A 3 BY 3 BLOCK OF
C     ELEMENTS IN MATRIX 'TRSTOR' TO MATRIX 'TR'.
C
      DIMENSION TR(3,3), TRSTOR(9,6)
      INTEGER P
C
      IF(T.EQ.37.Ø) JJ=Ø
      IF(T.EQ.7Ø.Ø) JJ=3
      IF(P.EQ.Ø) II=Ø
      IF(P.EQ.12Ø) II=3
      IF(P.EQ.24Ø) II=6
      DO 1 I=1,3
      DO 1 J=1,3
      K = I+II
      L = J+JJ
      TR(I,J) = TRSTOR(K,L)
```

```
    1 CONTINUE
      RETURN
      END
C
      SUBROUTINE MATMUL(ARRAYA,ARRAYB,ARRAYC,IA,JA,IB,JB)
C
C     POST MULTIPLICATION OF ARRAYA BY ARRAYB TO GIVE ARRAYC.
C
      DIMENSION ARRAYA(IA,JA),ARRAYB(IB,JB),ARRAYC(IA,JB)
      DO 1 I=1,IA
      DO 1 J=1,JB
      CIJ = Ø.Ø
      DO 2 K=1,JA
    2 CIJ = CIJ + ARRAYA(I,K) * ARRAYB(K,J)
    1 ARRAYC(I,J) = CIJ
      RETURN
      END
####S
        1
```

1 TOTAL NUMBER OF CONFORMATIONS = 12464

SUM OF WEIGHTED SQUARED DIPOLE MOMENTS = .28258E-Ø2
PARTITION FUNCTION = .15625E-Ø2

R.M.S. DIPOLE MOMENT = .13448E+Ø1

Program 4 Calculation of the Mean-Square Dipole Moment of a Cyclic Polymer

Matrix representation of the FCM model cannot be used directly to calculate the properties of cyclic molecules, since it is not known at the outset which conformations of the equivalent open chain correspond to those adopted by a cyclic molecule. However, the FCM model may still be utilized provided that one or two modifications are implemented. Essentially, all possible conformations, defined by a three-state rotational isomeric model, of the equivalent open chains are generated using this computer program and the relative positions and orientations of the terminal skeletal bonds of the chains are carefully examined. If certain geometrical criteria (see Chapter 7) are satisfied then the conformations are accepted to be those adopted by a cyclic molecule and their statistical weights and dipole moments are calculated.

The sample output following this program is a calculation of the mean-square dipole moment of the cyclic dimethyl siloxane oligomer having n = 12 skeletal bonds. Following the tabulation of the accepted conformations and their parameters, the conformations are then categorised in terms of their end-to-end distances. All distances are expressed in Angstroms and all dipole moments in Debyes.

```
JOB :EADXX,MBCYCD6,CP76(P1000,T2400,SP)
FTN(L=0,OPT=2,ROUND)
ATTACH(LIB,\:EAAXX.PMICLLIBRARY\,ST=S4S,FO=ASIS)
LIBRARY(LIB)
LDSET(MAP=B/ZZZZMP,PRESET=NGINF)
LGO(PL=2000)
CATALOG(MBR4,MBRES4,ST=S4S)
####S
      PROGRAM CYCLOD(INPUT,OUTPUT,MBR4,TAPE1=INPUT,TAPE2=MBR4)
C
C     THIS PROGRAM CALCULATES THE MEAN SQUARE DIPOLE MOMENT OF A CYCLIC
C     POLYMER MOLECULE OVER ALL CONFORMATIONS. THESE CONFORMATIONS ARE
C     GENERATED EXPLICITLY USING THE RELATED LINEAR MOLECULE AND TESTING
C     EACH TIME THAT THEY MAY CONFORM TO A CYCLIC STRUCTURE; REJECTING
C     THOSE THAT DO NOT.
C     EACH CONFORMATION ACCEPTED IS STATISTICALLY WEIGHTED BY READING IN
C     THE VALUES OF SIGMA, CAPITAL PHI AND OMEGA (THE STATISTICAL WEIGHTS
C     FOR THE INDIVIDUAL BOND CONFORMATIONS DEPENDENT UPON PHI) AND
C     APPLYING THESE THROUGH THE STATISTICAL WEIGHT MATRIX ARRAYU.
C
C      *** CALLS SUBROUTINES ***
C     FILMATU, FILLTR, TRANSEM, MATMUL.
C
      DIMENSION THETAS(40),ARRAYU(3,3),TR(3,3),TRSTOR(9,6),
     2 TEMP(3,3),SUM(3,1),SUMDIP(3,1),PROD(3,3),ENDIN1(3,1),BOND(3,1),
     3 TEMPU(3,1),REMEM(500,8)
      INTEGER ARPHI(1,40),CONFNO(500),SAVESW(1,40),SIGN
C
C     SET NUMBER OF CONFORMATIONS AND NUMBER OF BACKBONE BONDS.
C
      N = 12
      MULT = 3
      RAD = 0.0174532925199432957
C
C     SET THETAS.
C
      NLESS1 = N-1
      NLESS2 = N-2
      NLESS3 = N-3
      NLESS5 = N-5
      DO 2 I=1,NLESS1,2
    2 THETAS(I) = 37.0
      DO 3 I=2,NLESS2,2
    3 THETAS(I) = 70.0
C
C     SET STATISTICAL WEIGHTS AND FILL STATISTICAL WEIGHT MATRIX ARRAYU.
C
      SIG = 0.238
      CPHI = 1.0
      OMEG = 0.170
      CALL FILMATU(SIG,CPHI,OMEG,ARRAYU)
      SAVESW(1,N+1) = 0.0
C
C     FILL THE 9 BY 6 MATRIX TRSTOR WITH ALL THE TRANSFORMATION MATRICES
```

```
C     TO BE USED BY USING SUBROUTINE FILLTR.
C
      DO 26 I=1,7,3
      DO 26 J=1,4,3
      IF(J.EQ.1) T=37.Ø
      IF(J.EQ.4) T=7Ø.Ø
      IF(I.EQ.1) P=Ø.Ø
      IF(I.EQ.4) P=12Ø.Ø
      IF(I.EQ.7) P=24Ø.Ø
      CALL FILLTR(T,P,TR)
      DO 26 II=1,3
      DO 26 JJ=1,3
      K = II + (I-1)
      L = JJ + (J-1)
      TRSTOR(K,L) = TR(II,JJ)
   26 CONTINUE
C
C     READ IN STARTING VALUE OF MAIN DO LOOP COUNTER.
C
      READ(1,*)KOUNT
C
      WRITE(2,1ØØ)
  1ØØ FORMAT('1')
      WRITE(2,2ØØ)
  2ØØ FORMAT(1ØX,'ACCEPTABLE CYCLIC CONFORMATIONS FOR ',
     2 'MAXIMUM SCALAR OF 3.5 A')
      WRITE(2,3ØØ)
  3ØØ FORMAT(1ØX,'----------------------------------------------------',
     2 '----------',//)
      SUMWSDS = Ø.Ø
      KNOW = 1
C
C     MAIN DO LOOP STARTS HERE.
C
      DO 999 K=KOUNT,MULT
      KKK = (K-1)*59Ø49
      DO 99 KK=1,59Ø49
C
      KKK = KKK+1
      CONFNO(KNOW) = KKK
      REMEM(KNOW,6) = Ø.Ø
C
C     FILL ARRAY ARPHI WITH RELEVANT VALUES OF PHI AND
C     DETECT AND ELIMINATE ANY MIRROR IMAGE CONFORMATIONS.
C
      NUM = Ø
      NOTE = Ø
      A = FLOAT(KKK-1)
      DO 1 I=1,NLESS1
      C = A/3.Ø
      A = AINT(C)
      II = N-I
      ARPHI(1,II) = (NINT(3.Ø*(C-A))) * 12Ø
      IF(ARPHI(1,II).EQ.12Ø) NUM=NUM+1
```

```
      IF(ARPHI(1,II).EQ.240) NUM=NUM-1
      IF(NOTE.EQ.0) NOTE=NUM
    1 CONTINUE
      IF(NUM.EQ.0) NUM=NOTE
      IF(NUM.LT.0) GO TO 99
C
C     DETECT AND ELIMINATE ANY CONFORMATIONS WHERE FOUR BOND INTERACTION
C     BETWEEN METHYL GROUPS, OR BETWEEN A METHYL AND AN OXYGEN, ABOUT A
C     SILICON ATOM IS EXCESSIVE.
C
      DO 22 I=1,NLESS5,2
      IF((ARPHI(1,I+1).EQ.120).AND.(ARPHI(1,I+2).EQ.240))GO TO 11
      IF((ARPHI(1,I+1).NE.240).OR.(ARPHI(1,I+2).NE.120))GO TO 22
      IF((ARPHI(1,I).NE.120).AND.(ARPHI(1,I+3).NE.240))GO TO 99
      GO TO 22
   11 CONTINUE
      IF((ARPHI(1,I).NE.240).AND.(ARPHI(1,I+3).NE.120))GO TO 99
   22 CONTINUE
C
C     INITIALISE TEMPORARY MATRIX 'TEMP' PRIOR TO FORMING SERIAL PRODUCT
C     OF TRANSFORMATION MATRICES 'PROD'.
C     BOND AND DIPOLE MOMENT VECTORS ARE CONSIDERED AS UNIT VECTORS
C     AT THIS POINT.
C
      TEMP(1,1) = 1.0
      TEMP(2,2) = 1.0
      TEMP(3,3) = 1.0
      TEMP(1,2) = 0.0
      TEMP(1,3) = 0.0
      TEMP(2,1) = 0.0
      TEMP(2,3) = 0.0
      TEMP(3,1) = 0.0
      TEMP(3,2) = 0.0
      SUM(1,1) = 1.0
      SUM(2,1) = 0.0
      SUM(3,1) = 0.0
      SUMDIP(1,1) = 1.0
      SUMDIP(2,1) = 0.0
      SUMDIP(3,1) = 0.0
      SIGN = 1
      DO 5 II=1,NLESS1
      SIGN = -SIGN
C
C     FORM PRE-MULTIPLYING TRANSFORMATION PRODUCT 'PROD'.
C
      CALL TRANSFM(THETAS(II),ARPHI(1,II),TR,TRSTOR)
      CALL MATMUL(TEMP,TR,PROD,3,3,3,3)
      SUM(1,1) = SUM(1,1) + PROD(1,1)
      SUM(2,1) = SUM(2,1) + PROD(2,1)
      SUM(3,1) = SUM(3,1) + PROD(3,1)
      SUMDIP(1,1) = SUMDIP(1,1) + (PROD(1,1)*SIGN)
      SUMDIP(2,1) = SUMDIP(2,1) + (PROD(2,1)*SIGN)
      SUMDIP(3,1) = SUMDIP(3,1) + (PROD(3,1)*SIGN)
      IF(II.NE.NLESS2) GO TO 44
```

```
      ENDIN1(1,1) = SUM(1,1)
      ENDIN1(2,1) = SUM(2,1)
      ENDIN1(3,1) = SUM(3,1)
   44 CONTINUE
C
C     REINITIALISE ARRAY 'TEMP'.
C
      TEMP(1,1) = PROD(1,1)
      TEMP(1,2) = PROD(1,2)
      TEMP(1,3) = PROD(1,3)
      TEMP(2,1) = PROD(2,1)
      TEMP(2,2) = PROD(2,2)
      TEMP(2,3) = PROD(2,3)
      TEMP(3,1) = PROD(3,1)
      TEMP(3,2) = PROD(3,2)
      TEMP(3,3) = PROD(3,3)
    5 CONTINUE
C
C     MOLECULAR VECTOR IS NOW COMPLETE.
C     COMPUTE SCALAR PART OF MOLECULAR VECTOR.
C
      SCALAR = (SQRT(SUM(1,1)**2.Ø+SUM(2,1)**2.Ø+SUM(3,1)**2.Ø))*1.64
C
C     CHECK THIS END-TO-END DISTANCE IS WITHIN TOLERANCE.
C
      IF(SCALAR.GT.3.5)GO TO 99
      REMEM(KNOW,1) = SCALAR
C
C     CHECK ANGLE IS WITHIN LIMITS OF SUPPLEMENTARY BOND ANGLE.
C
      SCAL = SQRT(ENDIN1(1,1)**2.Ø + ENDIN1(2,1)**2.Ø +
     2 ENDIN1(3,1)**2.Ø)
      ANGLE = 18Ø.Ø - ((ACOS(ENDIN1(1,1)/SCAL))/RAD)
      IF((ANGLE.LT.55.Ø).OR.(ANGLE.GT.85.Ø)) GO TO 99
      REMEM(KNOW,2) = ANGLE
C
C     CHECK Y COMPONENT OF BOND N-1 IS NEGATIVE AND Z COMPONENT
C     APPROACHES ZERO IN COORDINATE SYSTEM OF FIRST BOND.
C     I.E. BOND N LIES IN XY PLANE BELOW X-AXIS.
C
      YCOORD = ENDIN1(2,1) * 1.64
      IF(YCOORD.GT.Ø.Ø)GO TO 99
      REMEM(KNOW,3) = YCOORD
      ZCOORD = ENDIN1(3,1) * 1.64
      IF(ZCOORD.GT.Ø.5)GO TO 99
      IF(ZCOORD.LT.-Ø.5)GO TO 99
      REMEM(KNOW,4) = ZCOORD
C
C     CHECK DIHEDRAL ANGLE IS OF RIGHT ORDER.
C     ANTI-CLOCKWISE ROTATION IS TAKEN TO BE POSITIVE LOOKING DOWN
C     THE XO POSITIVE AXIS TOWARDS THE ORIGIN.
C
      BOND(1,1) = Ø.Ø
      BOND(2,1) = -1.Ø
```

```
      BOND(3,1) = 0.0
      CALL MATMUL (PROD,BOND,TEMPU,3,3,3,1)
      BOND(1,1) = -COS(20.0*RAD)
      BOND(2,1) = SIN(20.0*RAD)
      A = TEMPU(1,1)*BOND(1,1) + TEMPU(2,1)*BOND(2,1)
      SCTEMPU = SQRT(TEMPU(1,1)**2.0 + TEMPU(2,1)**2.0 +
     2 TEMPU(3,1)**2.0)
      SCBOND = SQRT(BOND(1,1)**2.0 + BOND(2,1)**2.0)
      SCAL = SCTEMPU*SCBOND
      ANGLE = (ACOS(A/SCAL))/RAD
      IF(TEMPU(3,1).LE.0.0)GO TO 55
      ANGLE = 360.0 - ANGLE
   55 CONTINUE
      IF((ANGLE.GT.15.AND.ANGLE.LT.105).OR.
     2 (ANGLE.GT.135.AND.ANGLE.LT.225).OR.
     3 (ANGLE.GT.255.AND.ANGLE.LT.345)) GO TO 99
      REMEM(KNOW,5) = ANGLE
      ARPHI(1,N) = IFIX(ANINT(ANGLE/120.0)) * 120
      IF(ARPHI(1,N).EQ.360) ARPHI(1,N)=0
C
C     DETECT AND ELIMINATE CONFORMATIONS WHERE FOUR BOND INTERACTION
C     BETWEEN METHYL GROUPS, OR BETWEEN A METHYL AND AN OXYGEN,
C     ABOUT THE PENULTIMATE AND ULTIMATE SILICON ATOMS IN THE CHAIN
C     IS EXCESSIVE.
C
      IF((ARPHI(1,NLESS2).EQ.120).AND.(ARPHI(1,NLESS1).EQ.240))GO TO 27
      IF((ARPHI(1,NLESS2).NE.240).OR.(ARPHI(1,NLESS1).NE.120))GO TO 28
      IF((ARPHI(1,NLESS3).NE.120).AND.(ARPHI(1,N).NE.240))GO TO 99
      GO TO 28
   27 CONTINUE
      IF((ARPHI(1,NLESS3).NE.240).AND.(ARPHI(1,N).NE.120))GO TO 99
   28 CONTINUE
      IF((ARPHI(1,N).EQ.120).AND.(ARPHI(1,1).EQ.240))GO TO 29
      IF((ARPHI(1,N).NE.240).OR.(ARPHI(1,1).NE.120))GO TO 30
      IF((ARPHI(1,NLESS1).NE.120).AND.(ARPHI(1,2).NE.240))GO TO 99
      GO TO 30
   29 CONTINUE
      IF((ARPHI(1,NLESS1).NE.240).AND.(ARPHI(1,2).NE.120))GO TO 99
   30 CONTINUE
C
C     CALCULATE STATISTICAL WEIGHT OF ACCEPTED CYCLIC CONFORMATION.
C
      DO 9 I=1,N
      IF(ARPHI(1,I).EQ.0) SAVESW(1,I)=1
      IF(ARPHI(1,I).EQ.120) SAVESW(1,I)=2
      IF(ARPHI(1,I).EQ.240) SAVESW(1,I)=3
    9 CONTINUE
      STATW = 1.0
      II = SAVESW(1,N)
      JJ = SAVESW(1,1)
      DO 15 I=1,N
      STATW = ARRAYU(II,JJ) * STATW
      II = SAVESW(1,I)
      JJ = SAVESW(1,I+1)
```

```
   15 CONTINUE
      REMEM(KNOW,6) = STATW
C
C     COMPUTE THE SQUARE OF THE SCALAR OF THE MOLECULAR
C     DIPOLE MOMENT VECTOR OF THIS ACCEPTED CONFORMATION.
C
      SCDSQ = (SUMDIP(1,1)**2.Ø + SUMDIP(2,1)**2.Ø +
     2 SUMDIP(3,1)**2.Ø) * (Ø.6**2.Ø)
      REMEM(KNOW,7) = SCDSQ
      WSCDSQ = STATW * SCDSQ
      REMEM(KNOW,8) = WSCDSQ
      WRITE(2,156Ø)(ARPHI(1,I),I=1,N)
 156Ø FORMAT(1ØX,26I4)
      KNOW = KNOW+1
   99 CONTINUE
  999 CONTINUE
      IF(REMEM(KNOW,6).EQ.Ø.Ø) KNOW=KNOW-1
      WRITE(2,1575)
 1575 FORMAT('1')
      WRITE(2,16ØØ)
 16ØØ FORMAT(15X,'CONF NO',1X,'SCAL',1X,'THETAS',1X,'YCOMP',1X,
     2 'ZCOMP',3X,'PHIS',4X,'STATW',1X,'MSQMOM')
      DO 164Ø I=1,KNOW
 164Ø WRITE(2,165Ø)CONFNO(I),(REMEM(I,J),J=1,7)
 165Ø FORMAT(1ØX,I12,F5.2,F7.2,2F6.2,F7.2,E9.2,F7.4)
      TOL = 3.6
      DO 8 ITOL=1,35
      NCONFS = Ø
      SUMWSDS = Ø.Ø
      Z = Ø.Ø
      TOL = TOL-Ø.1
      DO 7 I=1,KNOW
      IF(REMEM(I,1).GT.TOL) GO TO 7
      SUMWSDS = SUMWSDS + REMEM(I,8)
      Z = Z + REMEM(I,6)
      NCONFS = NCONFS + 1
    7 CONTINUE
      IF(NCONFS.EQ.Ø)GO TO 9999
      WRITE(2,166Ø)TOL
 166Ø FORMAT(/,1ØX,'SCALAR LIMIT = ',F4.1,1X,'A')
      WRITE(2,1665)
 1665 FORMAT(1ØX,'----------------------')
      WRITE(2,167Ø)SUMWSDS
 167Ø FORMAT(/,1ØX,'SUM OF WEIGHTED SQUARED DIPOLE MOMENTS =',E14.5)
      WRITE(2,154Ø)Z
 154Ø FORMAT(1ØX,'PARTITION FUNCTION =',E14.5)
      WRITE(2,168Ø)NCONFS
 168Ø FORMAT(1ØX,'NUMBER OF ACCEPTED CONFORMATIONS =',I6)
      AVSQDIP = SUMWSDS / Z
      RMSDIP = SQRT(AVSQDIP)
      WRITE(2,169Ø)RMSDIP
 169Ø FORMAT(//,1ØX,'R.M.S. DIPOLE MOMENT = ',E14.5,//)
      WRITE(2,17ØØ)AVSQDIP
 17ØØ FORMAT(//,1ØX,'MEAN SQUARE DIPOLE MOMENT =',E14.5,////)
```

```
    8 CONTINUE
 9999 CONTINUE
      STOP
      END
C
      SUBROUTINE FILMATU (SIG, CPHI, OMEG, ARRAYU)
C
C     THIS SUBROUTINE FILLS THE STATISTICAL WEIGHT MATRIX 'U'
C     WITH THE RELEVANT VALUES OF SIGMA, CAPITAL PHI AND OMEGA.
C
      DIMENSION ARRAYU(3,3)
      ARRAYU(1,1) = 1.Ø
      ARRAYU(1,2) = SIG
      ARRAYU(1,3) = SIG
      ARRAYU(2,1) = 1.Ø
      ARRAYU(2,2) = SIG * CPHI
      ARRAYU(2,3) = SIG * OMEG
      ARRAYU(3,1) = 1.Ø
      ARRAYU(3,2) = SIG * OMEG
      ARRAYU(3,3) = SIG * CPHI
      RETURN
      END
C
      SUBROUTINE FILLTR (THETA,PHI,TR)
C
C     FILLS ORTHOGONAL MATRIX REQUIRED FOR TRANSFORMING A VECTOR FROM
C     ONE CARTESIAN COORDINATE SYSTEM TO ANOTHER.
C     ANGLES THETA (BOND ANGLE SUPPLEMENT) AND PHI (DIHEDRAL ANGLE)
C     MUST BE EXPRESSED IN RADIANS.
C
      DIMENSION TR(3,3)
      RAD = Ø.Ø174533
      THETA = THETA * RAD
      PHI = PHI * RAD
      COST = COS(THETA)
      SINT = SIN(THETA)
      COSP = COS(PHI)
      SINP = SIN(PHI)
      TR(1,1) = COST
      TR(1,2) = SINT
      TR(1,3) = Ø.Ø
      TR(2,1) = SINT * COSP
      TR(2,2) = -COST * COSP
      TR(2,3) = SINP
      TR(3,1) = SINT * SINP
      TR(3,2) = -COST * SINP
      TR(3,3) = -COSP
      RETURN
      END
C
      SUBROUTINE TRANSFM(T,P,TR,TRSTOR)
C
C     THIS SUBROUTINE IS CALLED MANY TIMES DURING THE CALCULATIONS. IT
C     PROVIDES THE PROGRAM WITH TRANSFORMATION MATRICES WHICH HAVE
```

```
C     PREVIOSLY BEEN FILLED. NO CALCULATIONS ARE PERFORMED OTHER THAN
C     THOSE NECESSARY TO TRANSFER THE CONTENTS OF A 3 BY 3 BLOCK OF
C     ELEMENTS IN MATRIX 'TRSTOR' TO MATRIX 'TR'.
C
      DIMENSION TR(3,3), TRSTOR(9,6)
      INTEGER P
C
      IF(T.EQ.37.Ø) JJ=Ø
      IF(T.EQ.7Ø.Ø) JJ=3
      IF(P.EQ.Ø) II=Ø
      IF(P.EQ.12Ø) II=3
      IF(P.EQ.24Ø) II=6
      DO 1 I=1,3
      DO 1 J=1,3
      K = I+II
      L = J+JJ
      TR(I,J) = TRSTOR(K,L)
    1 CONTINUE
      RETURN
      END
C
      SUBROUTINE MATMUL (ARRAYA,ARRAYB,ARRAYC,IA,JA,IB,JB )
C
C     POST MULTIPLICATION OF ARRAYA BY ARRAYB TO GIVE ARRAYC.
C
      DIMENSION ARRAYA(IA,JA),ARRAYB(IB,JB),ARRAYC(IA,JB)
      DO 1 I=1,IA
      DO 1 J=1,JB
      CIJ = Ø.Ø
      DO 2 K=1,JA
    2 CIJ = CIJ + ARRAYA(I,K) * ARRAYB(K,J)
    1 ARRAYC(I,J) = CIJ
      RETURN
      END
####S
       1
****
```

ACCEPTABLE CYCLIC CONFORMATIONS FOR MAXIMUM SCALAR OF 3.5 A

Ø	Ø	12Ø	24Ø	Ø	Ø	Ø	Ø	12Ø	24Ø	12Ø	24Ø
Ø	Ø	12Ø	24Ø	Ø	Ø	12Ø	24Ø	Ø	Ø	12Ø	24Ø
Ø	Ø	12Ø	24Ø	Ø	Ø	12Ø	24Ø	12Ø	Ø	Ø	24Ø
Ø	Ø	12Ø	24Ø	12Ø	Ø	Ø	24Ø	12Ø	24Ø	12Ø	24Ø
Ø	Ø	12Ø	24Ø	12Ø	Ø	12Ø	12Ø	12Ø	24Ø	24Ø	12Ø
Ø	Ø	12Ø	24Ø	24Ø	Ø	Ø	12Ø	12Ø	24Ø	12Ø	24Ø
Ø	Ø	24Ø	12Ø	Ø	Ø	Ø	Ø	24Ø	12Ø	12Ø	24Ø
Ø	Ø	24Ø	12Ø	Ø	Ø	24Ø	12Ø	Ø	Ø	12Ø	24Ø
Ø	Ø	24Ø	12Ø	Ø	Ø	24Ø	12Ø	12Ø	Ø	Ø	24Ø
Ø	Ø	24Ø	12Ø	12Ø	Ø	Ø	24Ø	24Ø	12Ø	12Ø	24Ø
Ø	Ø	24Ø	12Ø	24Ø	Ø	Ø	12Ø	24Ø	12Ø	12Ø	24Ø
Ø	12Ø	24Ø	12Ø	12Ø	24Ø	12Ø	Ø	12Ø	24Ø	12Ø	24Ø
Ø	24Ø	Ø	Ø	12Ø	24Ø	12Ø	24Ø	Ø	12Ø	Ø	12Ø
Ø	24Ø	Ø	Ø	12Ø	24Ø	12Ø	24Ø	Ø	12Ø	12Ø	24Ø
12Ø	Ø	12Ø	12Ø	24Ø	12Ø	24Ø	24Ø	Ø	24Ø	12Ø	24Ø
12Ø	Ø	12Ø	24Ø	12Ø	24Ø	12Ø	12Ø	Ø	24Ø	12Ø	24Ø
12Ø	Ø	24Ø	12Ø	24Ø	12Ø	Ø	Ø	12Ø	Ø	12Ø	24Ø
12Ø	12Ø	Ø	12Ø	12Ø	24Ø	24Ø	Ø	24Ø	24Ø	12Ø	24Ø
12Ø	12Ø	Ø	12Ø	24Ø	12Ø	12Ø	24Ø	Ø	12Ø	12Ø	24Ø
12Ø	12Ø	24Ø	12Ø	24Ø	24Ø	Ø	24Ø	24Ø	12Ø	12Ø	Ø
12Ø	24Ø	Ø	Ø	Ø	Ø	12Ø	24Ø	Ø	Ø	12Ø	24Ø
12Ø	24Ø	Ø	Ø	Ø	Ø	12Ø	24Ø	12Ø	Ø	Ø	24Ø
12Ø	24Ø	Ø	Ø	24Ø	12Ø	24Ø	12Ø	12Ø	12Ø	Ø	24Ø
12Ø	24Ø	Ø	Ø	24Ø	12Ø	24Ø	12Ø	12Ø	12Ø	12Ø	12Ø
12Ø	24Ø	12Ø	Ø	Ø	24Ø	12Ø	24Ø	Ø	Ø	12Ø	24Ø
12Ø	24Ø	12Ø	Ø	Ø	24Ø	12Ø	24Ø	12Ø	Ø	Ø	24Ø
12Ø	24Ø	12Ø	Ø	12Ø	12Ø	24Ø	12Ø	24Ø	Ø	Ø	24Ø
12Ø	24Ø	24Ø	Ø	Ø	12Ø	12Ø	24Ø	Ø	Ø	12Ø	24Ø
12Ø	24Ø	24Ø	Ø	Ø	12Ø	12Ø	24Ø	12Ø	Ø	Ø	24Ø
24Ø	Ø	24Ø	24Ø	12Ø	24Ø	12Ø	12Ø	Ø	12Ø	12Ø	24Ø
24Ø	12Ø	Ø	Ø	Ø	Ø	24Ø	12Ø	Ø	Ø	12Ø	24Ø
24Ø	12Ø	Ø	Ø	Ø	Ø	24Ø	12Ø	12Ø	Ø	Ø	24Ø
24Ø	12Ø	Ø	Ø	12Ø	24Ø	Ø	Ø	24Ø	12Ø	12Ø	24Ø
24Ø	12Ø	Ø	Ø	24Ø	12Ø	Ø	Ø	24Ø	12Ø	Ø	Ø
24Ø	12Ø	12Ø	Ø	Ø	24Ø	24Ø	12Ø	Ø	Ø	12Ø	24Ø
24Ø	12Ø	12Ø	Ø	Ø	24Ø	24Ø	12Ø	12Ø	Ø	Ø	24Ø
24Ø	12Ø	12Ø	24Ø	Ø	Ø	12Ø	24Ø	24Ø	12Ø	12Ø	24Ø
24Ø	12Ø	24Ø	Ø	Ø	12Ø	24Ø	12Ø	Ø	Ø	12Ø	24Ø
24Ø	12Ø	24Ø	Ø	Ø	12Ø	24Ø	12Ø	12Ø	Ø	Ø	24Ø
24Ø	24Ø	Ø	24Ø	24Ø	12Ø	12Ø	Ø	12Ø	12Ø	12Ø	24Ø
24Ø	24Ø	12Ø	24Ø	24Ø	12Ø	12Ø	24Ø	12Ø	12Ø	12Ø	24Ø

CONF NO	SCAL	THETAS	YCOMP	ZCOMP	PHIS	STATW	MSQMOM
1Ø952	2.46	8Ø.96	-3.56	.48	238.26	.15E-Ø6	1.8389
11Ø72	.7Ø	68.56	-.92	-.17	244.25	.89E-Ø6	1.5146
11Ø8Ø	1.19	75.31	-.85	-.14	245.45	.89E-Ø6	2.2624
11735	2.12	8Ø.14	-3.Ø8	.43	242.11	.25E-Ø9	2.5875
11790	2.57	79.83	-4.Ø8	.Ø9	122.6Ø	.2ØE-Ø8	.8961
12437	2.25	8Ø.99	-3.26	.24	241.28	.86E-Ø8	.1763

15332	2.65	80.96	-3.56	-.48	242.51	.89E-06	.5771
15500	1.63	68.56	-.92	.17	242.17	.89E-06	.4595
15508	1.37	75.55	-.92	.28	242.88	.53E-05	.1303
16115	2.35	80.99	-3.26	-.24	243.84	.51E-07	.3001
16817	2.29	80.14	-3.08	-.43	247.31	.15E-08	1.3732
36305	2.35	67.85	-2.64	-.45	232.12	.24E-11	1.0607
40720	2.21	66.21	-.64	.28	119.66	.21E-06	2.0889
40721	2.39	66.21	-.64	.28	230.60	.86E-08	.8502
69722	1.29	67.11	-1.26	.04	227.34	.14E-10	.9099
71315	3.24	58.22	-2.71	.16	232.12	.24E-11	1.1954
76070	3.21	59.93	-2.21	-.33	237.28	.15E-08	.6586
82322	.85	71.45	-2.22	.31	244.32	.49E-09	.4518
82760	2.44	80.85	-2.26	-.00	242.60	.83E-10	.2002
96062	1.06	79.78	-2.20	-.24	9.37	.49E-09	.5102
98552	2.22	64.74	-3.35	-.08	244.63	.15E-06	1.9161
98560	2.69	66.13	-3.28	-.01	249.76	.15E-06	3.0385
100318	2.02	60.69	-.94	.23	240.76	.35E-09	.6789
100319	1.71	60.69	-.94	.23	130.03	.49E-09	.3519
105599	1.73	61.64	-2.81	-.14	248.20	.25E-09	2.8345
105607	2.14	63.37	-2.75	-.07	247.11	.25E-09	2.6744
106156	3.36	61.95	-2.95	.34	234.97	.59E-10	.9540
111917	1.98	62.26	-2.96	-.07	244.54	.86E-08	.3221
111925	2.33	63.88	-2.91	.01	246.65	.86E-08	.2829
136922	.53	67.11	-1.26	-.04	234.30	.49E-09	.5312
137972	2.79	64.74	-3.35	.08	237.18	.89E-06	.7234
137980	2.80	66.40	-3.32	.17	240.81	.53E-05	.6283
139019	1.29	68.02	-2.02	.32	250.10	.86E-08	.2891
139504	.70	79.53	-1.20	-.02	347.31	.89E-06	1.5146
145019	2.32	62.26	-2.96	.07	240.88	.51E-07	.4820
145027	2.40	64.06	-2.93	.15	242.15	.30E-06	.6060
148874	2.55	80.20	-1.39	-.32	250.01	.83E-10	.3607
151337	2.38	61.64	-2.81	.14	242.26	.15E-08	1.6832
151345	2.27	63.71	-2.79	.23	239.56	.86E-08	.3478
163634	2.42	71.45	-2.22	-.31	239.40	.17E-07	.2022
170249	2.90	84.20	-1.87	-.15	239.39	.80E-12	.3957

SCALAR LIMIT = 3.5 A

SUM OF WEIGHTED SQUARED DIPOLE MOMENTS = .12009E-04
PARTITION FUNCTION = .17007E-04
NUMBER OF ACCEPTED CONFORMATIONS = 41

R.M.S. DIPOLE MOMENT = .84033E+00

MEAN SQUARE DIPOLE MOMENT = .70615E+00

SCALAR LIMIT = 3.4 A

SUM OF WEIGHTED SQUARED DIPOLE MOMENTS = .12009E-04
PARTITION FUNCTION = .17007E-04
NUMBER OF ACCEPTED CONFORMATIONS = 41

R.M.S. DIPOLE MOMENT = .84033E+00

MEAN SQUARE DIPOLE MOMENT = .70615E+00

SCALAR LIMIT = 3.3 A

SUM OF WEIGHTED SQUARED DIPOLE MOMENTS = .12009E-04
PARTITION FUNCTION = .17007E-04
NUMBER OF ACCEPTED CONFORMATIONS = 40

R.M.S. DIPOLE MOMENT = .84033E+00

MEAN SQUARE DIPOLE MOMENT = .70615E+00

SCALAR LIMIT = 3.2 A

SUM OF WEIGHTED SQUARED DIPOLE MOMENTS = .12008E-04
PARTITION FUNCTION = .17006E-04
NUMBER OF ACCEPTED CONFORMATIONS = 38

R.M.S. DIPOLE MOMENT = .84033E+00

MEAN SQUARE DIPOLE MOMENT = .70615E+00

SCALAR LIMIT = 3.1 A

SUM OF WEIGHTED SQUARED DIPOLE MOMENTS = .12008E-04
PARTITION FUNCTION = .17006E-04
NUMBER OF ACCEPTED CONFORMATIONS = 38

R.M.S. DIPOLE MOMENT = .84033E+00

MEAN SQUARE DIPOLE MOMENT = .70615E+00

SCALAR LIMIT = 3.0 A

SUM OF WEIGHTED SQUARED DIPOLE MOMENTS = .12008E-04
PARTITION FUNCTION = .17006E-04
NUMBER OF ACCEPTED CONFORMATIONS = 38

R.M.S. DIPOLE MOMENT = .84033E+00

MEAN SQUARE DIPOLE MOMENT = .70615E+00

SCALAR LIMIT = 2.9 A

SUM OF WEIGHTED SQUARED DIPOLE MOMENTS = .12008E-04
PARTITION FUNCTION = .17006E-04
NUMBER OF ACCEPTED CONFORMATIONS = 38

R.M.S. DIPOLE MOMENT = .84033E+00

MEAN SQUARE DIPOLE MOMENT = .70615E+00

SCALAR LIMIT = 2.8 A

SUM OF WEIGHTED SQUARED DIPOLE MOMENTS = .87083E-05
PARTITION FUNCTION = .11753E-04
NUMBER OF ACCEPTED CONFORMATIONS = 36

R.M.S. DIPOLE MOMENT = .86078E+00

MEAN SQUARE DIPOLE MOMENT = .74094E+00

SCALAR LIMIT = 2.7 A

SUM OF WEIGHTED SQUARED DIPOLE MOMENTS = .80624E-05
PARTITION FUNCTION = .10860E-04
NUMBER OF ACCEPTED CONFORMATIONS = 35

R.M.S. DIPOLE MOMENT = .86161E+00

MEAN SQUARE DIPOLE MOMENT = .74238E+00

SCALAR LIMIT = 2.6 A

SUM OF WEIGHTED SQUARED DIPOLE MOMENTS = .70858E-05
PARTITION FUNCTION = .98155E-05
NUMBER OF ACCEPTED CONFORMATIONS = 33

R.M.S. DIPOLE MOMENT = .84965E+00

MEAN SQUARE DIPOLE MOMENT = .72190E+00

SCALAR LIMIT = 2.5 A

SUM OF WEIGHTED SQUARED DIPOLE MOMENTS = .70839E-05
PARTITION FUNCTION = .98134E-05
NUMBER OF ACCEPTED CONFORMATIONS = 31

R.M.S. DIPOLE MOMENT = .84963E+00

MEAN SQUARE DIPOLE MOMENT = .72187E+00

SCALAR LIMIT = 2.4 A

SUM OF WEIGHTED SQUARED DIPOLE MOMENTS = .68014E-05
PARTITION FUNCTION = .96446E-05
NUMBER OF ACCEPTED CONFORMATIONS = 28

R.M.S. DIPOLE MOMENT = .83976E+00

MEAN SQUARE DIPOLE MOMENT = .70520E+00

SCALAR LIMIT = 2.3 A

SUM OF WEIGHTED SQUARED DIPOLE MOMENTS = .65693E-05
PARTITION FUNCTION = .92273E-05
NUMBER OF ACCEPTED CONFORMATIONS = 21

R.M.S. DIPOLE MOMENT = .84377E+00

MEAN SQUARE DIPOLE MOMENT = .71195E+00

SCALAR LIMIT = 2.2 A

SUM OF WEIGHTED SQUARED DIPOLE MOMENTS = .58281E-Ø5
PARTITION FUNCTION = .88443E-Ø5
NUMBER OF ACCEPTED CONFORMATIONS = 16

R.M.S. DIPOLE MOMENT = .81176E+ØØ

MEAN SQUARE DIPOLE MOMENT = .65896E+ØØ

SCALAR LIMIT = 2.1 A

SUM OF WEIGHTED SQUARED DIPOLE MOMENTS = .58267E-Ø5
PARTITION FUNCTION = .88438E-Ø5
NUMBER OF ACCEPTED CONFORMATIONS = 14

R.M.S. DIPOLE MOMENT = .81170E+ØØ

MEAN SQUARE DIPOLE MOMENT = .65885E+ØØ

SCALAR LIMIT = 2.Ø A

SUM OF WEIGHTED SQUARED DIPOLE MOMENTS = .58265E-Ø5
PARTITION FUNCTION = .88435E-Ø5
NUMBER OF ACCEPTED CONFORMATIONS = 13

R.M.S. DIPOLE MOMENT = .81169E+ØØ

MEAN SQUARE DIPOLE MOMENT = .65885E+ØØ

SCALAR LIMIT = 1.9 A

SUM OF WEIGHTED SQUARED DIPOLE MOMENTS = .58237E-Ø5
PARTITION FUNCTION = .88349E-Ø5
NUMBER OF ACCEPTED CONFORMATIONS = 12

R.M.S. DIPOLE MOMENT = .81190E+ØØ

MEAN SQUARE DIPOLE MOMENT = .65918E+ØØ

SCALAR LIMIT = 1.8 A

SUM OF WEIGHTED SQUARED DIPOLE MOMENTS = .58237E-Ø5
PARTITION FUNCTION = .88349E-Ø5
NUMBER OF ACCEPTED CONFORMATIONS = 12

R.M.S. DIPOLE MOMENT = .81190E+ØØ

MEAN SQUARE DIPOLE MOMENT = .65918E+ØØ

SCALAR LIMIT = 1.7 A

SUM OF WEIGHTED SQUARED DIPOLE MOMENTS = .58229E-Ø5
PARTITION FUNCTION = .88341E-Ø5
NUMBER OF ACCEPTED CONFORMATIONS = 1Ø

R.M.S. DIPOLE MOMENT = .81187E+ØØ

MEAN SQUARE DIPOLE MOMENT = .65913E+ØØ

SCALAR LIMIT = 1.6 A

SUM OF WEIGHTED SQUARED DIPOLE MOMENTS = .54125E-Ø5
PARTITION FUNCTION = .79412E-Ø5
NUMBER OF ACCEPTED CONFORMATIONS = 9

R.M.S. DIPOLE MOMENT = .82557E+ØØ

MEAN SQUARE DIPOLE MOMENT = .68157E+ØØ

SCALAR LIMIT = 1.5 A

SUM OF WEIGHTED SQUARED DIPOLE MOMENTS = .54125E-Ø5
PARTITION FUNCTION = .79412E-Ø5
NUMBER OF ACCEPTED CONFORMATIONS = 9

R.M.S. DIPOLE MOMENT = .82557E+ØØ

MEAN SQUARE DIPOLE MOMENT = .68157E+ØØ

SCALAR LIMIT = 1.4 A

SUM OF WEIGHTED SQUARED DIPOLE MOMENTS = .54125E-Ø5
PARTITION FUNCTION = .79412E-Ø5
NUMBER OF ACCEPTED CONFORMATIONS = 9

R.M.S. DIPOLE MOMENT = .82557E+ØØ

MEAN SQUARE DIPOLE MOMENT = .68157E+ØØ

SCALAR LIMIT = 1.3 A

SUM OF WEIGHTED SQUARED DIPOLE MOMENTS = .47281E-Ø5
PARTITION FUNCTION = .26888E-Ø5
NUMBER OF ACCEPTED CONFORMATIONS = 8

R.M.S. DIPOLE MOMENT = .13261E+Ø1

MEAN SQUARE DIPOLE MOMENT = .17584E+Ø1

SCALAR LIMIT = 1.2 A

SUM OF WEIGHTED SQUARED DIPOLE MOMENTS = .47256E-Ø5
PARTITION FUNCTION = .26802E-Ø5
NUMBER OF ACCEPTED CONFORMATIONS = 6

R.M.S. DIPOLE MOMENT = .13278E+Ø1

MEAN SQUARE DIPOLE MOMENT = .17631E+Ø1

SCALAR LIMIT = 1.1 A

SUM OF WEIGHTED SQUARED DIPOLE MOMENTS = .27Ø55E-Ø5
PARTITION FUNCTION = .17873E-Ø5
NUMBER OF ACCEPTED CONFORMATIONS = 5

R.M.S. DIPOLE MOMENT = .123Ø3E+Ø1

MEAN SQUARE DIPOLE MOMENT = .15137E+Ø1

SCALAR LIMIT = 1.Ø A

SUM OF WEIGHTED SQUARED DIPOLE MOMENTS = .27Ø52E-Ø5
PARTITION FUNCTION = .17868E-Ø5
NUMBER OF ACCEPTED CONFORMATIONS = 4

R.M.S. DIPOLE MOMENT = .12304E+Ø1

MEAN SQUARE DIPOLE MOMENT = .15140E+Ø1

SCALAR LIMIT = .9 A

SUM OF WEIGHTED SQUARED DIPOLE MOMENTS = .27Ø52E-Ø5
PARTITION FUNCTION = .17868E-Ø5
NUMBER OF ACCEPTED CONFORMATIONS = 4

R.M.S. DIPOLE MOMENT = .12304E+Ø1

MEAN SQUARE DIPOLE MOMENT = .15140E+Ø1

SCALAR LIMIT = .8 A

SUM OF WEIGHTED SQUARED DIPOLE MOMENTS = .27Ø5ØE-Ø5
PARTITION FUNCTION = .17863E-Ø5
NUMBER OF ACCEPTED CONFORMATIONS = 3

R.M.S. DIPOLE MOMENT = .12306E+Ø1

MEAN SQUARE DIPOLE MOMENT = .15143E+Ø1

SCALAR LIMIT = .7 A

SUM OF WEIGHTED SQUARED DIPOLE MOMENTS = .27050E-05
PARTITION FUNCTION = .17863E-05
NUMBER OF ACCEPTED CONFORMATIONS = 3

R.M.S. DIPOLE MOMENT = .12306E+01

MEAN SQUARE DIPOLE MOMENT = .15143E+01

SCALAR LIMIT = .6 A

SUM OF WEIGHTED SQUARED DIPOLE MOMENTS = .25872E-09
PARTITION FUNCTION = .48704E-09
NUMBER OF ACCEPTED CONFORMATIONS = 1

R.M.S. DIPOLE MOMENT = .72884E+00

MEAN SQUARE DIPOLE MOMENT = .53121E+00

Program 5 Perturbation of the Dihedral Angles of a Cyclic Conformation of the Equivalent Dimethyl Siloxane Chain

This computer program was used to conduct the calculations described in Section 7.05 on the cyclic conformations of the equivalent open dimethyl siloxane chain having n = 12 skeletal bonds. It could also be used to carry out perturbation calculations on any other conformation of any length of polymer chain. The sample calculation following this program shows the amount of perturbation which was required in order to reduce the end-to-end distance of this conformation from 2.33Å to less than 0.1Å. It may also be observed that the dipole moment of this conformation changes little due to this perturbation. All distances are expressed in Angstroms and all dipole moments in Debyes.

```
JOB :EADXX,MBPTLIM,CP76(P3000,TD320,SP)
FTN(L=0,OPT=2,ROUND)
ATTACH(LIB,\:EAAXX.PMICLLIBRARY\,ST=S4S,FO=ASIS)
LIBRARY(LIB)
LDSET(MAP=B/ZZZZMP,PRESET=NGINF)
LGO(PL=500000)
CATALOG(MBR5,MBRES5,ST=S4S)
####S
      PROGRAM PERTLIM(INPUT,OUTPUT,MBR5,TAPE1=INPUT,TAPE2=MBR5)
C
C     THIS PROGRAM READS IN A SET OF PHIS FOR A CONFORMATION AND THEN
C     PERTURBS ALL PERMUTATIONS OF THESE ORIGINAL PHIS BY A PREDECIDED
C     AMOUNT (IPERT). IT THEN CALCULATES THE NEW SCALAR OF
C     THE END-TO-END VECTOR AND THE DIPOLE MOMENT OF EACH SLIGHTLY
C     DIFFERENT CONFORMATION.
C     THE PROGRAM ONLY ACCEPTS CONFORMATIONS WHOSE SCALARS ARE LESS
C     THAN THE PRE-SET VALUE SCALMAX.
C     THE ACCEPTED VALUES ARE OUTPUT TO A FILE MBR5.
C
C      *** CALLS SUBROUTINES ***
C     FILLTR, MATMUL
C
      DIMENSION TR(3,3),TEMP(3,3),SUM(3,1),SUMDIP(3,1),PROD(3,3),
     2 TEMPU(3,1)
      INTEGER ARPHIN(1,40), ARPHI(1,40),THETAS(40),SIGN
C
C     SET NUMBER OF PERTURBATIONS AND NUMBER OF BACKBONE BONDS.
C
      N = 12
      MULT = 1
      RAD = 0.0174532925199432957
C
C     SET THETAS.
C
      NLESS1 = N-1
      NLESS2 = N-2
      DO 2 I=1,NLESS1,2
    2 THETAS(I) = 37
      DO 3 I=2,NLESS2,2
    3 THETAS(I) = 70
C
C     READ AMOUNT BY WHICH ALL THE PHIS ARE TO BE PERTURBED.
C
      READ(1,*) IPERT
      WRITE(2,10) IPERT
   10 FORMAT(///,10X,'AMOUNT OF PERTURBATION =',I4,1X,'DEGREES')
C
C     READ MAXIMUM SCALAR TO BE ACCEPTED.
C
      READ(1,*) SCALMAX
      WRITE(2,30) SCALMAX
   30 FORMAT(/,10X,'MAXIMUM SCALAR ACCEPTED =',F5.3,1X,'A')
      WRITE(2,15)
   15 FORMAT(///,10X,'STARTING CONFORMATION',/,
```

```
     2 10X,'----------------------',/)
C
C     READ INITIAL VALUES OF PHI.
C
      READ(1,*) (ARPHIN(1,I),I=1,N)
      WRITE(2,20) (ARPHIN(1,I),I=1,N)
   20 FORMAT(10X,2614)
      KKK=0
      GO TO 7
   11 CONTINUE
      WRITE(2,25)
   25 FORMAT(///,10X,'PERTURBED CONFORMATIONS',/,
     2 10X,'------------------------',/)
C
C     MAIN DO LOOP STARTS HERE.
C
      DO 999 K=1,MULT
      KKK = (K-1)*59049
      DO 99 KK=1,59049
C
      KKK = KKK+1
C
C     PERTURB VALUES OF PHI.
C
    7 CONTINUE
      DO 6 I=1,N
    6 ARPHI(1,I) = ARPHIN(1,I)
      IF(KKK.EQ.0) GO TO 4
      IF(KKK.EQ.1) GO TO 99
      A = FLOAT(KKK-1)
      DO 1 I=1,NLESS2
      C = A/3.0
      A = AINT(C)
      II = N-I
      PERT = ((NINT(3.0*(C-A)))-1) * IPERT
      ARPHI(1,II) = ARPHIN(1,II) + PERT
      IF(ARPHI(1,II).LT.0) ARPHI(1,II)=360+ARPHI(1,II)
    1 CONTINUE
    4 CONTINUE
C
C     INITIALISE TEMPORARY MATRIX TEMP PRIOR TO FORMING SERIAL PRODUCT
C     OF TRANSFORMATION MATRICES PROD.
C     BOND AND DIPOLE MOMENT VECTORS ARE CONSIDERED AS UNIT VECTORS
C     AT THIS POINT.
C
      TEMP(1,1) = 1.0
      TEMP(2,2) = 1.0
      TEMP(3,3) = 1.0
      TEMP(1,2) = 0.0
      TEMP(1,3) = 0.0
      TEMP(2,1) = 0.0
      TEMP(2,3) = 0.0
      TEMP(3,1) = 0.0
      TEMP(3,2) = 0.0
```

```
      SUM(1,1) = 1.Ø
      SUM(2,1) = Ø.Ø
      SUM(3,1) = Ø.Ø
      SUMDIP(1,1) = 1.Ø
      SUMDIP(2,1) = Ø.Ø
      SUMDIP(3,1) = Ø.Ø
      SIGN = 1
      DO 5 II=1,NLESS1
      SIGN = -SIGN
C
C     FORM PRE-MULTIPLYING TRANSFORMATION PRODUCT PROD.
C
      CALL FILLTR(THETAS(II),ARPHI(1,II),TR)
      CALL MATMUL(TEMP,TR,PROD,3,3,3,3)
      SUM(1,1) = SUM(1,1) + PROD(1,1)
      SUM(2,1) = SUM(2,1) + PROD(2,1)
      SUM(3,1) = SUM(3,1) + PROD(3,1)
      SUMDIP(1,1) = SUMDIP(1,1) + (PROD(1,1)*SIGN)
      SUMDIP(2,1) = SUMDIP(2,1) + (PROD(2,1)*SIGN)
      SUMDIP(3,1) = SUMDIP(3,1) + (PROD(3,1)*SIGN)
C
C     REINITIALISE ARRAY TEMP.
C
      TEMP(1,1) = PROD(1,1)
      TEMP(1,2) = PROD(1,2)
      TEMP(1,3) = PROD(1,3)
      TEMP(2,1) = PROD(2,1)
      TEMP(2,2) = PROD(2,2)
      TEMP(2,3) = PROD(2,3)
      TEMP(3,1) = PROD(3,1)
      TEMP(3,2) = PROD(3,2)
      TEMP(3,3) = PROD(3,3)
    5 CONTINUE
C
C     MOLECULAR VECTOR IS NOW COMPLETE.
C     COMPUTE SCALAR PART OF MOLECULAR VECTOR.
C
      SCALAR = (SQRT(SUM(1,1)**2.Ø+SUM(2,1)**2.Ø+SUM(3,1)**2.Ø))*1.64
C
C     ELIMINATE ALL THE CONFORMATIONS WITH A SCALAR GREATER THAN SCALMAX.
C
      IF((KKK.NE.Ø).AND.(SCALAR.GT.SCALMAX)) GO TO 99
C
C     COMPUTE THE SQUARE OF THE SCALAR OF THIS MOLECULAR
C     DIPOLE MOMENT VECTOR.
C
      SCDSQ = (SUMDIP(1,1)**2.Ø + SUMDIP(2,1)**2.Ø +
     2 SUMDIP(3,1)**2.Ø) * (Ø.6**2.Ø)
      DIPMOM = SQRT(SCDSQ)
      IF(KKK.EQ.Ø) GO TO 1565
      WRITE(2,156Ø)KKK,(ARPHI(1,I),I=1,N)
 156Ø FORMAT(1ØX,I15,3X,26I4)
 1565 WRITE(2,157Ø)SCALAR,DIPMOM,SCDSQ
 157Ø FORMAT(1ØX,'SCALAR =',F5.2,5X,'DIP. MOM. =',F5.2,5X,
```

```
    2 'DIP. MOM. SQUARED =',F5.2)
      IF(KKK.EQ.Ø)GO TO 11
   99 CONTINUE
  999 CONTINUE
      STOP
      END
C
      SUBROUTINE FILLTR (THETA,PHI,TR)
C
C     FILLS ORTHOGONAL MATRIX REQUIRED FOR TRANSFORMING A VECTOR FROM
C     ONE CARTESIAN COORDINATE SYSTEM TO ANOTHER.
C     ANGLES THETA (BOND ANGLE SUPPLEMENT) AND PHI (DIHEDRAL ANGLE)
C     MUST BE EXPRESSED IN RADIANS.
C
      DIMENSION TR(3,3)
      INTEGER THETA,PHI
      RAD = Ø.Ø1745329251994329577
      T = FLOAT(THETA) * RAD
      P = FLOAT(PHI) * RAD
      COST = COS(T)
      SINT = SIN(T)
      COSP = COS(P)
      SINP = SIN(P)
      TR(1,1) = COST
      TR(1,2) = SINT
      TR(1,3) = Ø.Ø
      TR(2,1) = SINT * COSP
      TR(2,2) = -COST * COSP
      TR(2,3) = SINP
      TR(3,1) = SINT * SINP
      TR(3,2) = -COST * SINP
      TR(3,3) = -COSP
      RETURN
      END
C
      SUBROUTINE MATMUL (ARRAYA,ARRAYB,ARRAYC,IA,JA,IB,JB )
C
C     POST MULTIPLICATION OF ARRAYA BY ARRAYB TO GIVE ARRAYC.
C
      DIMENSION ARRAYA(IA,JA),ARRAYB(IB,JB),ARRAYC(IA,JB)
      DO 1 I=1,IA
      DO 1 J=1,JB
      CIJ = Ø.Ø
      DO 2 K=1,JA
    2 CIJ = CIJ + ARRAYA(I,K) * ARRAYB(K,J)
    1 ARRAYC(I,J) = CIJ
      RETURN
      END
####S
        12
            Ø.1
    12Ø  24Ø  24Ø  Ø  Ø  12Ø  12Ø  24Ø  12Ø  Ø  Ø  24Ø
****
```

AMOUNT OF PERTURBATION = 12 DEGREES

MAXIMUM SCALAR ACCEPTED = .100 A

STARTING CONFORMATION

120 240 240 0 0 120 120 240 120 0 0 240
SCALAR = 2.33 DIP. MOM. = .53 DIP. MOM. SQUARED = .28

PERTURBED CONFORMATIONS

11343 120 228 240 12 348 120 132 228 108 348 12 240
SCALAR = .09 DIP. MOM. = .49 DIP. MOM. SQUARED = .24
17661 120 228 252 12 348 108 132 228 108 348 12 240
SCALAR = .07 DIP. MOM. = .54 DIP. MOM. SQUARED = .29

Program 6 Calculation of the Dihedral Angles of a Polymer Chain from its Atomic Coordinates

Bond dihedral angles of the crystallographic form of octamethylcyclotetrasiloxane were found from the atomic coordinates[185] by using this computer program. This conformation corresponds to structure E in Table 7.06 (see Section 7.08 for further details).

```
      MASTER FINDPHIS
C
C     THIS PROGRAM CALCULATES THE DIHEDRAL ANGLES (PHIS) OF THE BONDS OF
C     A CYCLIC POLYMER MOLECULE GIVEN THE COORDINATES OF EACH INDIVIDUAL
C     ATOM PRESENT.
C     ANTI-CLOCKWISE ROTATION IS TAKEN TO BE POSITIVE WHEN LOOKING DOWN
C     THE XO POSITIVE AXIS TOWARDS THE ORIGIN.
C
C      *** DATA INPUT ORDER ***
C     (1) NSETS              NUMBER OF SETS OF DATA.
C     (2) NCONF              NUMBER OF CONFORMATIONS.
C     (3) N                  NUMBER OF SKELETAL BONDS IN CHAIN.
C     (4) ATOM COORDINATES   READ INTO 'STORECOORDS'
C
C      *** CALLS SUBROUTINES ***
C     FILLREFLEC, MATMUL, MATSET, FILLROT, VECTANG, MATRAN
C
      DIMENSION STORECOORDS(3,100), TEMPCOORDS(3,4), REFLEC(3,3),
     2 ATOM1(3,1), ATOM2(3,1), ROTATE(3,3), ATOM4(3,1), PHIS(100)
C
C      *** COMMON TO SUBROUTINE REFLEC ***
      COMMON PHITURN
C
C     READ NUMBER OF SETS OF DATA.
C
      READ(1,100)NSETS
  100 FORMAT(I0)
      WRITE(2,120)
  120 FORMAT(/,10X,'DATA')
      WRITE(2,130)
  130 FORMAT(10X,'----')
      WRITE(2,150)NSETS
  150 FORMAT(/,10X,'NSETS =',I6)
      ICOUNT = 0
    1 CONTINUE
C
C     READ NUMBER OF CONFORMATIONS.
C
      READ(1,200)NCONF
  200 FORMAT(I0)
      WRITE(2,250)NCONF
  250 FORMAT(/,10X,'NCONF =',I6)
C
C     READ NUMBER OF BACKBONE BONDS.
C
      READ(1,300)N
  300 FORMAT(I0)
      WRITE(2,350)N
  350 FORMAT(/,10X,'N =',I6)
C
C     MAIN DO LOOP STARTS HERE.
C
      DO 97 K=1,NCONF
C
```

```
C     READ IN ATOM COORDINATES.
C     IN SILOXANES FIRST OXYGEN ATOM COORDINATES ARE READ FIRST.
C     FIRST SILICON ATOM COORDINATES ARE READ IN LAST, THUS
C     MAKING THIS ATOM N AND/OR ATOM ZERO.
C     THE FIRST DIHEDRAL ANGLE CALCULATED IS THEREFORE THAT OF
C     BOND SI(N/Ø)-O(1)   I.E. BOND ONE.
C
      DO 2 J=1,N
    2 READ(1,4ØØ)(STORECOORDS(I,J),I=1,3)
  4ØØ FORMAT(3FØ.Ø)
      WRITE(2,41Ø)
  41Ø FORMAT(//,1ØX,'ATOM COORDINATES')
      WRITE(2,42Ø)
  42Ø FORMAT(/,1ØX,'ATOM NO.',7X,'X',14X,'Y',14X,'Z')
      DO 43Ø J=1,N
      JLESS1 = J-1
  43Ø WRITE(2,44Ø)JLESS1,(STORECOORDS(I,J),I=1,3)
  44Ø FORMAT(1ØX,I5,1X,3F15.5)
      RAD = Ø.Ø174533
      NLESS2 = N-2
      DO 99 KK=1,N
      PHITURN = 1.Ø
C
C     FILL ARRAY 'TEMPCOORDS' WITH COORDINATES OF REQUIRED FOUR ATOMS.
C
C
      IF(KK.EQ.N)GO TO 42
      IF(KK.GE.3)GO TO 4Ø
      IF(KK.EQ.2)GO TO 37
      DO 35 J=1,2
      JJ = NLESS2 + J
      DO 35 I=1,3
   35 TEMPCOORDS(I,J) = STORECOORDS(I,JJ)
      DO 36 J=3,4
      JJ = J-2
      DO 36 I=1,3
   36 TEMPCOORDS(I,J) = STORECOORDS(I,JJ)
      GO TO 46
   37 CONTINUE
      DO 38 I=1,3
   38 TEMPCOORDS(I,1) = STORECOORDS(I,N)
      DO 39 J=2,4
      JJ = J-1
      DO 39 I=1,3
   39 TEMPCOORDS(I,J) = STORECOORDS(I,JJ)
      GO TO 46
   4Ø CONTINUE
      DO 41 J=1,4
      JJ = KK-(3-J)
      DO 41 I=1,3
   41 TEMPCOORDS(I,J) = STORECOORDS(I,JJ)
      GO TO 46
   42 CONTINUE
      DO 43 J=1,3
```

```
      JJ = N-(3-J)
      DO 43 I=1,3
   43 TEMPCOORDS(I,J) = STORECOORDS(I,JJ)
      DO 45 I=1,3
   45 TEMPCOORDS(I,4) = STORECOORDS(I,1)
   46 CONTINUE
C
C     TRANSLATE SECOND ATOM OF FOUR ATOM CHAIN TO BE CONSIDERED TO
C     ORIGIN OF COORDINATE AXIS SYSTEM.
C
      DO 18 I=1,3
      ATOM2(I,1) = TEMPCOORDS(I,2)
   18 CONTINUE
      DO 21 J=1,4
      DO 21 I=1,3
      TEMPCOORDS(I,J) = TEMPCOORDS(I,J) - ATOM2(I,1)
   21 CONTINUE
C
C     CHECK ALL COORDINATES OF THIRD ATOM IN FOUR ATOM CHAIN BEING
C     CONSIDERED ARE POSITIVE, AND IF THIS IS NOT SO MAKE THEM POSITIVE
C     BY REFLECTION THROUGH THE APPROPRIATE PLANE.
C
      DO 98 II=1,3
      IF(TEMPCOORDS(II,3).GE.0.0)GO TO 98
      CALL FILLREFLEC(REFLEC,3,3,II)
      DO 77 J=1,4
      DO 20 I=1,3
   20 ATOM1(I,1) = TEMPCOORDS(I,J)
      CALL MATMUL(REFLEC,ATOM1,ATOM2,3,3,3,1)
      DO 3 I=1,3
    3 TEMPCOORDS(I,J) = ATOM2(I,1)
   77 CONTINUE
   98 CONTINUE
C
C     POSITION SECOND BOND OF THREE BOND CHAIN UNDER CONSIDERATION ON
C     POSITIVE X AXIS.
C
      DO 555 II=2,3
      IF(II.EQ.3)GO TO 111
      M = 3
      GO TO 222
  111 CONTINUE
      M = 2
  222 CONTINUE
      IF(TEMPCOORDS(M,3).EQ.0.0)GO TO 555
      IF(TEMPCOORDS(1,3).EQ.0.0)GO TO 458
      ANGLE = ATAN(TEMPCOORDS(M,3)/TEMPCOORDS(1,3))
      ANGLE = ANGLE/RAD
      GO TO 459
  458 CONTINUE
      ANGLE = 90.0
  459 CONTINUE
      CALL FILLROT(ROTATE,ANGLE,II)
      DO 333 J=1,4
```

```
      DO 6 I=1,3
    6 ATOM1(I,1) = TEMPCOORDS(I,J)
      CALL MATMUL(ROTATE,ATOM1,ATOM2,3,3,3,1)
      DO 7 I=1,3
    7 TEMPCOORDS(I,J) = ATOM2(I,1)
  333 CONTINUE
  555 CONTINUE
C
C     CHECK Y AND Z COMPONENTS OF FIRST ATOM IN FOUR ATOM SEQUENCE BEING
C     CONSIDERED ARE BOTH NEGATIVE AND IF THEY ARE NOT MAKE THEM SO BY
C     REFLECTION THROUGH THE APPROPRIATE PLANE.
C
      DO 888 II=2,3
      IF(II.EQ.3)GO TO 463
      IF(TEMPCOORDS(2,1).LE.0.0)GO TO 888
      GO TO 464
  463 CONTINUE
      IF(TEMPCOORDS(3,1).LE.0.0)GO TO 888
  464 CONTINUE
      CALL FILLREFLEC(REFLEC,3,3,II)
      DO 666 J=1,4
      DO 10 I=1,3
   10 ATOM1(I,1) = TEMPCOORDS(I,J)
      CALL MATMUL(REFLEC,ATOM1,ATOM2,3,3,3,1)
      DO 12 I=1,3
   12 TEMPCOORDS(I,J) = ATOM2(I,1)
  666 CONTINUE
  888 CONTINUE
C
C     POSITION FIRST BOND OF THREE BOND CHAIN IN THE XY PLANE BY
C     ROTATING ABOUT THE X AXIS.
C
      IF(TEMPCOORDS(3,1).EQ.0.0)GO TO 999
      IF(TEMPCOORDS(2,1).EQ.0.0)GO TO 461
      ANGLE=ATAN(SQRT(TEMPCOORDS(3,1)**2.0)/SQRT(TEMPCOORDS(2,1)**2.0))
      ANGLE = ANGLE/RAD
      GO TO 462
  461 CONTINUE
      ANGLE = 90.0
  462 CONTINUE
      CALL FILLROT(ROTATE,ANGLE,1)
      DO 999 J=1,4
      DO 15 I=1,3
   15 ATOM1(I,1) = TEMPCOORDS(I,J)
      CALL MATMUL(ROTATE,ATOM1,ATOM2,3,3,3,1)
      DO 16 I=1,3
   16 TEMPCOORDS(I,J) = ATOM2(I,1)
  999 CONTINUE
C
C     CALCULATE DIHEDRAL ANGLES PHIS.
C
      CALL MATSET(ATOM1,3,1,0)
      ATOM1(2,1) = 1.0
      CALL MATSET(ATOM4,3,1,0)
```

```
      ATOM4(2,1) = TEMPCOORDS(2,4)
      ATOM4(3,1) = TEMPCOORDS(3,4)
      RAD = 0.0174533
      SCAL = SQRT(TEMPCOORDS(2,4)**2.0 + TEMPCOORDS(3,4)**2.0)
      IF((TEMPCOORDS(2,4)/SCAL).GE.1.0)GO TO 5
      IF((TEMPCOORDS(2,4)/SCAL).LE.-1.0)GO TO 8
      PHIS(KK) = (ACOS(TEMPCOORDS(2,4)/SCAL))/RAD
      GO TO 9
    5 ANGLE = 0.0
      GO TO 9
    8 ANGLE = 180.0
    9 CONTINUE
      IF(PHITURN.EQ.1.0)GO TO 4
      PHIS(KK) = 360.0-PHIS(KK)
      PHITURN = 0.0
    4 CONTINUE
      IF(TEMPCOORDS(3,4).GE.0.0)GO TO 99
      PHIS(KK) = 360.0-PHIS(KK)
   99 CONTINUE
C
C     WRITE OUT PHIS.
C
      WRITE(2,450)
  450 FORMAT(////)
      WRITE(2,460)
  460 FORMAT(10X,'RESULTS')
      WRITE(2,470)
  470 FORMAT(10X,'-------',/)
      WRITE(2,500)
  500 FORMAT(10X,'BOND NUMBER',10X,'PHIS')
      WRITE(2,520)
  520 FORMAT(30X,'(DEGREES)')
      DO 19 I=1,N
   19 WRITE(2,550)I,PHIS(I)
  550 FORMAT(10X,I6,15X,F6.2)
      WRITE(2,600)
  600 FORMAT('1')
C
   97 CONTINUE
C
      ICOUNT = ICOUNT + 1
      IF(ICOUNT.NE.NSETS)GO TO 1
C
      STOP
      END
C
      SUBROUTINE FILLREFLEC(REFLEC,IA,JA,KK)
C
C     THIS SUBROUTINE FILLS THE PRE-MULTIPLYING MATRIX REQUIRED TO
C     REFLECT A VECTOR IN A GIVEN PLANE.
C     THE PLANE IS DECIDED BY THE VALUE OF KK.
C     (1) YZ PLANE, (2) XZ PLANE, (3) XY PLANE
C
      DIMENSION REFLEC(IA,JA)
```

```
C
C     WHETHER REFLECTION HAS BEEN CARRIED OUT ON A PARTICULAR SET OF
C     FOUR ATOMS AN ODD OR EVEN NUMBER OF TIMES IS REMEMBERED BY
C     PHITURN.
C     THIS IS ESSENTIAL SINCE EACH TIME A REFLECTION TAKES PLACE PHI IS
C     CONVERTED TO (360.0-PHI).
C
      COMMON PHITURN
C
C     EXTERNAL STATEMENT LISTS SUBROUTINE TO BE CALLED TO
C     SUBROUTINE FILLREFLEC.
C
      EXTERNAL MATSET
C
      PHITURN = -PHITURN
      CALL MATSET(REFLEC,3,3,1)
      IF(KK.EQ.2)GO TO 1
      IF(KK.EQ.3)GO TO 2
      REFLEC(1,1) = -REFLEC(1,1)
      GO TO 3
    1 CONTINUE
      REFLEC(2,2) = -REFLEC(2,2)
      GO TO 3
    2 CONTINUE
      REFLEC(3,3) = -REFLEC(3,3)
    3 CONTINUE
      RETURN
      END
C
      SUBROUTINE MATMUL(ARRAYA,ARRAYB,ARRAYC,IA,JA,IB,JB)
C
C     POST MULTIPLICATION OF ARRAYA BY ARRAYB TO GIVE ARRAYC.
C
      DIMENSION ARRAYA(IA,JA),ARRAYB(IB,JB),ARRAYC(IA,JB),TEMPRE(20,20)
      DO 3 I=1,IA
      DO 3 J=1,JA
      TEMPRE(I,J) = ARRAYA(I,J)
    3 CONTINUE
      DO 1 I=1,IA
      DO 1 J=1,JB
      CIJ = 0.0
      DO 2 K=1,JA
    2 CIJ = CIJ + TEMPRE(I,K) * ARRAYB(K,J)
    1 ARRAYC(I,J) = CIJ
      RETURN
      END
C
      SUBROUTINE MATSET(ARRAYA,IA,JA,K)
C
C     IF K EQUALS 0 THEN ALL ELEMENTS SET TO ZERO ONLY.
C     IF K EQUALS 1 THEN IDENTITY IS FORMED.
C
      DIMENSION ARRAYA(IA,JA)
      DO 1 I=1,IA
```

```
      DO 1 J=1,JA
    1 ARRAYA(I,J) = 0.0
      IF(K.EQ.0)GO TO 3
      DO 2 I=1,IA
    2 ARRAYA(I,I) = 1.0
    3 CONTINUE
      RETURN
      END
C
      SUBROUTINE FILLROT(ROTATE,ANGLE,KK)
C
C     THIS SUBROUTINE FILLS THE PRE-MULTIPYLING MATRIX REQUIRED TO
C     ROTATE A VECTOR THROUGH THE GIVEN ANGLE IN A GIVEN PLANE.
C     THE PLANE IS DECIDED BY THE VALUE OF KK.
C     (1) YZ PLANE, (2) XZ PLANE, (3) XY PLANE.
C
      DIMENSION ROTATE(3,3)
C
C     EXTERNAL STATEMENT LISTS SUBROUTINES TO BE CALLED TO
C     SUBROUTINE FILLROT.
C
      EXTERNAL MATSET
      CALL MATSET(ROTATE,3,3,1)
      RAD = 0.0174533
      ANGLE = ANGLE*RAD
      IF(KK.EQ.2)GO TO 1
      IF(KK.EQ.3)GO TO 2
      ROTATE(2,2) = COS(ANGLE)
      ROTATE(2,3) = SIN(ANGLE)
      ROTATE(3,2) = -SIN(ANGLE)
      ROTATE(3,3) = COS(ANGLE)
      GO TO 3
    1 CONTINUE
      ROTATE(1,1) = COS(ANGLE)
      ROTATE(1,3) = SIN(ANGLE)
      ROTATE(3,1) = -SIN(ANGLE)
      ROTATE(3,3) = COS(ANGLE)
      GO TO 3
    2 CONTINUE
      ROTATE(1,1) = COS(ANGLE)
      ROTATE(1,2) = SIN(ANGLE)
      ROTATE(2,1) = -SIN(ANGLE)
      ROTATE(2,2) = COS(ANGLE)
    3 CONTINUE
      RETURN
      END
C
      SUBROUTINE VECTANG(ARRAYA,ARRAYB,ANGLE)
C
C     THIS SUBROUTINE FINDS THE ANGLE IN DEGREES BETWEEN ANY TWO
C     VECTORS REPRESENTED IN THE SAME COORDINATE SYSTEM.
C
      DIMENSION ARRAYA(3,1), ARRAYB(3,1), ARRAYAT(1,3), A(1,1)
C
```

```
C     EXTERNAL STATEMENT LISTS SUBROUTINES TO BE CALLED TO
C     SUBROUTINE VECTANG.
C
      EXTERNAL MATRAN, MATMUL
C
      CALL MATRAN(ARRAYA,ARRAYAT,3,1)
      CALL MATMUL(ARRAYAT,ARRAYB,A,1,3,3,1)
      SCALARA = SQRT(ARRAYA(1,1)**2.Ø + ARRAYA(2,1)**2.Ø +
     2 ARRAYA(3,1)**2.Ø)
      SCALARB = SQRT(ARRAYB(1,1)**2.Ø + ARRAYB(2,1)**2.Ø +
     2 ARRAYB(3,1)**2.Ø)
      SCALSQ = SCALARA * SCALARB
      RAD = Ø.Ø174533
      ANGLE = (ACOS(A(1,1)/SCALSQ))/RAD
      RETURN
      END
C
      SUBROUTINE MATRAN(ARRAYA,ARRAYB,IA,JA)
C
C     FINDS THE TRANSPOSE OF A RECTANGULAR MATRIX ARRAYA.
C     NOTE - IF ARRAY IS ORTHOGONAL THEN ITS TRANSPOSE IS ITS INVERSE.
C
      DIMENSION ARRAYA(IA,JA), ARRAYB(JA,IA)
      DO 1 I=1,IA
      DO 1 J=1,JA
    1 ARRAYB(J,I) = ARRAYA(I,J)
      RETURN
      END
      FINISH
```

DATA

NSETS = 1

NCONF = 1

N = 8

ATOM COORDINATES

ATOM NO.	X	Y	Z
Ø	1.82740	-Ø.37510	Ø.11650
1	1.09000	-1.84830	-Ø.04530
2	-Ø.29460	-1.76300	-Ø.93490
3	-1.76780	-1.04970	-Ø.96730
4	-1.82740	Ø.37510	-Ø.11780
5	-1.09000	1.84830	Ø.04660
6	Ø.29460	1.76300	Ø.93820
7	1.76780	1.05000	Ø.96400

RESULTS

BOND NUMBER	PHIS (DEGREES)
1	127.Ø6
2	259.34
3	120.21
4	204.16
5	233.14
6	100.63
7	239.99
8	155.46

Program 7 Calculation of the Molecular Polarizability Tensor and the Square of the Optical Anisotropy for each Conformation of a Polymer Chain.

This computer program is analogous to Program 1 which transforms and sums group dipole moment vectors to form a molecular dipole moment vector. This program reads group polarizability tensors, together with geometrical data, and transforms and sums these tensors to form the molecular polarizability tensor. The square of the optical anisotropy may then be calculated from this molecular polarizability tensor. Facilities are available in the program to perform these calculations on several different conformations of a polymer chain, and by reading their respective statistical weights the mean-square optical anisotropy averaged over all these conformations may be produced.

The sample output following this program is a calculation of the molecular polarizability tensors and the square of the optical anisotropy for each conformation of n-pentane. The bond anisotropies of the C-C and C-H bonds calculated by Denbigh[214] have been used to construct the group polarizability tensors[194]. The statistical weights of each conformation have also been input to enable the mean-square optical anisotropy over all conformations to be calculated. The value so produced agrees well with the corresponding value calculated by an implicit matrix method in the following program, and with the value calculated by Ishikawa and Nagai[198]. All squares of the optical anisotropies are expressed as $\gamma^2(\times 10^{50}/cm^6)$.

```
C
      MASTER ALPHAADD
C
C     THIS PROGRAM CALCULATES THE MOLECULAR POLARIZABILITY
C     TENSOR AND THE SQUARE OF THE OPTICAL ANISOTROPY (GAMMA) FOR EACH
C     CONFORMATION OF A POLYMER CHAIN .
C     THE BOND POLARISABILITY TENSOR (ALPHA), THE BOND ANGLE
C     SUPPLEMENT (THETA) AND THE DIHEDRAL ANGLE (PHI) ARE FIRST READ IN
C     AND THE APPROPRIATE TRANSFORMING AND SUMMING PROCEDURES ARE
C     CARRIED OUT TO PRODUCE GAMMA SQUARED.
C     BY READING IN THE CONFORMATIONAL STATISTICAL WEIGHTS, THESE GAMMA
C     SQUARES MAY THEN BE COMBINED TO PRODUCE THE STATISTICAL MECHANICAL
C     AVERAGE OF THE SQUARED OPTICAL ANISOTROPY FOR THE CHAIN MOLECULE
C     OVER ALL CONFORMATIONS.
C
C     FOR LONG POLYMER CHAINS IT IS MORE CONVENIENT TO USE THE MATRIX
C     METHODS DEVELOPED BY FLORY TO PRODUCE THE AVERAGE SQUARED OPTICAL
C     ANISOTROPY. - SEE PROGRAM 'LITESCAT'.
C
C       *** CALLS SUBROUTINES ***
C     MATSET,FILLTR,MATMUL,MATADD,MATEQU,MATRAN
C
      DIMENSION ALPHASUM(3,3), TEMP(3,3), TEMP1(3,3), TEMP2(3,3),
     2 TEMPT(3,3), TR(3,3), TRT(3,3), TRPROD(3,3), TRTPROD(3,3),
     3 ALPHA(3,3), ALPHASUMT(3,3), GAMMA(9,1), GAMMAT(1,9), GSQ(1,1)
      INTEGER CONFNO,ARPHI(100)
C
C     READ NUMBER OF CONFORMATIONS.
C
      READ(1,100)NCONFS
  100 FORMAT(I0)
C
C     READ NUMBER OF BACKBONE BONDS.
C
      READ(1,200)N
  200 FORMAT(I0)
C
C     WRITE OUT FIRST HEADINGS AND DATA.
C
      WRITE(2,220)
  220 FORMAT(/,10X,'DATA',/,10X,'----')
      WRITE(2,240)NCONFS
  240 FORMAT(/,10X,'NCONFS =',I6)
      WRITE(2,260)N
  260 FORMAT(/,10X,'N =',I6)
C
C     INITIALISE VARIABLES
C
      STATWSUM = 0.0
      ICOUNT = 0
      SWGS = 0.0
    1 CONTINUE
      RAD = 0.0174532925199432957
C
```

```
C     READ THE TENSOR OF THE FIRST BOND INTO 'ALPHASUM'.
C
      READ(1,300)((ALPHASUM(I,J),J=1,3),I=1,3)
  300 FORMAT(3F0.0)
      CALL MATSET(TRPROD,3,3,1)
      CALL MATSET(TRTPROD,3,3,1)
C
C     MAIN DO LOOP STARTS HERE.
C
      DO 99 II=1,N
C
C     READ IN NUBETTA AND NUANGS.
C
      READ(1,370)NUBETTA,NUANGS
  370 FORMAT(2I0)
      IF(NUBETTA.EQ.0)GO TO 11
C
C     READ IN TENSOR FOR (II)TH BOND.
C
      READ(1,400)((ALPHA(I,J),J=1,3),I=1,3)
  400 FORMAT(3F0.0)
   11 CONTINUE
      IF(NUANGS.EQ.0)GO TO 22
C
C     READ IN SUPPLEMENTARY BOND ANGLE THETA AND DIHEDRAL ANGLE PHI.
C
      READ(1,500)THETA,PHI
  500 FORMAT(2F0.0)
      THETA = THETA * RAD
      ARPHI(II) = IFIX(PHI)
      PHI = PHI * RAD
   22 CONTINUE
C
C     FORM SERIAL PRODUCTS OF TRANSFORMATION MATRICES AND TRANSFORM
C     (II)TH TENSOR INTO COORDINATE SYSTEM OF FIRST BOND.
C
      CALL FILLTR(THETA,PHI,TR)
      CALL MATMUL(TRPROD,TR,TEMP,3,3,3,3)
      CALL MATRAN(TR,TRT,3,3)
      CALL MATMUL(TRT,TRTPROD,TEMPT,3,3,3,3)
      CALL MATEQU(TRPROD,TEMP,3,3)
      CALL MATEQU(TRTPROD,TEMPT,3,3)
      CALL MATMUL(TRPROD,ALPHA,TEMP1,3,3,3,3)
      CALL MATMUL(TEMP1,TRTPROD,TEMP2,3,3,3,3)
      CALL MATADD(ALPHASUM,TEMP2,ALPHASUM,3,3)
   99 CONTINUE
C
C     FORM THE SQUARE OF THE OPTICAL ANISOTROPY OF THIS CONFORMATION.
C
      GAMMASQ = 0.5*(((ALPHASUM(1,1)-ALPHASUM(2,2))**2) +
     2 ((ALPHASUM(1,1)-ALPHASUM(3,3))**2) +
     3 ((ALPHASUM(2,2)-ALPHASUM(3,3))**2)) +
     4 3.0*((ALPHASUM(1,2)**2) + (ALPHASUM(1,3)**2) +
     5  (ALPHASUM(2,3)**2))
```

```
C
C     READ IN STATISTICAL WEIGHT OF THIS CONFORMATION.
C
      READ(1,550)STATW
  550 FORMAT(F0.0)
C
C     WRITE OUT DATA AND RESULTS FOR (II)TH CONFORMATION.
C
      CONFNO = ICOUNT + 1
      WRITE(2,600)CONFNO
  600 FORMAT(///,10X,'*** DATA AND RESULTS FOR CONFORMATION ',
     2 'NUMBER',I6,' ***',/)
      WRITE(2,605)(ARPHI(I),I=1,N)
  605 FORMAT(10X,'CONFORMATION :',100I4)
      WRITE(2,610)
  610 FORMAT(/,10X,'OPTICAL POLARISABILITY TENSOR')
      WRITE(2,620)((ALPHASUM(I,J),J=1,3),I=1,3)
  620 FORMAT(10X,3E14.5)
      WRITE(2,630)GAMMASQ
  630 FORMAT(/,10X,'SQUARE OF THE OPTICAL ANISOTROPY =',E14.5)
      WRITE(2,640)STATW
  640 FORMAT(/,10X,'STATISTICAL WEIGHT =',F14.5)
C
C     START TO FORM THE PARTITION FUNCTION.
C
      STATWSUM = STATWSUM + STATW
C
C     START TO FORM THE STATISTICALLY WEIGHTED SUM OF THE SQUARE OF
C     THE OPTICAL ANISOTROPY.
C
      SWGS = SWGS + (GAMMASQ*STATW)
      ICOUNT = ICOUNT + 1
C
C     RETURN TO START NEXT CONFORMATION.
C
      IF(ICOUNT.NE.NCONFS)GO TO 1
C
C     ON COMPLETION OF ALL CONFORMATIONS COMPUTE THE MEAN SQUARED
C     AVERAGE OF THE OPTICAL ANISOTROPY.
C
      GAMMASQ = SWGS/STATWSUM
C
C     WRITE OUT THE MEAN RESULTS OVER ALL CONFORMATIONS.
C
      WRITE(2,700)
  700 FORMAT(/////,10X,'*** MEAN RESULTS OVER ALL CONFORMATIONS ***')
      WRITE(2,720)STATWSUM
  720 FORMAT(/,10X,'PARTITION FUMCTION =',E14.5)
      WRITE(2,740)SWGS
  740 FORMAT(/,10X,'SUM OF THE WEIGHTED GAMMA SQUARES =',E14.5)
      WRITE(2,760)GAMMASQ
  760 FORMAT(//,10X,'THE AVERAGE MEAN SQUARE OPTICAL ANISOTROPY ',
     2 /,10X,'OVER ALL CONFORMATIONS IS',//,30X,E14.5)
      STOP
```

```
      END
C
      SUBROUTINE MATSET (ARRAYA,IA,JA,K)
C
C     IF K EQUALS Ø THEN ALL ELEMENTS SET TO ZERO ONLY.
C     IF K EQUALS 1 THEN IDENTITY IS FORMED
C
      DIMENSION ARRAYA(IA,JA)
      DO 1 I=1,IA
      DO 1 J=1,JA
    1 ARRAYA(I,J) = Ø.Ø
      IF (K.EQ.Ø) GO TO 3
      DO 2 I=1,IA
    2 ARRAYA(I,I) = 1.Ø
    3 CONTINUE
      RETURN
      END
C
      SUBROUTINE FILLTR(THETA,PHI,TR)
C
C     FILLS ORTHOGONAL MATRIX REQUIRED FOR TRANSFORMING VECTOR FROM
C     ONE CARTESIAN COORDINATE SYSTEM TO ANOTHER.
C     ANGLES THETA (BOND ANGLE SUPPLEMENTS) AND PHI (DIHEDRAL ANGLE)
C     MUST BE EXPRESSED IN RADIANS.
C
      DIMENSION TR(3,3)
      COST = COS(THETA)
      SINT = SIN(THETA)
      COSP = COS(PHI)
      SINP = SIN(PHI)
      TR(1,1) = COST
      TR(1,2) = SINT
      TR(1,3) = Ø.Ø
      TR(2,1) = SINT*COSP
      TR(2,2) = -COST*COSP
      TR(2,3) = SINP
      TR(3,1) = SINT*SINP
      TR(3,2) = -COST*SINP
      TR(3,3) = -COSP
      RETURN
      END
C
      SUBROUTINE MATMUL(ARRAYA,ARRAYB,ARRAYC,IA,JA,IB,JB)
C
C     POSTMULTIPLICATION OF ARRAYA BY ARRAYB TO GIVE ARRAYC.
C
      DIMENSION ARRAYA(IA,JA),ARRAYB(JA,JB),ARRAYC(IA,JB)
      DO 1 I=1,IA
      DO 1 J=1,JB
      CIJ = Ø.Ø
      DO 2 K=1,JA
    2 CIJ = CIJ + ARRAYA(I,K) * ARRAYB(K,J)
    1 ARRAYC(I,J) = CIJ
      RETURN
```

```
      END
C
      SUBROUTINE MATADD(ARRAYA,ARRAYB,ARRAYC,IA,JA)
C
C     ADDS TWO MATRICES ARRAYA AND ARRAYB TO GIVE ARRAYC.
C
      DIMENSION ARRAYA(IA,JA),ARRAYB(IA,JA),ARRAYC(IA,JA)
      DO 1 I=1,IA
      DO 1 J=1,JA
    1 ARRAYC(I,J) = ARRAYA(I,J) + ARRAYB(I,J)
      RETURN
      END
C
      SUBROUTINE MATEQU(ARRAYA,ARRAYB,IA,JA)
C
C     MATRIX A BECOMES EQUAL TO MATRIX B.
C
      DIMENSION ARRAYA(IA,JA),ARRAYB(IA,JA)
      DO 1 I=1,IA
      DO 1 J=1,JA
    1 ARRAYA(I,J) = ARRAYB(I,J)
      RETURN
      END
C
      SUBROUTINE MATRAN (ARRAYA, ARRAYB, IA, JA)
C
C     FINDS THE TRANSPOSE OF A RECTANGULAR MATRIX ARRAYA.
C     NOTE - IF ARRAY IS ORTHOGONAL THEN ITS TRANSPOSE IS ITS INVERSE.
C
      DIMENSION ARRAYA(IA,JA),ARRAYB(JA,IA)
      DO 1 I=1,IA
      DO 1 J=1,JA
    1 ARRAYB(J,I) = ARRAYA(I,J)
      RETURN
      END
      FINISH
```

```
DATA
----

NCONFS =      9

N =      4


*** DATA AND RESULTS FOR CONFORMATION NUMBER      1 ***

CONFORMATION :   Ø   Ø   Ø   Ø

OPTICAL POLARISABILITY TENSOR
   Ø.11735E Ø3   Ø.10221E Ø2   Ø.00000E ØØ
   Ø.10221E Ø2   Ø.10909E Ø3   Ø.00000E ØØ
   Ø.00000E ØØ   Ø.00000E ØØ   Ø.84353E Ø2

SQUARE OF THE OPTICAL ANISOTROPY =   Ø.11981E Ø4

STATISTICAL WEIGHT =        1.00000


*** DATA AND RESULTS FOR CONFORMATION NUMBER      2 ***

CONFORMATION :   Ø   Ø 120   Ø

OPTICAL POLARISABILITY TENSOR
   Ø.11735E Ø3   Ø.26098E Ø1   Ø.43942E Ø1
   Ø.26098E Ø1   Ø.99814E Ø2  -Ø.53580E Ø1
   Ø.43942E Ø1  -Ø.53580E Ø1   Ø.93634E Ø2

SQUARE OF THE OPTICAL ANISOTROPY =   Ø.61872E Ø3

STATISTICAL WEIGHT =        Ø.43000


*** DATA AND RESULTS FOR CONFORMATION NUMBER      3 ***

CONFORMATION :   Ø   Ø 240   Ø

OPTICAL POLARISABILITY TENSOR
   Ø.11735E Ø3   Ø.26098E Ø1  -Ø.43942E Ø1
   Ø.26098E Ø1   Ø.99814E Ø2   Ø.53580E Ø1
  -Ø.43942E Ø1   Ø.53580E Ø1   Ø.93634E Ø2

SQUARE OF THE OPTICAL ANISOTROPY =   Ø.61872E Ø3

STATISTICAL WEIGHT =        Ø.43000
```

*** DATA AND RESULTS FOR CONFORMATION NUMBER 4 ***

CONFORMATION : Ø 12Ø Ø Ø

OPTICAL POLARISABILITY TENSOR

Ø.1Ø4Ø2E Ø3	Ø.78891E Ø1	Ø.32958E Ø1
Ø.78891E Ø1	Ø.11316E Ø3	-Ø.61389E Ø1
Ø.32958E Ø1	-Ø.61389E Ø1	Ø.93629E Ø2

SQUARE OF THE OPTICAL ANISOTROPY = Ø.61871E Ø3

STATISTICAL WEIGHT = Ø.43ØØØ

*** DATA AND RESULTS FOR CONFORMATION NUMBER 5 ***

CONFORMATION : Ø 12Ø Ø Ø

OPTICAL POLARISABILITY TENSOR

Ø.1Ø325E Ø3	Ø.1Ø88ØE Ø1	-Ø.29692E ØØ
Ø.1Ø88ØE Ø1	Ø.1Ø335E Ø3	-Ø.79305E ØØ
-Ø.29692E ØØ	-Ø.79305E ØØ	Ø.1Ø42ØE Ø3

SQUARE OF THE OPTICAL ANISOTROPY = Ø.65301E Ø1

STATISTICAL WEIGHT = Ø.1849Ø

*** DATA AND RESULTS FOR CONFORMATION NUMBER 6 ***

CONFORMATION : Ø 12Ø 24Ø Ø

OPTICAL POLARISABILITY TENSOR

Ø.11630E Ø3	Ø.15682E Ø1	Ø.4Ø973E Ø1
Ø.15682E Ø1	Ø.1ØØ83E Ø3	-Ø.61510E Ø1
Ø.4Ø973E Ø1	-Ø.61510E Ø1	Ø.93671E Ø2

SQUARE OF THE OPTICAL ANISOTROPY = Ø.57268E Ø3

STATISTICAL WEIGHT = Ø.ØØ277

*** DATA AND RESULTS FOR CONFORMATION NUMBER 7 ***

CONFORMATION : Ø 24Ø Ø Ø

OPTICAL POLARISABILITY TENSOR

Ø.1Ø4Ø2E Ø3	Ø.78875E Ø1	-Ø.32934E Ø1
Ø.78875E Ø1	Ø.11316E Ø3	Ø.61380E Ø1
-Ø.32934E Ø1	Ø.61380E Ø1	Ø.93634E Ø2

```
SQUARE OF THE OPTICAL ANISOTROPY =    Ø.61844E Ø3

STATISTICAL WEIGHT =          Ø.43ØØØ


*** DATA AND RESULTS FOR CONFORMATION NUMBER      8 ***

CONFORMATION :    Ø 24Ø 12Ø   Ø

OPTICAL POLARISABILITY TENSOR
   Ø.11630E Ø3    Ø.15682E Ø1  -Ø.40973E Ø1
   Ø.15682E Ø1    Ø.1ØØ83E Ø3   Ø.61510E Ø1
  -Ø.40973E Ø1    Ø.61510E Ø1   Ø.93671E Ø2

SQUARE OF THE OPTICAL ANISOTROPY =    Ø.57268E Ø3

STATISTICAL WEIGHT =          Ø.ØØ277


*** DATA AND RESULTS FOR CONFORMATION NUMBER      9 ***

CONFORMATION :    Ø 24Ø 12Ø   Ø

OPTICAL POLARISABILITY TENSOR
   Ø.1Ø325E Ø3    Ø.1Ø88ØE Ø1   Ø.29692E ØØ
   Ø.1Ø88ØE Ø1    Ø.1Ø335E Ø3   Ø.79305E ØØ
   Ø.29692E ØØ    Ø.79305E ØØ   Ø.1Ø42ØE Ø3

SQUARE OF THE OPTICAL ANISOTROPY =    Ø.653Ø1E Ø1

STATISTICAL WEIGHT =          Ø.1849Ø


*** MEAN RESULTS OVER ALL CONFORMATIONS ***

PARTITION FUMCTION =    Ø.3Ø953E Ø1

SUM OF THE WEIGHTED GAMMA SQUARES =    Ø.22677E Ø4


THE AVERAGE MEAN SQUARE OPTICAL ANISOTROPY
OVER ALL CONFORMATIONS IS

                        Ø.73263E Ø3
```

Program 8 Calculation of the Mean-Square Optical Anisotropy over all Conformations of a Polymer Chain.

Implicit matrix methods, analogous to those for the calculation of the mean-square dipole moment or end-to-end distance of a polymer, are available to calculate the mean-square optical anisotropy of a polymer chain molecule[194]. This computer program employs these matrix methods to evaluate Equation 8.7.

The sample output following this program is the result of the calculation of mean-square optical anisotropy, $\langle\gamma^2\rangle(x10^{50}/cm^6)$, of n-alkane chains having n = 1 to n = 30 skeletal bonds. The bond anisotropies calculated by Denbigh[214] were used for this purpose, and the results agree well with those calculated by Ishikawa and Nagai[198]. The discrepancy between these results and those presented by Jernigan and Flory[194] has been discussed in Section 8.04.

```
C
      MASTER LITESCAT
C
C     THIS PROGRAM CALCULATES THE STATISTICAL MECHANICAL
C     AVERAGE OF THE SQUARED OPTICAL ANISOTROPY FOR CHAIN
C     MOLECULES AVERAGED OVER ALL CONFORMATIONS.
C     MATRIX FORMULATION IS USED THROUGHOUT (SEE R.L.JERNIGAN
C     AND P.J.FLORY, J.CHEM.PHYS., VOL.47, P1999, (1967) ).
C
C     EACH ROTATABLE SKELETAL BOND OF THE CHAIN BACKBONE IS
C     ASSIGNED A LOCAL REFERENCE CARTESIAN COORDINATE
C     SYSTEM. GROUP ELECTRO-OPTICAL POLARIZABILITIES
C     REPRESENTED IN THIS COORDINATE SYSTEM ARE ASSUMED
C     TO BE INVARIANT TO CONFORMATIONAL CHANGES.
C
C     THE PROGRAM INPUTS ROTATIONAL STATISTICAL WEIGHTS AND
C     FORMS U FOR EACH ROTATABLE SKELETAL BOND.
C     FOR A ROTATIONAL ISOMERIC STATE MODEL (T,G+,G-) THE
C     DIMENSIONS OF U WILL BE 3X3. ADDITIONAL DATA ARE BOND
C     ANGLE SUPPLEMENTS, DIHEDRAL ANGLES AND GROUP ELECTRO-
C     OPTICAL POLARIZABILITY TENSORS.
C
C           *** CALLS THE SUBROUTINES ***
C     MATSET,FILLMATU,FILLBETA,SCALMUL,MATADD,FILLTR,FILLP,
C     MATKRO,MATMUL,MATEQU
C
      DIMENSION UTEMP(3,3),UPROD(3,3),THETA(100),BETA(3,3)
      REAL PTEMP(33,33),PPROD(33,33),PMAT(33,33)
      COMMON U(3,3),GAMMA(9,1),GAMMAT(1,9),E9(9,9),T1(3,3),
     2 T2(3,3),T3(3,3)
C
C     READ NUMBER OF SETS OF DATA.
C
      READ(1,100)NSETS
  100 FORMAT(I0)
      ICOUNT = 0
    1 CONTINUE
C
C     READ NUMBER OF BACKBONE BONDS.
C
      READ(1,200)N
  200 FORMAT(I0)
C
C     READ DELTA ALPHA C-C AND DELTA ALPHA C-H.
C
      READ(1,250)DACC,DACH
  250 FORMAT(2F0.0)
C
C     WRITE OUT FIRST HEADINGS AND DATA.
C
      WRITE(2,300)
  300 FORMAT(/,10X,'DATA',/,10X,'----')
      WRITE(2,400)NSETS
  400 FORMAT(/,10X,'NSETS =',I6)
```

```
      WRITE(2,500)N
  500 FORMAT(/,10X,'N =',I6)
C
C     INITIALISE VARIABLES AND ARRAYS.
C
      RAD = 0.0174532925199432957
      CALL MATSET(E9,9,9,1)
      CALL MATSET(PTEMP,33,33,1)
      CALL MATSET(UTEMP,3,3,1)
      NPLUS1 = N+1
C
C     BEGIN MAIN DO LOOP TO CONSTRUCT SERIAL PRODUCT OF
C     P MATRICES.
C
      DO 3 II=1,NPLUS1
C
C     READ NUSW, NUGAM, NUTHET AND NUPHI.
C
      READ(1,600)NUSW,NUGAM,NUTHET,NUPHI
  600 FORMAT(4I0)
      IF(NUSW.EQ.0)GO TO 11
C
C     READ IN STATISTICAL WEIGHTS AND FILL MATRIX U FOR
C     (II)TH BOND.
C     IF NUSW EQUALS 2 THEN U IS FILLED AS AN IDENTITY.
C
      IF(NUSW.NE.2)GO TO 77
      CALL MATSET(U,3,3,1)
      GO TO 11
   77 CONTINUE
      READ(1,650)SIG,CPHI,OMEG
  650 FORMAT(3F0.0)
      CALL FILLMATU(SIG,CPHI,OMEG,U)
   11 CONTINUE
      IF(NUGAM.EQ.0)GO TO 22
C
C     READ IN THETA(1), XI AND PHI.
C     FILL TRACELESS BOND POLARISABILITY TENSOR BETA.
C
      IF(II.NE.1)GO TO 111
      READ(1,660)THETA(1),XI,PSI
  660 FORMAT(3F0.0)
      THETA(1) = THETA(1)*RAD
      XI = XI*RAD
      PSI = PSI*RAD
      CALL FILLBETA(DACC,DACH,THETA(1),XI,PSI,BETA,1)
      GO TO 333
  111 CONTINUE
      IF(II.EQ.NPLUS1)GO TO 222
      READ(1,670)PSI
  670 FORMAT(F0.0)
      PSI = PSI*RAD
      CALL FILLBETA(DACC,DACH,THETA(II),0.0,PSI,BETA,2)
      GO TO 333
```

```
  222 CONTINUE
      READ(1,680)XI,PSI
  680 FORMAT(2F0.0)
      XI = XI*RAD
      PSI = PSI*RAD
      CALL FILLBETA(DACC,DACH,0.0,XI,PSI,BETA,3)
  333 CONTINUE
C
C     FILL COLUMN AND ROW FORMS OF GAMMA FROM BETA.
C
      DO 2 I=1,3
      DO 2 J=1,3
      K = (I-1)*3 + J
      GAMMA(K,1) = BETA(I,J)
      GAMMAT(1,K) = BETA(I,J)
    2 CONTINUE
   22 CONTINUE
      THETA(II+1) = THETA(II)
      IF(NUTHET.EQ.0)GO TO 33
C
C     READ BOND ANGLE SUPPLEMENT THETA.
C
      READ(1,700)THETA(II+1)
  700 FORMAT(F0.0)
   33 CONTINUE
      IF(NUPHI.EQ.0)GO TO 44
C
C     READ DIHEDRAL ANGLES PHI.
C
      READ(1,800)PHI1,PHI2,PHI3
  800 FORMAT(3F0.0)
   44 CONTINUE
C
C     WRITE OUT DATA FOR (II)TH BOND.
C
      WRITE(2,1050)II
 1050 FORMAT(/,10X,'*** DATA FOR BOND',I3,' ***',/)
      WRITE(2,900)NUSW,NUGAM,NUTHET,NUPHI
  900 FORMAT(/,10X,'NUSW, NUGAM, NUTHET',/10X,
     2 'AND NUPHI ARE RESPECTIVELY',4I6)
      WRITE(2,1060)
 1060 FORMAT(/,10X,'STATISTICAL WEIGHT MATRIX',14X,
     2 'TRACELESS TENSOR X E-25',/)
      DO 8 I=1,3
    8 WRITE(2,50)U(I,1),U(I,2),U(I,3),BETA(I,1),BETA(I,2),
     2 BETA(I,3)
   50 FORMAT(/,10X,3F10.4,10X,3E14.5)
      WRITE(2,1070)THETA(II+1),PHI1,PHI2,PHI3
 1070 FORMAT(/,10X,'GEOMETRICAL DATA... THETA=',F10.4,5X,
     2 'PHI1=',F10.4,
     2 5X,'PHI2=',F10.4,5X,'PHI3=',F10.4)
      IF(NUPHI.EQ.0)GO TO 55
      PHI1 = PHI1*RAD
      PHI2 = PHI2*RAD
```

```
      PHI3 = PHI3*RAD
   55 CONTINUE
      IF(NUTHET.EQ.Ø)GO TO 66
      THETA(II+1) = THETA(II+1)*RAD
   66 CONTINUE
C
C     FILL TRANSFORMATION MATRICES.
C
      CALL FILLTR(THETA(II+1),PHI1,T1)
      CALL FILLTR(THETA(II+1),PHI2,T2)
      CALL FILLTR(THETA(II+1),PHI3,T3)
C
C     FILL PMAT AND FORM SERIAL PRODUCT OF THIS AND THE
C     STATISTICAL WEIGHT MATRIX U.
C
      CALL FILLP(PMAT)
      CALL MATMUL(PTEMP,PMAT,PPROD,33,33,33,33)
      CALL MATMUL(UTEMP,U,UPROD,3,3,3,3)
      CALL MATEQU(PTEMP,PPROD,33,33)
      CALL MATEQU(UTEMP,UPROD,3,3)
C
C     END OF MAIN DO LOOP.
C
    3 CONTINUE
C
C     FORM THE CONFORMATIONAL PARTITION FUNCTION Z.
C
      Z = UPROD(1,1) + UPROD(1,2) + UPROD(1,3)
C
C     NOTE THAT ONLY ELEMENTS (1,31),(1,32) AND (1,33) OF
C     PPROD ARE REQUIRED.
C
      TEMP = PPROD(1,31) + PPROD(1,32) + PPROD(1,33)
      ANISOT = 2*TEMP/Z
      WRITE(2,1Ø8Ø)ANISOT
 1Ø8Ø FORMAT(/,1ØX,'STATISTICAL MECHANICAL AVERAGE OF THE ',
     2 'SQUARE OF THE OPTICAL',/,1ØX,'ANISTROPY ',
     3 '(GAMMA SQUARED) X E-5Ø IS',//,3ØX,E14.5)
      GOVERN = ANISOT/N
      WRITE(2,11ØØ)GOVERN
 11ØØ FORMAT(//,1ØX,'GAMMA SQUARED X E-5Ø / NUMBER OF',
     2 ' BACKBONE BONDS IS',//,3ØX,E14.5)
C
      ICOUNT = ICOUNT + 1
      IF(ICOUNT.NE.NSETS)GO TO 1
C
      STOP
      END
C
      SUBROUTINE MATSET(ARRAYA,IA,JA,K)
C
C     IF K EQUALS Ø THEN ALL ELEMENTS SET TO ZERO ONLY.
C     IF K EQUALS 1 THEN IDENTITY IS FORMED.
C
```

```
      DIMENSION ARRAYA(IA,JA)
C
      DO 1 I=1,IA
      DO 1 J=1,JA
    1 ARRAYA(I,J) = 0.0
      IF(K.EQ.0) GO TO 3
      DO 2 I=1,IA
    2 ARRAYA(I,I) = 1.0
    3 CONTINUE
      RETURN
      END
C
      SUBROUTINE FILLMATU (SIG, CPHI, OMEG, ARRAYU)
C
C     THIS SUBROUTINE FILLS THE STATISTICAL WEIGHT MATRIX U
C     WITH THE RELEVANT VALUES OF SIGMA, CAPITAL PHI AND
C     OMEGA.
C
      DIMENSION ARRAYU(3,3)
      ARRAYU(1,1) = 1.0
      ARRAYU(1,2) = SIG
      ARRAYU(1,3) = SIG
      ARRAYU(2,1) = 1.0
      ARRAYU(2,2) = SIG * CPHI
      ARRAYU(2,3) = SIG * OMEG
      ARRAYU(3,1) = 1.0
      ARRAYU(3,2) = SIG * OMEG
      ARRAYU(3,3) = SIG * CPHI
      RETURN
      END
C
      SUBROUTINE FILLBETA(DACC,DACH,THETA,XI,PSI,BETA,K)
C
C     THIS SUBROUTINE FILLS THE 3*3 TRACELESS TENSOR BETA
C     FOR THE N-ALKANE CHAINS USING THE MATRICES DERIVED BY
C     R.L.JERNIGAN AND P.J.FLORY, J.CHEM.PHYS., VOL.47,
C     P1999, (1967).
C
C     IF K EQUALS 1 THEN TENSOR FOR BOND ONE IS FILLED.
C     IF K EQUALS 2 THEN TENSOR FOR BOND I IS FILLED.
C     IF K EQUALS 3 THEN TENSOR FOR BOND N+1 IS FILLED.
C
      DIMENSION BETA(3,3),AA(3,3),BB(3,3)
C
      CALL MATSET(BETA,3,3,0)
      CALL MATSET(AA,3,3,0)
      CALL MATSET(BB,3,3,0)
      COST = COS(THETA)
      SINT = SIN(THETA)
      COSTSQ = COST**2.0
      SINTSQ = SINT**2.0
      COSX = COS(XI)
      SINX = SIN(XI)
      COSXSQ = COSX**2.0
```

```
      SINXSQ = SINX**2.Ø
      COSPSISQ = COS(PSI)**2.Ø
      SINPSISQ = SIN(PSI)**2.Ø
      THIRD = 1.Ø/3.Ø
      IF(K.NE.1)GO TO 11
      AA(1,1) = (2.Ø*THIRD*DACC)+(2.Ø*((COSXSQ*COSPSISQ)-
     2 THIRD)*DACH)
      AA(1,2) = -2.Ø*(SINX*COSX*COSPSISQ)*DACH
      AA(2,1) = AA(1,2)
      AA(2,2) = (-THIRD*DACC)+(2.Ø*((SINXSQ*COSPSISQ)-THIRD)
     2 *DACH)
      AA(3,3) = (-THIRD*DACC)+(2.Ø*(SINPSISQ-THIRD)*DACH)
      S = SQRT(1.5)
      CALL SCALMUL(AA,S,AA,3,3)
      BB(1,1) = COSTSQ-THIRD
      BB(1,2) = SINT*COST
      BB(2,1) = BB(1,2)
      BB(2,2) = SINTSQ-THIRD
      BB(3,3) = -THIRD
      S = SQRT(1.5)*DACH
      CALL SCALMUL(BB,S,BB,3,3)
      CALL MATADD(AA,BB,BETA,3,3)
      GO TO 33
   11 CONTINUE
      IF(K.NE.2)GO TO 22
      AA(1,1) = (2.Ø*THIRD*DACC)+((((1.Ø-COST)*COSPSISQ)-
     2 (2.Ø*THIRD))*DACH)
      AA(1,2) = -((SINT*COSPSISQ)*DACH)
      AA(2,1) = AA(1,2)
      AA(2,2) = (-THIRD*DACC)+((((1.Ø+COST)*COSPSISQ)-
     2 (2.Ø*THIRD))*DACH)
      AA(3,3) = (-THIRD*DACC)+(2.Ø*(SINPSISQ-THIRD)*DACH)
      S = SQRT(1.5)
      CALL SCALMUL(AA,S,BETA,3,3)
      GO TO 33
   22 CONTINUE
      AA(1,1) = COSXSQ*COSPSISQ
      AA(1,2) = -SINX*COSX*COSPSISQ
      AA(2,1) = AA(1,2)
      AA(2,2) = (SINXSQ*COSPSISQ)-Ø.5
      AA(3,3) = SINPSISQ-Ø.5
      S = SQRT(6.Ø)*DACH
      CALL SCALMUL(AA,S,BETA,3,3)
   33 CONTINUE
      RETURN
      END
C
      SUBROUTINE SCALMUL (ARRAYA,S,ARRAYB,IA,JA)
C
C     MULTIPLIES ARRAYA BY A SCALAR S TO GIVE ARRAYB.
C
      DIMENSION ARRAYA(IA,JA),ARRAYB(IA,JA)
      DO 1 I=1,IA
      DO 1 J=1,JA
```

```
      ARRAYB(I,J) = S * ARRAYA(I,J)
    1 CONTINUE
      RETURN
      END
C
      SUBROUTINE MATADD(ARRAYA,ARRAYB,ARRAYC,IA,JA)
C
C     ADDS TWO MATRICES ARRAYA AND ARRAYB TO GIVE ARRAYC.
C
      DIMENSION ARRAYA(IA,JA),ARRAYB(IA,JA),ARRAYC(IA,JA)
      DO 1 I=1,IA
      DO 1 J=1,JA
    1 ARRAYC(I,J) = ARRAYA(I,J) + ARRAYB(I,J)
      RETURN
      END
C
      SUBROUTINE FILLTR(THETA,PHI,TR)
C
C     FILLS ORTHOGONAL MATRIX REQUIRED FOR TRANSFORMING
C     VECTOR FROM ONE CARTESIAN COORDINATE SYSTEM TO ANOTHER.
C     ANGLES THETA (BOND ANGLE SUPPLEMENT) AND PHI (DIHEDRAL
C     ANGLE) MUST BE EXPRESSED IN RADIANS.
C
      DIMENSION TR(3,3)
C
      COST = COS(THETA)
      SINT = SIN(THETA)
      COSP = COS(PHI)
      SINP = SIN(PHI)
      TR(1,1) = COST
      TR(1,2) = SINT
      TR(1,3) = Ø.Ø
      TR(2,1) = SINT*COSP
      TR(2,2) = -COST*COSP
      TR(2,3) = SINP
      TR(3,1) = SINT*SINP
      TR(3,2) = -COST*SINP
      TR(3,3) = -COSP
      RETURN
      END
C
      SUBROUTINE FILLP(PMAT)
C
C     THIS SUBROUTINE IS REQUIRED FOR THE CALCULATION OF
C     THE SQUARE OF THE OPTICAL ANISOTROPY OF A CHAIN
C     MOLECULE AVERAGED OVER ALL CONFORMATIONS.
C     THE SUBROUTINE FILLS A 33*33 MATRIX PMAT WITH
C     INFORMATION RELATING TO A REPEAT UNIT OR SKELETAL BOND
C     SUCH AS CONFORMATIONAL PROBABILITIES, ELECTRO-OPTICAL
C     POLARIZABILITY TENSORS AND LOCAL GEOMETRY.
C
      REAL PMAT(33,33)
      DIMENSION ARRAYA(3,27),ARRAYB(27,27),ARRAYC(3,27),
     2 ARRAYD(9,9),ARRAYE(27,3),ARRAYF(27,27),TDPT(27,27),
```

```
     3 GAMSQ(1,1)
       COMMON U(3,3),GAMMA(9,1),GAMMAT(1,9),E9(9,9),T1(3,3),
     2 T2(3,3),T3(3,3)
C
C      *** CALLS SUBROUTINES ***
C     MATSET,MATKRO,MATMUL
C
       CALL MATSET(PMAT,33,33,0)
       DO 1 I=1,3
       DO 1 J=1,3
     1 PMAT(I,J) = U(I,J)
       CALL MATSET(TDPT,27,27,0)
       CALL MATKRO(T1,T1,ARRAYD,3,3,3,3,9,9)
       DO 2 I=1,9
       DO 2 J=1,9
     2 TDPT(I,J) = ARRAYD(I,J)
       CALL MATKRO(T2,T2,ARRAYD,3,3,3,3,9,9)
       DO 3 I=10,18
       DO 3 J=10,18
     3 TDPT(I,J) = ARRAYD(I-9,J-9)
       CALL MATKRO(T3,T3,ARRAYD,3,3,3,3,9,9)
       DO 4 I=19,27
       DO 4 J=19,27
     4 TDPT(I,J) = ARRAYD(I-18,J-18)
C
       CALL MATKRO(U,GAMMAT,ARRAYA,3,3,1,9,3,27)
       CALL MATMUL(ARRAYA,TDPT,ARRAYC,3,27,27,27)
       DO 5 I=1,3
       DO 5 J=4,30
     5 PMAT(I,J) = ARRAYC(I,J-3)
C
       CALL MATKRO(U,E9,ARRAYB,3,3,9,9,27,27)
       CALL MATMUL(ARRAYB,TDPT,ARRAYF,27,27,27,27)
C
       DO 6 I=4,30
       DO 6 J=4,30
     6 PMAT(I,J) = ARRAYF(I-3,J-3)
C
       CALL MATKRO(U,GAMMA,ARRAYE,3,3,9,1,27,3)
       DO 7 I=4,30
       DO 7 J=31,33
     7 PMAT(I,J) = ARRAYE(I-3,J-30)
C
       DO 8 I=31,33
       DO 8 J=31,33
     8 PMAT(I,J) = U(I-30,J-30)
C
       CALL MATMUL(GAMMAT,GAMMA,GAMSQ,1,9,9,1)
       G = 0.5 * GAMSQ(1,1)
       DO 9 I=1,3
       DO 9 J=1,3
       K = J+30
       PMAT(I,K) = U(I,J) * G
     9 CONTINUE
```

```
      RETURN
      END
C
      SUBROUTINE MATKRO(ARRAYA,ARRAYB,ARRAYC,IA,JA,IB,JB,IC,
     2 JC)
C
C     FORMS THE KRONECKER PRODUCT (DIRECT PRODUCT) OF TWO
C     MATRICES.
C
      DIMENSION ARRAYA(IA,JA),ARRAYB(IB,JB),ARRAYC(IC,JC)
C
      DO 1 I=1,IA
      DO 1 J=1,JA
      TEMP = ARRAYA(I,J)
      DO 1 K=1,IB
      DO 1 L=1,JB
      II = (I-1)*IB + K
      JJ = (J-1)*JB + L
    1 ARRAYC(II,JJ) = TEMP*ARRAYB(K,L)
      RETURN
      END
C
      SUBROUTINE MATMUL(ARRAYA,ARRAYB,ARRAYC,IA,JA,IB,JB)
C
C     POSTMULTIPLICATION OF ARRAYA BY ARRAYB TO GIVE ARRAYC.
C
      DIMENSION ARRAYA(IA,JA),ARRAYB(IB,JB),ARRAYC(IA,JB)
C
      DO 1 I=1,IA
      DO 1 J=1,JB
      CIJ = 0.0
      DO 2 K=1,JA
    2 CIJ = CIJ + ARRAYA(I,K) * ARRAYB(K,J)
    1 ARRAYC(I,J) = CIJ
      RETURN
      END
C
      SUBROUTINE MATEQU(ARRAYA,ARRAYB,IA,JA)
C
C     MATRIX A BECOMES EQUAL TO MATRIX B.
C
      DIMENSION ARRAYA(IA,JA),ARRAYB(IA,JA)
C
      DO 1 I=1,IA
      DO 1 J=1,JA
    1 ARRAYA(I,J) = ARRAYB(I,J)
      RETURN
      END
      FINISH
****
```

DATA

NSETS = 3Ø

N = 1

DACC =18.6Ø

DACH = 2.1Ø

RESULTS

N	GAMMASQ	GAMMASQ/N
1	Ø.2Ø736E Ø3	Ø.2Ø736E Ø3
2	Ø.29792E Ø3	Ø.14896E Ø3
3	Ø.54ØØ4E Ø3	Ø.18ØØ1E Ø3
4	Ø.73279E Ø3	Ø.1832ØE Ø3
5	Ø.1Ø185E Ø4	Ø.2Ø37ØE Ø3
6	Ø.12485E Ø4	Ø.2Ø8Ø9E Ø3
7	Ø.15373E Ø4	Ø.21962E Ø3
8	Ø.17845E Ø4	Ø.22Ø6E Ø3
9	Ø.2Ø698E Ø4	Ø.22998E Ø3
1Ø	Ø.23254E Ø4	Ø.23254E Ø3
11	Ø.26Ø66E Ø4	Ø.23697E Ø3
12	Ø.28671E Ø4	Ø.23892E Ø3
13	Ø.3145lE Ø4	Ø.24193E Ø3
14	Ø.34Ø87E Ø4	Ø.24348E Ø3
15	Ø.36843E Ø4	Ø.24562E Ø3
16	Ø.395ØØE Ø4	Ø.24688E Ø3
17	Ø.42240E Ø4	Ø.24847E Ø3
18	Ø.44911E Ø4	Ø.2495lE Ø3
19	Ø.47639E Ø4	Ø.25Ø73E Ø3
2Ø	Ø.5Ø32ØE Ø4	Ø.2516ØE Ø3
21	Ø.53Ø4ØE Ø4	Ø.25257E Ø3
22	Ø.55728E Ø4	Ø.2533lE Ø3
23	Ø.58442E Ø4	Ø.2541ØE Ø3
24	Ø.61134E Ø4	Ø.25473E Ø3
25	Ø.63845E Ø4	Ø.25538E Ø3
26	Ø.66540E Ø4	Ø.25592E Ø3
27	Ø.69248E Ø4	Ø.25647E Ø3
28	Ø.71946E Ø4	Ø.25695E Ø3
29	Ø.74652E Ø4	Ø.25742E Ø3
3Ø	Ø.7735lE Ø4	Ø.25784E Ø3

Program 9 Calculation of the Molar Kerr Constant

This program calculates the molar Kerr constant using the components of the molecular electro-optical polarizability tensor and the components of the molecular permanent dipole vector. Thus, this computer program may be used to evaluate Equation (10.12). It is also possible to calculate values of the molar Kerr constant corresponding to different temperatures.

The results of a trial calculation of the molar Kerr constant ($x10^{12}$/cgs units) at various temperatures for an imaginary molecule. is presented immediately following this program listing. The values computed for the molar Kerr constant were checked by hand calculation and found to be correct. All dipole moments are listed in Debyes and all polarizations in cm^3.

```
C
      MASTER MOLARK
C
C     THIS PROGRAM CALCULATES THE MOLECULAR KERR CONSTANT USING
C     COMPONENTS OF THE MOLECULAR ELECTRO-OPTICAL POLARIZABILITY TENSOR
C     AND THE COMPONENTS OF THE MOLECULAR PERMANENT DIPOLE VECTOR.
C
C     THE DISTORTION POLARIZATION (DP), ELECTRONIC POLARIZATION (EP)
C     AND THE ABSOLUTE TEMPERATURE ARE REQUIRED.
C     EVALUATION AT DIFFERENT TEMPERATURES IS POSSIBLE.
C
C     CERTAIN AREAS OF THE PROGRAM ARE SKIPPED IF THERE IS
C     ZERO PERMANENT DIPOLE MOMENT.
C
      INTEGER YES
      REAL MKCONS
      DIMENSION TEMP(1ØØ),MKCONS(1ØØ),T(3,3),U(3)
C
C     T AND U REFER TO THE POLARIZABILITY TENSOR AND THE DIPOLE
C     VECTOR RESPECTIVELY.
C
C      *** CALLS SUBROUTINES ***
C           STATIC, PERMAN
C
C     SUBROUTINE STATIC RETURNS THE INDUCED COMPONENT OF THE
C     MOLAR KERR CONSTANT (WITHOUT 1/45KT FACTOR)
C     SUBROUTINE PERMAN RETURNS THE DIPOLAR COMPONENT OF THE
C     MOLAR KERR CONSTANT (WITHOUT 1/45KT FACTOR)
C
C      *** DATA INPUT ORDER ***
C     (Ø) NSETS           NUMBER OF SETS OF DATA.
C     (1) NURA,NUTEMPS,   ALL MAY BE EITHER ZERO
C         NUTENS,NUDIP    OR UNITY.
C     (2) GANS            RATIO OF DP TO EP.
C     (3) NTEMP           NUMBER OF DIFFERT TEMPERATURES.
C     (4) TEMP(I)         TEMPERATURE VALUES.
C     (5) T(3,3)          ELECTRO-OPTICAL POLARIZABILITY TENSOR  X E24
C     (6) YES             ZERO IF THERE IS NO DIPOLE TERM,
C                         UNITY IF THERE IS A DIPOLE TERM.
C     (7) U(3)            DIPOLE MOMENT VECTOR (NOT REQUIRED IF YES = Ø)
C                         (READ IN ROW-BY-ROW) X E18
C
C     IF ZERO INPUT FOR NURA,NUTEMPS,NUTENS OR NUDIP INITIAL VALUES OF
C     RATIO, TEMPS, TENSOR OR DIPOLE ARE TO BE USED FOR EACH INDIVIDUAL
C     CALCULATION. IF UNITY NEW VALUES ARE TO BE INPUT EACH TIME.
C
      BOLTZ = 1.38Ø54E-16
      AVOGAD = 6.Ø2252E23
      PI = 3.141593
      ICOUNT = Ø
      READ(1,1ØØ)NSETS
  1ØØ FORMAT(IØ)
  15Ø CONTINUE
      WRITE(2,11Ø)
```

```
110 FORMAT(/,10X,'DATA',/,10X,'----')
    WRITE(2,120)NSETS
120 FORMAT(/,10X,'NSETS =',I6)
    READ(1,200)NURA,NUTEMPS,NUTENS,NUDIP
200 FORMAT(4I0)
    WRITE(2,250)NURA,NUTEMPS,NUTENS,NUDIP
250 FORMAT(/,10X,'NURA, NUTEMPS, NUTENS',/,10X,
   2 'AND NUDIP ARE RESPECTIVELY',4I6)
    IF(NURA.EQ.0) GO TO 11
    READ(1,300)GANS
300 FORMAT(F0.0)
    WRITE(2,350)GANS
350 FORMAT(/,10X,'GANS =',F10.4)
 11 CONTINUE
    IF(NUTEMPS.EQ.0) GO TO 22
    READ(1,400)NTEMP
400 FORMAT(I0)
    WRITE(2,450)NTEMP
450 FORMAT(/,10X,'NTEMP =',I6)
    READ(1,500) (TEMP(I), I=1,NTEMP)
500 FORMAT(100F0.0)
    WRITE(2,550) (TEMP(I),I=1,NTEMP)
550 FORMAT(/,10X,'TEMPERATURES =',100F11.4)
 22 CONTINUE
    IF(NUTENS.EQ.0) GO TO 33
    DO 1 I=1,3
  1 READ(1,600)  (T(I,J), J=1,3)
600 FORMAT(9F0.0)
    WRITE(2,650)
650 FORMAT(//,10X,'ELECTRO-OPTICAL POLARIZABILITY TENSOR * E24')
    WRITE(2,670) ((T(I,J),J=1,3),I=1,3)
670 FORMAT(/,10X,3F15.5,/,10X,3F15.5,/,10X,3F15.5)
    DO 9 I=1,3
    DO 9 J=1,3
  9 T(I,J) = T(I,J) * 1.0E-24
 33 CONTINUE
    IF(NUDIP.EQ.0) GO TO 44
    READ(1,700)YES
700 FORMAT(I0)
    WRITE(2,750)YES
750 FORMAT(/,10X,'YES =',I6)
    IF(YES.EQ.0) GO TO 44
    READ(1,800)  (U(I),I=1,3)
800 FORMAT(3F0.0)
    WRITE(2,850)
850 FORMAT(//,10X,'DIPOLE MOMENT VECTOR * E18')
    WRITE(2,870)
870 FORMAT(/,19X,'X',14X,'Y',14X,'Z')
    WRITE(2,890)(U(I),I=1,3)
890 FORMAT(10X,3F15.5)
    DO 10 I=1,3
 10 U(I) = U(I) * 1.0E-18
 44 CONTINUE
C
```

```
      CALL STATIC(A,T)
      IF(YES.EQ.Ø) GO TO 55
      CALL PERMAN(B,T,U)
   55 CONTINUE
      A=A*GANS
C
      DO 4 I=1,NTEMP
      CONSTA = 1/(45*BOLTZ*TEMP(I))
      TERMA = CONSTA * A
      TERMB = Ø.Ø
      IF(YES.EQ.Ø) GO TO 66
      CONSTB = CONSTA/(BOLTZ * TEMP(I))
      TERMB  = CONSTB * B
   66 CONTINUE
      MKCONS(I) = 2*PI*AVOGAD*(TERMA+TERMB)/9
    4 CONTINUE
C
C     WRITE OUT MOLAR KERR CONSTANTS.
C
      WRITE(2,9ØØ)
  9ØØ FORMAT(////,1ØX,'RESULTS',/,1ØX,'-------')
      WRITE(2,13ØØ)
 13ØØ FORMAT(//,1ØX,'MOLAR KERR CONST * E12      TEMPERATURE(K)')
      DO 8 I=1,NTEMP
      MKCONS(I) = MKCONS(I) * 1.ØE12
      WRITE(2,14ØØ)MKCONS(I),TEMP(I)
 14ØØ FORMAT(1ØX,F15.5,9X,F15.5)
    8 CONTINUE
      WRITE(2,15ØØ)
 15ØØ FORMAT('1')
      ICOUNT = ICOUNT + 1
      IF(ICOUNT.NE.NSETS) GO TO 15Ø
      STOP
      END
C
      SUBROUTINE STATIC(A,T)
C
C     THIS SUBROUTINE CALCULATES THE STATIC COMPONENT OF THE
C     MOLAR KERR CONSTANT FROM THE ELECTRO-OPTICAL POLARIZABILITY
C     TENSOR (WHICH NEED NOT BE DIAGONALISED)
C     THE 1/45KT FACTOR IS NOT INCLUDED
C
      DIMENSION T(3,3)
      A = (T(1,1) - T(2,2)) * (T(1,1) - T(2,2)) +
     1    (T(2,2) - T(3,3)) * (T(2,2) - T(3,3)) +
     2    (T(3,3) - T(1,1)) * (T(3,3) - T(1,1)) +
     3    3*T(1,2) * T(1,2) + 3*T(2,1) * T(2,1) +
     4    3*T(1,3) * T(1,3) + 3*T(3,1) * T(3,1) +
     5    3*T(2,3) * T(2,3) + 3*T(3,2) * T(3,2)
      RETURN
      END
C
      SUBROUTINE PERMAN(B,T,U)
C
```

```
C     THIS SUBROUTINE CALCULATES THE DIPOLAR TERM
C     OF THE MOLAR KERR CONSTANT USING THE COMPONENTS OF
C     THE ELECTRO-OPTICAL POLARIZABILITY TENSOR (WHICH NEED
C     NOT BE DIAGONAL FORM) AND THE COMPONENTS OF THE
C     PERMANENT DIPOLE MOMENT VECTOR.
C     THE 1/45KT FACTOR IS NOT INCLUDED.
C
      DIMENSION T(3,3), U(3)
      B = (T(1,1) - T(2,2)) * (U(1) * U(1) - U(2) * U(2)) +
     1    (T(2,2) - T(3,3)) * (U(2) * U(2) - U(3) * U(3)) +
     2    (T(3,3) - T(1,1)) * (U(3) * U(3) - U(1) * U(1)) +
     3    3*U(1) * U(2) * T(1,2) + 3*U(2) * U(3) * T(2,3) +
     4    3*U(1) * U(3) * T(1,3) + 3*U(2) * U(1) *T(2,1) +
     5    3*U(3) * U(2) * T(3,2) + 3*U(3)* U(2) * T(3,1)
      RETURN
      END
      FINISH
```

DATA

NSETS = 2

NURA, NUTEMPS, NUTENS
AND NUDIP ARE RESPECTIVELY 1 1 1 1

GANS = 1.1000

NTEMP = 5

TEMPERATURES = 273.0000 283.0000 293.0000 303.0000 313.0000

ELECTRO-OPTICAL POLARIZABILITY TENSOR * E24

5.70000	0.00000	0.00000
0.00000	6.60000	0.00000
0.00000	0.00000	0.00000

YES = 1

DIPOLE MOMENT VECTOR * E18

X	Y	Z
3.79000	1.03000	0.00000

RESULTS

MOLAR KERR CONST * E12	TEMPERATURE(K)
526.82070	273.00000
490.96180	283.00000
458.68746	293.00000
429.53392	303.00000
403.11016	313.00000

DATA

NSETS = 2

NURA, NUTEMPS, NUTENS
AND NUDIP ARE RESPECTIVELY 0 0 0 1

YES = 0

RESULTS

MOLAR KERR CONST * E12	TEMPERATURE(K)
20.95968	273.00000
20.21905	283.00000
19.52898	293.00000
18.88446	303.00000
18.28112	313.00000

Program 10 Calculation of the Molar Kerr Constant Averaged over all Conformations of a Polymer Chain.

Matrix methods are available to calculate the molar Kerr constant of a polymer chain averaged over all conformations.[195] These methods are applied here in this computer program in order to evaluate Equation (8.19) (See section 8.06 for further details of the theory involved). This program has been specifically structured to calculate the molar Kerr constant of poly(oxyethylene glycols), however, only very slight adjustments are required in order that calculations might be performed upon any other linear polymer.

The results of a calculation of the molar Kerr constants (cgs units) for a series of poly(oxyethylene glycols) having n = 5 to n = 74 skeletal bonds forms the sample output immediately following this program. The values obtained are in good agreement with those calculated by Ishikawa and Nagai[198]. Each value of the molar Kerr constant is also resolved into a dipolar and an induced term (see Equation (10.12)).

```
JOB :EADXX,MBETH2,CP76(P1000,TD1280,SP)
FTN(L=0)
ATTACH(LIB,\:EAAXX.PMICLLIBRARY\,ST=S4S,FO=ASIS)
LIBRARY(LIB)
LDSET(MAP=B/ZZZZMP,PRESET=NGINF)
LGO.
CATALOG(MBR10,MBRES10,ST=S4S)
####S
C
      PROGRAM ETHGLY(INPUT,OUTPUT,MBR10,TAPE1=INPUT,TAPE2=MBR10)
C
C     THIS PROGRAM CALCULATES THE MOLAR KERR CONSTANT OF A LINEAR
C     OXYETHYLENE GLYCOL POLYMER.
C     MATRIX FORMULATION IS USED THROUGHOUT (SEE P.J.FLORY AND
C     R.L.JERNGAN, THE JOURNAL OF CHEMICAL PHYSICS, VOLUME 48,
C     P3823, (1968)).
C     THE DATA IS WRITEN OUT ON A CHAIN-BY-CHAIN BASIS.
C
C     THE PROGRAM READS ELECTRO-OPTICAL POLARIZABILITY TENSORS AND
C     DIPOLE MOMENTS FOR EACH BOND AS WELL AS VARIOUS GEOMETRICAL DATA.
C     GANS, THE RATIO OF THE DISTORTION (PE+PA) TO THE ELECTRONIC
C     POLARIZATION, IS ALSO REQUIRED.
C
C     THE POLARIZABILITY TENSORS ARE ASSUMED TO BE INVARIANT WITH
C     CONFORMATIONAL CHANGES.
C
C             *** CALLS THE SUBROUTINES ***
C     FILMATU,MATSET,MATEQU,FILLTR,FILTD,FILTDP,FILARS,MATRAN,
C     SCALMUL,MATKRO,MATMUL,
C
      DIMENSION ARRAYUA(3,3),ARRAYUB(3,3),ATEMP(60,60),QTEMP(78,78),
     2 UTEMP(3,3),GAMMAOC(9,1),BOND(3,1),T1(3,3),T2(3,3),T3(3,3),
     3 ARA(60,60),ARQ(78,78),APROD(60,60),QPROD(78,78),UPROD(3,3),
     4 ARRAYUC(3,3),ARRAYUD(3,3)
      REAL MOLARK,KMDIVN
      COMMON U(3,3),E3(3,3),E9(9,9),TRDIAG(9,9),TDPT(27,27)
C
C     READ NUMBER OF SETS OF DATA.
C
      READ(1,*)NSETS
      ICOUNT = 0
    1 CONTINUE
C
C     READ THE NUMBER OF BACKBONE BONDS (N).
C
      READ(1,*)N
      IF(ICOUNT.NE.0)GO TO 11
C
C     READ THE TEMPERATURE IN KELVIN AND USE THIS TO CALCULATE THE
C     STATISTICAL WEIGHTS AND FILL THE STATISTICAL WEIGHT MATRICES.
C
      READ(1,*)TEMP
      SIGD = 1.5
      SIG = 0.156
```

```
      CPHI = 1.Ø
      OMEG1 = Ø.Ø
      OMEG2 = Ø.22
      OMEG3 = 1.Ø
      CALL FILMATU(SIGD,CPHI,OMEG2,ARRAYUA)
      CALL FILMATU(SIG,CPHI,OMEG1,ARRAYUC)
      CALL FILMATU(SIG,CPHI,OMEG2,ARRAYUB)
      CALL FILMATU(SIGD,CPHI,OMEG3,ARRAYUD)
C
C     READ THE VALUE OF THE RATIO 'GANS' (PD/PE).
C
      READ(1,*)GANS
C
C     WRITE OUT FIRST HEADINGS AND DATA.
C
      WRITE(2,5ØØ)
  5ØØ FORMAT('1')
      WRITE(2,6ØØ)
  6ØØ FORMAT(/,1ØX,'KERR EFECT OF LINEAR POLYMER FROM ',
     2 'MATRIX PROGRAM.',/,
     3 1ØX, '-------------------------------------------------',/)
      WRITE(2,7ØØ)NSETS
  7ØØ FORMAT(/,1ØX,'NSETS =',I6)
      WRITE(2,85Ø)TEMP
  85Ø FORMAT(/,1ØX,'TEMP =',F8.2)
      WRITE(2,9ØØ)GANS
  9ØØ FORMAT(/,1ØX,'GANS (PD/PE) =',F5.2)
      WRITE(2,95Ø)
  95Ø FORMAT(////,11X,'N  PART.FUNC.    DIP.TERM    ',
     2 'IND.TERM  MOLAR KERR        KM/N',/)
C
C     SET THE DIHEDRAL ANGLES (PHIS).
C
      RAD = Ø.Ø1745329251994329 57
      PHI1 = Ø.Ø
      PHI2 = 12Ø.Ø*RAD
      PHI3 = 24Ø.Ø*RAD
   11 CONTINUE
C
C     INITIALISE VARIABLES AND ARRAYS.
C
      CALL MATSET(E3,3,3,1)
      CALL MATSET(E9,9,9,1)
      CALL MATSET(ATEMP,6Ø,6Ø,1)
      CALL MATSET(QTEMP,78,78,1)
      CALL MATSET(UTEMP,3,3,1)
      NPLUS1 = N+1
      NLESS1 = N-1
      NLESS2 = N-2
C
C     BEGIN MAIN DO LOOP TO CONSTRUCT SERIAL PRODUCT OF MATRICES.
C
      DO 99 II=1,N
C
```

```
C     FILL THE TRACELESS BOND POLARIZABILITY TENSOR, DIPOLE MOMENT
C     VECTOR AND BOND ANGLE SUPPLEMENT THETA.
C
      CALL MATSET(U,3,3,1)
      CALL MATSET(BOND,3,1,Ø)
      CALL MATSET(GAMMAOC,9,1,Ø)
      IF((II.NE.1).AND.(II.NE.N))GO TO 44
      GAMMAOC(1,1) = 1.4667
      GAMMAOC(5,1) = -Ø.7333
      GAMMAOC(9,1) = -Ø.7333
      BOND(1,1) = 1.7
      IF(II.EQ.N)BOND(1,1) = -BOND(1,1)
      THETA = 72.Ø*RAD
      GO TO 77
   44 CONTINUE
      IF(II.GT.((INT((FLOAT(II))/3.Ø))*3))GO TO 55
      GAMMAOC(1,1) = 9.6
      GAMMAOC(5,1) = -4.8
      GAMMAOC(9,1) = -4.8
      THETA = 7Ø.528781*RAD
      CALL MATEQU(U,ARRAYUA,3,3)
      IF(II.EQ.3)CALL MATEQU(U,ARRAYUD,3,3)
      GO TO 77
   55 CONTINUE
      GAMMAOC(1,1) = 5.1333
      GAMMAOC(5,1) = -2.5667
      GAMMAOC(9,1) = -2.5667
      THETA = 7Ø.528781*RAD
      IF((II.NE.2).AND.(II.NE.NLESS1))GO TO 88
      IF(II.EQ.2)BOND(1,1) = -1.Ø
      IF(II.EQ.NLESS1)BOND(1,1) = 1.Ø
      U(1,2) = 1.Ø
      U(1,3) = 1.Ø
      U(2,1) = 1.Ø
      U(2,3) = 1.Ø
      U(3,1) = 1.Ø
      U(3,2) = 1.Ø
      GO TO 77
   88 IF(II.GT.(((INT((FLOAT(II-2))/3.Ø))*3)+2))GO TO 66
      CALL MATEQU(U,ARRAYUC,3,3)
      BOND(1,1) = -1.Ø
      GO TO 77
   66 CONTINUE
      CALL MATEQU(U,ARRAYUB,3,3)
      BOND(1,1) = 1.Ø
   77 CONTINUE
      CALL SCALMUL(GAMMAOC,1.ØE-25,GAMMAOC,9,1)
      CALL SCALMUL(BOND,1.ØE-18,BOND,3,1)
C
C     FILL ALL APPROPRIATE TRANSFORMATION ARRAYS.
C
      CALL FILLTR(THETA,PHI1,T1)
      CALL FILLTR(THETA,PHI2,T2)
      CALL FILLTR(THETA,PHI3,T3)
```

```
      CALL FILTD(T1,T2,T3,TRDIAG)
      CALL FILTDP(T1,T2,T3,TDPT)
C
C     FILL THE GENERATOR MATRICES 'ARA' AND 'ARQ', AND FORM THE SERIAL
C     PRODUCTS OF THESE AND THE STATISTICAL WEIGHT MATRIX 'U'.
C
      CALL FILARS(BOND,GAMMAOC,GANS,ARA,ARQ)
      CALL MATMUL(ATEMP,ARA,APROD,60,60,60,60)
      CALL MATMUL(QTEMP,ARQ,QPROD,78,78,78,78)
      CALL MATMUL(UTEMP,U,UPROD,3,3,3,3)
      CALL MATEQU(ATEMP,APROD,60,60)
      CALL MATEQU(QTEMP,QPROD,78,78)
      CALL MATEQU(UTEMP,UPROD,3,3)
C
C     END OF MAIN DO LOOP.
C
   99 CONTINUE
C
C     FORM THE CONFORMATIONAL PARTITION FUNCTION Z.
C     NOTE THAT ONLY ELEMENTS (1,1),(1,2) AND (1,3) OF
C     'UPROD' ARE REQUIRED.
C
      Z = UPROD(1,1) + UPROD(1,2) + UPROD(1,3)
C
C     NOTE THAT ONLY ELEMENTS (1,58),(1,59) AND (1,60) OF 'APROD', AND
C     (1,76),(1,77) AND (1,78) OF 'QPROD' ARE REQUIRED.
C
      SERA = APROD(1,58) + APROD(1,59) + APROD(1,60)
      SERQ = QPROD(1,76) + QPROD(1,77) + QPROD(1,78)
      TRGOGS = SERA/Z
      BOLTZ = 1.38054E-16
      AVOGAD = 6.02252E23
      PI = 3.1415926
      FACTR = ((2.0*PI*AVOGAD)/(15.0*BOLTZ*TEMP))
      TRGOGS = FACTR * TRGOGS
      BTGOB = (SERQ*2.0)/Z
      BTGOB = (FACTR*(BTGOB/(BOLTZ*TEMP)))
C
C     CALCULATE THE MOLAR KERR CONSTANT.
C
      MOLARK = TRGOGS + BTGOB
      KMDIVN = MOLARK/N
      WRITE(2,1000)N,Z,BTGOB,TRGOGS,MOLARK,KMDIVN
 1000 FORMAT(9X,I3,5E12.4)
C
      ICOUNT = ICOUNT+1
      IF(ICOUNT.NE.NSETS)GO TO 1
C
      STOP
      END
C
      SUBROUTINE FILMATU(SIG,CPHI,OMEG,ARRAYU)
C
C     THIS SUBROUTINE FILLS THE STATISTICAL WEIGHT MATRIX 'U'
```

```
C     WITH THE RELEVANT VALUES OF SIGMA, CAPITAL PHI AND OMEGA.
C
      DIMENSION ARRAYU(3,3)
      ARRAYU(1,1) = 1.Ø
      ARRAYU(1,2) = SIG
      ARRAYU(1,3) = SIG
      ARRAYU(2,1) = 1.Ø
      ARRAYU(2,2) = SIG*CPHI
      ARRAYU(2,3) = SIG*OMEG
      ARRAYU(3,1) = 1.Ø
      ARRAYU(3,2) = SIG*OMEG
      ARRAYU(3,3) = SIG*CPHI
      RETURN
      END
C
      SUBROUTINE MATSET(ARRAYA,IA,JA,K)
C
C     IF K EQUALS Ø THEN ALL ELEMENTS ARE SET TO ZERO ONLY.
C     IF K EQUALS 1 THEN AN IDENTITY IS FORMED.
C
      DIMENSION ARRAYA(IA,JA)
      DO 1 I=1,IA
      DO 1 J=1,JA
    1 ARRAYA(I,J) = Ø.Ø
      IF(K.EQ.Ø)GO TO 3
      DO 2 I=1,IA
    2 ARRAYA(I,I) = 1.Ø
    3 CONTINUE
      RETURN
      END
C
      SUBROUTINE MATEQU(ARRAYA,ARRAYB,IA,JA)
C
C     MATRIX 'A' BECOMES EQUAL TO MATRIX 'B'.
C
      DIMENSION ARRAYA(IA,JA),ARRAYB(IA,JA)
C
      DO 1 I=1,IA
      DO 1 J=1,JA
    1 ARRAYA(I,J) = ARRAYB(I,J)
      RETURN
      END
C
      SUBROUTINE FILLTR(THETA,PHI,TR)
C
C     FILLS ORTHOGONAL MATRIX REQUIRED FOR TRANSFORMING A VECTOR FROM
C     ONE CARTESIAN COORDINATE SYSTEM TO ANOTHER.
C     ANGLES THETA (BOND ANGLE SUPPLEMENT) AND PHI (DIHEDRAL ANGLE)
C     MUST BE EXPRESSED IN RADIANS.
C
      DIMENSION TR(3,3)
C
      COST = COS(THETA)
      SINT = SIN(THETA)
```

```
      COSP = COS(PHI)
      SINP = SIN(PHI)
      TR(1,1) = COST
      TR(1,2) = SINT
      TR(1,3) = Ø.Ø
      TR(2,1) = SINT*COSP
      TR(2,2) = -COST*COSP
      TR(2,3) = SINP
      TR(3,1) = SINT*SINP
      TR(3,2) = -COST*SINP
      TR(3,3) = -COSP
      RETURN
      END
C
      SUBROUTINE FILTD(TRA,TRB,TRC,TRDIAG)
C
C     FORMS PSEUDO-DIAGONAL MATRIX 'TRDIAG' CONSISTING OF
C     SMALLER MATRICES 'TRA', 'TRB' AND 'TRC'.
C
      DIMENSION TRA(3,3),TRB(3,3),TRC(3,3),TRDIAG(9,9)
      CALL MATSET(TRDIAG,9,9,Ø)
      DO 1 I=1,3
      DO 1 J=1,3
    1 TRDIAG(I,J) = TRA(I,J)
      DO 2 I=1,3
      DO 2 J=1,3
      II = I+3
      JJ = J+3
    2 TRDIAG(II,JJ) = TRB(I,J)
      DO 3 I=1,3
      DO 3 J=1,3
      II = I+6
      JJ = J+6
    3 TRDIAG(II,JJ) = TRC(I,J)
      RETURN
      END
C
      SUBROUTINE FILTDP(TRA,TRB,TRC,TDPT)
C
C     THIS SUBROUTINE FILLS THE PSEUDO-DIAGONAL MATRIX 'TDPT' WITH
C     THE DIRECT PRODUCT OF EACH OF THE SMALLER ARRAYS 'TRA','TRB'
C     AND 'TRC' WITH THEMSELVES.
C
C      *** CALLS SUBROUTINES ***
C     MATSET AND MATKRO
C
      DIMENSION TRA(3,3),TRB(3,3),TRC(3,3),TDPT(27,27),ARRAYA(9,9)
      CALL MATSET(TDPT,27,27,Ø)
      CALL MATKRO(TRA,TRA,ARRAYA,3,3,3,3,9,9)
      DO 1 I=1,9
      DO 1 J=1,9
    1 TDPT(I,J) = ARRAYA(I,J)
      CALL MATKRO(TRB,TRB,ARRAYA,3,3,3,3,9,9)
      DO 2 I=1Ø,18
```

```
      DO 2 J=10,18
    2 TDPT(I,J) = ARRAYA(I-9,J-9)
      CALL MATKRO(TRC,TRC,ARRAYA,3,3,3,3,9,9)
      DO 3 I=19,27
      DO 3 J=19,27
    3 TDPT(I,J) = ARRAYA(I-18,J-18)
      RETURN
      END
C
      SUBROUTINE FILARS(BOND,GAMMAOC,GANS,ARA,ARQ)
C
C     THIS SUBROUTINE IS REQUIRED FOR THE CALCULATION OF THE MOLAR
C     KERR CONSTANT OF A CHAIN MOLECULE.
C     THE SUBROUTINE FILLS TWO MATRICES 'ARA'(60*60) AND 'ARQ'(78*78) WITH
C     INFORMATION RELATING TO A REPEAT UNIT OR SKELETAL BOND SUCH AS
C     CONFORMATIONAL PROBABILITIES, ELECTRO-OPTICAL POLARIZABILITY
C     TENSORS, BOND DIPOLE MOMENTS AND LOCAL GEOMETRY.
C
      DIMENSION ARA(60,60),ARQ(78,78),S(1,1),GAMMAO(3,3),GAMMAOC(9,1),
     2 GAMMAOR(1,9),GAMMASC(9,1),GAMMASR(1,9),BOND(3,1),BONDT(1,3),
     3 ARRAYA(9,9),ARRAYB(9,9),ARRAYC(27,27),ARRAYD(27,27),ARRAYE(3,9),
     4 ARRAYF(3,9),ARRAYG(3,27),ARRAYH(3,27),ARRAYI(9,3),ARRAYJ(1,3),
     5 ARRAYK(9,1),ARRAYL(3,3),ARRAYM(9,27),ARRAYN(9,27),ARRAYO(3,1),
     6 ARRAYP(27,9),ARRAYQ(27,9),ARRAYR(27,3)
      COMMON U(3,3),E3(3,3),E9(9,9),TRDIAG(9,9),TDPT(27,27)
C
      CALL MATRAN(BOND,BONDT,3,1)
      CALL SCALMUL(GAMMAOC,GANS,GAMMASC,9,1)
      CALL MATRAN(GAMMAOC,GAMMAOR,9,1)
      CALL MATRAN(GAMMASC,GAMMASR,9,1)
      CALL MATSET(ARA,60,60,0)
      CALL MATSET(ARQ,78,78,0)
      DO 1 I=1,3
      DO 1 J=1,3
      ARA(I,J) = U(I,J)
      ARQ(I,J) = U(I,J)
      ARA(I+57,J+57) = U(I,J)
      ARQ(I+75,J+75) = U(I,J)
    1 CONTINUE
      CALL MATKRO(U,E3,ARRAYA,3,3,3,3,9,9)
      CALL MATMUL(ARRAYA,TRDIAG,ARRAYB,9,9,9,9)
      DO 2 I=1,9
      DO 2 J=1,9
      ARQ(I+3,J+3) = ARRAYB(I,J)
      ARQ(I+66,J+66) = ARRAYB(I,J)
    2 CONTINUE
      CALL MATKRO(U,E9,ARRAYC,3,3,9,9,27,27)
      CALL MATMUL(ARRAYC,TDPT,ARRAYD,27,27,27,27)
      DO 3 I=1,27
      DO 3 J=1,27
      ARQ(I+12,J+12) = ARRAYD(I,J)
      ARQ(I+39,J+39) = ARRAYD(I,J)
      ARA(I+3,J+3) = ARRAYD(I,J)
      ARA(I+30,J+30) = ARRAYD(I,J)
```

```
3 CONTINUE
  CALL MATKRO(U,BONDT,ARRAYE,3,3,1,3,3,9)
  CALL MATMUL(ARRAYE,TRDIAG,ARRAYF,3,9,9,9)
  DO 4 I=1,3
  DO 4 J=1,9
4 ARQ(I,J+3) = ARRAYF(I,J)
  CALL MATKRO(ARRAYE,BONDT,ARRAYG,3,9,1,3,3,27)
  CALL SCALMUL(ARRAYG,Ø.5,ARRAYH,3,27)
  CALL MATMUL(ARRAYH,TDPT,ARRAYG,3,27,27,27)
  DO 5 I=1,3
  DO 5 J=1,27
5 ARQ(I,J+39) = ARRAYG(I,J)
  CALL MATKRO(U,GAMMAOR,ARRAYG,3,3,1,9,3,27)
  CALL MATMUL(ARRAYG,TDPT,ARRAYH,3,27,27,27)
  DO 6 I=1,3
  DO 6 J=1,27
  ARQ(I,J+12) = ARRAYH(I,J)
  ARA(I,J+3) = ARRAYH(I,J)
6 CONTINUE
  CALL MATKRO(BOND,E3,ARRAYI,3,1,3,3,9,3)
  CALL MATMUL(GAMMAOR,ARRAYI,ARRAYJ,1,9,9,3)
  CALL MATKRO(U,ARRAYJ,ARRAYE,3,3,1,3,3,9)
  CALL MATMUL(ARRAYE,TRDIAG,ARRAYF,3,9,9,9)
  DO 7 I=1,3
  DO 7 J=1,9
7 ARQ(I,J+66) = ARRAYF(I,J)
  CALL MATKRO(BOND,BOND,ARRAYK,3,1,3,1,9,1)
  CALL MATMUL(GAMMAOR,ARRAYK,S,1,9,9,1)
  SC = S(1,1) * Ø.5
  CALL SCALMUL(U,SC,ARRAYL,3,3)
  DO 8 I=1,3
  DO 8 J=1,3
8 ARQ(I,J+75) = ARRAYL(I,J)
  CALL MATKRO(ARRAYA,BONDT,ARRAYM,9,9,1,3,9,27)
  CALL MATMUL(ARRAYM,TDPT,ARRAYN,9,27,27,27)
  DO 9 I=1,9
  DO 9 J=1,27
9 ARQ(I+3,J+39) = ARRAYN(I,J)
  DO 1Ø I=1,3
  DO 1Ø J=1,3
  K = (I-1)*3 + J
1Ø GAMMAO(I,J) = GAMMAOR(1,K)
  CALL MATKRO(U,GAMMAO,ARRAYA,3,3,3,3,9,9)
  CALL MATMUL(ARRAYA,TRDIAG,ARRAYB,9,9,9,9)
  DO 11 I=1,9
  DO 11 J=1,9
11 ARQ(I+3,J+66) = ARRAYB(I,J)
  CALL MATKRO(E3,BONDT,ARRAYE,3,3,1,3,3,9)
  CALL MATMUL(ARRAYE,GAMMAOC,ARRAYO,3,9,9,1)
  CALL MATKRO(U,ARRAYO,ARRAYI,3,3,3,1,9,3)
  DO 12 I=1,9
  DO 12 J=1,3
12 ARQ(I+3,J+75) = ARRAYI(I,J)
  CALL MATKRO(U,BOND,ARRAYI,3,3,3,1,9,3)
```

```
      CALL MATKRO(ARRAYI,E3,ARRAYP,9,3,3,3,27,9)
      CALL MATMUL(ARRAYP,TRDIAG,ARRAYQ,27,9,9,9)
      DO 13 I=1,27
      DO 13 J=1,9
   13 ARQ(I+12,J+66) = ARRAYQ(I,J)
      CALL MATKRO(U,BOND,ARRAYI,3,3,3,1,9,3)
      CALL MATKRO(ARRAYI,BOND,ARRAYR,9,3,3,1,27,3)
      CALL SCALMUL(ARRAYR,0.5,ARRAYR,27,3)
      DO 14 I=1,27
      DO 14 J=1,3
   14 ARQ(I+12,J+75) = ARRAYR(I,J)
      CALL MATKRO(U,GAMMAOC,ARRAYR,3,3,9,1,27,3)
      DO 15 I=1,27
      DO 15 J=1,3
      ARQ(I+39,J+75) = ARRAYR(I,J)
      ARA(I+30,J+57) = ARRAYR(I,J)
   15 CONTINUE
      CALL MATKRO(U,BOND,ARRAYI,3,3,3,1,9,3)
      DO 16 I=1,9
      DO 16 J=1,3
   16 ARQ(I+66,J+75) = ARRAYI(I,J)
      CALL MATKRO(U,GAMMASR,ARRAYG,3,3,1,9,3,27)
      CALL MATMUL(ARRAYG,TDPT,ARRAYH,3,27,27,27)
      DO 17 I=1,3
      DO 17 J=1,27
   17 ARA(I,J+30) = ARRAYH(I,J)
      CALL MATMUL(GAMMAOR,GAMMASC,S,1,9,9,1)
      SC = S(1,1)
      CALL SCALMUL(U,SC,ARRAYL,3,3)
      DO 18 I=1,3
      DO 18 J=1,3
   18 ARA(I,J+57) = ARRAYL(I,J)
      SC = S(1,1)
      CALL SCALMUL(U,SC,ARRAYL,3,3)
      DO 18 I=1,3
      DO 18 J=1,3
   18 ARA(I,J+57) = ARRAYL(I,J)
      CALL MATKRO(U,GAMMASC,ARRAYR,3,3,9,1,27,3)
      DO 19 I=1,27
      DO 19 J=1,3
   19 ARA(I+3,J+57) = ARRAYR(I,J)
      RETURN
      END
C
      SUBROUTINE MATRAN(ARRAYA,ARRAYB,IA,JA)
C
C     FINDS THE TRANSPOSE OF A RECTANGULAR MATRIX 'ARRAYA'.
C     NOTE - IF ARRAY IS ORTHOGONAL THEN ITS TRANSPOSE IS ITS INVERSE.
C
      DIMENSION ARRAYA(IA,JA),ARRAYB(JA,IA)
      DO 1 I=1,IA
      DO 1 J=1,JA
    1 ARRAYB(J,I) = ARRAYA(I,J)
      RETURN
```

```
      END
C
      SUBROUTINE SCALMUL(ARRAYA,S,ARRAYB,IA,JA)
C
C     MULTIPLIES 'ARRAYA' BY A SCALAR 'S' TO GIVE 'ARRAYB'.
C
      DIMENSION ARRAYA(IA,JA),ARRAYB(IA,JA)
      DO 1 I=1,IA
      DO 1 J=1,JA
    1 ARRAYB(I,J) = S * ARRAYA(I,J)
      RETURN
      END
C
      SUBROUTINE MATKRO(ARRAYA,ARRAYB,ARRAYC,IA,JA,IB,JB,IC,JC)
C
C     FINDS DIRECT PRODUCT OF 'ARRAYA' AND 'ARRAYB' TO GIVE 'ARRAYC'.
C     IA * IB MUST EQUAL IC AND JA * JB MUST EQUAL JC.
C
      DIMENSION ARRAYA(IA,JA),ARRAYB(IB,JB),ARRAYC(IC,JC)
      DO 1 I=1,IA
      DO 1 J=1,JA
      DO 1 K=1,IB
      DO 1 L=1,JB
      II = (I-1) * IB + K
      JJ = (J-1) * JB + L
      ARRAYC(II,JJ) = ARRAYA(I,J) * ARRAYB(K,L)
    1 CONTINUE
      RETURN
      END
C
      SUBROUTINE MATMUL(ARRAYA,ARRAYB,ARRAYC,IA,JA,IB,JB)
C
C     POST MULTIPLICATION OF 'ARRAYA' BY 'ARRAYB' TO GIVE 'ARRAYC'.
C
      DIMENSION ARRAYA(IA,JA),ARRAYB(IB,JB),ARRAYC(IA,JB),TEMPRE(78,78)
      DO 3 I=1,IA
      DO 3 J=1,JA
      TEMPRE(I,J) = ARRAYA(I,J)
    3 CONTINUE
      DO 1 I=1,IA
      DO 1 J=1,JB
      CIJ = Ø.Ø
      DO 2 K=1,JA
    2 CIJ = CIJ+TEMPRE(I,K)*ARRAYB(K,J)
    1 ARRAYC(I,J) = CIJ
      RETURN
      END
####S
        24
         5
       298
       1.1
         8
       11
```

```
          14
          17
          20
          23
          26
          29
          32
          35
          38
          41
          44
          47
          50
          53
          56
          59
          62
          65
          68
          71
          74
****
```

KERR EFECT OF LINEAR POLYMER FROM MATRIX PROGRAM.

NSETS = 24

TEMP = 298.ØØ

GANS (PD/PE) = 1.1Ø

N	PART.FUNC.	DIP.TERM	IND.TERM	MOLAR KERR	KM/N
5	.36ØØE+Ø2	-.9Ø58E-11	.8Ø48E-11	-.1Ø1ØE-11	-.2Ø2ØE-12
8	.2111E+Ø3	.3338E-1Ø	.2183E-1Ø	.5521E-1Ø	.6901E-11
11	.124ØE+Ø4	.8995E-1Ø	.3514E-1Ø	.1251E-Ø9	.1137E-1Ø
14	.728ØE+Ø4	.1389E-Ø9	.4837E-1Ø	.1872E-Ø9	.1337E-1Ø
17	.4275E+Ø5	.1421E-Ø9	.6168E-1Ø	.2Ø38E-Ø9	.1199E-1Ø
2Ø	.2511E+Ø6	.1253E-Ø9	.7496E-1Ø	.2ØØ3E-Ø9	.1ØØ1E-1Ø
23	.1474E+Ø7	.1ØØØE-Ø9	.8824E-1Ø	.1883E-Ø9	.8186E-11
26	.8659E+Ø7	.7237E-1Ø	.1Ø15E-Ø9	.1739E-Ø9	.6688E-11
29	.5Ø85E+Ø8	.4427E-1Ø	.1148E-Ø9	.1591E-Ø9	.5486E-11
32	.2986E+Ø9	.1614E-1Ø	.1281E-Ø9	.1442E-Ø9	.4507E-11
35	.1754E+1Ø	-.1195E-1Ø	.1414E-Ø9	.1294E-Ø9	.3698E-11
38	.1Ø3ØE+11	-.4ØØ3E-1Ø	.1547E-Ø9	.1146E-Ø9	.3Ø17E-11
41	.6Ø49E+11	-.681ØE-1Ø	.1679E-Ø9	.9984E-1Ø	.2435E-11
44	.3552E+12	-.9618E-1Ø	.1812E-Ø9	.85Ø5E-1Ø	.1933E-11
47	.2Ø86E+13	-.1243E-Ø9	.1945E-Ø9	.7Ø27E-1Ø	.1495E-11
5Ø	.1225E+14	-.1523E-Ø9	.2Ø78E-Ø9	.5547E-1Ø	.1109E-11
53	.7195E+14	-.18Ø4E-Ø9	.2211E-Ø9	.4Ø68E-1Ø	.7676E-12
56	.4225E+15	-.2Ø85E-Ø9	.2344E-Ø9	.2589E-1Ø	.4623E-12
59	.2481E+16	-.2366E-Ø9	.2477E-Ø9	.1109E-1Ø	.188ØE-12
62	.1457E+17	-.2646E-Ø9	.2609E-Ø9	-.3709E-11	-.5981E-13
65	.8558E+17	-.2927E-Ø9	.2742E-Ø9	-.1851E-1Ø	-.2847E-12
68	.5Ø26E+18	-.3208E-Ø9	.2875E-Ø9	-.3331E-1Ø	-.4899E-12
71	.2952E+19	-.3489E-Ø9	.3ØØ8E-Ø9	-.4811E-1Ø	-.6777E-12
74	.1733E+2Ø	-.377ØE-Ø9	.3141E-Ø9	-.6292E-1Ø	-.85Ø2E-12

REFERENCES

1. Blythe, A.R., 'Electrical Properties of Polymers', Cambridge Univ. Press, (1979).

2. Debye, P., 'Polar Molecules', Chem. Catalog, New York, (1929).

3. Debye, P., 'Polar Molecules', Dover Publications, New York, (1945).

4. Smyth, C.P., 'Dielectric Behaviour and Structure', McGraw-Hill, (1955).

5. Smith, J.W., 'Electric Dipole Moments', Butterworths, (1955).

6. Fröhlich, H.,'Theory of Dielectrics : Dielectric Constant', 2nd edn., Oxford Press, (1958).

7. McCrum, N.G., Read, B.E. and Williams, G., 'Anelastic and Dielectric Effects in Polymeric Solids', John Wiley, (1967).

8. Böttcher, C.J.F., 'Theory of Electric Polarization', 2nd edn., Elsevier, (1973).

9. Burfoot, J.C. and Taylor, G.W., 'Polar Dielectrics and their Applications', Macmillan, (1979).

10. 'Encyclopedia of Polymer Science and Technology', Vol 1, p 856, John Wiley, (1972).

11. Sessler, G.M., editor, 'Electrets', Topics in Appl. Phys., Vol 33, Springer-Verlag, (1980).

12. Sessler, G.M. and West, J.E., 'Charging of Polymer Foils with Momoenergetic Low-Energy Electron Beams', Appl. Phys. Lett., Vol. 17, p507-509, (1970).

13. Labes, M.M., 'Conductivity in Polymeric Solids', Pure and Appl. Chem., Vol. 12(1-4), p275-285, (1966).

14. Goodings, E.P., 'Conductivity and Superconductivity in Polymers', Chem. Soc. Reviews, Vol. 5, p95-123, (1976).

15 Block, H., 'The Nature and Application of Electrical Phenomena in Polymers', Adv. Polym. Sci., Vol 33, p 93-167, (1979).

16 Mort, J. and Pfister, G., editors, 'Electronic Properties of Polymers', John Wiley, (1982).

17. 'New Conducting Polymers join Polyacetylene', Phys. Today, Vol. 32(9), p 19-21, (1979).

18. Diaz, A.F., Kanazawa, K.K. and Gardini, G.P., 'Electrochemical Polymerization of Pyrrole', J.C.S., Chem. Comm., Vol 19, p635-636, (1979)

19. Kanazawa, K.K., Diaz, A.F., Geiss, R.H., Gill, W.D., Kwak, J.F., Logan, J.A., Rabolt, J.F. and Street, G.B., 'Organic Metals: Polypyrrole, a Stable Synthetic Metallic Polymer', J.C.S., Chem. Comm., Vol 19, p854-855, (1979).

20. Diaz, A.F. and Kanazawa, K.K., 'Polypyrrole: An Electrochemical Approach to Conducting Polymers', in Miller, J.S., editor, 'Extended Linear Chain Compounds', Vol. 3, p417-441, Plenum Publ., (1983).

21. 'Encyclopedia of Polymer Science and Technology', Vol 11, p338-364, John Wiley, (1972).

22. Penwell, R.C., Ganguly, B.N. and Smith, T.W., 'Poly(N-Vinyl Carbazole): A Selective Review of its Polymerization, Structure, Properties and Electrical Characteristics', J. Polymer Sci., Macro. Reviews, Vol. 13, p 63-160, (1978).

23. Hoegl, H., Süs, O. and Neugebauer, German Patents, 1 111 935, 1 068 115.

24. Hoegl, H., 'The Photoelectric Effects in Polymers and their Sensitisation by Dopants', J. Phys, Chem., Vol 69, p755-766, (1965).

25. Klöpffer, W., 'Transfer of Electronic Exitation Energy in Poly(Vinyl Carbazole)', J. Chem. Phys., Vol. 50, p2337-2343, (1969).

26. Maxwell, J.C., 'Electricity and Magnetism', p452, Oxford University Press, (1892).

27. Wagner, K.W., Arch. Elektrotechn., Vol.2, p371, (1914).

28. Sillars, R.W., 'The Properties of a Dielectric Containing Semi-Conducting Particles of Various Shapes', J. Instn. Electr. Engrs., Vol. 80, p 378-394, (1937).

29. Hamon, B.V., 'Maxwell-Wagner Loss and Absorption Currents in Dielectrics', Austral. J. Phys., Vol. 6, p304-315. (1953).

30. Flory, P.J., 'Principles of Polymer Chemistry', Cornell University Press, New York, (1953).

31. Flory, P.J., 'Statistical Mechanics of Chain Molecules', Interscience, New York, (1969).

32. Volkenstein, M.V., 'Configurational Statistics of Polymer Chains', English Translation, Interscience, New York, (1963).

33. Birshtein, T.M., and Ptitsyn, O.B., 'Conformations of Macromolecules', English Translation, Interscience, New York, (1966).

34. Karasz F.E., editor, 'Dielectric Properties of Polymers', Plenum Press, (1972).

35. Hedvig, P., 'Dielectric Spectroscopy of Polymers', Adam Hilger, (1977).

36. Le Fèvre, C.G. and Le Fèvre, R.J.W., 'The Kerr Effect: Its Measurement and Applications in Chemistry', Rev. Pure Appl. Chem., Vol 5(4), p261-318, (1955).

37. Le Fèvre, C.G. and Le Fèvre, R.J.W., 'The Kerr Effect', in Weissberger, A, editor, 'Physical Methods of Chemistry', Vol. 1, Part IIIc, p 399-452, John Wiley, (1972).

38. Fredericq, E. and Houssier, C., Electric Dichroism and Electric Birefringence', Clarendon Press, Oxford, (1973).

39. O'Konski, C.T., editor, 'Molecular Electro-Optics. Part 1 and 2', Marcel Dekker, (1976).

40. Krause, S., editor, 'Molecular Electro-Optics', NATO Advan. Stud. Inst., Plenum Press, (1981).

41. Le Fèvre, R.J.W., 'Molecular Refractivity and Polarizability', Advan. Phys. Organ. Chem., Vol. 3, p 1-90, (1965).

42. Le Fèvre, R.J.W., 'Dipole Moments', Methuen, (1953).

43. Jernigan, R.L. and Thompson, D.S., 'Flexible Polymers', Ch. 5 of Ref. 39.

44. Patterson, G.D. and Flory, P.J., 'Depolarized Rayleigh Scattering and the Mean-Squared Optical Anisotropies of n-Alkanes in Solution', J.C.S., Faraday II, Vol. 68, p1098-1110, (1972).

45. Dodgson, K. and Semlyen, J.A., 'Studies of Cyclic and Linear Poly (Dimethyl Siloxanes): 1. Limiting Viscosity Number-Molecular Weight Relationships', Polymer, Vol. 18, p1265-1268, (1977).

46. Dodgson, K., Sympson, D. and Semlyen, J.A., 'Studies of Cyclic and Linear Poly(Dimethyl Siloxanes): 2. Preparative Gel Permeation Chromatography', Polymer, Vol. 19, p 1285-1290, (1978).

47. Higgins, J.S., Dodgson, K. and Semlyen, J.A., 'Studies of Cyclic and Linear Poly(Dimethyl Siloxanes): 3 Neutron Scattering Measurements of Rings and Chain Polymers', Polymer, Vol. 20, p553-558, (1979).

48. Dodgson, K., Bannister, D.J. and Semlyen, J.A., 'Studies of Cyclic and Linear Poly(Dimethyl Siloxanes). 4. Bulk Viscosities', Polymer, Vol. 21, p 663-667, (1980).

49. Edwards, C.J.C., Stepto, R.F.T. and Semlyen, J.A., 'Studies of Cyclic and Linear Poly(Dimethyl Siloxanes): 5. Diffusion Behaviour in Dilute Solution', Polymer. Vol. 21, p 781-786, (1980).

50. Bannister, D.J. and Semlyen, J.A., 'Studies of Cyclic and Linear Poly(Dimethyl Siloxanes): 6. Effect of Heat', Polymer, Vol. 22, p 377-381, (1981).

51. Edwards, C.J.C., Stepto, R.F.T. and Semlyen, J.A., 'Studies of Cyclic and Linear Poly(Dimethyl Siloxanes): 7. Diffusion Behaviour in a Poor Solvent', Polymer, Vol. 23, p865-868, (1982).

52. Edwards, C.J.C., Stepto, R.F.T. and Semlyen, J.A., 'Studies of Cyclic and Linear Poly(Dimethyl Siloxanes): 8. Light Scattering Measurements in Good and Poor Solvents', Polymer, Vol. 23, p 869-872, (1982).

53. Edwards, C.J.C., Bantle, S., Burchard, W. Stepto, R.F.T. and Semlyen, J.A., 'Studies of Cyclic and Linear Poly(Dimethyl Siloxanes): 9 Quasi-Elastic Light Scattering and Concentration Dependence of Diffusion Coefficients', Polymer, Vol. 23, p 873-876, (1982).

54. Edwards, C.J.C., Rigby, D., Stepto, R.F.T., Dodgson, K. and Semlyen, J.A., 'Studies of Cyclic and Linear Poly(Dimethyl Siloxanes): 10. Calculations of Radii of Gyration', Polymer, Vol. 24, p391-394, (1983).

55. Edwards, C.J.C., Rigby, D., Stepto, R.F.T. and Semlyen, 'Studies of Cyclic and Linear Poly(Dimethyl Siloxanes) : 11. Shapes of Ring and Chain Molecules', Polymer, Vol. 24, p 395-399, (1983).

56. Higgins, J.S., Ma, K. Nicholson, L.K., Hayter, J.B., Dodgson, K. and Semlyen, J.A., 'Studies of Cyclic and Linear Poly(Dimethyl Siloxanes): 12. Observation of Diffusion Behaviour by Quasielastic Neutron Scattering', Polymer, Vol. 24, p793-799, (1983).

57. Mark, J.E., 'The Use of Dipole Moments to Characterize Configurations of Chain Molecules', Acc. Chem. Res., Vol. 7, p 218-225, (1974).

58. Marchal, J. and Benoit, H., 'Contribution des Moments Électriques a L'Etude des Solutions de Macromolécules en Chaine', J. Chim. Phys. Physicochim. Biol., Vol. 52, p818-825, (1955).

59. Marchal, J. and Benoit, H., 'Comparaison Entre les Résultats Fournis par la Determination des Dimensions et du Moment Électrique Moyen des Chaînes Macromoléculaires', J. Polym, Sci., Vol. 23, p223-232, (1957).

60. Stockmayer, W.H., 'Dielectric Dispersion in Solutions of Flexible Polymers'. Pure Appl. Chem., Vol. 15, p 539-554, (1967).

61. Nagai, K. and Ishikawa, T., 'Excluded Volume Effect on Dipole Moments of Polymer Chains', Polymer J., Vol. 2(3), p 416-421, (1971).

62. Doi, M. 'Excluded-Volume Effect on Dipole Moment of Polar Macromolecules', Polymer J., Vol. 3(2), p 252-253, (1972).

63. Liao, S.C. and Mark, J.E., 'Effect of Excluded Volume on the Dipole Moments of Chain Molecules', J. Chem. Phys. Vol. 59(7), p 3825-3830, (1973).

64. Dasgupta, S. and Smyth, C.P., 'Microwave Absorption and Molecular Structure in Liquids. LXX. Dipole Moment, Atomic Polarization, and Dielectric Relaxation in Polymethylpolysiloxanes', J. Chem. Phys., Vol. 47(8), p 2911-2916, (1967).

65. Sutton, C. and Mark, J.E., 'Dipole Moments of Dimethyl Siloxane Oligomers and Poly(Dimethyl Siloxane)', J. Chem. Phys., Vol 54(12), p 5011-5014, (1971).

66. Crescenzi, V. and Flory, P.J. 'Configuration of the Poly(Dimethyl Siloxane) Chain. II Unperturbed Dimensions and Specific Solvent Effects', J.A.C.S., Vol. 86, p 141-146, (1964).

67. Mark, J.E., 'Dipole Moments of Dimethyl Siloxane Chains', J. Chem., Phys., Vol. 49(3), p 1398-1402, (1968).

68. Flory, P.J., Crescenzi, V. and Mark J.E., 'Configuration of the Poly(Dimethyl Siloxane) Chain III. Correlation of Theory and Experiment', J.A.C.S., Vol. 86, p146-152, (1964).

69. Yu, C.U. and Mark, J.E., 'Specific Solvent Effects in Swollen Polymer Networks', Macromolecules, Vol. 7(2), p229-232, (1974).

70. Mark, J.E. and Flory, P.J., 'The Configuration of the Polyoxyethylene Chain', J.A.C.S., Vol. 87, p 1415-1423, (1965).

71. Mark, J.E. and Flory, P.J., 'Dipole Moments of Chain Molecules. I. Oligomers and Polymers of Oxyethylene', J.A.C.S., Vol 88, p 3702-3703, (1966).

72. Mark, J.E., 'Dipole Moments of Chain Molecules. II. Poly(Tetramethylene Oxide)', J.A.C.S., Vol. 88, p3708-3711, (1966).

73. Mark, J.E., 'Chain Dimensions and Dipole Moments of Poly(Trimethylene Oxide)', J. Polym. Sci., Part B, Vol. 4, p 825-831, (1966).

74. Flory, P.J. and Mark, J.E., 'The Configuration of the Polyoxymethylene Chain', Makromol. Chem, Vol. 75, p 11-21, (1964).

75. Uchida, T. Kurita, Y. and Kubo, M., 'The Dipole Moments and the Structures of Polyoxymethylene Dimethyl Ethers', J. Polym. Sci., Vol. 19, p 365-372, (1956).

76. Porter, C.H., Lawler, J.H.L. and Boyd, R.H., 'A Dielectric Study of Molecular Relaxation in Polyoxymethylene at High Temperatures', Macromolecules, Vol. 3, p 308-314, (1970).

77. Uchida, T., Kurita, Y., Koizumi, H. and Kubo, M., 'Dipole Moments and the Structures of Polyethylene Glycols', J. Polm. Sci., Vol. 21, p 313-322, (1956).

78. Kotera, A., Suzuki, K., Matsumura, K., Nakano, T., Oyama, T. and Kambayashi, U., 'Dipole Moments of Polyethylene Glycol Diethyl Ethers', Bull. Chem. Soc. Jap., Vol. 35, p797-801, (1962).

79. Bak, K., Elefante, G. and Mark J.E., 'Configurational Properties of Poly(Ethylene Oxide) and Poly(Tetramethylene Oxide), J. Phys. Chem., Vol. 71, p 4007-4011, (1967).

80. Aroney, M., Le Fèvre, R.J.W. and Parkins, G.M., 'Molecular Polarizability. The Molar Kerr Constants and Dipole Moments of Six Polyethylene Glycols as Solutes in Benzene', J.C.S., p2890-2895, (1960).

81. Loveluck, G.D., 'Dipole Moment Studies on Polyethylene and Polypropylene Glycols of Low Molecular Weight', J.C.S., p2729-2732, (1961).

82. Yamamoto, K., Teramoto, A. and Fujita, H., 'Limiting Viscosity Number versus Molecular Weight Relations for Polyoxacyclobutane', Polymer, Vol. 7, p 267-273, (1966).

83. Kurata, M., Utiyama, H. and Kamada, K., 'Unperturbed Dimensions of Poly(Tetrahydrofuran)', Makromol Chem., Vol. 88, p 281-293, (1965).

84. Leonard, W.J., Jernigan, R.L. and Flory, P.J., 'Dipole Moments in Relation to Configuration of n-Alkane Chains Bearing α, ω Dipolar Substituents', J. Chem. Phys., Vol. 43(7), p 2256-2261, (1965).

85. Hayman, H.J.G. and Eliezer, I., 'Dipole Moments of α, ω - Dibromoparaffins and their Temperature Dependence', J. Chem. Phys., Vol. 35(2), p 644-648, (1961).

86. Abbe, A., Jernigan, R.L. and Flory, P.J., 'Conformational Energies of n-Alkanes and the Random Configuration of Higher Homologs Including Polymethylene', J.A.C.S., Vol. 88, p 631-639, (1966).

87. Flory, P.J. and Jernigan, R.L., 'Second and Fourth Moments of Chain Molecules', J. Chem, Phys., Vol. 42(10), p 3509-3519, (1964).

88. Le Févre, C.G., Le Févre, R.J.W. and Parkins, G.M., 'Molecular Polarizability. The Specific Kerr Constants and Polarizations of Various Polystyrenes dissolved in Carbon Tetrachloride', J.C.S., p 1468-1474, (1958).

89. Le Févre, C.G., Le Févre, R.J.W. and Parkins, G.M., 'Molecular Polarizability. The Specific Kerr Constants and Polarizations of Vinyl Acetate and Various Polyvinyl Acetates dissolved in Carbon Tetrachloride or Benzene', J.C.S., p 1814-1819, (1960).

90. Le Févre, R.J.W. and Sundaram, K.M.S., 'Molecular Polarizability Molar Kerr Constants and Dipole Moments of Vinyl Chloride and Six Polyvinyl Chlorides as Solutes in Dioxan', J.C.S., p 1494-1502, (1962).

91. Le Févre, R.J.W. and Sundaram, K.M.S., 'Molecular Polarizability Molar Kerr Constants and Dipole Moments of Vinyl Bromide and Six Polyvinyl Bromides as Solutes in Dioxan', J.C.S. p 4003-4008, (1962).

92. Le Févre, R.J.W. and Sundaram, K.M.S., 'Molecular Polarizability. Molar Kerr Constants of Methyl Methacrylate and its Polymers', J.C.S., p 1880-1887, (1963).

93. Le Févre, R.J.W., Sundaram, A. and Sundaram, K.M.S., 'Molecular Polarizability. The Molar Kerr Constants and Conformations of Eight Polyaryls as Solutes', J.C.S., p 3180-3188, (1963).

94. Le Févre, R.J.W. and Sundaram, K.M.S., 'Molecular Polarizability. The Molar Kerr Constants, Apparent Dipole Moments, etc., of Methyl Acrylate and Five of its Polymers', J.C.S., p 3188-3193, (1963).

95. Le Févre, R.J.W. and Sundaram, K.M.S., 'Molecular Polarizability. The Molar Kerr Constants, Dipole Moments, etc., of Isoprene , Polyisoprenes, and Some Related Hydrocarbons', J.C.S., p3547-3554, (1963).

96. Le Févre, R.J.W. and Sundaram, K.M.S., 'Molecular Polarizability. The Molar Kerr Constants, Apparent Dipole Moments, etc., of Indene and Eight Polyindenes as Solutes in Benzene', J.C.S., p556-562, (1964).

97. Le Févre, R.J.W. and Sundaram, K.M.S., 'Molecular Polarizability. The Molar Kerr Constants and Apparent Dipole Moments of Cyclopentadiene and Some of its Polymers', J.C.S., p 3518-3523, (1964).

98. Suter, U.W. and Flory, P.J., 'Optical Anisotropy of Polystyrene and Its Low Molecular Analogues', J.C.S., Faraday II, Vol. 73, p 1521-1537, (1977).

99. Saiz, E., Suter, U.W., and Flory, P.J., 'Optical Anisotropies of para-Halogenated Polystyrenes and Related Molecules', J.C.S., Faraday II, Vol. 73, p 1538-1552, (1977).

100. Tonelli, A.E., 'Possible Characterization of Homopolymer Configuration and Copolymer Sequence Distribution by Comparison of Measured and Calculated Molar Kerr Constants', Macromolecules, Vol. 10, p 153-157, (1977).

101. Khanarian, G., Schilling, F.C., Cais, R.E. and Tonelli, A.E., 'Kerr Effect and Dielectric Study of Poly(Vinyl Chloride) and its Oligomers', Macromolecules, Vol. 16, p 287-291, (1983).

102. Mattice, W.L., 'Generator Matrix and Monte Carlo Treatments of Simple Chains with Excluded Volume. Asymmetry and Overall Expansion of Finite Chians', Macromolecules, Vol. 14, p 1485-1490, (1981).

103. Mattice, W.L., 'Subchain Expansion in Generator Matrix and Monte Carlo Treatments of Simple Chains with Excluded Volume', Macromolecules, Vol. 14, p 1491-1495, (1981).

104. Mattice, W.L. and Carpenter, D.K., 'Mean-Square Dipole Moments in Rotational Isomeric State Chains Containing Atoms which Behave as Hard Spheres', Macromolecules, in press.

105. Khanarian, G. and Tonelli, A., 'Kerr Effect and Dielectric Study of Poly(Oxyethylene Glycols)', Macromolecules, Vo. 15, p 145-148, (1982).

106. Davies, M., Senior Reporter, 'Dielectric and Related Molecular Processes', Chem. Soc. Spec. Per. Rep.; Vol. 1, (1972); Vol. 2 (1975); Vol 3 (1977).

107. Le Févre, C.G. and Le Févre, R.J.W., 'Molecular Polarizability. The Measurement of Molecular Kerr Constants in Solution', J.C.S., p 4041-4050, (1953).

108. O'Konski, C.T. and Farinato, R.S., 'Electro-Optic Measurement of γ-Ray Induced Damage in DNA', in Jennings, B.R., editor, 'Electro-Optics and Dielectrics of Macromolecules and Colloids', p 133-142, Plenum Press, New York, (1979).

109. O'Konski, C.T., 'Note on Electro-Optic Measurements of Vesicles to Study Proteins in Membranes', in Sund, H. and Blauer, G., editors, 'Transport by Proteins', p 231-233, Walter de Gruyter, (1978).

110. O'Konski, C.T. and Pritchard, A.E., 'Dynamics of Superhelical DNA and Its Complexes with Ethidium Bromide from Electro-Optic Relaxation Measurements', Ann. New York Acad. of Sciences, Vol 303, p 159-169, (1977).

111. O'Konski, C.T., Highsmith, S, Kretzschmar, K.M. and Morales, M.F., 'Flexibility of Myosin Rod, Light Meromyosin and Myosin Subfragment-2 in Solution', Proc. Natl. Acad. Sci., Vol. 74, p 4986-4990, (1977).

112. Beevers, M.S., Khanarian, G. and Moore, W.J., 'Kerr Constants of Naturally-Occuring α-Amino Acids in Aqueous Solution', in Jennings, B.R., editor, 'Electro-Optics and Dielectrics of Macromolecules and Colloids', p 269-275, Plenum Press, New York, (1979).

113. Beevers, M.S. and Khanarian, G., 'Measurement of Kerr Constants of Conducting Liquids', Aust. J. Chem., Vol. 32, p 263-269, (1979).

114. Beevers, M.S., 'The Electro-Optical Kerr Effect in Solutions of the Nematogen N-(p-Methoxybenzylidene)-p-n-butylaniline Mol. Cryst. Liq. Cryst., Vol. 31, p333-348, (1975).

115. Davies, M., Moutran, R. Price, A.H., Beevers, M.S. and Williams, G., 'Dielectric and Optical Studies of Nematogen 4, 4'-n-Heptyl-Cyanobiphenyl', J.C.S., Faraday II, Vol. 72, p 1447-1458, (1972).

116. Beevers, M.S. and Williams, G., 'Electro-Optical Kerr Effect in Solutions of Benzylidene Aniline and its Derivatives', J.C.S., Faraday Trans II, Vol. 72, p 2171-2177, (1976).

117. Beevers, M.S., Garrington, D.C. and Williams, G., 'Dielectric and Dynamic Kerr Effect Studies of Poly(n-Butyl Isocyanate) and Poly(n-Octyl Isocyanate) in Solution', Polymer, Vol. 18, p 540-546, (1977).

118. Beevers, M.S., Elliott, D.A. and Williams, G., 'Studies of Cholesteryl Oleyl Carbonate in its Isotropic and Homeotropic States Using Optical Rotation, Kerr Effect and Light Scattering', Mol. Cryst. Liq. Cryst., Vol. 80, p 135-156, (1982).

119. Krause, S. and O'Konski, C.T., 'Electric Birefringence Dynamics' p 147-162 of ref. 40, (1981).

120. Kerr, K., 'A New Relation Between Electricity and Light Dielectrified Media Birefringent', Phil. Mag., Vol 50(4), p 337-348, (1875).

121. Kerr, J., 'A New Relation Between Electricity and Light Dielectrified Media Birefringent. (Second Paper)', Phil. Mag., Vol. 50(4), p 446-458, (1875).

122. Gans, R., 'Asymmetrie von Gasmolekeln. Ein Beitragzur Bestimmungder-molekularen Form', Annalen der Physik, Vol. 65(10), p 97-123, (1921).

123. Debye, P., 'Handbuch Radiol', Vol. 6, p 597 and p 760, (1925).

124. Debye, P. and Sack, H., 'Handbuch der Radiologie', Vol. 6, Ch. 2, p 69 and p 179, (1934).

125. Stuart, H.A., 'Die Struktur des freien Molekuls', Chapter 7, p 415, Springer, Berlin, (1952).

126. Stuart, H.A., in Euchen, A. and Wolf, K.S., editors, 'Hand-und Jahrbuch der Chemischen Physik', Vol. 10, Part 3, (1939).

127. Debye, P. and Bueche, F., 'Electric Moments of Polar Polymers in Relation to their Structure', J. Chem. Phys., Vol. 19, p589-594, (1951).

128. Weast, R.C., 'Handbook of Chemistry and Physics', CRC Press Inc., 1981-1982 edn.

129. Morrison, R.T. and Boyd, R.N., 'Organic Chemistry', Chapter 4, p 119-120, Third Edn., Allyn and Bacon Inc., (1977).

130. Champion, J.V., Meeton, G.H. and Whittle, C.D., 'Temperature Dependence of the Kerr Effect and Depolarization Ratio in Liquids', J. Chem. Phys., Vol. 67, p 1864-1869, (1970).

131. Aroney, M.J., Battaglia, M.R. Ferfoglia, R., Millar, D. and Pierens, R.K., 'The Kerr Constant of Water and other Pure Liquids at 633nm', J.C.S., Faraday II, Vol. 72, p 724-726, (1976).

132. Kipping, F.S. and Robinson, R., 'Organic Derivatives of Silicon. Part XXI. The Condensation Products of Diphenylsilicanediol', J.C.S., Vol. 105, p 484-500, (1914).

133. Hyde, J.F. and Delong, R.C., 'Condensation Products of the Organo-Silane Diols', J.A.C.S., Vol. 63, p1194-1196, (1941).

134. Hunter, M.J., Hyde, J.F., Warrick, E.L. and Fletcher, H.J., 'Organo-Silicon Polymers. The Cyclic Dimethyl Siloxanes', J.A.C.S., Vol. 68, p 667-672, (1946).

135. Patnode, W. and Wilcock, D.F., 'Methylpolysiloxanes', J.A.C.S., Vol. 68, p 358-363, (1946).

136. Brown, J.F. and Slusarczuk, G.M.J, 'Macrocyclic Polydimethylsiloxanes', J.A.C.S., Vol. 87, p 931-932, (1965).

137. Clemo, E.R. and Perkin, W.H., Jr, 'Vinyl Derivatives especially of Carbazole and Tetrahydrocarbazole and their Behaviour with Acids', J.C.S., Vol. 125, p 1804-1814, (1924).

138. Reppe, W. and Keyssmer, E. (to General Aniline and Film Corp.), German Patent 618, 120, (1935).

139. Frisch, K.C., 'N-Vinylcarbazole', in Blout, E.R. and Mark, H., editors, 'Monomers', Interscience Publishers Inc., New York, (1951).

140. Okamoto, K., Yamada, M., Itaya, A., Kimura, T. and Kusabayashi, S., 'Polymerization of N-Vinylcarbazole, N-Vinyl-5H-Benzo(b)carbazole and N-Vinyl-7H-Benzo(c)carbazole', Macromolecules, Vol. 9, p 645-649, (1976).

141. Williams, D.J. and Froix, M., 'The Stereoregularity of Poly(N-Vinylcarbazole)', Polymer Preprints, Vol. 18, p 445-449, (1977).

142. Kawamura, T. and Matsuzaki, K., 'Carbon-13 Nuclear Magnetic Resonance Studies of Poly(N-Vinyl Carbazole)', Makromol. Chem., Vol. 179, p 1003-1010, (1978).

143. Scot, R.P.W., 'The Construction of High-Efficiency Columns for the Separation of Hydrocarbons', in Desty, D.H., editor, 'Gas Chromatography', Chapter 15, p 189-199, Butterworths, (1958).

144. Purnell, J.H., 'The Development of Highly Efficient Gas-Liquid Chromatography Columns', Ann. N.Y. Acad. Sci., Vol. 72, p 592-605, (1958).

145. Bohemen, J., Langer, S.H., Perrett, R.H. and Purnell, J.H., 'A Study of the Adsorptive Properties of Firebrick in Relation to its use as a Solid Support in Gas-Liquid Chromatography', J.C.S., Part 2, p 2444-2451, (1960).

146. Hurd, C.B., 'Studies on Siloxanes. 1. The Specific Volume and Viscosity in Relation to Temperature and Constitution', J.A.C.S., Vol. 68, p 364-370, (1946).

147. Heller, J., Tiezen, D.O. and Parkinson, D.B., 'Polymerization of N-Vinyl Carbazole with Ziegler-Type Catalyst Systems', J. Polym. Sci., Part A, Vol. 1, p 125-138, (1963).

148. Yoshimoto, S., Akana, Y., Kimura, A., Hirata, H., Kusabayashi, S. and Mikawa, H., 'The Nuclear Magnetic Resonance Spectrum of Poly (N-Vinyl Carbazole), J.C.S. Section D: Chemical Communications, p 987, (1969).

149. Williams, D.J., 'Nuclear Magnetic Resonance Studies of Poly(N-Vinyl Carbazole)', Macromolecules, Vol. 3, p 602-605, (1970).

150. Tsuchihashi, N., Hatano, M. and Somha, J., 'Carbon-13 and Proton Magnetic Resonance Studies of Poly(N-Vinyl Carbazole)', Makromol. Chem., Vol. 177, p2739-2747, (1976).

151. Sauer, R.O. and Mead, D.J., 'Dipole Moments of Linaer and Cyclic Polymethylpolysiloxanes', J.A.C.S., Vol. 68, p 1794-1797, (1946).

152. Kurita, Y. and Kondo, M., 'Dipole Moments of Cyclic Siloxanes and Thiosiloxanes', Bull. Chem. Soc. Japan, Vol. 27,p 160-163, (1954).

153. Dasgupta, S. and Smyth, C.P., 'Microwave Absorption and Molecular Structure in Liquids. LXXVII. Relaxation Mechanisms in Hexamethyldisiloxane and Hexaphenyldisiloxane', J. Chem. Phys., Vol. 54(11), p 4648-4650, (1971).

154. Dasgupta, S., Garg, S.K. and Smyth, C.P., 'Microwave Absorption and Molecular Structure in Liquids. LXIX. Atomic Polarization and Relaxation in Several Siloxanes and Hexamethyldisilazane', J.A.C.S., Vol. 89(10), p 2243-2246, (1967).

155. Baker, E.B. Barry, A.J. and Hunter, M.J., 'Dielectric Constants of Dimethyl Siloxane Polymers', Ind. Eng. Chem., Vol. 38, p 1117-1120, (1946).

156. Flory, P.J., 'Configuration-Dependent Properties of Polymer Chains', Pure Appl. Chem., Vol. 26, p 309-326, (1971).

157. Onsager, L., 'Electric Moments of Molecules in Liquids', J.A.C.S., Vol. 58, p 1486-1493, (1936).

158. Guggenheim, E.A., 'A Proposed Simplification in the Procedure for Computing Electric Dipole Moments', Trans. Far. Soc., Vol. 45, p 714-720, (1949).

159. Freiser, H., Eagle, M.V. and Speiser, J., 'Electron Moments and Structures of Organosilicon Compounds. III The Oxygen-Silicon Bond', J.A.C.S., Vol. 75, p 2824-2827, (1953).

160. Aggarwal, E.H. and Bauer, S.H., 'The Structures of Hexamethylcyclotrisiloxane as Determined by the Diffraction of Electrons on the Vapour', J. Chem. Phys., Vol. 18(1), p 42-50, (1950).

161. Frevel, L.K. and Hunter, M.J., 'The Structure of Hexamethylcyclooctasiloxane', J.A.C.S., Vol. 67, p 2275, (1945).

162. Holland, R.S. and Smyth, C.P., 'The Dielectric Properties and Molecular Structure of Hexamethyldisiloxane', J.A.C.S., Vol. 77, p 268-271, (1955).

163. Mizushima, S., 'Structure of Molecules and Internal Rotation', Academic Press. Inc., New York, (1954).

164. Lifson, S., 'Neighbor Interactions and Internal Rotations in Polymer Molecules. III Statistics of Interdependent Rotations and Their Applications to the Polyethylene Molecule', J. Chem. Phys., Vol. 30, p 964-967, (1959).

165. Birshtein, T.M. and Ptitsyn, O.B., Zh, Tekh, Fiz., Vol 29, p 1048, (1959), (Sov. Phys-Tech. Fiz., Vol. 4, p 954, (196)); Birshtein, T.M., Vysokomolekul. Soedin., Vol. 1, p 798 and p 1086, (1959); Ptitsyn, O.B., Usp. Fiz. Nauk., Vol. 69, p 371, (1959), (Sov. Phys. - Usp., Vol. 2, p 797, (1960)).

166. Nagai, K., 'Local Steric Hinderances and Configurations of Linear Macromolecules in Solutions I. Formulation', J. Chem. Phys., Vol. 31(5), p 1169-1174, (1959).

167. Hoeve, C.A.J., 'Unperturbed Chain Dimensions of Polymeric Chains', J. Chem. Phys., Vol. 32(3), p 888-893, (1960).

168. Flory, P.J., 'Mean-Square Moments of Chain Molecules', Proc. Natl. Acad. Sci. (U.S.), Vol 51, p 1060-1067, (1964).

169. References 71, 84 and 170-178 are representative studies from what is a very extensive body of literature.

170. Brant, D.A. and Flory, P.J., 'The Configuration of Random Polypeptide Chains. II. Theory', J.A.C.S., Vol. 87, p 2791-2800, (1965).

171. Mark, J.E., 'Interpretation ofRandom-Coil Configurations of trans-1, 4-Polybutadiene and trans-1, 4-Polyisoprene', J.A.C.S., Vol. 89,, p 6829-6835, (1967).

172. Bates, T.W. and Stockmayer, W.H., 'Conformational Energies of Perfluoroalkanes. II. Dipole Moments of $H(CH_2)_nH$', Macromolecules, Vol. 1, p12-17, (1968).

173. Miller, W.G. and Flory, P.J., 'Dimensions of Polypeptide Chains in Helicogenic Solvents', J. Mol. Biol., Vol. 15. p 298-314, (1966).

174. Flory, P.J. and Semlyen, J.A., 'Macrocyclization Equilibrium Constants and the Statistical Configuration of Poly(Dimethyl Siloxane) Chains', J.A.C.S., Vol. 88, p 3209-3212, (1966).

175. Flory, P.J., 'Stereochemical Equilibrium in Chain Molecules', J.A.C.S., Vol. 89, p 1798-1804, (1967).

176. Nagai, K. and Ishikawa, T. 'Internal Rotation and Kerr Effect in Polymer Molecules', J. Chem. Phys., Vol. 43(12), p 4508-4515, (1965).

177. Nagai, K. 'Photoelastic Property of Cross-Linked Amorphous Polyethylene', J. Chem. Phys., Vol. 40(10), p 2818-2826, (1964).

178. Flory, P.J., Jernigan, R.L. and Tonelli, A.E., 'Strain Birefringence of Polymer Chains', J. Chem, Phys., Vol. 48, p 3822-3823, (1968).

179. Flory, P.J., 'Lectures in Materials Science', Benjamin Inc. New York, Amsterdam, (1963).

180. Jacobson, H. and Sockmayer, W.H., 'Intramolecular Reaction in Polycondensations. I. The Theory of Linear Systems', J. Chem. Phys., Vol. 18(12), p1600-1606, (1950).

181. Semlyen, J.A. and Wright, P.V., 'Equilibrium Ring Concentrations and the Statistical Conformations of Polymer Chains. I Oligomeric Dimethyl Siloxanes', Polymer, Vol. 10, p 543-553, (1969).

182. Beevers, M.S. and Semlyen, J.A., 'Equilibrium Ring Concentrations and the Statistical Conformations of Polymer Chains: Part 5. Stereoisomeric Cyclic in Poly(Phenylmethylsiloxane) Equilibriates', Polymer, Vol. 12, p 373-382, (1971).

183. Beevers, M.S. and Semlyen, J.A., 'Equilibrium Ring Concentrations and the Statistical Conformations of Polymer Chains; Part 8. Calculation of Small Ring Concentrations in Polydihydrogensiloxane and Polydimethylsiloxane Equilibriates', Polymer, Vol. 13, p 385-390, (1972).

184. Beevers, M.S. and Semlyen, J.A., 'Equilibrium Ring Concentrations and the Statistical Conformations of Polymer Chains: Part 10. Cyclics in a Polymeric Paraffin-Siloxane', Polymer, Vol. 13, p 523-526, (1972).

185. Steinfink, H., Post, B. and Fankuchen, I., 'The Crystal Structure of Octamethyl Cyclotetrasiloxane', Acta. Cryst., Vol. 8, p 420-424, (1955).

186. Yokoi, M., 'Electron Diffraction Investigation on the Molecular Structures of Some Organosilicon Compounds. I', Bull. Chem. Soc. Japan, Vol. 30, p 100-106, (1957).

187. Carmichael, J.B. and Kinsinger, J.B., 'A Theoretical Study of Ring Closure. Application to the Cyclic-Linear Distribution in Polydimethylsiloxane', Can. J. Chem., Vol. 42, p 1996-2007, (1964).

188. Applequist, J., Carl, J.R. and Fung, K.K., 'An Atom Dipole Interaction Model for Molecular Polarizability. Application to Polyatomic Molecules and Determination of Atom Polarizabilities', J.A.C.S., Vol. 94, p 2952-2960, (1972).

189. Ladanyi, B.M. and Keyes, T., 'Effect of Internal Fields on Depolarized Light Scattering from n-Alkane Gases', Mol. Phys., Vol. 37, p 1809-1821, (1971).

190. Armstrong, R.S., Aroney, M.J., Higgs, B.S. and Skamp, K.R., 'Molecular Polarizability. Anisotropy of Silicon Containing Groups', J.C.S., Faraday Trans. 2, Vol. 77, p 55-60, (1981).

191. Smith, R.P. and Mortensen, E.M., 'Bond and Molecular Polarizability Tensors. I. Mathematical Treatment of Bond Tensor Additivity', J. Chem. Phys., Vol 32(2). p 502-507, (1960).

192. Clement, C. and Bothorel, P., 'Étude de l'Anisotropie Optique Moléculaire d'Alcanes Normaux, Ramifiés et Halogénés. Effect de Solvent', J. Chim. Phys., Vol. 61, p 878-883, (1964).

193. Clement, C. and Bothorel, P., 'Étude de l'Anisotropie Optique des Alcanes Normaux: Différence d'Energie Entre Isomères de Rotation Anisotropies Optiques des Liaisons Atomiques C-C et C-H', J. Chim. Phys., Vol. 61, p 1262-1270, (1964).

194. Jernigan. R.L. and Flory, P.J., 'Optical Anisotropy of Chain Molecules. Theory of Depolarization of Scattered Light with Application to n-Alkanes', J. Chem. Phys., Vol. 47(6), p 1999-2007, (1967).

195. Flory, P.J. and Jernigan, R.L., 'Kerr Effect in Polymer Chains', J. Chem. Phys., Vol. 48, p 3823-3824, (1968).

196. Gans, R., 'Dielektrizitatskonstante und Elektrische Doppelbrechung', Ann. Physik, Vol. 64, p 481-512, (1921).

197. Lemaire, B. Fourche, G. and Sanchez, E., 'Excluded-Volume Effect for Various Chain Models. 1. Applications to Optical Anisotropy and End-To-End Distance of Linear Polymers', J. Polym. Sci., Polym. Phys. Ed., Vol. 12, p 417-429, (1974).

198. Ishikawa, T. and Nagai, K., 'Theoretical Interpretation of Kerr Constants of Polymer Chains. n-Alkanes, Poly(Oxyethylene Glycol)s and Poly(Oxyethylene Dimethyl Ether)s', Polymer J. Vol. 2(2), p 263-273, (1971).

199. North, A.M. and Phillips, P.J., 'Dielectric Properties of Poly(N-Vinyl Carbazole) Solutions', Chemical Communications, Vol. 21, p 1340-1341, (1968).

200. North, A.M. and Phillips, P.J., 'Correlation of Dielectric and Visco-Elastic Relaxation in Polymer Solutions', British Polym. J., Vol. 1(2), p 76-80, (1969).

201. Dev, S.B., Lochhead, R.Y. and North, A.M., 'Dielectric and Viscoelastic Relaxation in Dilute Solutions of some Non-Gaussian Chains', Discuss. Faraday Soc., Vol. 49, p 244-256, (1970).

202. Pochan, J.M., Hinman D.F., Froix, M.F. and Nash, R.W., 'Dielectric Relaxation Studies of Poly(N-Vinyl Carbazole) and Poly(3-Chloro-N-Vinyl Carbazole) Including the Effects of Sorbed Oxygen', Polymer Preprints, A.C.S., Div. Polym. Chem., p 570-575, (1975).

203. Froix, M.F., Williams, D.J., Pochan, J.M. and Geodde, A.O.,'Anomalous Relaxation in Carbazole Polymers', Polymer Preprints, A.C.S., Div. Polym. Chem. p576-582, (1975).

204. Pochan, J.M., Hinmann, D.F. and Nash, R., 'Dielectric Relaxation Studies of Poly(N-Vinyl Carbazole) and Poly(3-Chloro-N-Vinyl Carbazole) Including the Effects of Sorbed Oxygen', J. Appl. Phys., Vol. 46(10), p 4115-4119, (1975).

205. Fujiwara, Y. and Flory, P.J., 'Second and Forth Moments of Vinyl Polymer Chains', Macromolecules, Vol. 3, p 280-288, (1970).

206. Tonelli, A.E. and Schilling, F.C., 'Carbon-13 Chemical Shifts and the Microstructure of Polymers', Acc. Chem. Res., Vol. 14, p 233-238, (1981).

207. Khanarian. G. and Tonelli, A.E., 'A Kerr Effect and Dielectric Study of α, ω - Dibromoalkanes', J. Chem. Phys., Vol. 75(10), p 5031-5036, (1981).

208. Cowley, E.G. and Partington, J.R., 'Studies of Dielectric Polarization. Part XV. The Dipole Moments of Five Membered Nitrogen Ring Compounds:- Indole, Skatole, Carbazole, Isatin, Phthalimide and Succinimide', J.C.S., Part 1, p 47-50, (1936).

209. Liptay, W. 'Die Beeinflussung der Optischen Absorption von Molekulen durch ein Ausseres Elektrisches Feld. V. Ubergangsmomentrichtungen und Dipolmomente der Niedrigen Elektronenzustrande in 4-Nitranilin, 1-Nitro-3, 5- Diaminobenzol, 3, 5 Dinitroanilin, Carbazole und 3, 6-Dinitrocarbazol', Ber. Bunsenges. Phys. Chem., Vol. 71, p 548-559, (1967).

210. Kimura, A., Yoshimoto, S., Akana, Y., Hirata, H., Kusabayashi, S., Mikawa, H. and Kasai, N., 'Crystallinity of Poly(N-Vinyl Carbazole)', J. Polym. Sci., A-2, Vol. 8, p 643-648, (1970).

211. Crystal, R.C., 'The Crystalline Morphology of Poly(N-Vinyl Carbazole)', Macromolecules, Vol. 4, p 379-384, (1971).

212. Griffiths, C.H., 'Structural Characterization of Poly(N-Vinyl Carbazole)', in Characterization of Metal and Polymer Surfaces (Symp), Vol. 2, p 333-358, (1976).

213. Champion, J.V., Meeton, G.H. and Southwell, G.W., 'Electro-Optic Kerr Birefringence of Polystyrene in Dilute Solutions', Polymer, Vol. 17, p 651-655, (1976).

214. Denbigh, K.G., 'The Polarizabilities of Bonds-I', Trans. Faraday Soc., Vol. 36, p936-948, (1940).